Voorwoord

Een thesis schrijven leek me een ondoenbare klus, een voorwoord daarentegen leek me 'peanuts'. Nu ik eraan begin realiseer ik me wel dat dit de meest gelezen bladzijden zullen zijn! Dus aan allen die dit nu lezen: schenk niet te veel aandacht aan de volgorde en manier van bedanken, jullie verdienen het allemaal ook al vind ik misschien niet altijd de gepaste woorden. En doe nu verdorie ook eens de moeite om wat verder te lezen!

Zoals het een goed voorwoord past wil ik zeker beginnen met het bedanken van mijn promotor prof. dr. Dirk Vanderzande en mijn co-promotor prof. dr. Jan Gelan. Zij hebben altijd in mij geloofd waarvoor dank (en af en toe de nodige verwondering). Dankzij hen kon ik me in hun labo zowel op wetenschappelijk als sociaal vlak de afgelopen vier jaar verder ontwikkelen. Dirk, ik ben er me ten sterkste van bewust dat deze thesis het nodige 'verbeterwerk' heeft gevraagd en dat ik af en toe misschien wat veeleisend was.

Een dergelijk werk komt natuurlijk niet enkel tot stand door een doctorandus en zijn promotoren. De volgende mensen hebben ook meer dan hun steentje bijgedragen. Dr. Laurence Lutsen was voor het labo de rechterhand als het aankwam op het schrijven van de vereiste projecten en project-rapporten. Prof. dr. Peter Adriaensens verdient van mij een speciaal woord van dank: hij heeft me de waarde en de kracht van NMR technieken leren kennen en geen avond was hem te veel voor het verbeteren van artikels en teksten. Dr. Jan Czech heeft er nooit een probleem van gemaakt eender welk massaspectrum op te nemen en hierbij, indien nodig, de gepaste uitleg te geven. Daniel en Guy stonden in voor de TGA en ook Huguette, duizend maal dank voor al het werk rond de UV-Vis en FT-IR metingen.

De mensen waar je tijdens je vier jaar onderzoek het meest mee hebt vertoefd, zijn toch wel je 'mede-lotgenoten'. Hoewel een groot deel reeds de werkvloer heeft verlaten, ben ik jullie zeker niet vergeten. Lieve en Els, hopelijk worden al jullie dromen werkelijkheid in jullie nieuwe woning, Stijn en Robby, veel succes met jullie nieuwe rol als vader en Joachim, je moet binnenkort zeker eens 'croissankes' komen eten. Bart, ook al zat je maar een jaartje bij ons, we hebben het allemaal geweten. Liesbet, tof dat je nog wat langer kan blijven, wie weet kunnen we nu nog samen wat voor zwarte piet spelen. Anne, bedankt om drie weken

voor mij af te leggen, hierdoor heb ik je nog veel kunnen vragen, ik duim in ieder geval voor brave studentjes.

Veerle, gelukkig ben je snel weer hier terug op het LUC geraakt. Het was immers altijd fijn je langs mijn zijde te hebben voor een goede babbel. Iris, niet alleen bedankt voor de kleine dingen die je voor me deed in het labo maar ook voor het luisterend oor. Filip, je 'in de gloria' immitaties zal ik zeker in mijn gedachten bewaren. Hilde, ik vond het altijd tof je als jaargenootje te hebben, hopelijk kunnen we de band nog een tijdje aanhouden. Roel, waar we ook terecht mogen komen, ik ben ervan overtuigd dat jij de stilste zal blijven en ik de luidruchtigste maar we zullen er maar van uitgaan dat dit ons siert, niet? Ook de mensen die nog maar een jaar van ons labo deel uitmaken: Lien, Kristof, Ine en Sofie, bedankt voor de geweldige tijd samen. Jullie blazen een frisse wind door het labo en hopelijk mogen jullie nog veel plezier bij OS beleven. Het is mede dankzij jullie dat de fantastische sfeer in het labo behouden kan worden!

For the people who did a post-doc in our lab: Iwona, Pawel, Pierre-Henri, Mael and Wojtek: it was nice to have you here in Belgium. Iwona, thank you for the work you did on the polyisothianaphtene derivatives, I'm sure you will read chapter two carefully.

Aan alle mensen die bij ons hun stage hebben gedaan: hopelijk vonden jullie het leuk in ons labo en bedankt voor de toffe momenten. Vooral Annelies zou ik hierbij extra willen bedanken voor haar bijdrage aan de inhoud van hoofdstuk vier.

Daarnaast zijn er nog een aantal personen die achter de schermen alles draaiende houden: niet alleen alle mensen van het secretariaat, ook Christel Rappoort, bedankt voor het steeds opnieuw bezorgen van het nodige labo-materiaal, Koen Van Vinckenroye voor de opnames van de talrijke NMR spectra en Jos Kaelen voor de reparaties van ons glaswerk.

Zonder Ludwig Goris en Martin Knipper van het IMO, Tom Aernouts en Wim Geens van IMEC Leuven en Patrick Baesjou van Philips Eindhoven, zou ik nooit feed-back hebben gekregen over het gebruik van mijn materialen in zonnecellen en transistoren. Mannen, ik geef het toe, ik zal nog veel moeten leren over de fysica en wij scheikundigen hebben jullie nodig. Daarom ook dank aan Jean Manca voor de fysische uitleg. Hopelijk blijft een goede samenwerking in de toekomst verzekerd.

Al dat harde werken vereist natuurlijk ook de nodige ontspanning. Al de mensen die hiertoe bijgedragen hebben verdienen dan ook een woordje van aandacht. Mijn vrienden en

vooral vriendinnen ‘thuis’: babes, hopelijk weten jullie nu wat ik hier in Diepenbeek de afgelopen vier jaar verricht heb, iedereen die ooit mee geweest is op de labo-weekends, de badmintonners die net zoals ik altijd weer uitkeken naar de vrijdagmiddag, de mensen van het cafetaria,…; allemaal hebben ze bijgedragen om de afgelopen jaren ontzettend aangenaam voor mij te maken.

Voor de financiële steun heb ik gedurende vier jaar mogen rekenen op het Instituut voor de aanmoediging van Innovatie door Wetenschap en Technologie in Vlaanderen (IWT) waarvoor ik natuurlijk zeer erkentelijk ben. Maar vooral mijn ouders hebben mij zover gebracht: dankzij hen heb ik me nooit zorgen moeten maken over het financiële aspect van studeren en het is door hun steun dat ik zover ben geraakt. Rob, als elektrotechnicus ben jij misschien nog wel degene met wie ik thuis het meest over mijn onderzoek heb kunnen vertellen.

Ook Tom, mijne chocoprins, wil ik bedanken voor alles wat hij voor mij al gedaan heeft (en hopelijk nog lang blijft doen). Het zou heel wat moeilijker zijn geweest zonder jou…

Dank je wel!

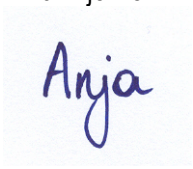

Contents

Chapter 1
General introduction

1.1 Conductive polymers

Conductive polymers are build up of a sequence of alternating single and double bonds, forming an extended π-conjugated system. The simplest example of such a conjugated polymer is poly(acetylene) (PA). This organic polymer was first prepared in 1958 when Natta *et al.*[1] polymerised acetylene in hexane using $AlEt_3/Ti(OPr)_4$ as the initiator system. It was known as an insoluble and air sensitive black powder when in 1974 it was again prepared as a silvery film by Shirakawa and co-workers from acetylene, using a Ziegler-Natta catalyst[2, 3]. However, in its neutral state it was not a conductor, indicating that the π-conjugated system still does not answer for the conductivity. It was not until the findings of Alan J. Heeger, Alan G. MacDiarmid and Hideki Shirakawa in 1977; one knew what made a material conductive. They discovered that oxidation with chlorine, bromine or iodine vapour made PA films 10^9 times more conductive than they were originally[4, 5]. Treatment with such oxidants was called 'doping' by analogy with the doping of semiconductors. It was for this discovery, which is seen as a major breakthrough in the research in conductive polymers that the Royal Swedish Academy of Sciences had decided to award the Nobel Prize in Chemistry for 2000 to these three scientists. Polymers then were already known for their favourable physical properties: low density, mechanical strength, low cost, flexibility and easy processability. The combination of the ability to conduct electricity with these favourable physical properties gave a new dimension to the fast expanding area of the synthesis of conjugated polymers. Another major breakthrough was established in 1990 with the observation of electroluminescence (EL) from another conjugated polymer, poly(*p*-phenylene vinylene) (PPV)[6]. This event gave a new boost to this research area and in the last ten years, it became clear that these conjugated polymers have a semiconductor behaviour that is as diverse as this of the classical inorganic

semiconductors. In this new research area of “plastic electronics”, an intense cooperation between chemists, physicists and engineers is needed to develop this new domain of technology further.

1.2 Low band gap (LBG) polymers

In the class of conjugated polymers, low band gap polymers form a separate class of materials. If we describe the electrical properties of a material with the band model, the definition of a low band gap material becomes more obvious.

In this model, bands arise from the overlap of the atomic orbitals of each atom with its neighbouring atoms in order to give rise to molecular orbitals which on their turn combine to energy bands. The way in which atoms or molecules interact with each other determines the dispersion of the bands. The highest occupied molecular band or the valence band (VB) is generated by the π-orbitals. The lowest unoccupied molecular band or the conduction band (CB) is produced by the π^*-orbitals. The band gap (E_g), the energy spacing between these two bands, determines whether we are dealing with an insulator (E_g > 2 eV), a semiconductor ($E_g \leq$ 2 eV) or a metal (E_g = 0 eV). For inorganic semiconducting materials as well as for conventional conjugated polymers, conductivity is only possible when we have partially empty valence bands or partially filled conduction bands. With this band theory, we can now visualise the doping-induced changes in the electronic structure, explaining the conductivity of doped PA found by Hideki Shirakawa, Alan G. MacDiarmid and Alan J. Heeger. By doping, extra charge carriers are created by adding electron donors or electron acceptors. In the case of electron donors, electrons are brought into the conduction band (reduction or n-doping), in the other case, holes are created in the valence band by the electron acceptors (oxidation or p-doping). In both cases extra localised energy levels are created between the VB and the CB which on extensive doping lowers the band gap and increases the conductivity. (Figure 1.1)

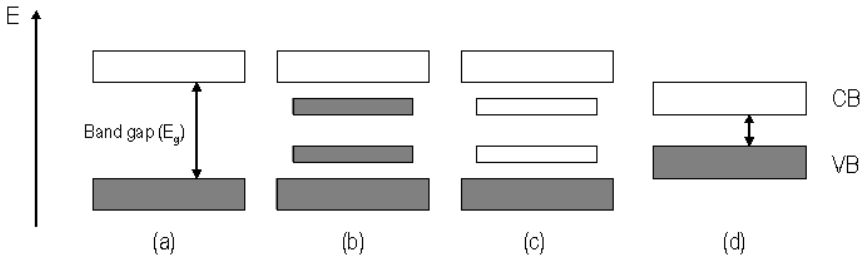

***Figure 1.1**: (a) Band model of a conventional conjugated polymer; (b) Band model of an n-doped conjugated polymer; (c) Band model of a p-doped conjugated polymer and (d) Band model of a low band gap polymer*

On this model, we can see clearly that the extra energy bands created by doping the conjugated semiconductor, can either be filled or be empty. They reduce the original band gap which facilitates the excitation of electrons from the new valence band to the new conduction band and answers for the conductivity. Investigations showed that the conductivity of conjugated polymers results from the formation of solitons or polarons and bipolarons[7]. In the case of p-doping, a hole -a position where an electron is missing- is created and can be filled by an electron jumping in from a neighbouring position. As a result, a new hole is created and so on, which allows charge to migrate along a certain distance of the conjugated backbone. However, the vacancy does not delocalise completely, as would be expected from the classical band theory. If an electron is removed locally, a radical cation, a polaron, is created. If a second electron is removed from an already oxidised section of the polymer, either a second independent polaron may be created or, if it is the unpaired electron of the first polaron that is removed, a bipolaron is formed. So in general: polarons are radical ions (radical cation or radical anion) and bipolarons are either dications or dianions. Both polymer chain defects can be formed upon reduction or oxidation. Solitons are other localised defects in the chain which only occur for π-systems with a degenerated ground state. In such cases, three types can be distinguished: a neutral soliton (a stable free radical), a cationic soliton or an anionic soliton.

Within this framework to explain the conductivity of conjugated polymers, a low band gap material can be defined. Nowadays there is still some discussion about the precise definition of low band gap polymers. The band gap of a conjugated polymer varies between 1 and 4 eV. According to some people poly(2,5-thienylene vinylene) (PTV) with a band gap of 1.8 eV[8] is on the borderline[9], others define a 'low band gap' as a conjugated material with an energy gap smaller than 1.5 eV[10, 11]. A typical property of this type of conjugated

polymer is the fact that they show intrinsic conductivity: the band gap is small enough to redistribute the electrons easily in an -even weak- electrical field. This property may be very useful for some possible applications because one normally dopes the polymers to obtain the wanted electrical or optical properties. Doping, however, is an oxidation or reduction process in which -often unstable- charged species are created by -most of the time- toxic dopants. In this way the created polymers are very unstable to oxygen in the air and to humidity. Often very high doping levels are needed which can change the mechanical properties of the materials. In this regard, low band gap polymers, which are conductive without the addition of dopant, can offer an alternative. Reducing the band gap will increase the population of the conduction band, increasing the number of intrinsic charge carriers. This type of polymers can also be doped which reduces the band gap even more. As a result, these polymers absorb light in the near infrared instead of in the visible area of the spectrum so that they often become transparent upon doping.

1.3 Synthesis of low band gap polymers

Control of the band gap is a research issue of ongoing interest because this “band gap engineering” may give the polymer its desired electrical and optical properties. There are different tools to manipulate and minimise the band gap of conjugated polymers. Two major approaches towards reduction of the band gap are the minimisation of the bond length alternation along the main chain and the alternation of electron-donors and electron-acceptors in the main chain[12]. This second approach will not be discussed since no materials of this class will be presented in this dissertation. Before reporting how to find out what the band gap is, the factors determining the band gap are dealt with first.

1.3.1 Parameters influencing the band gap

According to Roncali[11], the band gap of polyaromatic conjugated polymers can be viewed at as the result of five contributions i.e. the energy related to the bond length alternation ($E^{\Delta r}$), the mean deviation from planarity (E^{θ}), the aromatic resonance energy (E^{res}), the inductive or mesomeric electronic effects of substituents (E^{sub}) and the

intermolecular or interchain coupling in the solid state (E^{int}). All parameters are visualised in figure 1.2.

$$E_g = E^{\Delta r} + E^{\theta} + E^{res} + E^{sub} + E^{int} \qquad (1\text{-}1)$$

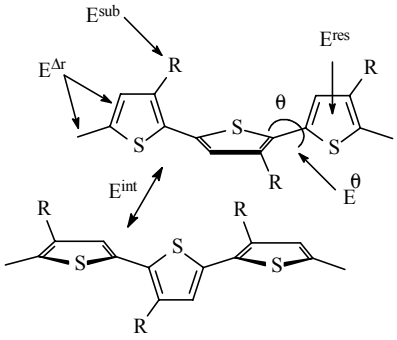

***Figure 1.2**: Parameters determining the band gap*

Kürti *et al.*[13] claimed that the energy gap can be approximated as given in equation (1-2).

$$E_g = E_g^{Peierls} + E_g^{non\text{-}plan} + E_g^{hetero} + E_g^{1\text{-}3,4\ldots} + E_g^{ch\text{-}ch} \qquad (1\text{-}2)$$

This is another way to express the different contributors to the band gap but in fact the two equations mean the same. $E_g^{Peierls}$ is proportional to the average bond length alternation, $E_g^{non\text{-}plan}$ depends on the planarity of the polymer (cf. E^{θ}), E_g^{hetero} describes the effect of heteroatoms (which indirectly determine the resonance energy), $E_g^{1\text{-}3,4\ldots}$ arises from the second and higher neighbour interactions and $E_g^{ch\text{-}ch}$ describes the effect of interchain interactions.

The band gap mainly depends on $E^{\Delta r}$. This contribution is related to the difference between single and double bond lengths. The bond length alternation (Δr) is defined as the maximum difference between the length of a C-C bond inclined relative to the chain axis and a C-C bond parallel to the chain axis[14]. An aromatic and a quinoid geometry can be distinguished for all polyaromatics. In the aromatic structure of PT for example, the thiophene rings are connected by single bonds whereas in the quinoid geometry the inter-ring bond is a double bond. (Figure 1.3) For the aromatic geometry Δr is negative and tends to be more and more positive as the quinoid contribution to the geometry increases. In most cases the quinoid form has a smaller band gap[15]. In figure 1.3 the decrease in band gap for

poly(thiophene) (PT) is shown as the contribution of the aromatic mesomeric form decreases[14].

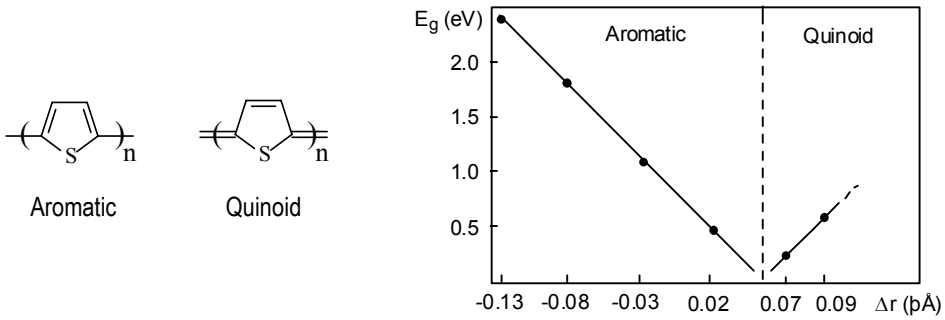

***Figure 1.3**: The band gap (E_g) of PT as a function of Δr*

By means of theoretical studies, J. L. Brédas calculated the band gap of some polyaromatics. He found that the calculated E_g for aromatic PT is 2 eV, a value that approaches the experimental value very well, and for quinoid PT is 0.47 eV[16]. Most polyaromatics, including PT, have a non-degenerate ground state which means that the two alternative geometries, aromatic and quinoid, are not energetically equivalent. For PT, the aromatic form is more stable than the quinoid form and thus preferred.

The second parameter influencing E_g is the departure from planarity. Since the bonds between the aromatic units are essentially single bonds, they allow rotations between the rings. The orbital overlap varies approximately with the cosine of the torsion angle (θ)[17, 18] so that any deviation from coplanarity results in an increase of the band gap. This is visualised in figure 1.4 where the band gap of PT is plotted as a function of the torsion angle.

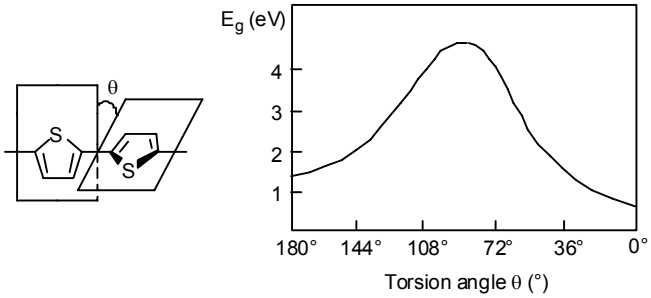

***Figure 1.4**: The band gap of PT as a function of the torsion angle θ*

A decrease of interring twisting -and thus a reduction of the band gap- was demonstrated with the synthesis of regioregular poly(3-alkylthiophenes) (P3ATs or P3RThs). Since the discovery of insoluble PT and the determination of its electroconductivity in 1980[19, 20], many studies have been completed to improve its processability. A breakthrough was accomplished in 1985 when poly(3-alkylthiophene) was synthesised as a soluble, processable and stable polymer[21-23]. Several different synthetic methods for polymer synthesis were developed including electrochemical polymerisation[24], oxidative polymerisation[25-27] and polymerisation by catalysed dedihalogenation of 2,5-dihalo-3-alkylthiophene, such as nickel-catalyzed coupling of thiophene Grignard reagents[22, 23] or dihalothiophene monomers[28]. Irregularly substituted PTs have structures where unfavourable head-to-head couplings cause a sterically driven twist of thiophene rings, resulting in a loss of conjugation. Therefore, the challenge to develop a method which would yield regioregular P3ATs remained. In the early nineties this goal was achieved by different research groups[29] and it was proven that these highly regioregular polymers with long side chains tend to organise themselves in regularly ordered planar structures. The dense packing of these polymers in the solid state therefore decreased the band gap[30, 31].

The third factor influencing the band gap is the aromatic resonance energy. In 1971, B. A. Hess and L. J. Schaad reported on a new method of predicting aromaticity[32] and extended this approach to a variety of aromatic systems in the subsequent years[33-35]. By comparing these calculated resonance energy per electron (REPE) values of the monomer with the values of the band gap of the polymer[36], one can conclude that the band gap decreases when the REPE value of the corresponding monomer is decreasing. For example: REPE (benzene) = 0.065 and E_g (PPP) = 3 eV, REPE (pyrrole) = 0.039 and E_g (PPy) = 2.5 eV, REPE (thiophene) = 0.032 and E_g (PT) = 2 eV, etc. This trend however is limited by the chemical stability of the monomer. Furan with an REPE of 0.007 has a lower stability than benzene and pyrrole which can be an explanation for the high band gap of PF (2.3 eV).

Introducing substituents can modify both the HOMO and LUMO levels of a π–electron system and thus affect the band gap. When grafting an electron donating group, especially the HOMO will be increased; lowering the oxidation potential of the polymer (it is easier to withdraw electrons from the HOMO). With an electron accepting group especially the LUMO is decreased and as a result the reduction potential is lowered (it is easier to put

electrons in the LUMO and the imported electron is better stabilised). Consequently, substituting can not only guarantee the solubility of a polymer but also will lower its band gap.

The last determining aspects of the band gap are possible interchain interactions between single polymers in the solid state. Due to interchain interactions the macroscopic functional properties in the solid phase can differ significantly from the intrinsic properties of conjugated polymer chains in solution. Whereas $\pi-\pi$ interchain interactions between π-conjugated polymer chains are generally detrimental for luminescence efficiencies, they are beneficial for charge carrier mobilities. This can be illustrated with poly(3-alkylthiophene)s[37-39]. The regioirregular P3RThs form essentially amorphous films with no supramolecular order and have low charge carrier mobilities ($\leq 10^{-5}$ cm^2 $V^{-1}s^{-1}$). The regioregular P3RThs form microcrystalline domains in which the polymer chains self-organise into lamella structures with two-dimensional conjugated sheets formed by interchain stacking. The mobilities inside these ordered domains are significantly higher (0.01-0.1 cm^2 $V^{-1}s^{-1}$) and the regioregular polymers exhibit a band gap of 1.7 eV which is 0.4 eV lower than of the regiorandom polymer. The $\pi-\pi$ interactions between two different regioregular poly(3-alkylthiophene-2,5-diyl) (P3RTh) strains are visualised in figure 1.5. As mentioned before, a decrease in E_g in thin films can be attributed to these interactions which will contribute to the adaptation of a more planar structure.

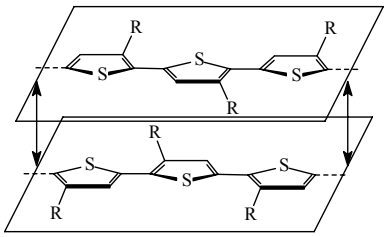

***Figure 1.5**: $\pi-\pi$ interactions in P3RTh*

These five different parameters are evidently often related to each other: the substitution of an alkyl group on each thiophene unit in PT not only lowers E^{sub} but will also affect the interring twisting (E^{θ}) due to interchain interactions (E^{int}) in the solid state.

1.3.2 Determination of the band gap

To deduce the value of E_g, several techniques can be applied. Predictions of the band gap can be made by theoretical calculations. A method that has been widely used to predict the band structure of conjugated polymers is the valence effective Hamiltonian (VEH) pseudo potential technique[40]. The, in this way calculated, band gaps have usually been in good agreement with experimental data. The experimental determination can be performed either by electrochemistry (cyclic voltammetry (CV)), ultraviolet-visible (UV-Vis) spectroscopy or conductivity measurements.

The relationship of optical and electrochemical parameters is shown schematically in figure 1.6[41].

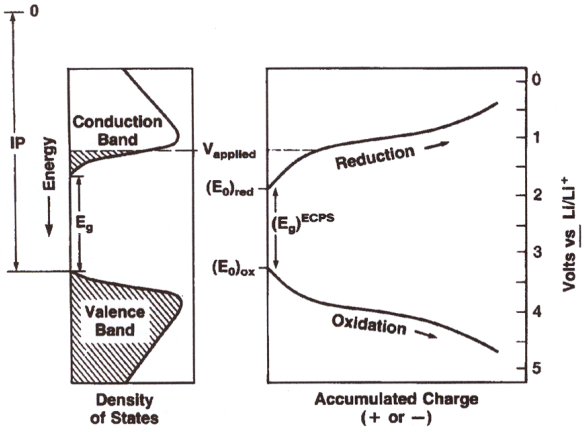

***Figure 1.6**: Relationship between electrochemically measured onset potentials and the band gap*

On the left-hand side of figure 1.6, the density of states of the valence and conduction band is drawn. On the right-hand side, the potentials for a reduction or oxidation cycle as a function of accumulated charge are shown. In the case of the oxidation process no charges will be removed from the polymer electrode until the applied voltage reaches an onset value which corresponds to the highest occupied states in the valence band. The onset voltage of the reduction cycle corresponds to the lowest unoccupied states in the conduction band. So one can say that the band gap is proportional to the difference between the start of the oxidation (E_0^{ox}) and the start of reduction (E_0^{red})[11] and that the value of these two energies can be derived from the waves obtained in the CV

measurements. The electrolyte system, of course, has to allow one to perform both reduction and oxidation in the same system.

To determine E_g from a UV-Vis spectrum (figure 1.7), the tangent on the low energetic side of the absorption spectrum is drawn. The intersection of this tangent and the abscissa gives a value for the band gap.

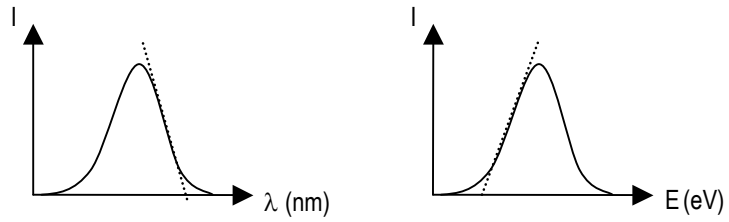

***Figure 1.7**: Determination of the band gap from a UV-Vis spectrum*

Normally, in a UV-Vis spectrum, the absorbance is plotted as a function of the wavelength. To make the conversion of nanometre to electronvolt, one can use the equation of Planck (equation 1-3).

$$E = h\nu = hc/\lambda \qquad (1\text{-}3)$$

In this equation, E is the energy (in J), h is the Planck constant (6.626 10^{-34} Js), c is the speed of light (3 10^8 ms^{-1}), ν is the frequency (in s^{-1} or Hz) and λ is the wavelength (in m). Knowing that 1 eV equals 1.602 10^{-19} J, calculations can be made for the conversion leading to the simple conversion equation (1-4).

$$E\ (eV) = 1240{,}8/\lambda\ (nm) \qquad (1\text{-}4)$$

A third method derives the band gap from the evolution of the conductivity in function of the temperature. For inorganic materials, the conductivity is related to the band gap by an Arrhenius-like equation ($\sigma = \sigma_0.e^{-Ea/kT}$) where sigma is the conductivity, k is the Boltzmann constant (1.381 JK^{-1}) and two times the activation energy (E_a) equals the band gap[42]. However it has been found that this is not a good method to determine the E_g of polymers[43]. Since in this dissertation we will thus not make use of this method, it will not be further discussed.

1.3.3 Approaches towards low band gap materials

Ever since the first low band gap material, poly(isothianaphthene) (PITN), was synthesised in 1984 by Wudl *et al.*[44], scientists were eager to synthesise more of these small band gap polymers. A problem however in the synthesis of conjugated polymers is the insolubility of conjugated polymers due to their very rigid backbone. In order to obtain processable polymers, we have to make them soluble. Two possible solutions are within reach. First, we can make the polymer soluble by introducing long and flexible side chains on the conjugated structure. Secondly, one can use precursor routes to circumvent the problem of insolubility. Here, first a soluble, non-conjugated precursor polymer is synthesised that can easily be processed. After processing this polymer, the precursor can be converted to the fully conjugated polymer by a simple (e.g. thermal) elimination of a small molecule. Today, four different precursor routes are known (scheme 1.1): the dehalogenation or Gilch precursor route[45], the sulphonium or Wessling-Zimmerman precursor route[46, 47], the xanthate precursor route[48] and the sulphinyl precursor route[49-51]. Initially they all were focussed on the synthesis of PPV and were later -if possible- adopted to deal with the synthesis of other poly(heteroarylene vinylenes). These four routes differ by their polymerisation conditions (base, solvent, reaction temperature and reaction time), leaving group (L) and eliminable group (P).

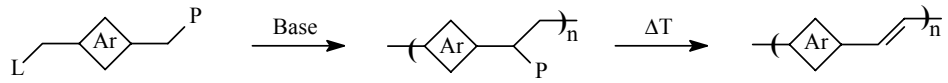

***Scheme 1.1**: Precursor routes towards poly(arylene vinylene)s: Wessling-Zimmerman: L = P = $\oplus SR_2$; Gilch: L = P = Cl; Xanthate: L = P = SC(S)OR; Sulphinyl: L = Cl, P = S(O)R*

The main difference between polymers synthesised via either the side chain approach or the precursor approach, is their solubility in the conjugated form. The precursor approach allows synthesis of conjugated polymers without side chains but as a result, these polymers are not soluble after elimination. Only on the precursor stage these polymers are soluble and thus can be processed.

Very comprehensive reviews on low band gap materials have been published by Tour[52], Roncali[11], Kaeriyama[53], Scherf[54] and Pomerantz[10]. It would be impossible to discuss all the classes of LBG materials. For that reason, the history of certain polymers

(PITN and its derivatives and PTV and its derivatives) will be presented more in detail in the introduction of chapter two and three.

1.4 Applications

Since the report of Bourroughes in 1990 on the EL from PPV[6], the research into the use of organic π-conjugated polymers as the active semiconductor in light-emitting diodes has advanced rapidly. About four years ago, a pilot line for the commercial production of polymer light-emitting diodes (PLEDs) has been realised[55]. Low band gap materials, however, do not have their (possible) emission in the visible area but in the IR area of the electromagnetic spectrum and they have low fluorescence efficiencies. For this reason mostly broad band gap polymers are used in this type of device and LBG polymers are applicable in devices where luminescence is not important. Although they can be potentially useful for the fabrication of LEDs operating in the IR[56], this device will not be discussed in detail. Conjugated polymers have also been proven to be useful as active layer in chemical and biochemical sensors. Also here a large number of this type of sensors has already been tested. In a gas sensor for example, the electrical resistance changes when a specific volatile is present. Different molecules between the polymer chains can change the number or the mobility of the charge carriers in a different way so that each sensor has its own response to a certain gas or odour.

Today, the number of possible applications of conductive polymers seems unlimited. They are being developed for corrosion inhibitors, antistatic coatings, electromagnetic shielding, compact capacitors, batteries, organic lasers,… Since this dissertation will focus on the development of new low band gap materials with possible application in organic field-effect transistors or in solar cells, only these devices will be discussed in detail. Thus, all materials discussed in the next chapters were designed with an eye to further testing in such device structures.

1.4.1 Photovoltaic (solar cell) device

The strong interest nowadays in research towards organic solar cells is driven by the necessity to reduce the production cost of solar cells in order to have a viable alternative for energy production. The low cost can be realised thanks to, on the one hand the small

amounts of material needed and on the other hand the relative ease by which large scale production techniques potentially can be introduced. Even a rather low efficiency (5%) would be good enough to compete with classical silicon-based (inorganic) solar cells. The fact that polymers are thin and flexible of course opens a whole range of possibilities.

In 1998, the first conference devoted to organic solar cells was held in France[57]. Here three types of organic solar cells were discussed: the sensitisation solar cells or dye-sensitised solar cells of which the Grätzel cell[58, 59] is the best known, the molecular organic solar cells and the polymer organic solar cells. The third type of organic solar cell is the youngest and its research field grows rapidly. It is this type of photovoltaic device we will use to test our new synthesised materials. From this viewpoint low band gap materials are excellent candidates for photovoltaic applications since the optical absorption of this class of conjugated materials covers most of the solar spectrum. The photovoltaic effect involves the production of electrons and holes under illumination, and their subsequent collection at the opposite electrodes[60, 61]. Thus, photovoltaic cells are devices, which transform radiation energy into electricity and in this respect they can be considered as inverse to LEDs. The photophysics of a polymeric photovoltaic cell device is based on an extremely fast electron transfer from light absorbing (donor-type) semiconducting conjugated polymers to embedded fullerene (C_{60}) molecules or acceptor-type conjugated polymers (e.g. CN-PPV). After this electron transfer, the charges are transported to the electrodes: the electrons via hopping through the fullerene network and the holes are carried by the conjugated polymer. Time-resolved spectroscopic studies have shown that the photoinduced electron transfer in donor-acceptor (D-A) mixtures of conjugated polymers and methanofullerenes occurs on a time scale of about 45 fs[62]. Since this is several orders of magnitude faster than the radiative and non-radiative decay of photoexcitations, the quantum efficiency for charge transfer and charge separation is close to unity. The electron transfer is also reversible but the back electron transfer is many orders of magnitude slower than the photoinduced forward electron transfer. Hence, polymer photovoltaic cells are considered to be promising devices for solar energy production. However, the conversion efficiency in π-conjugated polymer/fullerene solar cells, is limited[63, 64]. Efficient charge separation occurs only at the D-A interface: photoexcitations created far from the D-A junction recombine before diffusing to the heterojunction. Even if charges are separated at the D-A interface, the efficiency is limited by the low carrier collection efficiency. To overcome this limitation, an

interpenetrating donor/acceptor network approach has been suggested[60, 63, 65]. In such a single composite photoactive film, where donors and acceptors are blended, a "bulk heterojunction" is formed between the electron donors and acceptors. Significant improvement of the power conversion efficiency of the photovoltaic cells is achieved in this way compared to the photovoltaic cell device in which a fullerene layer is introduced between the anode and the polymer layer. These two device constructions are presented in figure 1.8[9]. The main difference between a device with a bulk heterojunction and a device with a linear heterojunction of two organic thin films is the effective interaction area between the donor and acceptor components. In the first it is dispersed over the entire volume of the composite layer, in the second it is the geometrical interface.

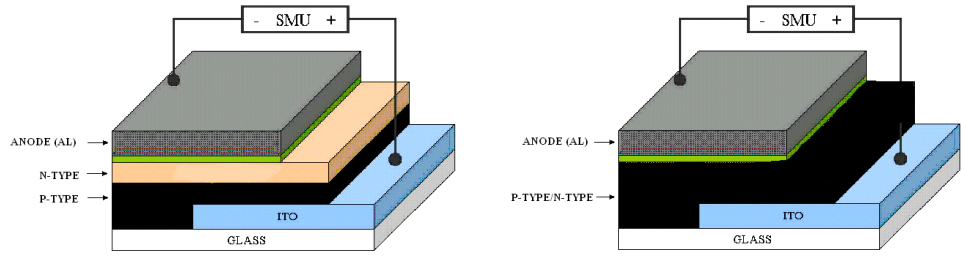

(a) bilayer *(b) composite*

***Figure 1.8**: Device construction of an organic photovoltaic cell*

Nowadays, strategies to achieve higher efficiencies are explored by looking at a whole range of different aspects. Physicists look further into the device construction and the optimalisation of the film morphology. To improve the energy conversion efficiency of a device, the absorption of light, the charge carrier generation and the selective transport and collection of charges at the electrodes have to be optimised. A challenge to chemists is the synthesis of new and better materials. In this respect, low band gap materials are promising since they may improve the efficiency by increasing the absorption in the visible and near infrared region of the solar spectrum[66]. Reports however on such low band gap systems are scarce[9, 66-68] and various aspects need to be considered when designing new low band gap polymers for photovoltaic applications. After all, a drawback of reducing the band gap is the decrease of the open circuit voltage (V_{oc}) of the device. As a consequence the optimum band gap of a photovoltaic device is at 1.35 eV[69] or, as other theoretical calculations

indicate, at 1.4 to 1.5 eV[70]. In our design of a low band gap polymer for application in bulk heterojunction photovoltaic cells we aim at a band gap in the 1.3-1.7 eV region, as this seems a reasonable compromise at the moment of optical absorption and expected open circuit voltage. First conjugated polymeric photovoltaic devices showed efficiencies below 0.05%[71]. However major increases in efficiency are obtained since. In 2001, Saraciftci *et al.* reported an efficiency of more than 2.5%[72], a year ago an efficiency of nearly 3%[73] was reached and in the beginning of this year photovoltaic devices with an efficiency of around 3.5% were produced[74]. This only indicates the progress made in this research field and the potential for further improvement.

1.4.2 Organic Field-Effect Transistor (OFET)

The principle of the field-effect transistor (FET) was first proposed by Lilienfeld in 1930[75]. Essentially, a FET operates as a capacitor where one plate is a conducting channel between the source and drain electrodes. The density of charge carriers in the channel is modulated by the voltage applied to the second plate of the capacitor, the gate electrode. Thus with no voltage between the source and the gate electrodes the FET is in its insulating state. By application of a voltage between these electrodes, the device can be switched to the conducting state, which results in the creation of charge carriers. Three types of FETs can be distinguished[76]: a metal-insulator-semiconductor FET (MISFET), a metal-semi-conductor (MESFET) and a thin film transistor (TFT). Organic field-effect transistors were fist described in 1986 by Koezuka and co-workers[77, 78]. The conjugated polymer that was used was PT and the transistor yielded a carrier mobility of about 10^{-5} cm^2 $V^{-1}s^{-1}$. In this paragraph, only the architecture of the OTFTs will be discussed. Already a lot of reviews concerning these OTFT have been published[76, 79-88] and for a detailed description of the used materials, designs and applications we would like to refer to them. In figure 1.9 two common device configurations used in OTFTs are shown[86]. In the top-contact device (a), the source and drain electrodes are evaporated onto the organic semiconducting layer while in the bottom-contact device (b), the organic semiconductor is deposited onto (prefabricated) source and drain electrodes. Since the majority of organic semiconductors exhibit p-type behaviour, the conductivity is carried by holes. The magnitude of the negative

voltage applied to the gate determines the amount of current flowing between the source and the drain.

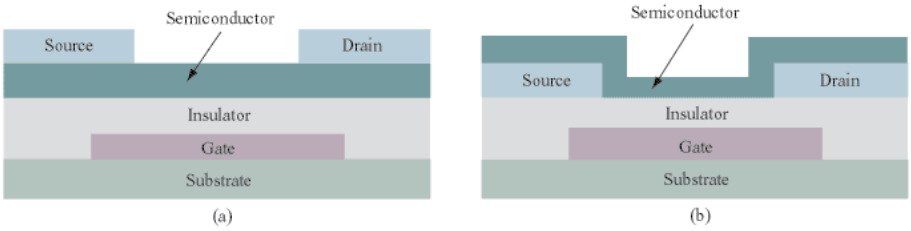

***Figure 1.9**: OTFT device configurations: (a) Top-contact device (b) Bottom-contact device*

The crucial parameter of the application of FETs in electronics is the switching speed, also called modulation or on-off ratio (I_{on}/I_{off}). This is the ratio of the conductivities with the gate voltage switched on and off, respectively. To obtain the high on-off ratios of > 10^6 required in practice, a high mobility of the charge carries (the holes) is required. This is the weakest point of FETs. A high on-off ratio can also be achieved if the pristine semiconductor contains a very small number of charge carriers as shown in equation (1-5). As a consequence, the material needs to be extremely pure. Incomplete purification of the polymers results sometimes in the presence of minute amounts of dopants, which create charge carriers in the polymeric semiconductors. These carriers are undesirable since they increase the conductivity in the OFF-state and consecutively lower the on-off ratio.

$$I_{on}/I_{off} \sim \mu/\sigma \text{ and } \sigma = \mu N e \qquad (1\text{-}5)$$

In this equation, σ is the conductivity, μ the mobility (in $cm^2 V^{-1}s^{-1}$), N the number of charge carries and e the electron charge. The mobility gives a measure of how easily holes (or electrons) drift through the semiconductor in response to an electric field. This field-effect mobility μ_{FE} can be determined from the current-voltage (I-V) characteristics of the transistor with the formula (1-6)[86, 89].

$$I_{ds,sat} = \mu_{FE} C_i (W/2L) (V_{gs} - V_t)^2 \qquad (1\text{-}6)$$

In this formula, W and L are the width and the length of the channel between the source and the drain, C_i is the capacity of the isolating layer, V_{gs} is the gate voltage and V_t is the threshold voltage. By plotting the square root of $I_{ds,sat}$ as a function of V_{gs}, μ_{FE} can be determined from the slope of the straight line and V_t from the extrapolation to the V_{gs} axis.

When looking to the progress in performance of OTFTs from 1986 to the present, one can observe an impressive increase in mobility which was achieved either by improving the processes used to the fabrication of the transistors or by synthesising new organic materials. Thus, also in this field of research, an extended collaboration between physicists and chemists is vital to gain better device performances. These field-effect transistors are promising for use in low-cost applications such as displays, smart cards, electronic (identification) tags, anti-theft markers and sensors.

1.5 Aim and outline of the thesis

The aim of the research that is described in this dissertation is to discover well defined and reliable synthetic pathways towards new low band gap materials which are all based on a thiophene unit. The reason for the need of these well defined pathways is their limited number existing today. In this way we can measure the intrinsic properties of these materials. As mentioned before, a problem in the synthesis of such materials is the processability. Due to their high rigidity, their processability is poor which complicates their use in the introduced devices. In chapter 2 we will overcome this problem by implanting long alkyl chains on the monomer. These groups will increase the solubility of the corresponding polymers. In this chapter, the synthesis and characterisation of substituted poly(isothianaphthene)s is presented. Despite the rather low molecular weights, the material is also tested in a photovoltaic device. Another way to overcome the difficulties in the use of the polymers is to work via a precursor route. Both the sulphinyl as the xanthate precursor route will be used in the synthesis of 3,4-disubstituted poly(2,5-thienylene vinylene) derivatives. The latter only will be used when the sulphinyl route is not an option due to problems in the monomer synthesis. This monomer synthesis as well as the polymerisation is described in chapter 3. Chapter 4 deals with the synthesis of poly(2,5-thienylene vinylene) (PTV) via the xanthate route. Also other xanthate groups -as the conventional *O*-ethyl xanthate- are explored. In chapter 5, a new precursor route is investigated and applied in

the synthesis of PPV and PTV. Here, also the copolymerisation behaviour of these monomers is studied. The synthesis and characterisation of another group of materials is presented in chapter 6. Two different thienyl substituted premonomers towards substituted poly(*p*-phenylene vinylene) are described. Some ideas for future work are presented in chapter 7 and the dissertation is completed with two summaries: one in English, followed by one in Dutch.

1.6 References

1. G. Natta, G. Mazzanti, P. Corraddini, *Atti Accad. Naz. Lincei Rend. Cl. Sci. Fis., Mat. Natur.* **1958**, 25, 3.
2. T. Ito, H. Shirakawa, S. Ikeda, *J. Polym. Sci., Part A: Polym. Chem.* **1974**, 12, 11.
3. H. Shirakawa, S. Ikeda, *J. Polym. Sci., Part A: Polym. Chem.* **1974**, 12, 929.
4. H. Shirakawa, E. J. Louis, A. G. MacDiarmid, C. K. Chiang, A. J. Heeger, *J. Chem. Soc., Chem. Commun.* **1977**, 578.
5. C. K. Chiang, C. R. Fincher, Y. W. Park, A. J. Heeger, H. Shirakawa, E. J. Louis, S. C. Gau, A. G. MacDiarmid, *Phys. Rev. Lett.* **1977**, 39, 1098.
6. J. H. Bourroughes, D. D. C. Bradley, A. R. Brown, R. N. Marks, K. MacKay, R. H. Friend, P. L. Burn, A. B. Holmes, *Nature* **1990**, 347, 539.
7. J. L. Brédas, G. B. Street, *Acc. Chem. Res.* **1985**, 18, 309.
8. K. Kaeriyama, in: H. S. Nalwa, *Handbook of Organic Conductive Molecules and Polymers*, John Wiley & Sons, Chichester, **1997**, 296.
9. C. J. Brabec, N. S. Sariciftci, J. C. Hummelen, *Adv. Funct. Mater.* **2001**, 11, 1, 15.
10. M. Pomerantz, in: T. A. Skotheim, R. L. Elsenbaumer, J. R. Reynolds, *Handbook of Conducting Polymers*, Marcel Dekker, New York, **1998**, 277.
11. J. Roncali, *Chem. Rev.* **1997**, 97, 1, 173.
12. H. A. M. van Mullekom, J. A. J. M. Vekemans, E. E. Havinga, E. W. Meijer, *Materials Science and Engineering* **2001**, 32, 1, 1.
13. J. Kürti, P. R. Surjan, M. Kertesz, G. Frapper, *Synth. Met.* **1992**, 49-50, 537.
14. J. L. Brédas, *Synth. Met.* **1987**, 17, 115.
15. J. L. Brédas, *J. Chem. Phys.* **1985**, 82, 8, 3808.
16. J. L. Brédas, *Mol. Cryst. Liq. Cryst* **1985**, 118, 49.

17. J. L. Brédas, G. B. Street, B. Thémans, J. M. André, *J. Chem. Phys.* **1985**, 83, 1323.
18. R. S. Mulliken, C. A. Rieke, W. G. Brown, *J. Am. Chem. Soc.* **1941**, 63, 41.
19. J. W. P. Lin, L. P. Dudek, *J. Polym. Sci., Polym. Chem. Ed.* **1980**, 18, 9, 2869.
20. T. Yamamoto, K. Sanechika, A. Yamamoto, *J. Polym. Sci., Polym. Lett. Ed.* **1980**, 18, 1, 9.
21. K.-Y. Jen, R. Oboodi, R. L. Elsenbaumer, *Polym. Mater. Sci. Eng.* **1985**, 53, 79.
22. R. L. Elsenbaumer, K.-Y. Jen, R. Oboodi, *Synth. Met.* **1986**, 15, 169.
23. K.-Y. Jen, G. G. Miller, R. L. Elsenbaumer, *J. Chem. Soc., Chem. Commun.* **1986**, 1346.
24. M. Sato, S. Tanaka, K. Kaeriyama, *J. Chem. Soc., Chem. Commun.* **1986**, 873.
25. K. Yoshino, S. Nakajima, M. Onada, R. Sugimoto, *Synth. Met.* **1989**, 28, C349.
26. J.-E. Osterholm, J. Laakso, P. Nyholm, H. Isotalo, H. Stubb, O. Inganäs, W. R. Salaneck, *Synth. Met.* **1989**, 28, C435.
27. R. Sugimoto, S. Takeda, H. B. Gu, K. Yoshino, *Chem. Express* **1986**, 1, 635.
28. T. Yamamoto, A. Morita, Y. Miyazaki, t. Maruyama, H. Wakayama, Z.-H. Zhou, Y. Nakamura, T. Kanbara, S. Sasaki, K. Kubota, *Macromolecules* **1992**, 25, 1214.
29. R. D. McCullough, R. D. Lowe, M. Jayaraman, D. L. Anderson, *J. Org. Chem.* **1993**, 58, 904.
30. R. Österbacka, C. P. An, X. M. Jiang, Z. V. Vardeny, *Science* **2000**, 287, 5454, 839.
31. R. Österbacka, C. P. An, X. M. Jiang, Z. V. Vardeny, *Synth. Met.* **2001**, 116, 1-3, 317.
32. B. A. Hess, L. J. Schaad, *J. Am. Chem. Soc.* **1971**, 93, 2, 305.
33. B. A. Hess, L. J. Schaad, C. W. Holyoke, *Tetrahedron* **1972**, 28, 3657.
34. B. A. Hess, L. J. Schaad, *J. Am. Chem. Soc.* **1973**, 95, 12, 3907.
35. B. A. Hess, L. J. Schaad, C. W. Holyoke, *Tetrahedron* **1975**, 31, 295.
36. E. M. Conwell, in: H. S. Nalwa, *Handbook of Organic Conductive Molecules and Polymers*, John Wiley & Sons, Chichester, **1997**, 2.
37. T.-A. Chen, X. Wu, R. D. Rieke, *J. Am. Chem. Soc.* **1995**, 117, 1, 233.
38. T. Yamamoto, D. Komarundin, *Polymer Journal* **1997**, 29, 11, 952.
39. Y. Yamamoto, D. Komarudin, M. Arai, B.-L. Lee, H. Suganuma, N. Asakawa, Y. Inoue, K. Kubota, S. Sasaki, T. Fukuda, H. Matsuda, *J. Am. Chem. Soc.* **1998**, 120, 2047.
40. J.-L. Brédas, in: T. A. Skotheim, *Handbook of Conducting Polymers*, Dekker, New York, **1986**, 859.
41. H. Eckhardt, L. W. Shacklette, K.-Y. Jen, R. L. Elsenbaumer, *J. Chem. Phys.* **1989**, 91, 2, 1303.
42. D. F. Shriver, P. W. Atkins, C. H. Langford, *Inorganic chemistry*, 2nd ed., Oxford University Press, Oxford, **1994**, p. 98.

43. J. Manca, internal discussions.
44. F. Wudl, M. Kobayashi, A. J. Heeger, *J. Org. Chem.* **1984**, 49, 18, 3382.
45. H. G. Gilch, W. L. Wheelwright, *J. Polym. Sci.* **1966**, 4, 1337.
46. R. A. Wessling, R. G. Zimmerman, *U.S. Patent No 3401152*, **1968**.
47. R. A. Wessling, *J. Polym. Sci., Polym. Symp.* **1985**, 72, 55.
48. S. Son, A. Dodabalapur, A. J. Lovinger, M. E. Galvin, *Science* **1995**, 269, 376.
49. F. Louwet, D. Vanderzande, J. Gelan, *Synth. Met.* **1992**, 52, 125.
50. F. Louwet, D. Vanderzande, J. Gelan, *Synth. Met.* **1995**, 69, 509.
51. F. Louwet, D. Vanderzande, J. Gelan, J. Mullens, *Macromolecules* **1995**, 28, 1330.
52. J. M. Tour, *Adv. Mater.* **1994**, 6, 190.
53. K. Kaeriyama, in: H. S. Nalwa, *Handbook of Organic Conductive Molecules and Polymers*, John Wiley & Sons, Chichester, **1997**, 271.
54. U. Scherf, in: T. A. Skotheim, R. L. Elsenbaumer, J. R. Reynolds, *Handbook of Conducting Polymers*, Marcel Dekker, New York, **1998**, 363.
55. H. Huibers, C. T. H. Liedenbaum, R.-J. Visser, *Chemisch2Weekblad* **1999**, 24, 13.
56. D. R. Baigent, P. J. Hamer, R. H. Friend, S. C. Moratti, A. B. Holmes, *Synth. Met.* **1995**, 71, 2175.
57. D. Meissner, *Photon* **1999**.
58. J. Desilvestro, M. Grätzel, L. Kavan, J. Moser, J. Augustynski, *J. Am. Chem. Soc.* **1985**, 107, 2988.
59. T. Gerfin, M. Grätzel, L. Walder, *Prog. Inorg. Chem.* **1997**, 44, 345.
60. J. J. M. Halls, C. A. Walsh, N. C. Greenham, E. A. Marseglia, R. H. Friend, S. C. Moratti, A. B. Holmes, *Nature* **1995**, 376, 498.
61. J.-F. Nierengarten, G. Hadziioannou, N. Armaroli, *Materials Today* **2001**, 4, 2, 16.
62. C. J. Brabec, G. Zerza, G. Cerullo, S. De Silvestri, S. Luzzati, J. C. Hummelen, N. S. Sariciftci, *Chem. Phys. Lett.* **2001**, 340, 232.
63. G. Yu, J. Gao, J. C. Hummelen, F. Wudl, A. J. Heeger, *Science* **1995**, 270, 1789.
64. N. S. Sariciftci, D. Braun, C. Zhang, V. I. Srdanov, A. J. Heeger, G. Stucky, F. Wudl, *Appl. Phys. Lett.* **1993**, 62, 6, 585.
65. N. S. Sariciftci, L. Smilowitz, A. J. Heeger, F. Wudl, *Science* **1992**, 258, 1474.
66. A. Dhanabalan, J. K. J. van Duren, P. A. van Hal, J. L. J. van Dongen, R. A. J. Janssen, *Adv. Funct. Mater.* **2001**, 11, 4, 255.

67. S. E. Shaheen, D. Vangeneugden, R. Kiebooms, D. Vanderzande, T. Fromherz, F. Padinger, C. J. Brabec, N. S. Sariciftci, *Synth. Met.* **2001**, 121, 1583.

68. C. Winder, D. Mühlbacher, H. Neugebauer, N. S. Sariciftci, C. J. Brabec, R. A. J. Janssen, J. C. Hummelen, *Mol. Cryst. Liq. Cryst* **2002**, 385, 93.

69. S. M. Sze, in: *Physics of Semiconductor Devices*, Wiley, New York, **1981**,

70. C. R. M. Grovenor, in: B. Cantor, *Microelectronic Materials*, **1994**, 430.

71. G. Yu, C. Zhang, A. J. Heeger, *Appl. Phys. Lett.* **1994**, 64, 12, 1540.

72. S. E. Shaheen, C. J. Brabec, F. Padinger, T. Fromherz, J. C. Hummelen, N. S. Sariciftci, *Appl. Phys. Lett.* **2001**, 78, 6, 841.

73. T. Munters, T. Martens, L. Goris, V. Vrindts, J. V. Manca, L. Lutsen, P. De Ceuninck, D. Vanderzande, L. De Schepper, J. Gelan, N. S. Sariciftci, C. J. Brabec, *Thin Solid Films* **2002**, 403, 247.

74. F. Padinger, R. S. Rittberger, N. S. Sariciftci, *Adv. Funct. Mater.* **2003**, 13, 1, 85.

75. J. E. Lilienfeld, *U.S. Patent No 1745175*, **1930**.

76. G. Horowitz, *Adv. Mater.* **1998**, 10, 5, 365.

77. A. Tsumura, H. Koezuka, T. Ando, *Appl. Phys. Lett.* **1986**, 49, 1210.

78. H. Koezuka, A. Tsumura, T. Ando, *Synth. Met.* **1987**, 18, 699.

79. G. Horowitz, *Adv. Mater.* **1990**, 2, 287.

80. S. Hotta, K. Waragai, *Adv. Mater.* **1993**, 5, 896.

81. A. J. Lovinger, L. J. Rothberg, *J. Mater. Res.* **1996**, 11, 1581.

82. H. E. Katz, *J. Mater. Chem.* **1997**, 7, 369.

83. A. R. Brown, C. P. Jarrett, D. de Leeuw, M. Matters, *Synth. Met.* **1997**, 88, 37.

84. F. Garnier, *Chem. Phys.* **1998**, 227, 253.

85. H. E. Katz, Z. Bao, *J. Phys. Chem. B* **2000**, 104, 671.

86. C. D. Dimitrakopoulos, D. J. Mascaro, *IBM J. Res. & Dev.* **2001**, 45, 1, 11.

87. H. E. Katz, Z. Bao, S. L. Gilat, *Acc. Chem. Res.* **2001**, 34, 5, 359.

88. A. Kraft, *Chem. Phys. Chem.* **2001**, 2, 163.

89. A. R. Brown, D. M. de Leeuw, E. E. Havinga, A. Pomp, *Synth. Met.* **1994**, 68, 1, 65.

Chapter 2
Soluble isothianaphthene based polymers: poly(isothianaphthene) (PITN) and poly(1,3-dithienylisothianaphthene) (PDTI) derivatives

2.1 Poly(isothianaphthene)*

2.1.1 Introduction

As already mentioned in chapter one, poly(isothianaphthene) (PITN) was the first low band gap polymer to be synthesised[1]. Wudl *et al.* obtained the polymer via electrochemical polymerisation of isothianaphthene. The idea of synthesising PITN came with the idea that it would exhibit a higher stability and perhaps a higher conductivity than poly(thiophene) (PT). On explaining the factors that determine the band gap (chapter one), it was already stated that the contribution of the quinoid resonance structure should be increased in order to reduce the band gap of aromatic PT. By fusing a diene in the 3- and 4-positions of PT, and thus creating PITN, this was accomplished. A joint experimental and theoretical study of the structure of PITN[2, 3] showed that PITN has a quinoid structure with a band gap of 1.1 eV, one full electronvolt smaller than that of PT. Nevertheless, the aromatic geometry of PITN was calculated to possess an even lower band gap of 0.6 eV[4]. This can be explained by the model which indicates that on going from PT to PITN, the minimum in bond length alternation has been passed (figure 1.3) and that the quinoid geometry has been stabilised too much.

* Part of this work has been published in *J. Polym. Sci.: Part A: Polym. Chem.* **2003**, 41, 1034-1045.

Since the discovery of PITN, many papers have appeared which describe the synthesis with a variety of chemical and electrochemical methods. The different routes that are presently known are presented in scheme 2.1.

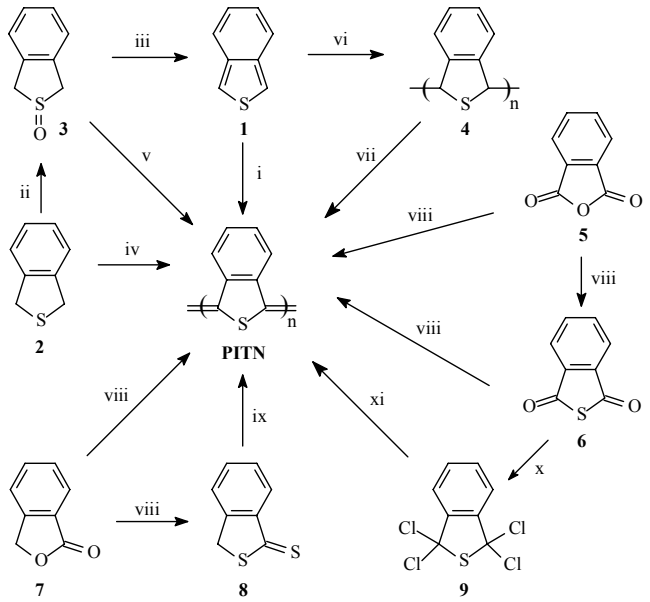

Scheme 2.1*: Different synthetic routes towards PITN:*
i) electrochemical polymerisation or H_2SO_4; ii) $NaIO_4$ or H_2O_2; iii) Al_2O_3; iv) $FeCl_3$, O_2 or NCS; v) H_2SO_4 or NCS; vi) electrochemical polymerisation or CH_3SO_3H; vii) SO_2Cl_2, $SOCl_2$, NCS or electrochemical oxidation; viii) P_4S_{10}; ix) ΔT; x) PCl_5; xi) tBuSH/CF_3COOH or NaSC(S)OEt

Several groups reported on the synthesis of PITN, based on the electrochemical polymerisation of isothianaphthene **1**[1, 5-9]. Isothianaphthene **1** was prepared in two steps from 1,3-dihydrobenzo(c)thiophene **2** via 1,3-dihydrobenzo(c)thiophene-2-oxide **3**[10]. Since **1** was unstable, Jen and Elsenbaumer showed an easy route to PITN by chemical oxidation of **2** with iron(III)chloride[11]. The conversion of **2** into PITN could also be performed with O_2 or with *N*-chlorosuccinimide (NCS)[3]. The polymerisation of **3** with sulphuric acid and the dehydrogenation of the precursor poly(1,3-dihydroisothianaphthene) **4** with sulphuryl chloride (SO_2Cl_2)[12] or thionyl chloride vapour ($SOCl_2$)[13] are the last possibilities in the list of the "classical pathways" towards PITN. These routes however are difficult and too expensive to perform on an industrial scale. In the last decade, there has been performed extensive work in our research group on the development of a straightforward chemical

polymerisation route towards PITN, in which various isothianaphthene derivatives were utilised[14-17]. In 1991 it was found that it is possible to treat phthalic anhydride **5** or phthalide **7** with phosphorus pentasulphide (P_4S_{10}) to obtain PITN in one step in a reasonable yield[14]. Mechanistic studies were performed and based on the observed intermediates; it was proposed that both reactions occurred by a sequence of thionation, isomerisation, and polymerisation reactions[15]. The first step is a substitution reaction in which a carbonyl (C=O) is converted to a thiocarbonyl (C=S) functionality. Recently, also the polymerisation of dithiophthalide **8** and 1,1,3,3-tetrachlorothiophthalan **9** towards PITN were described[17].

Already since halfway the eighties, low band gap conjugated polymers have aroused extensive interest because of their peculiar behaviour and properties which are quite different from those of "classical" broad band gap conjugated polymers. Still, at the moment, few reports are available that lead to good processable materials, which would open possibilities for thorough characterisation. PITN fulfils all expectations of a low band gap polymer (highly conductive, transparent after doping) but has the disadvantage of being insoluble and thus not processable. A possible answer to this problem is the synthesis of substituted analogues of isothianaphthene as new monomer precursors to soluble PITN[18-27]. Few substituted PITNs have been described to date. (Figure 2.1) This is probably due to the perceived difficulty in synthesising suitable monomers.

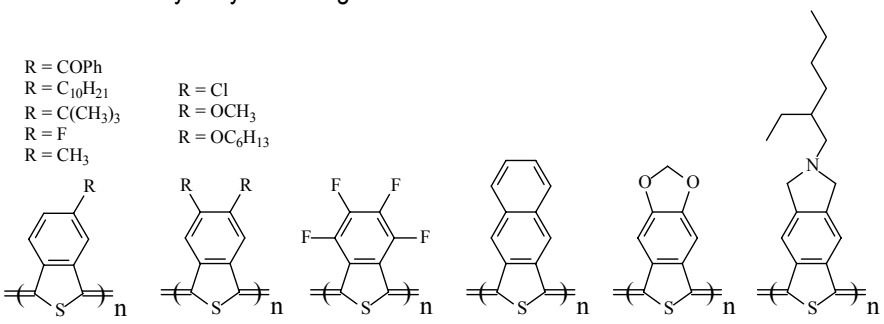

***Figure 2.1**: Substituted PITNs described in literature*

Introduction of substituents will not only increase the solubility but at the same time will influence the ionisation potential or the electron affinity. Theoretical calculations indicate that when alkyl chains are grafted onto the 5- and/or 6-position, the influence on the band gap is in general rather low[28, 29]. Another possibility to introduce processability of PITN consists of the synthesis of processable precursor polymers which may be converted to

PITN in a simple way. Recently, such a stable and soluble precursor was obtained by cationic, low temperature polymerisation of 2-thioalkylisothianaphthene[30].

In the following paragraphs, a convenient and new procedure towards the synthesis of dithiophthalides substituted by alkyloxy and thioalkyl groups is presented. Also, the thermal and non-oxidative polymerisation of these monomers towards poly(5,6-dioctyloxyisothianaphthene) and poly(5,6-dithiooctylisothianaphthene) is discussed.

2.1.2 Monomer synthesis

It has been demonstrated previously that dithiophthalides are excellent precursor monomers towards PITN[17]. (Scheme 2.1) Consequently a search for new synthetic routes towards substituted dithiophthalides seemed to be absolutely needed. In scheme 2.2 an overview of the full monomer synthesis is presented.

Starting from 4,5-dichlorophthalic acid **10**, the carboxylic groups were protected by esterification with ethanol. A nucleophilic substitution with thiooctyl anions generated from sodium thiooctalate was performed. Although for this type of reaction, dimethylformamide (DMF) or dioxane is usually used as a solvent, we found that a toluene/*N*-methylpyrrolidone (NMP) solution in a 20:1 ratio assured the effective reaction course[31]. As the preparation of the thiol salt, either with sodium metal or a sodium hydride suspension, always generates noticeable quantities of disulphides, a twofold stoichiometric excess of thiol was used to support a sufficient concentration of the octylthiolate. After heating at 120°C, the desired diethyl 4,5-dithiooctylphthalate **12** was purified by column chromatography. To obtain the respective 4,5-dialkyloxylated diester **17**, we adapted a synthetic method for phthalocyanines that was published by Drager and O'Brien[32]. The commercially available 2,3-butadione **13** was first converted into 2,3-bis(trimethylsilyloxy)butadiene **14**[33], which then underwent a Diels-Alder condensation with dimethyl acetylenedicarboxylate to give the adequate cyclohexanedione **15**. The latter was then aromatised by the reaction with bromine; next, the obtained catechol (4,5-dihydroxyphthalic acid dimethyl ester **16**) gave **17** in a Williamson ether synthesis with 1-octylbromide.

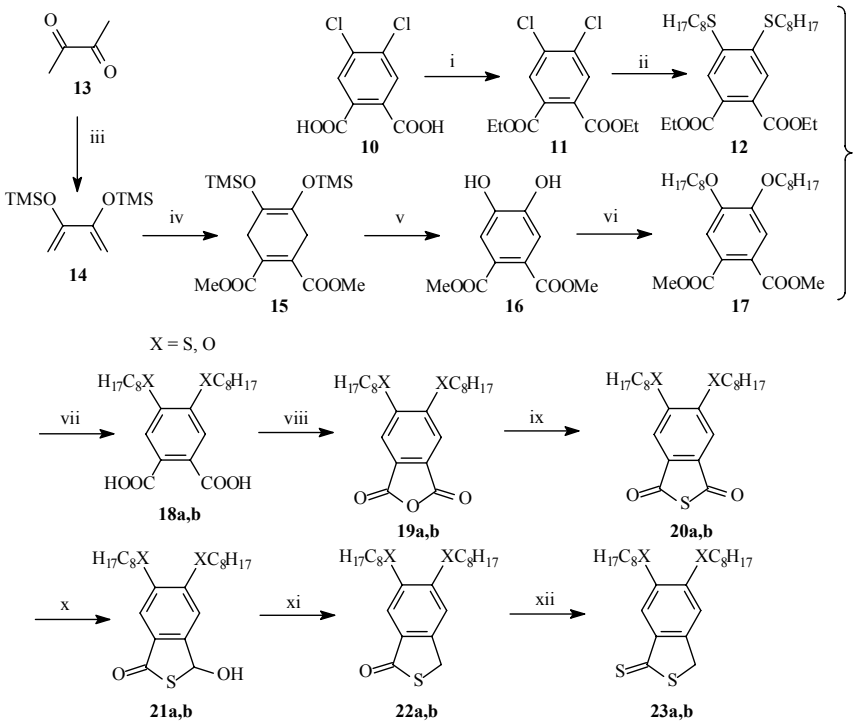

***Scheme 2.2**: Synthesis of 5,6-dithiooctyl- and 5,6-dioctyloxythiophthalides **23a,b**:*
i) EtOH, toluene, H_2SO_4 cat., reflux; ii) $C_8H_{17}SNa$, toluene-NMP (20/1), 120°C, 20 h; iii) TMSCl, LiBr/Et_3N; iv) dimethyl acetylenedicarboxylate, DA; v) Br_2/CCl_4; vi) $C_8H_{17}Br$, K_2CO_3, acetone, reflux, 48 h; vii) KOH, MeOH, 40°C, 12 h; viii) Ac_2O, 120°C, 2 h; ix) $Na_2S.4H_2O$, CH_2Cl_2, 40°C; x) $NaBH_4$, THF, -5°C; xi) AcOH/HI 57% aq. soln., 120°C, 2 h; xii) P_4S_{10}, $NaHCO_3$, CH_2Cl_2, 40°C, 40 h

Both the intermediate 4,5-dithioalkyldiester **12** and 4,5-dialkyloxydiester **17** were then hydrolysed in a 20% methanolic solution of KOH, and this was followed by the acidification of the resultant salts with diluted HCl[34]. After extraction, diacids 4,5-dithiooctylphthalic acid **18a** and 4,5-dioctyloxyphthalic acid **18b** were obtained in almost quantitative yields. These last two compounds were dehydrated via heating with Ac_2O to form the respective anhydrides 5,6-dithiooctylphthalic anhydride **19a** and 5,6-dioctyloxyphthalic anhydride **19b**[35]. The next step was the conversion of the anhydrides to their corresponding thio analogues, 5,6-dithiooctylphtalic thioanhydride **20a** and 5,6-dioctyloxyphtalic thioanhydride **20b**, by a reaction with sodium disulphide. After the use of commercially available sodium sulphide nonahydrate, which only yielded about 20% of the desired thioanhydride, the efficiency could be substantially improved by drying the nonahydrate by means of an azeotropic distillation with toluene. The obtained orange sodium disulphide tetrahydrate

seemed to be a better reagent, and **20a** was obtained in a yield of 75%; **20b** was obtained in a moderate yield of 43%.

Recently, dr. I. Polec in our group developed an efficient procedure for a 2-step reduction reaction, to convert thioanhydrides to 2-thiophthalides[36]. Regarding the generality of this process, we applied it also here. After a low-temperature reduction of thioanhydrides with sodium borohydride, the respective 5,6-disubstituted 3-hydroxylated intermediates 5,6-dithiooctyl-3-hydroxy-2-thiophthalide **21a** and 5,6-dioctyloxy-3-hydroxy-2-thiophthalide **21b** were synthesised with a yield of 90%. The reduction with AcOH/HI led to the corresponding 2-thiophthalides, 5,6-dithiooctyl-2-thiophthalide **22a** and 5,6-dioctyloxy-2-thiophthalide **22b**. The effectiveness and high selectivity of this transformation were in good agreement with our previous experiences. The expected dithiophthalides 5,6-dithiooctyldithiophthalide **23a** and 5,6-dioctyloxydithiophthalide **23b** were finally obtained in the thionation reaction performed in the presence of P_4S_{10}.

2.1.3 Polymerisation

The thermal polymerisation of **23a** was performed at 155-160°C in a 0.4 M *o*-xylene solution and in the presence of a catalytical amount of *p*-toluenesulphonic acid (*p*-TsOH). (Scheme 2.3) After treatment with methanol (MeOH) and removal of the solvent, a Soxhlet extraction of **24a** with acetone gave an oligomer fraction (15%, M_w = 1167, PD = 1.05) and a "polymer fraction" (73%, M_w = 6667, PD = 2.26)†. The polymer had a very good solubility in chloroform, chlorobenzene and other commonly used organic solvents.

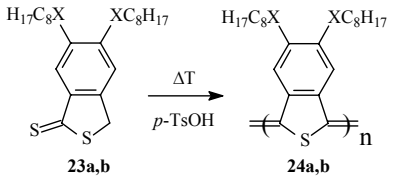

***Scheme 2.3**: Polymerisation of dithiophthalides **23a,b** (X = S (a), O (b))*

† M_w (weight-average molecular weight) and M_n (number-average molecular weight) were obtained via GPC (gel permeation chromatrography) with DMF as the eluent. The polydispersity was calculated from PD = M_w/M_n

Monomer **23b** was polymerised in a 0.4 M *o*-xylene solution at 155-160°C, with a trace of *p*-TsOH as a catalyst (15 mol%). Poly(5,6-dioctyloxyisothianapthene) **24b** with a molecular weight of 5918 (PD = 2.35) was obtained as a black, shinny material after treatment with MeOH. The degree of polymerisation (DP = 14) was very similar to this obtained for **23a**.

2.1.4 Characterisation of monomers and polymers by NMR spectroscopy (T_1 determination)

When the ^{1}H NMR spectra of polymers **24a** and **24b** were recorded, the aromatic resonances were not clearly visible. Therefore the spin-lattice relaxation times (T_1) were determined. The knowledge of these relaxation times is indispensable to acquire a quantitative spectrum since in that case a preparation delay of five times the longest T_1 relaxation decay time has to be respected between consecutive pulses in order to let the magnetisation return to equilibrium.

Under normal circumstances, two relaxation processes of proton nuclei are possible: spin-spin relaxation and spin-lattice relaxation. Two factors mainly determine the spin-lattice relaxation time: i) the environment i.e. the number of protons: the more protons are present, the faster the relaxation can occur and ii) the mobility: the more mobile the chain segment, the longer the relaxation time. The same is true for the relaxation of carbon nuclei. In chapter six, T_{1C} values of all the carbons in the synthesised monomer are presented. The T_1 decay times of all proton (or carbon) resonances of a material can be determined by means of an inversion recovery experiment. Here a series of ^{1}H NMR spectra were recorded using the pulse sequence shown in figure 2.2[37].

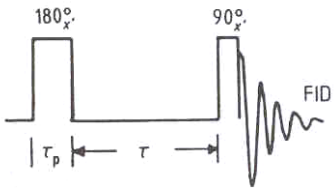

***Figure 2.2**: Pulse sequence for determining the spin-lattice relaxation time T_1*

After the 180° pulse, M_0 lies along the (-z) direction. (Figure 2.3) During the variable time τ the system relaxes with the rate constant $k = T_1^{-1}$ (the spin-lattice relaxation is a first-order process). When $\tau = 0$, $M_z \sim - M_0$, but M_z tends to be more and more less negative when τ becomes longer. The situation in which $M_z = 0$, is important for the quantitative measurement of T_1 and here $\tau = \tau_{zero}$. For greater values of τ, M_z again becomes positive and gets more and more positive until the system has finally returned to the equilibrium value $M_z = M_0$.

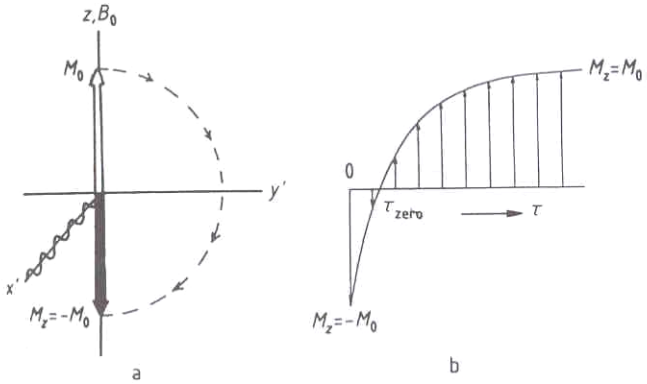

***Figure 2.3**: Evolution of the magnetisation M_z with time τ after a 180° pulse*

In view of the fact that M_0 and M_z are not directly measurable quantities, the magnetisation component M_z is rotated into the direction of the y'-axis by a 90° pulse in the second phase of the pulse sequence after the delay τ. In this way a transverse magnetization component $M_{y'}$ is given which can be observed. The intensities I of the NMR signals obtained after the Fourier transformation are proportional to the components $M_{y'}$. The spin-lattice relaxation process can therefore be described by equation (2-1) from which T_1 can be calculated.

$$I = I_0 (1 - 2 \exp(-\tau/T_1)) \qquad (2\text{-}1)$$

The T_1 decay times of all proton resonances of the side chain of the polymers **24a** and **24b**, determined through an inversion recovery experiment, are listed in table 2.1 and 2.2. Since the longest T_1 decay times are of the order of 1.1 sec, preparation delay times of at least 5.5 sec (a total acquisition time of 42 minutes for 460 repetitions) are needed.

Hydrogen atom	δ (ppm)	T_{1H} (sec)
-C**H**$_2$S-	3.11	0.29
-C**H**$_2$CH$_2$S-	1.74	0.37
CH$_3$(C**H**$_2$)$_5$CH$_2$CH$_2$S-	1.23	0.73
C**H**$_3$-	0.86	1.12

Table 2.1**: T_{1H} values of the side chains of **24a

Hydrogen atom	δ (ppm)	T_{1H} (sec)
-C**H**$_2$O-	4.08	0.31
-C**H**$_2$CH$_2$O-	1.87	0.25
CH$_3$(C**H**$_2$)$_5$CH$_2$CH$_2$O-	1.27	0.64
C**H**$_3$-	0.87	1.01

Table 2.2**: T_{1H} values of the side chains of **24b

The ^{1}H NMR spectra of monomer **23a** and polymer **24a** are presented in figure 2.4. For **23a**, the aromatic protons *4* and *7* are assigned to the resonances around 7.9 and 7.3 ppm (overlap with residual $CHCl_3$ line) respectively. The benzylic protons in the 3-position appear at 4.4 ppm. The methylene groups directly connected to the sulphur in the thiooctyl chain appear at 4.4 ppm. The other methylene and methyl resonances of the side chain are situated between 0.7 and 1.9 ppm. In the polymer fraction, one can notice the absence of the signal at 4.4 ppm. Because we are dealing with a rather rigid polymer system and the molecular mobility is correlated with the spin-spin relaxation time (T_2), a short T_2 value will lead to broad NMR signals. The protons of the rigid aromatic rings are so broad that they even become difficult to detect: a broad band with superimposed sharp peaks is observed. The latter can be assigned to the aromatic protons of oligomers whereas the broad line arises from higher molecular weight chains. The methylene groups directly connected to the sulphur in the thiooctyl chain appear in the region 3.4 – 2.8 ppm.

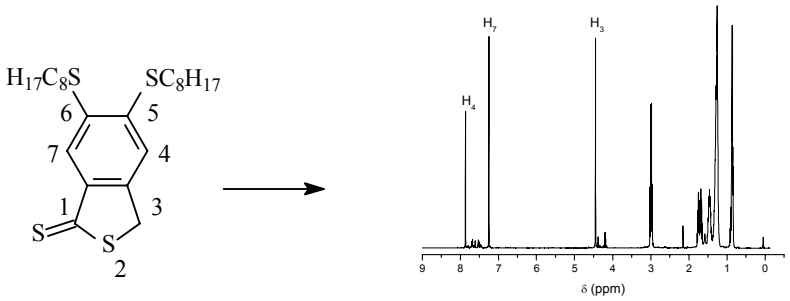

Figure 2.4a**: ^{1}H NMR spectrum of **23a

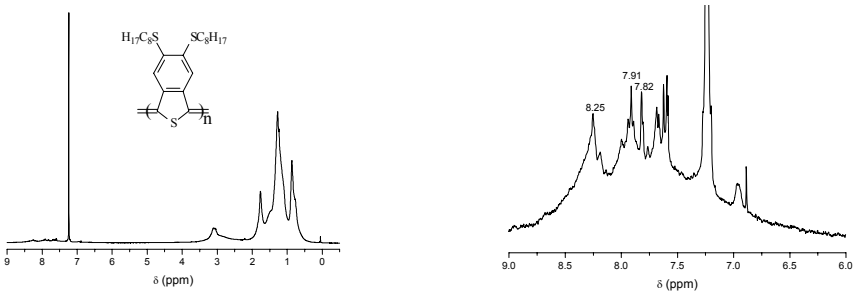

***Figure 2.4b**: [1]H NMR spectrum of **24a** (the spectrum at the right shows the aromatic region blown up approximately 35 times)*

The [1]H NMR spectrum of polymer **24b** is very similar compared to the spectrum of polymer **24a**: the benzylic protons, in the 3-position of monomer **23b** (at 4.4 ppm), also disappear in the spectrum of the polymer. Also in this spectrum, it becomes difficult to detect the signals of the aromatic protons, and a broad band with superimposed sharp peaks is observed. The broad peak in the region 4.2-3.9 ppm is consistent with the protons of the methylene group next to the oxygen.

2.1.5 UV-Vis spectroscopy and cyclic voltammetry (CV)

A further spectroscopic study through UV-Vis spectroscopy was performed on the polymers **24a** and **24b**. As already mentioned in chapter one, the band gap can be estimated in this way. The two soluble PITN derivatives were also investigated via CV which implies another way to determine the optical gap of the material. The results of both analyses are presented in this paragraph.

UV-Vis spectroscopy:

Films of the polymers were prepared via spin-coating from a chloroform solution (1.5 wt%) on a quartz disc at 1000 rpm (rotations per minute). For **24a**, the polymer absorption shows two broad features peaking around 3.8 eV or 329 nm and 1.7 eV or 710 nm, the latter is corresponding to the $\pi \rightarrow \pi^*$ transition. (Figure 2.5) From the low-frequency onset (dotted line) of this absorption, a band gap of approximately 1.2 eV was estimated. Exactly the same could be seen for compound **24b**: also here a band gap of approximately 1.2 eV was deduced from the spectrum.

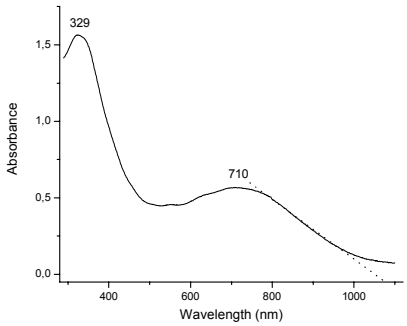

Figure 2.5**: UV-Vis spectrum of **24a

Cyclic voltammetry:

CV was applied to investigate the redox behaviour of the polymers and to estimate the HOMO and LUMO energy levels. Figure 2.6 shows the traces of the n-doping and p-doping processes for each polymer. Both presented stable p-doping (oxidation) upon cycling, whereas n-doping (reduction) proved to be less stable. The anodic peak was exhibited at about 0.80 V for **24a** with a corresponding cathodic peak at 0.65 V. The anodic peak was not clearly observed for **24b** and the re-reduction (p-dedoping) was located at 0.74 V. In the reduction curve, no peak was clearly defined, but two re-oxidative peaks were revealed at - 0.96 V and - 0.83 V for **24a**, and - 0.99 V and - 0.80 V for **24b**.

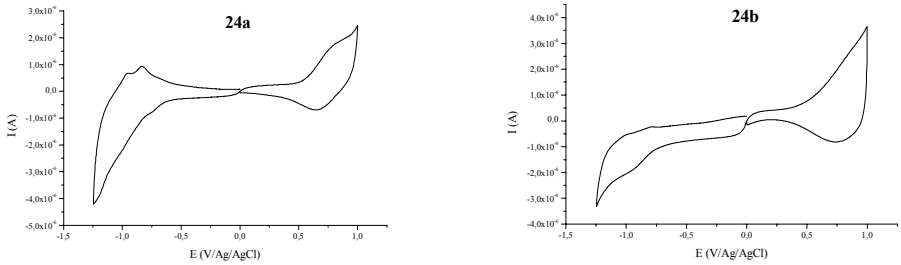

***Figure 2.6**: Cyclic voltammograms of the polymer films of **24a** and **24b**, drop-casted on Pt in an electrolytic solution of Bu_4NClO_4 (0.1 M) in CH_3CN at a scan rate of 50 mV s^{-1}*

The energy values of LUMO and HOMO were estimated from the onset potentials of both n- and p-doping and were calculated under the premise that the energy level of

ferrocene/ferrocenium is 4.8 eV below the vacuum level[38, 39]. The onset potentials were determined from the intersection of the two tangents drawn at the rising current and baseline charging current of the CV traces. The correlation can be expressed as follows: E_{LUMO} = - (4.8 + E_{onset}^{red}) eV and E_{HOMO} = - (4.8 + E_{onset}^{ox}) eV. The onset potentials in reduction and in oxidation were determined, respectively, at - 0.64 and 0.52 V for **24a** and at - 0.72 and 0.50 V for **24b** versus Ag/AgCl, corresponding to - 1.07 and 0.09 V for **24a** and - 1.15 and 0.07 V for **24b** versus F_c/F_c^+ ($E°'$ F_c/F_c^+ = 0.43 V vs. Ag/AgCl). Therefore, the LUMO and HOMO levels as well as the electrochemical band gap (E_g^{el}) can be estimated. The redox data and the energy levels are listed in table 2.3. The band gaps obtained here are in good agreement with the ones derived from UV-Vis measurements.

Polymer	E_{onset}^{ox} (V)	E_{onset}^{red} (V)	E_{HOMO} (eV)	E_{LUMO} (eV)	E_g^{el} (eV)
24a	0.52	-0.64	4.89	3.73	1.16
24b	0.50	-0.72	4.87	3.65	1.22

Table 2.3**: Electrochemical characteristics of polymer **24a** and **24b

2.1.6 Exploratory measurements for applications in organic solar cells

As stated in chapter one, low band gap polymers are interesting materials for their application in plastic photovoltaic cells. To obtain more insight into the nature of the species generated upon illumination, photoinduced absorption (PIA) measurements were performed by Ludwig Goris at the Johannes Kepler University in Linz, Austria. Such photophysical measurements can provide essential information about the possibility to implement a certain material in organic solar cells. PIA spectroscopy in the visible and near-infrared regions on polymer **24a** revealed the existence of charged excitations upon illumination[40, 41].

Photovoltaic studies on solar cell devices with **24b** as electron donor and (6,6)-phenyl-C_{61}-butyric-acid or 1-(3-(methoxycarbonyl)propyl)-1-phenyl[6,6]C_{61} ([6,6]-PCBM) as electron acceptor (figure 2.7) were performed by Wim Geens at IMEC in Leuven. The motivation for the use of [6,6]-PCBM instead of plain C_{60} is its improved solubility. This methanofullerene derivative was first synthesised by J.C. Hummelen *et al.* in order to improve the photoinduced electron transfer efficiency[42].

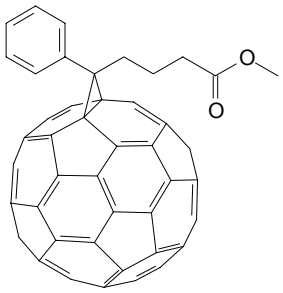

***Figure 2.7**: [6,6]-PCBM*

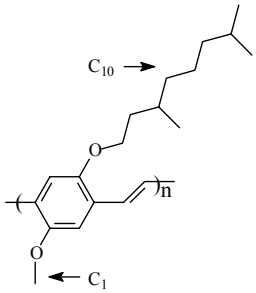

***Figure 2.8**: OC_1C_{10}-PPV*

Devices were made from a (1:4) blend of the polymer and the C_{60} derivative and from a (1:1:8) blend of the polymer, OC_1C_{10}-PPV (figure 2.8) and [6,6]-PCBM. The alkoxy substituted PPV derivative, OC_1C_{10}-PPV or MDMO-PPV (poly(2-methoxy-5-(3',7'-dimethyloctyloxy)-1,4-phenylene vinylene)), was used here since it shows a great performance in various devices. The compounds were dissolved in chlorobenzene in a concentration of 1% (w:v%) and stirred overnight. After the films were spin-coated, the gold top contacts were deposited. (Figure 2.9)

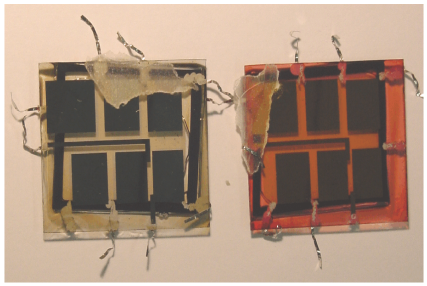

***Figure 2.9**: Solar cell device of poly(5,6-dioctyloxyisothianapthene): PCBM (1:4) (left) and poly(5,6-dioctyloxyisothianapthene):OC_1C_{10}-PPV:PCBM (1:1:8) (right)*

Photovoltaic studies on solar cell devices with **24a** and [6,6]-PCBM were also performed by Ludwig Goris in the group of professor N.S. Sariciftci in Linz. Solar cells, constructed with the pristine material and a (1:1) mixture with PCBM as active layer, showed a photovoltaic effect. However, adding the strong electron acceptor PCBM clearly improved the diode behaviour[40].

Drawing the current-voltage (I/V) curve of a cell in the dark and under illumination (P_{in} = 100 mW/cm^2), permits an evaluation of most of its photovoltaic performances as well as its electric behaviour[43]. The short circuit current I_{sc} is the current which crosses the cell at zero

applied voltage and the open circuit voltage V_{oc} is measured when current in the cell is zero. The fill factor FF is the ratio of the maximum power P_{max} or P_{out} delivered by the cell to the external short and open circuit values ($FF = P_{max}/V_{oc} \times I_{sc} = V_{max} \times I_{max}/V_{oc} \times I_{sc}$) and J_{sc} is the short circuit current density. An overview of the measured characteristics of the four different photovoltaic devices is presented in table 2.4. Efficiencies ($\eta = P_{out}/P_{in}$) of 0.0075% and 0.0066% were measured.

Blend	J_{sc} ($\mu A/cm^2$)	I_{sc} (μA)	V_{oc} (mV)	FF (%)	$\eta_{AM1.5}$ (%)
24b (1:4)	45	*	550	30	0.0075
24b (1:1:8)	49	*	550	25	0.0066
24a (pristine)	*	14	350	*	*
24a (1:1)	*	42	200	*	*

***Table 2.4**: Device characteristics, *not determined*

The results do not look very promising (low power conversion efficiencies). The main problem here was the low molecular weight which resulted in lousy films. Thus, if we can find a way to improve the molecular weight, this may lead to better characteristics.

2.2 Poly(1,3-dithienylisothianaphthene)

2.2.1 Introduction

Although progress has been made on the development of a straightforward polymerisation route to PITN, it has not yet found wide application in the development of electronic devices, partly due to the lack of a polymerisation route leading to a processable, high molecular weight material. Therefore, it is also interesting to look for other monomeric isothianaphthene derivatives which can combine the interesting properties of isothianaphthene with the possibility to improve the stability and processability of the resulting polymer. An example of such a monomer is 1,3-di(2-thienyl)isothianaphthene (DTI). In the early nineties four different groups reported on the synthesis of DTI[3, 44-46]. Kiebooms *et al.*[47, 48] revised the synthesis reported in literature and Vangeneugden *et al.*[49-

[51] synthesised soluble DTI derivatives. In scheme 2.4 the optimised synthesis for DTI derivatives towards soluble PDTIs is presented. The implementation of the latter as the active layer in a gas-sensing device[49], in an amperiometric sensor[52] and in photovoltaic devices[53-55], was already successfully tested.

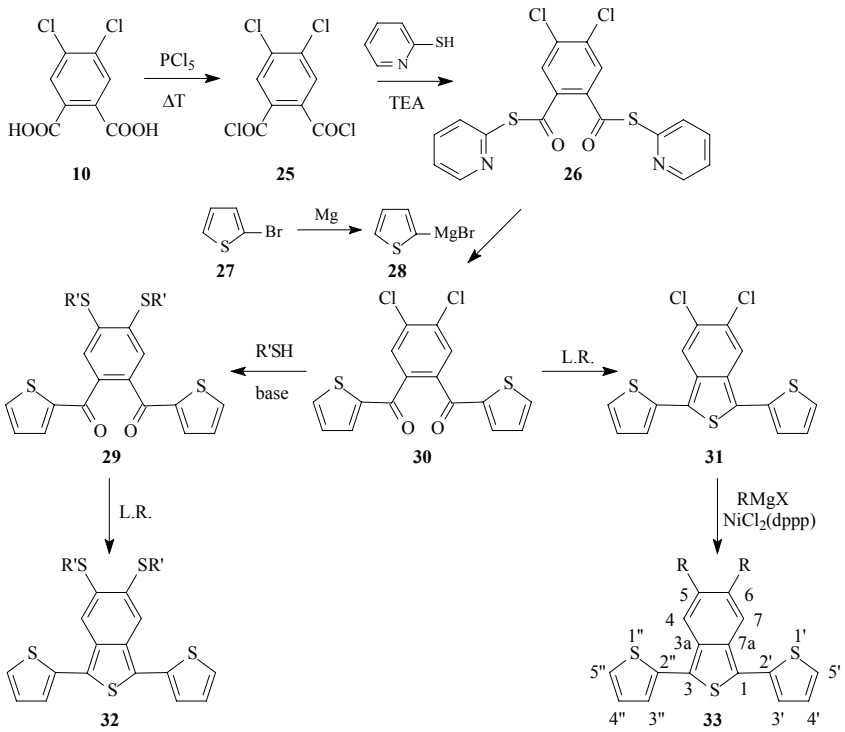

***Scheme 2.4**: Monomer synthesis of 5,6-disubstituted DTIs (R' = C_8H_{17}, $C_{12}H_{25}$; R = C_4H_9, C_8H_{17}, $C_{12}H_{25}$)*

The polymerisation of these monomers leads to "formal" copolymers of bithiophene and isothianaphthene. Detailed optoelectronic studies on the non-substituted polymer provided values of approximately 1.6-1.7 eV for its band gap[44, 46], a value intermediate between that of PITN and PT. For the substituted polymers values between 1.4 and 1.5 eV were found[50]. The polymerisation routes described in literature are electrochemical polymerisations and chemical, oxidative polymerisations of the DTI monomers. However, by applying the oxidative polymerisation with $FeCl_3$, some difficulties were experienced. Not only a large amount of DTI dimer was formed, but also oxidant remained preventing the recording of NMR spectra. Additionally, the traces of iron in the material are unfavourable

for electronic applications. For this reasons it seems better to use a reductive polymerisation route in order to circumvent the problem of the low reactivity of DTI (derivatives) and prevent doping of the material due to the use of $FeCl_3$. It is favourable that the applied reductive coupling does not need high temperatures. The Kumada or Grignard, the Suzuki and the Negishi coupling fulfil this condition[56]. The first is a cross coupling reaction between a Grignard reagent (RMgX) and an organohalide (R'X) and is catalysed by a Ni or Pd complex (e.g. $NiCl_2$(dppe), $NiCl_2$(dppp), $PdCl_2$(dppb) with dppe, dppp and dppb = 1,3-bis(diphenyl-phosphino)ethane, -propane and -butane)). The second is a cross coupling reaction between an organoboron reagent ($RB(OR')_2$) and an unsaturated halide, triflate or sulphonate and is usually catalysed by tetrakis(triphenylphosphine)palladium(0) ($Pd(PPh_3)_4$). Finally, the Negishi coupling is a cross coupling reaction between an organozinc intermediate (RZnX) and an unsaturated halide and is also catalysed by a Ni or Pd complex.

2.2.2 Monomer synthesis

The 5,6-disubstituted DTI derivatives were synthesised as presented in scheme 2.4. However, to polymerise the DTI monomers by means of a reductive coupling, the 5'- and 5''-position had to be functionalised in a proper way. All the suggested reductive polymerisation methods require a dihalide. We therefore attempted the synthesis of 5,6-dichloro-1,3-di(5'-bromothienyl)isothianaphthene **36**. (Scheme 2.5) When 5,6-dichloro-1,3-di(5'-bromo-thienoyl)benzene **35** was synthesised, attempts were made to obtain **36** by mixing the diketon with Lawesson's reagent (L.R.). The main product, however, appeared to be diClDTI **31**. This was in perfect agreement with the previous results for the non-substituted DTI obtained by R. Kiebooms[47]. Since the bromines are removed during the ring closure, another method was tried. It involved the free radical bromination of **31** using *N*-bromosuccinimide (NBS) in a mixture of $CHCl_3$ and acetic acid as a solvent. After extraction, it was almost impossible to purify the mixture of brominated products by means of column chromatography since the R_f values of the products in the reaction mixture (dibrominated DTI **36**, monobromide and starting product) were very similar.

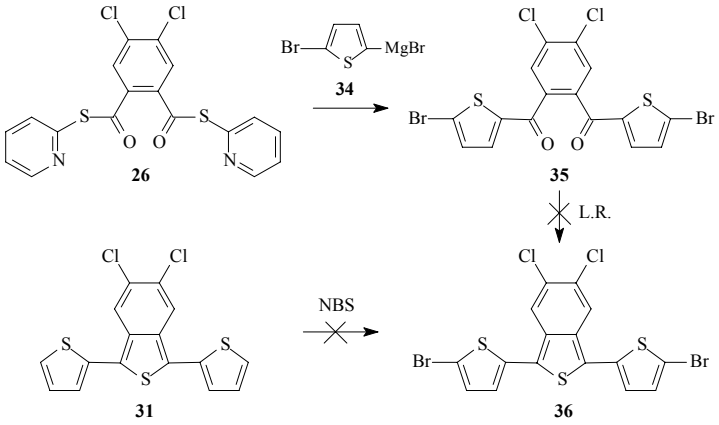

Scheme 2.5**: Synthesis of 1,3-di(5'-bromothienyl)isothianaphthene **36

Another interesting approach was the reductive coupling of difunctionalised thiophenes with DTIs. In this way a "formal" copolymer of trithiophene and isothianaphthene would be obtained. The advantage here is the commercial availability of 2,5-dibromothiophene which implies that compound **36**, the dibromo DTI derivative, does not need to be synthesised anymore. In this way of course another appropriate DTI monomer, functionalised on its 5'- and 5''-positions, had to be synthesised first. In a Grignard and in a Negishi coupling the Grignard reagent and the organozinc compound respectively, are synthesised from the corresponding halide. For this reason, these two couplings were excluded. Hensel *et al.*[57] reported on the synthesis of an organoboron reagent, not only from the corresponding halide, but also from a silyl compound. This opened a way to use a Suzuki coupling of 2,5-dibromothiophene and 5,6-dichloro-1,3-di(thienyl-5'-boronic acid)isothianaphthene. From this viewpoint, we were able to synthesise 5,6-dichloro-1,3-di(5'-trimethylsilylthienoyl)benzene **39**. (Scheme 2.6)

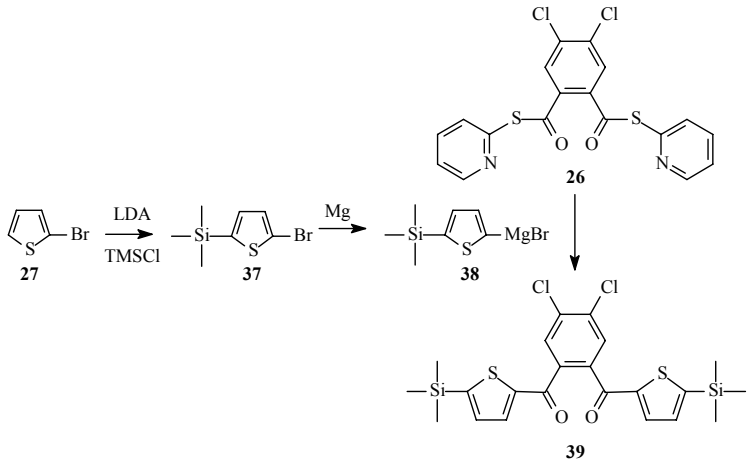

Scheme 2.6**: Synthesis of silyl substituted compound **39

Unfortunately, the same problem occurred as during the bromination reaction: the trimethylsilyl groups were removed totally or partially during ring closure with Lawesson's reagent.

2.3 Conclusion

The interesting properties of PITN have been described in literature ever since it was first synthesised. For the reason that it is infusible and insoluble, substitution of the monomers with suitable side chains seemed appropriate to solve this problem. The synthesis of 5,6-disubstituted dithiophthalides involved a seven- or eight-step procedure in which we made use of a new temperature dependent two-step reduction of a phthalic thioanhydride towards a phthalide. Thermal and non-oxidative polymerisation of these dithiophthalide monomers led to soluble PITN derivatives. As predicted by theoretical calculations, the band gap of the obtained polymers was comparable to the band gap of PITN itself. PIA spectroscopy in the visible and IR regions was performed, and evidence for the existence of charged excitations upon photoinduction was found. Although photovoltaic studies indicated that the power conversion efficiencies were rather low, a clear contribution of the measured photocurrent could be attributed to the polymer. When in the future a method to increase the molecular weight can be found, it is very likely that this will improve the film forming properties and as a result also the device characteristics.

PDTI derivatives could also be of great interest for the development of semiconducting materials. Since some problems occurred with the oxidative polymerisation of the DTI derivatives, the reductive polymerisation was investigated. Here, we experienced difficulties in the synthesis of the functionalised DTI monomers. As a consequence, the reductive polymerisation could not be valorised.

2.4 Experimental part

Materials: All solvents used in the synthesis were distilled before use. Tetrahydrofuran (THF) was refluxed under nitrogen with sodium metal and benzophenone until a blue colour persisted and was then distilled. Compound **10** was purchased from Fluka, and the other commercially available products were purchased from Acros or Aldrich.

Characterisation: ^{1}H NMR spectra were taken on a Varian Inova 300 spectrometer. For all synthesised compounds, ^{1}H NMR spectra were recorded in deuterated chloroform unless otherwise stated; the chemical shift at 7.24 ppm was used as a reference (relative to tetramethylsilane (TMS)).

CV was performed with an Autolab PGSTAT 20 potentiostat from Eco Chemie B.V., which was equipped with General Purpose Electrochemical System (GPES) software (version 4.9 for windows), in an electrolytic solution of tetrabutylammonium perchlorate (0.1 M) in acetonitrile, at a scan rate of 50 mV s^{-1}, at room temperature and under pressure of dry nitrogen. A platinum disc (area = 1.6 mm^2) with a thin drop-cast film was used as the working electrode, and a platinum wire was used as the counter electrode. All potentials were relative to the Ag/AgCl reference electrode.

The molecular weights and molecular weight distributions were determined relative to polystyrene standards (Polymer Labs) by Size Exclusion Chromatography (SEC). Chromatograms were recorded on a Spectra series P100 (Spectra Physics) equipped with two Mixed-B columns (10 µm, 2 x 30 cm, Polymer Labs) and a refractive index (RI) detector (Shodex) at 70°C. A DMF solution of oxalic acid (1.1 10^{-3} M) was used as the eluent at a flow rate of 1.0 mL/min. Toluene was used as a flow-rate marker.

Gas chromatography/mass spectrometry (GC/MS) analyses were carried out with TSQ – 70 and Voyager mass spectrometers (Thermoquest); the capillary column was a Chrompack Cpsil5CB or Cpsil8CB. Melting points (uncorrected) were measured with a

digital melting-point apparatus (Electrothermal IA 9000 series). Thin-layer chromatography (TLC) analyses were made on Merck aluminium sheets (20 x 20 cm) covered with silica gel 60 F_{254}.

Diethyl 4,5-dichlorophthalate (11)

To a suspension of 23.5 g (100 mmol) of 4,5-dichlorophthalic acid **10**, stirred in 150 mL of toluene, 50 mL of ethanol (1 mol, 46 g) and approximately 2 mL of concentrated H_2SO_4 were added. The mixture was kept under reflux, and an azeotrope of toluene/H_2O was collected in a Dean - Stark apparatus. After 6 hours, the reaction was completed. The obtained solution was washed with 100 mL of water, 100 mL of $NaHCO_3$ (5%) and again with 100 mL of water, dried over $MgSO_4$, and filtered. The filtrate was concentrated in the rotavapor, and the obtained diester was crystallised from hexane. The product (27.6 g) was obtained as white crystals (95% yield). Mp: 62-63°C; R_f = 0.41 (hexane/EtOAc, 9/1, v/v); ^{1}H NMR ($CDCl_3$): 7.77 (s, 2H, aromatic), 4.30 (2q, J = 7.2 Hz, 4H, aliphatic), 1.31 (2t, J = 7.2 Hz, 6H, aliphatic)

Diethyl 4,5- dithiooctylophthalate (12)

NaH (4.8 g, 120 mmol; 60% dispersion in mineral oil) was suspended in 200 mL of dry toluene. Then, 23.2 g (160 mmol) of 1-octanethiol, dissolved in 100 mL of dry toluene was carefully dropped into a stirred suspension of NaH. The liberation of H_2 was observed. During the addition, the mixture was not allowed to reach a temperature higher than 35–40°C. When the addition of the thiol was finished, the mixture was heated to 50°C, and this was followed by a one-portion addition of 14.5 g (50 mmol) of diethyl 4,5-dichlorophthalate **11**. The temperature was increased to 80°C and 10 mL of NMP was added. The temperature was again increased up to 120°C, and the reaction mixture was stirred for 20 hours. Then, at room temperature, it was transferred to a separating funnel, 200 mL of EtOAc and 200 mL of H_2O were added and an extraction was made. The organic layer was dried over $MgSO_4$ and filtered, and the solvents were evaporated. After column chromatography was performed on silica gel (eluent: hexane/EtOAc, in gradient, v/v) 20.95 g of the product was obtained as a yellow oil (yield: 82%). R_f = 0.43 (hexane/EtOAc, 9/1, v/v); ^{1}H NMR ($CDCl_3$): 7.46 (s, 2H, aromatic), 4.28 (2q, J = 7.2 Hz, 4H), 2.91 (2t, J = 7.2 Hz,

4H), 1.62 (2qu, J = 7.2 Hz, 4H), 1.37-1.45 (m, 4H), 1.30 (2t, J = 7.2 Hz, 6H), 1.22-1.28 (m, 16H), 0.81 (2t, J = 7.2 Hz, 6H); GC/MS: 510 (M^+), 398 (100), 286; 240, 213, 57, 43

4,5-Dithiooctylphthalic acid (18a)

Diethyl 4,5-dithiooctylphthalate **12** (25.95 g, 50.9 mmol) was stirred at a temperature of 40-45°C in a KOH/MeOH solution (KOH (16.8 g, 300 mmol) dissolved in 250 mL of MeOH). After 2 hours, the reaction was completed, methanol was evaporated, and the residue was dissolved in 300 mL of H_2O; this was followed by acidification with 3N HCl to pH~1-2. The acidified mixture was extracted with Et_2O (3 x 200 mL). The organic layers were dried over $MgSO_4$ and filtered, the solvent was evaporated, and the residue was precipitated from hexane. The pure acid (22.0 g) was obtained as white crystals (95% yield). Mp: 79.8-81.2°C; R_f = 0.67 (EtOAc/MeOH, 85/15, v/v); ^{1}H NMR (deuterated acetone): 7.97 (s, 2H, aromatic), 3.41 (2t, J = 7.2 Hz, 4H), 2.38-2.40 (m, 2H, 2 – O**H**), 2.01 (qu, J = 7.2 Hz, 4H), 1.62-1.88 (m, 20H), 1.18-1.22 (2t, J = 6.8 Hz, 6H); DIP MS: 455 (M^+ + 1), 345 (100), 329, 261, 217, 114, 95

5,6-Dithiooctylphthalic anhydride (19a)

4,5-Dithiooctylphthalic acid **18a** (22.0 g, 48.5 mmol) was refluxed for 1 hour in 20 mL of acetic anhydride. The reaction mixture was then cooled to room temperature, and 50 mL of hexane was added; this was followed by cooling to 0°C. The liquid layer was filtered off, and the solid residue was dried in air. The anhydride (19.95 g) was obtained as white crystals (94% yield). Mp 73.8-74.2°C; R_f = 0.45 (hexane/EtOAc, 95/5, v/v); ^{1}H NMR ($CDCl_3$): 7.61(s, 2H, aromatic), 3.03 (2t, J = 7.6 Hz, 4H), 1.71 (2qu, J = 7.6 Hz, 4H), 1.52-1.25 (m, 20 H), 0.84 (2t, J = 7.6 Hz, 6H); GC/MS: 436 (M^+), 324, 212 (100), 71, 57, 43

5,6-Dithiooctylphtalic thioanhydride (20a)

5,6-Dithiooctylphthalic anhydride **19a** (19.95 g, 45.6 mmol) was dissolved in a mixture of 100 mL of hexane and 100 mL of dichloromethane and was added to 16.0 g of $Na_2S.{\sim}4H_2O$, obtained from the azeotropic removal of water from 25.6 g (110 mmol) of $Na_2S.9H_2O$. This two-phase reaction mixture was stirred at room temperature for 60 hours (pH~7-8). Then, it was acidified with a 10% HCl aqueous solution to pH~1–2. Dichloromethane was distilled off. To the rest, 100 mL of H_2O was added, and the mixture was extracted with EtOAc (3 x

150 mL). Organic layers were separated, dried over $MgSO_4$, filtered and the solvents were evaporated. After flash column chromatography on silica gel (eluent: hexane/EtOAc, in gradient, v/v), 15.4 g (75% yield) of pure thioanhydride was obtained as a yellow solid. Mp: 47.4-48.3°C; R_f = 0.60 (hexane/EtOAc, 95/5, v/v); ^{1}H NMR ($CDCl_3$): 7.55 (s, 2H, aromatic), 3.02 (2t, J = 7.5 Hz, 4H), 1.20-1.79 (m, 24H), 0.83-0.88 (m, 6H); GC/MS: 452 (M^+), 340, 228 (100), 168, 71, 57, 43

5,6-Dithiooctyl-3-hydroxy-2-thiophthalide (21a)

$NaBH_4$ powder (98%, 1.42 g, 37.6 mmol) was suspended (under an atmosphere of N_2) in 100 mL of dry THF, and cooled to -20°C (NaCl - ice-bath). Then, 17.0 g (37.6 mmol) of 5,6-dithiooctylphthalic thioanhydride **20a** in 100 mL of THF was added drop by drop to this suspension. The reaction mixture was then stirred at –5°C, and this was followed by careful acidification with an approximately 5% HCl aqueous solution. The mixture was transferred to a separatory funnel, 100 mL of a saturated NaCl solution was added, and extraction with 100 mL of Et_2O was made. The water layer was additionally extracted with 150 mL of Et_2O. Organic layers were combined, dried over $MgSO_4$, and filtered, and the solvents were distilled. The crude product (16.45 g) was obtained, and crystallisation from hexane/EtOAc (8/2, v/v) gave 15.1 g (88%) of the pure product as a yellow solid. Mp: 47.5-49.3°C; R_f = 0.28 (hexane/EtOAc, 9/1,v/v); ^{1}H NMR ($CDCl_3$): 7.36 (s, 1H, aromatic), 7.34 (s, 1H, aromatic), 6.59 (s, 1H, C**H**OH), 2.86-3.02 (m, 4H), 1.25-1.78 (m, 24H), 0.82-0.87 (m, 6H); DIP MS: 454 (M^+), 340, 228 (100), 168, 97, 84, 57

5,6-Dithiooctyl-2-thiophthalide (22a)

5,6-Dithiooctyl-3-hydroxy-2-thiophthalide **21a** (15.1 g, 33.2 mmol) was added to a solution of 15 mL of AcOH and 5 mL of a 57% HI aqueous solution. The reaction mixture was kept at 120°C for 2 hours. Then, it was cooled to room temperature and poured carefully into 100 mL of 1 N NaOH containing 5 g $NaHSO_3$. The mixture was extracted with 250 mL of Et_2O. The organic layer was additionally washed with a saturated aqueous solution of $NaHCO_3$, for removal of the rest of the acetic acid, and it was then dried over $MgSO_4$ and filtered; the solvent was evaporated. The product (12.4 g, 85% yield) was obtained as a slightly brown solid. Mp: 38.6-39.8°C; R_f = 0.34 (hexane/EtOAc, 9/1, v/v), 0.33 (hexane/chloroform, 7/3, v/v); ^{1}H NMR ($CDCl_3$): 7.57 (s, 1H, aromatic), 7.22 (s, 1H, aromatic), 4.36 (s, 2H, C**H**$_2$ from

thiolactone ring), 2.91-2.98 (m, 4H), 1.24-1.77 (m, 24H) 0.82-0.86 (m, 6H); GC/MS: 438 (M^+), 326, 214 (100), 181, 153, 109, 69, 57; HR MS: calculated 438.20848; found 438.20839

5,6-Dithiooctyldithiophthalide (23a)

5,6-Dithiooctyl-2-thiophthalide **22a** (10.95 g, 25 mmol) was dissolved in 300 mL of dichloromethane. To this stirred solution, 19.05 g (85.8 mmol) P_4S_{10} and 3.6 g (42.9 mmol) $NaHCO_3$ were added. The resulted mixture was kept at 40°C for 40 hours, and this was followed by the addition of a saturated aqueous solution of $NaHCO_3$ to reach pH~6-7. After conventional layer separation, the aqueous layer was additionally extracted with 200 mL of dichloromethane; the organic layers were combined, dried over $MgSO_4$, and filtered; and the solvent was evaporated. The result was 10.4 g of a crude postreaction mixture. The crude product underwent column chromatography on silica gel (eluent: hexane/chloroform, gradient of eluents), and after purification, 4.80 g (42% yield) of the product was obtained as a brown solid. Mp: 47.5-48.5°C; R_f = 0.36 (hexane/EtOAc, 9/1, v/v), 0.44 (hexane/ chloroform, 7/3, v/v); ^{1}H NMR ($CDCl_3$): 7.85 (s, 1H, aromatic), 7.24 (s, 1H, aromatic), 4.45 (s, 2H, thiolactone), 2.96-3.02 (m, 4H), 1.26-1.76 (m, 24H), 0.84-0.90 (m, 6H); GC/MS: 454 (M^+), 421, 341 (100), 309 (100), 230, 198, 167, 121, 69, 55; HR MS: calculated 454.18564; found 454.18557

4,5-Dioctyloxyphthalic acid dimethyl ester (17)

4,5-Dihydroxyphthalic acid dimethyl ester **16**[32] (14.4 g, 64.3 mmol), 43.4 g (225 mmol, 38.9 mL) of octyl bromide and 42.0 g (300 mmol) of K_2CO_3 were refluxed for 48 hours. Then, acetone was evaporated, 500 mL of water was added to the reaction mixture, and this was followed by extraction with Et_2O (3 x 200 mL). The organic layer was dried over $MgSO_4$ and filtered, the solvent was evaporated, and column chromatography was performed (eluent: hexane/EtOAc, in gradient, v/v). This resulted in 23.6 g (82% yield) of the product as a white solid. Mp: 39.3-40.9°C; R_f = 0.44 (hexane/EtOAc, 8/2, v/v); ^{1}H NMR ($CDCl_3$): 7.15 (s, 2H, aromatic), 3.99 (t, 4H, J = 6.9 Hz), 3.85 (s, 6H), 1.76-1.85 (m, 4H), 1.25-1.48 (m, 20 H), 0.83 (m, 6H); GC/MS: 450 (M^+), 419, 338, 307, 226 (100), 195, 71, 57

4,5-Dioctyloxyphthalic acid (18b)

4,5-Dioctyloxyphthalic acid dimethyl ester **17** (30.5 g, 67.8 mmol) was treated with 15.1 g (270 mmol) of KOH dissolved in 300 mL of MeOH. The mixture was stirred at 40°C for 12 hours, the solvent was evaporated, and 200 mL of water was added to the reaction mixture; this was followed by careful acidification with aqueous HCl. Next, an extraction with Et_2O was performed (3 x 200 mL), and after drying over $MgSO_4$, filtration, solvent evaporation, and precipitation from hexane, 27.5 g of the product was obtained as a white solid (96% yield). Mp: 137.1-139.5°C; R_f = 0.44 (EtOAc/MeOH, 85/15, v/v); ^{1}H NMR (acetone deuterated): 7.32 (s, 2H, aromatic), 4.09 (2t, 6H, J = 6.6 Hz), 1.77-1.88 (m, 4H), 1.31-1.58 (m, 20H), 0.86-0.92 (m, 6H); DIP MS: 423 (M^+ + 1) (100), 309

5,6-Dioctyloxyphthalic anhydride (19b)

4,5-Dioctyloxyphthalic acid **18b** (25.0 g, 59.2 mmol) was refluxed with 65 mL of acetic anhydride for 1 hour. After a workup procedure analogous to that described for the 5,6-dithiooctylphthalic anhydride **19a** synthesis, 22.1 g (92% yield) of the product was obtained as a white solid. M.p.: 118.6-119.5°C; R_f = 0.64 (hexane/EtOAc, 8/2, v/v); ^{1}H NMR ($CDCl_3$): 7.28 (s, 2H, aromatic), 4.07 (t, 4H, J = 6.6 Hz), 1.81-1.90 (m, 4H), 1.26-1.51 (m, 20H), 0.84-0.88 (m, 6H); GC/MS: 404 (M^+), 293 (100), 193, 180, 112, 71, 57

5,6-Dioctyloxyphthalic thioanhydride (20b)

5,6-Dioctylphthalic anhydride **19b** (20.2 g, 50.0 mmol) was dissolved in 300 mL of dichloromethane with 12.6 g of $Na_2S.4H_2O$, and kept for 40 hours at 45 – 50°C. After a workup procedure analogous to that described for the 5,6-dithiooctylphthalic thioanhydride **20a** synthesis, 9.0 g of the product was obtained as a yellow solid (43% yield). Mp: 96.3-98.5°C; R_f = 0.69 (hexane/EtOAc, 9/1, v/v); ^{1}H NMR ($CDCl_3$): 7.27 (s, 2H, aromatic), 4.06 (2t, 4H, J = 6.6 Hz), 1.80-1.90 (m, 4H), 1.23-1.51 (m, 20H), 0.84-0.89 (m, 6H); GC/MS: 420 (M^+), 309, 209, 196 (100), 180, 112, 71, 57; HR MS: calculated 420.23343; found 420.23408

5,6-Dioctyloxy-*3*-hydroxy-*2*-thiophthalide (21b)

5,6-Dioctyloxyphthalic thioanhydride **20b** (8.4 g, 20 mmol) was treated with 0.74 g (20 mmol) of $NaBH_4$. The reaction conditions were analogous to those applied for the 5,6-dithiooctylphthalic thioanhydride **20a** reduction. After crystallisation from hexane/EtOAc, 7.8

g of the product was obtained as a slightly yellow solid (92% yield). Mp: 68.5-71.0°C; R_f = 0.37 (hexane/EtOAc, 8/2, v/v); ^{1}H NMR ($CDCl_3$): 6.99 (s, 1H, aromatic) 6.93 (s, 1H, aromatic), 6.49 (s, 1H, C**H**OH, hydroxythiolactone), 3.97-4.04 (m, 2H), 3.88-3.94 (m, 2H), 1.75-1.88 (m, 4H), 1.23-1.45 (m, 20H), 0.84-0.88 (m, 6H); DIP MS: 423 (M^+ + 1), 422, 389, 310, 277, 198 (100), 165, 137, 71, 57, 43; HR MS: calculated 422.24908; found 422.24915

5,6-Dioctyloxy-2-thiophthalide (22b)

5,6-Dioctyloxy-*3*-hydroxy-*2*-thiophthalide **21b** (7.3 g, 17.3 mmol) was treated with a mixture of 9 mL of AcOH and 3.7 mL of a 57% aqueous solution of HI and kept at 120°C for 1 hour. After a workup analogous to that applied for the 5,6-dithiooctyl-*2*-thiophthalide **22a** synthesis, which was followed by column chromatography on silica gel (eluent: hexane/EtOAc, 1/0, 9/1 and 8/2, v/v), 5.95 g of the product was obtained as a slightly yellow solid (84% yield). Mp: 50.5–51.9°C; R_f = 0.67 (hexane/EtOAc, 8/2, v/v); R_f = 0.47 (hexane/$CHCl_3$, 6/4, v/v); ^{1}H NMR ($CDCl_3$): 7.18 (s, 1H, aromatic) 6.89 (s, 1H, aromatic), 4.32 (s, 2H, thiolactone ring), 3.98-4.06 (m, 4H), 1.77-1.90 (m, 4H), 1.26-1.49 (m, 20H), 0.84- 0.88 (m, 6H); GC/MS: 406 (M^+), 294, 195, 182 (100), 154, 71, 57; HR MS: calculated 406.25417; found 406.25422

5,6-Dioctyloxydithiophthalide (23b)

5,6-Dioctyloxy-*2*-thiophthalide **22b** (5.6 g, 13.8 mmol) was dissolved in 75 mL of dichloromethane; 2.3 g (27 mmol) of $NaHCO_3$ and 10.4 g (47 mmol) of P_4S_{10} were then added. The mixture was kept at 40-45°C for 40 hours, and this was followed by the addition of a saturated aqueous solution of $NaHCO_3$ to reach pH~6-7. After a workup analogous to that applied for the 5,6-dithiooctyldithiophthalide **23a**, followed by the purification of the crude product by column chromatography on silica gel (eluent: hexane/$CHCl_3$, in gradient, v/v), 3.1 g of the pure product was obtained as a brown solid (53% yield). Mp: 47.9–49.9°C, R_f = 0.60 (hexane/$CHCl_3$, 6/4, v/v); ^{1}H NMR ($CDCl_3$): 7.41 (s, 1H, aromatic), 6.89 (s, 1H, aromatic), 4.35 (s, 2H, thiolactone), 3.98-4.07 (m, 4H), 1.78-1. 90 (m, 4H), 1.22-1.51 (m, 20 H), 0.83-0.87 (m, 6H); GC/MS: 422 (M^+), 389, 359, 323, 309, 293, 211, 198 (100), 71, 57; HR MS: calculated 422.23133; found 422.23120

Polymerisation of 5,6-dithiooctyldithiophthalide (24a)

5,6-Dithiooctyldithiophthalide **23a** (908 mg, 2 mmol) was dissolved in 5 mL of *o*-xylene, and 57 mg (0.3 mmol) of *p*-TsOH.H_2O was added. The mixture was stirred for 30 hours at a temperature of 155–160°C under an atmosphere of N_2. Then, the mixture was cooled to room temperature, and the solvent was removed under reduced pressure. The black, sticky residue was treated with a MeOH/H_2O solution (200 mL), which was removed; this led to a decanted, sticky solid. As it was still not in the precipitate form, more MeOH (150 mL) was added, and the mixture was refluxed for 1 hour. During this refluxing, the mass agglomerated in one piece. The MeOH solution was removed, and the solid was transferred to a Soxhlet tube. First, an extraction with acetone (24 hours) was performed to collect the lower oligomer fraction (M_w = 1167). After solvent evaporation and drying of the residue in vacuo, 122.6 mg (15%) of this fraction was obtained in the form of a black solid. Then, an extraction with chloroform was performed for the residue left in the Soxhlet tube. This resulted in 611.9 mg (73%) of the polymer fraction after solvent evaporation and precipitation of the residue with methanol (M_w = 6667). ^{1}H NMR ($CDCl_3$): 8.25 (br), 7.92 (br), 7.59 (br), 3.11 (br, 4H), 1.74 (br, 4H), 1.23 (br, 20H), 0.86 (br, 6H)

Polymerisation of 5,6-dioctyloxydithiophthalide (24b)

5,6-Dioctyloxydithiophthalide **23b** (844 mg, 2 mmol) was dissolved in 5 mL of *o*-xylene and 57 mg (0.3 mmol) of *p*-TsOH.H_2O was added. The mixture was stirred for 30 hours at a temperature of 155-160°C under an atmosphere of N_2. Then, the mixture was cooled to room temperature, and the *o*-xylene was removed under reduced pressure. The residue was treated with a MeOH/H_2O solution (200 mL). The black precipitate that was formed, was filtered and transferred into a Soxhlet extraction tube. An extraction for 24 hours with MeOH was performed, followed by a 24-hour extraction with acetone for the removal of lower oligomeric fractions. Both fractions were evaporated and after a period of drying in vacuo, 109.4 mg (14%, M_w = 809) of a methanol-soluble fraction and 134.4 mg (17%, M_w = 6138) of an acetone-soluble fraction were obtained. Finally, the polymer was extracted with chloroform. No precipitation occurred with the addition of methanol to the chloroform solution, so all solvents were evaporated, and the residue was treated only with MeOH. The black precipitate then formed easily. After a period of drying in vacuo, 358.4 mg of this polymer fraction was obtained (46%, M_w = 5918). As the M_w values for the two last fractions

were practically the same, they were combined, and the yield of the polymerisation was estimated as the combined yield of these two (64%). ^{1}H NMR ($CDCl_3$): 7.67 (br), 7.59 (br), 7.53 (br), 4.08 (br, 4H), 1.87 (br, 4H), 1.27 (br, 20H), 0.87 (br, 6H)

The synthesis of compounds **25** to **33** is described elsewhere[50].

2-Bromo-5-trimethylsilylthiophene (37)[58]

2-Bromothiophene **27** (4.0 g, 0.0245 mol) was dissolved in 40 mL of THF and cooled to -78°C. Then, 12.5 mL of a LDA (lithium diisopropylamide) solution (2 M in THF/hexane) was added with a syringe and the mixture was stirred at -78°C for 40 minutes. To this stirred solution, TMSCl (trimethylsilyl chloride) (3.1 g, 0.0287 mol) was added and the mixture was stirred for 12 hours. The mixture was quenched with a saturated aqueous solution of NH_4Cl (20 mL) and extracted with Et_2O (3 x 100 mL). The combined organic layers were washed with water (2 x 100 mL) and brine (1 x 100 mL), and it was then dried over $MgSO_4$ and filtered. The crude product underwent a vacuum distillation which yielded the pure product as a colourless liquid (5.1 g, 89%). ^{1}H NMR ($CDCl_3$): 7.06 (d, 1H, J = 3.6 Hz), 6.96 (d, 1H, J = 3.6 Hz), 0.29 (s, 9H); GC/MS (EI): 234 (M^+), 219 (M^+ - CH_3), 139 (M^+ - CH_3 - Br)

5,6-Dichloro-1,3-di(5'-trimethylsilylthienoyl)benzene (39)

A solution of 2-bromo-5-trimethylsilylthiophene **37** (2.0 g, 8.511 mmol) in 40 mL of THF was added drop by drop to iodine activated Mg (204 mg, 8.511 mmol) in 40 mL of THF. After refluxing for one and a half hours, the obtained Grignard reagent **38** was cooled down and slowly added to a solution of **26** (1.62 g, 3.869 mmol) in 60 mL of THF at 0°C. The mixture was stirred for 30 minutes after which 40 mL of HCl (5%) was added. Extraction with Et_2O (3 x 100 mL) and washing of the combined organic layers with NaOH (10%) was followed with drying over $MgSO_4$. The crude product was further purified by column chromatography (silica, $CHCl_3$) and this gave 1.4 g (71%) of the pure product. ^{1}H NMR ($CDCl_3$): 7.79 (s, 2H), 7.47 (d, 2H, J = 3.6 Hz), 7.17 (d, 2H, J = 3.6 Hz), 0.30 (s, 18H); GC/MS (EI): 510 (M^+), 495 (M^+ - CH_3)

2.5 References

1. F. Wudl, M. Kobayashi, A. J. Heeger, *J. Org. Chem.* **1984**, 49, 18, 3382.
2. I. Hoogmartens, P. Adriaensens, D. Vanderzande, J. Gelan, C. Quattrocchi, R. Lazzaroni, J. L. Brédas, *Macromolecules* **1992**, 25, 26, 7347.
3. I. Hoogmartens, D. Vanderzande, H. Martens, J. Gelan, *Synth. Met.* **1992**, 47, 367.
4. J. L. Brédas, B. Themans, J. M. Andre, *Synth. Met.* **1985**, 11, 343.
5. N. Colaneri, M. Kobayashi, A. J. Heeger, F. Wudl, *Synth. Met.* **1986**, 14, 45.
6. H. Yashima, M. Kobayashi, K.-B. Lee, T. C. Chung, A. J. Heeger, F. Wudl, *J. Electrochem. Soc.* **1987**, 134, 46.
7. P. A. Christensen, J. C. H. Kerr, S. J. Higgins, A. Hamnet, *Faraday Discuss. J. Chem. Soc.* **1989**, 88, 261.
8. S. M. Dale, A. Glide, A. R. Hillman, *J. Mater. Chem.* **1992**, 2, 99.
9. M. Onoda, S. Morita, H. Nakayama, K. Yoshino, *Jpn. J. Appl. Phys.* **1993**, 32, 3534.
10. M. P. Cava, N. M. Pollack, O. A. Mamer, M. J. Mitchell, *J. Org. Chem.* **1971**, 36, 25, 3932.
11. K.-Y. Jen, R. L. Elsenbaumer, *Synth. Met.* **1986**, 16, 379.
12. T. L. Rose, M. C. Liberto, *Synth. Met.* **1989**, 31, 395.
13. F. Wang, A. B. Kon, T. L. Rose, *Synth. Met.* **1997**, 84, 69.
14. R. Van Asselt, I. Hoogmartens, D. Vanderzande, J. Gelan, P. E. Froehling, M. Aussems, O. Aagaard, R. Schellekens, *Synth. Met.* **1995**, 74, 65.
15. R. Van Asselt, D. Vanderzande, J. Gelan, P. E. Froehling, O. Aagaard, *J. Polym. Sci., Part A: Polym. Chem.* **1996**, 34, 8, 1553.
16. H. Paulussen, B. Ottenbourgs, D. Vanderzande, P. Adriaensens, J. Gelan, *Polymer* **1997**, 38, 20, 5221.
17. R. Van Asselt, D. Vanderzande, J. Gelan, P. E. Froehling, O. Aagaard, *Synth. Met.* **2000**, 110, 1, 25.
18. Y. Ikenoue, F. Wudl, A. J. Heeger, *Synth. Met.* **1991**, 40, 1.
19. M. Pomerantz, B. Chaloner-Gill, L. O. Harding, J. J. Tseng, W. J. Pomerantz, *Synth. Met.* **1993**, 55, 2-3, 960.
20. J. S. Burbridge, H. Page, A. Drury, A. P. Davey, J. Callaghan, W. Blau, *J. Mod. Opt.* **1994**, 41, 6, 1217.
21. G. King, S. J. Higgins, *J. Mater. Chem.* **1995**, 5, 3, 447.

22. H. Paulussen, *Ph. D. Dissertation* **1996**, Limburgs Universitair Centrum, Diepenbeek, Belgium.
23. H. Paulussen, D. Vanderzande, J. Gelan, *Synth. Met.* **1997**, 84, 415.
24. A. Drury, S. Burbridge, A. P. Davey, W. J. Blau, *J. Mater. Chem.* **1998**, 8, 11, 2353.
25. T.-S. Hung, S.-A. Chen, *Polymer* **1999**, 40, 3881.
26. H. Meng, Y. Chen, F. Wudl, *Macromolecules* **2001**, 34, 6, 1810.
27. J. Swann, G. Brooke, D. Bloor, *Synth. Met.* **1993**, 55-57, 281.
28. J. L. Brédas, A. J. Heeger, F. Wudl, *J. Chem. Phys.* **1986**, 85, 8, 4673.
29. J. L. Brédas, *Synth. Met.* **1987**, 17, 115.
30. H. Haitjema, D. Vanderzande, J. Gelan, **1998**, Unpublished data, LUC Diepenbeek, Belgium.
31. J. March, *Advanced Organic Chemistry: Reactions, Mechanisms, and Structure*, Wiley-Interscience, New York, **1992**, p. 655.
32. A. S. Drager, D. F. O'Brien, *J. Org. Chem.* **2000**, 65, 7, 2257.
33. L. Hansson, R. Carlson, *Acta Chem. Scand.* **1989**, 43, 304.
34. L. Van Hijfte, R. D. Little, J. L. Petersen, K. D. Moeller, *J. Org. Chem.* **1987**, 52, 21, 4647.
35. B. S. Furniss, A. J. Hannaford, P. W. G. Smith, A. R. Tatchell, *Vogel's Textbook of Practical Organic Chemistry*, 5th ed., Longman: New York, **1989**, p. 1074.
36. I. Polec, L. Lutsen, D. Vanderzande, J. Gelan, *Eur. J. Org. Chem.* **2002**, 1033.
37. H. Friebolin, *Basic One- and Two-Dimensional NMR Spectroscopy*, Weinheim, **1991**, p. 149.
38. J. Pommerehne, H. Vestweber, W. Guss, R. F. Mahrt, H. Bässler, M. Porsch, J. Daub, *Adv. Mater.* **1995**, 7, 6, 551.
39. Y. Liu, S. M. Liu, A. K.-Y. Jen, *Acta Polym.* **1999**, 50, 105.
40. L. Goris, M. A. Loi, A. Cravino, H. Neugebauer, N. S. Sariciftci, I. Polec, L. Lutsen, E. Andries, J. Manca, L. De Schepper, D. Vanderzande, *Synth. Met.* **2003**, 138, 1-2, 249.
41. I. Polec, A. Henckens, L. Goris, M. Nicolas, M. A. Loi, P. Adriaensens, L. Lutsen, J. V. Manca, D. Vanderzande, N. S. Sariciftci, *J. Polym. Sci., Part A: Polym. Chem.* **2003**, 41, 7, 1034.
42. J. C. Hummelen, B. W. Knight, F. LePeq, F. Wudl, *J. Org. Chem.* **1995**, 60, 532.
43. J.-M. Nunzi, *C. R. Physique* **2002**, 3, 523.
44. D. Lorcy, M. P. Cava, *Adv. Mater.* **1992**, 4, 9, 562.
45. P. Bäuerle, G. Götz, P. Emerle, H. Port, *Adv. Mater.* **1992**, 4, 9, 564.
46. S. Musmanni, J. P. Ferraris, *J. Chem. Soc., Chem. Commun.* **1993**, 172.
47. R. Kiebooms, *Ph. D. Dissertation* **1995**, Limburgs Universitair Centrum, Diepenbeek, Belgium.

48. R. H. L. Kiebooms, P. J. A. Adriaensens, D. J. M. Vanderzande, J. M. J. V. Gelan, *J. Org. Chem.* **1997**, 62, 1473.

49. D. Vangeneugden, R. Kiebooms, P. Adriaensens, D. Vanderzande, J. Gelan, J. Desmet, G. Huyberechts, *Acta Polymerica* **1998**, 49, 12, 687.

50. D. Vangeneugden, *Ph. D. Dissertation* **1999**, Limburgs Universitair Centrum, Diepenbeek, Belgium.

51. D. L. Vangeneugden, R. H. L. Kiebooms, D. J. M. Vanderzande, J. M. J. V. Gelan, *Synth. Met.* **1999**, 101, 1-3, 120.

52. E. Staes, D. Vangeneugden, L. J. Nagels, D. Vanderzande, J. Gelan, *Electroanalysis* **1999**, 11, 1, 65.

53. S. E. Shaheen, D. Vangeneugden, R. Kiebooms, D. Vanderzande, T. Fromherz, F. Padinger, C. J. Brabec, N. S. Sariciftci, *Synth. Met.* **2001**, 121, 1583.

54. D. Gebeyehu, C. J. Brabec, N. S. Sariciftci, D. Vangeneugden, R. Kiebooms, D. Vanderzande, F. Kienberger, H. Schindler, *Synth. Met.* **2001**, 125, 3, 279.

55. D. Vangeneugden, D. J. M. Vanderzande, J. Salbeck, P. A. van Hal, R. A. J. Janssen, J. C. Hummelen, C. J. Brabec, S. E. Shaheen, N. S. Sariciftci, *J. Phys. Chem. B* **2001**, 105, 45, 11106.

56. L. Groenendaal, *Ph. D. Dissertation* **1996**, Technische Universiteit Eindhoven, The Netherlands, and references therein.

57. V. Hensel, A.-D. Schlüter, *Liebigs Ann./Recueil* **1997**, 303.

58. J. K. Herema, *Ph. D. Dissertation* **1996**, University of Groningen, the Netherlands.

Chapter 3
3,4-Disubstituted poly(2,5-thienylene vinylene)s

3.1 Introduction

Of all heteropolymers, thiophene derivatives seem to be most promising as semi-conductor in FET devices. When looking in literature more than 80% of the research towards materials for organic transistor applications involves thiophene based conductive polymers. Poly(2,5-thienylene vinylene) (PTV) proved already to be useful in plastic transistors[1] and photovoltaic devices. This polymer can be regarded as an alternating copolymer of thiophene and acetylene and thus should have properties of PT and PA[2]. Due to the extra vinylene double bond in PTV, compared to PT, the band gap of PTV is smaller. This is the result of two effects (i) a decrease in the overall aromatic character of the π-conjugated system, allowing a better delocalisation of π-electrons over the whole polymer chain, and (ii) a limitation in rotational disorder due to the presence of ethylenic linkages of defined configuration[3].

In 1970, PTV was prepared for the first time by Kossmehl *et al.*[4]. The polymer was synthesised as an insoluble powder via a Wittig reaction of thiophene-2,5-dicarbaldehyde **40** and 2,5-bis(triphenylphosphoniomethyl)thiophene dichloride **41**. (Scheme 3.1) During this reaction, cis and trans vinylene units were formed. By a catalytic amount of iodine, cis vinylene units could be isomerised into their trans isomers in boiling aromatic solvents. The major drawback however in this synthesis was the difficulty to process the material due to the insolubility of the PTV powder.

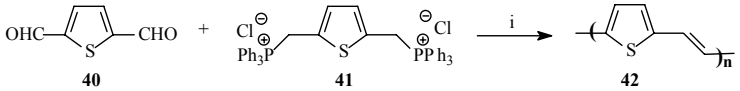

40 **41** **42**

***Scheme 3.1**: Synthesis of PTV via a Wittig reaction: i) base, DMF*

More than a decade later Kossmehl *et al.* synthesised PTV via the self-condensation of 5-methylthiophene-2-carbaldehyde **43**[5]. (Scheme 3.2) The polymers were identical with the polymers synthesised from the Wittig reaction and the vinylene units were trans configurated because of the trans elimination of water during the synthesis.

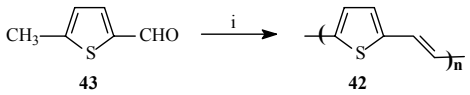

43 **42**

***Scheme 3.2**: Synthesis of PTV via an Aldol condensation: i) KtBuO, DMF, reflux*

Later, this aldol polycondensation toward poly(2,5-heteroarylene vinylene)s was patented and used by other research groups[6-8]. Kreja *et al.* suggested that two kinds of repeating units were present in the obtained polymers: aldol (-CHOH-CH_2-) and vinylene structural units[7]. (Figure 3.1) The vinylene form was produced by dehydration of the intermediate aldol form. This dehydration (-H_2O) is a consecutive reaction following the aldol condensation. Normally drastic conditions are necessary for the E_2-elimination of an alcohol but here the improved acidity of the α-proton and the conjugational stabilisation of the final product increase the reaction rate. If the polymer had mainly aldol structural units it should be soluble in water, when it contained mainly vinylene structural units, in our view it is expected to be insoluble in virtually every solvent. Therefore, production of the polymer in the aldol form should enable processing and the transformation into the vinylene form by means of a thermal treatment. However, when **43** was used as a substrate, the reaction equilibrium was always shifted toward the formation of mainly vinylene moieties. Average molecular weights for the polymer fractions were not determined due to the insolubility of the PTV **42** in THF and other suitable eluents.

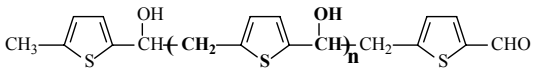

repeating unit aldol form

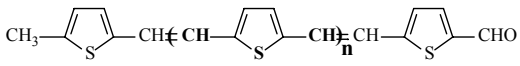

repeating unit vinylene form

Figure 3.1**: Aldol and vinylene form obtained after aldol condensation of **43

An indirect synthesis via a precursor polymer could be a solution to achieve processability. In 1984, Harper and Watson[9] noticed that in the patents of Wessling and Zimmerman[10] and in the report of Kanbe and Okawara[11], only the synthesis towards water soluble precursors of PPV and its derivatives was reported and that they did not mention the poly(heteroaromatic vinylene)s. Despite the fact that Harper and Watson patented the indirect route towards PTV, it was not until 1987, when Elsenbaumer *et al.*[12-14] first polymerised 2,5-bis(tetrahydrothiophenonium methyl)thiophene dichloride in water, that research was accelerated. They found that the polymerisation of the tetrahydrothiophenonium salt yielded a higher molecular weight polymer than the polymerisation of the dimethylsulphonium salt. However, the obtained precursor polymer was not stable and a spontaneous elimination to the unprocessable PTV could occur. The electrochemical, optical and magnetic properties of this polymer during electrochemical *p*-type doping were investigated by Onada *et al.*[15]. This complemented earlier work on the electronic properties of PTV[16]. Saito *et al.*[17-20] and Murase *et al.*[21, 22] independently reported on the synthesis of a precursor polymer bearing methoxy leaving groups. (Scheme 3.3) This polymer precipitated from the reaction mixture when the water soluble sulphonium precursor was treated with methanol. This precursor was soluble in organic solvents which was favourable for the characterisation and processability of the polymer. The electro-optic nonlinearity in PTV was studied by Gelsen *et al.*[23] using spectroscopic methods. Later, also Eevers *et al.*[24, 25] and Xie *et al.*[26] reported on a preparation method for PTV from a methoxy precursor polymer.

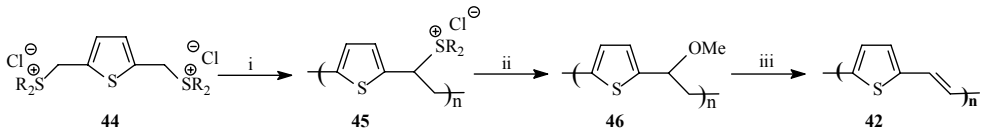

***Scheme 3.3**: Synthesis of PTV via a soluble precursor route (R_2 = Me_2 or $(CH_2)_4$): i) NaOH, H_2O; ii) MeOH, H_2O; iii) ΔT, HCl*

In 1989, Iwatsuki *et al.*[27] described an alternative method to prepare a film of fully conjugated PTV by a dehydrogenation reaction in dioxane from a poly(2,5-thienylene ethylene) (PTE) **50** film by using 2,3-dichloro-5,6-dicyano-1,4-benzoquinone (DDQ) as an oxidising reagent. (Scheme 3.4) The PTE film was obtained in the vapour deposition process with [2.2](2,5)thiophenophane **47** as a starting material[28]. The vapour phase

pyrolysis of heterophane **47** formed a reactive *p*-quinodimethane intermediate **48** and the subsequent polymerisation led to PTE. Another way to obtain a PTE film was by vapour pyrolysis of (5-methyl-2-thienyl)methyl benzoate **49** to obtain 2,5-dimethylene-2,5-dihydrothiophene **48**[29] which again spontaneously polymerised via a diradical intermediate[30, 31].

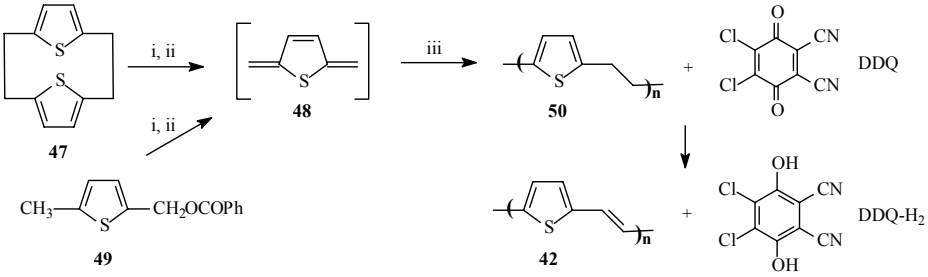

***Scheme 3.4**: Synthesis of PTV via hydrogen transfer of PTE with DDQ: i) vaporising; ii) pyrolysis; iii) deposition*

More recently, Philips Eindhoven patented another method to obtain PTV involving the polymerisation of 2,5-bisthioalkylmethylthiophenes[32].

Up till now, no reproducible, versatile, high yield polymerisation process toward PTV is developed. After all, the commonly used synthesis of PTV via the adapted Wessling route is not ideal. The synthesis is cumbersome and the reproducibility is rather poor. Due to the high reactivity, originating from the electron rich thiophene ring, monomer and thus polymer synthesis is difficult. Additionally, an alkoxy leaving group precursor polymer as **46** requires acid catalysis for the conversion process. Since this is incompatible with device fabrication, this PTV is not a suitable candidate for device applications. For that reason an effort to develop the synthesis of PTV via the sulphinyl precursor route was started in our lab[33]. However we encountered major difficulties in the synthesis of the sulphinyl monomer. Solvent substitution and instability of the intermediary products, caused by the high reactivity of the "benzylic" chlorine atoms, were the main problems. Due to these synthetical problems it was almost impossible to apply the sulphinyl route in the synthesis of PTV. This finally resulted in testing another precursor route for PTV synthesis (see chapter four). In a parallel approach, we also started with substituting the 3- and 4-position of the thiophene ring. In this way we wanted to facilitate the monomer synthesis by creating more stable intermediary products. The first time poly(2,5-thienylene vinylene) was substituted on its 3-

and/or 4-position was in 1987 when Elsenbaumer *et al.* synthesised the 3-methoxy and 3-ethoxy variant[34]. They used a Grignard reaction to couple trans-1,2-dichloroethylene with 3-alkoxy-2-litiated thiophene. (Scheme 3.5)

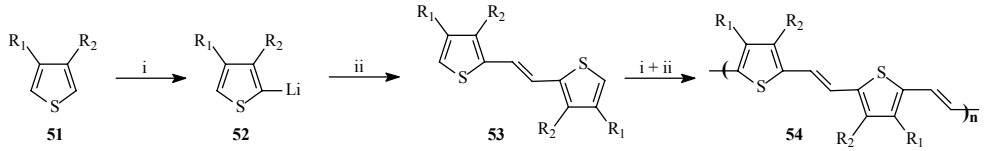

Scheme 3.5*: Grignard route to substituted PTV derivatives: i) BuLi; ii) $MgBr_2.Et_2O$, $NiCl_2(dppp)$, ClCH=CHCl (Elsenbaumer: R_1 = H, R_2 = OMe or OEt; Blohm: R_1 = R_2 = OBu; Peeters: R_1 = H, R_2 = octyl and R_1 = R_2 = butyl, octyl or 2'-ethylhexyl)*

A few year later, Blohm *et al.*[35-38] performed the nickel catalysed coupling of 3,4-dibutoxy-2,5-dilithiothiophene with 1,2-dichloroethylene to obtain poly(3,4-dibutoxy-2,5-thienylene vinylene) and Peeters *et al.*[39] synthesised poly(3-octyl-2,5-thienylene vinylene), poly(3,4-dibutyl-2,5-thienylene vinylene), poly(3,4-dioctyl-2,5-thienylene vinylene) and poly[3,4-di(2'-ethylhexyl)-2,5-thienylene vinylene] via the same Grignard coupling.

A second possible route that leads to substituted PTV derivatives is the Stille coupling. This is a cross coupling of organo stannanes with aryl halides[40]. The main advantage of the Stille coupling is its compatibility with a wide variety of functional groups. Disadvantages are the relative long reaction times (days) and quite elevated temperatures (100°C) required. Bolognesi *et al.*[41-43] used this method for the first time in the palladium catalysed coupling reaction of alkyl-substituted 2,5-diiodothiophene and 1,2-bistributylstannylethylene. (Scheme 3.6) In the same way Havinga *et al.*[44] synthesised four different alkoxy-substituted poly(2,5-thienylene vinylene)s and recently, in the group of McCullough[45] attempts to prepare poly(3-dodecyl-2,5-thienylene vinylene) by a Stille polymerisation led to a polymer that is at least 90% regioregular.

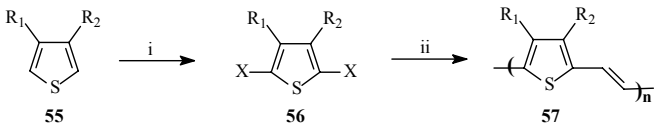

Scheme 3.6*: Stille variant of the Heck route to substituted PTV derivatives: i) I_2, HNO_3 (X = I) or NBS (X = Br); ii) $Bu_3SnCH=CHSnBu_3$, $Pd[(PPh_3)(CH_3COO)_2]_2$ or $Pd(PPh_3)_4$ (Bolognesi: R_1 = R_2 = decyl and R_1 = H, R_2 = butyl; Havinga: R_1 = H, R_2 = $OC_{12}H_{25}$, R_1 = R_2 = OC_4H_9, R_1 = R_2 = $OC_{12}H_{25}$, $OCH_2CH(C_6H_{13})O$; McCullough: R_1 = H, R_2 = dodecyl)*

Another method to synthesise substituted PTV derivatives is the McMurry reaction which is a titanium-induced reductive coupling of carbonyls to olefins[46, 47]. (Scheme 3.7) Poly(3,4-dibutoxy-2,5-thienylene vinylene), already synthesised by Blohm *et al.*, was somewhat later obtained by Iwatsuki *et al.*[48] by subjection of 3,4-dibutoxythiophene-2,5-dicarbaldehyde to the McMurry reaction. In the late nineties this route was used further in the group of S. Iwatsuki to synthesise poly(5-hexyloxybenzo[c]thiophene-1,3-vinylene)[49]. The group of E. W. Meijer reported on the synthesis of poly(3,4-bis[(S)-2-methylbutoxy]2,5-thienylene vinylene)[50], the first example of a PTV derivative with optically active side chains, and of poly(2,5-thienylene vinylene)s with chiral thioether side chains[51]. Cheng *et al.*[52] presented the synthesis of poly(3-hexyl-2,5-thienylene vinylene) on the International Conference on Science and Technology of Synthetic Metals (ICSM 2002) in Shanghai, China.

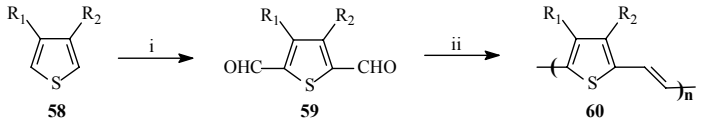

58 **59** **60**

***Scheme 3.7**: McMurry route to substituted PTV derivatives: i) BuLi, DMF; ii) $TiCl_4$/Zn (Iwatsuki: $R_1 = R_2 = OBu$, $CHCHC(C_6H_{13})CH$; Meijer: $R_1 = R_2 = OCH_2CH(CH_3)CH_2CH_3$, $R_1 = R_2 = SCH_2CH_2CH(CH_3)CH_3$ or $SCH_2CH(CH_3)CH_2CH_3$; Cheng: $R_1 = H$, $R_2 =$ hexyl)*

A final example of a substituted PTV derivative came from Bicknell *et al.*[53]. They synthesised an insoluble crown-ether ($(O(CH)_2)_4O$) containing PTV from a direct base catalysed polymerisation[54] of the unstable 2,5-bis(chloromethyl) derivative.

The methods described above are all direct methods in which the conjugated polymer is formed in one step. An indirect method was reported in 1995 by Elsenbaumer *et al.*[55] and was based on the sulphinyl precursor route[chapter one]. Previous attempts to use the Gilch and the Wessling-Zimmerman precursor route in the preparation of electron rich polymers[53, 56] were not successful due to the high reactivity and instability of the monomers as indicated before. The preparation by a precursor route thus needs a less reactive leaving group such as the phenylsulphoxide group used in the group of Elsenbaumer. In their route, the bis(sulphoxomethylene) monomer **65** could be prepared as shown in scheme 3.8 and with potassium *tert*-butoxide (K*t*BuO) it polymerised to the precursor polymer **66**. The sulphoxide group in the polymer could be thermally eliminated at moderate temperature (80°C) to provide the double bond[57]. The molecular weight of the polymers obtained in this

way (M_n = 87 000), was higher compared to the same polymers synthesised by a Grignard reaction[38] (M_n = 57 000) or a McMurry reaction[48] (M_n = 35 000).

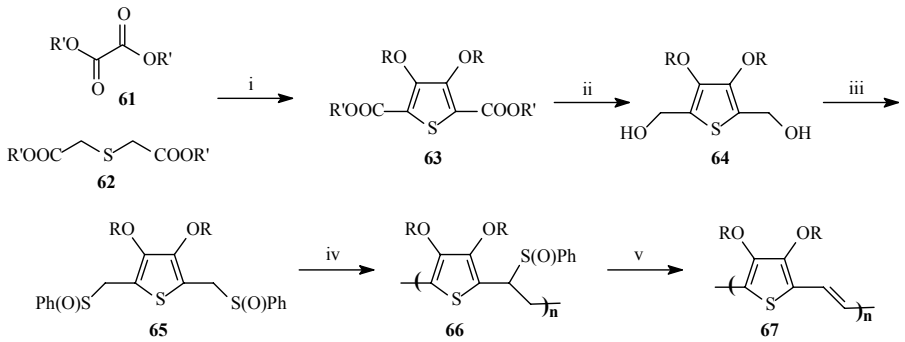

***Scheme 3.8**: Bis-sulphoxide route to poly(3,4-dialkoxy-2,5-thienylene vinylene)s: i) R'O-, RX; ii) $LiAlH_4$, MeOH; iii) PhSH, ZnI_2, MCPBA; iv) KtBuO, THF; v) ΔT*

Substitution with alkoxy or alkyl groups was mainly performed to guarantee the solubility and processability of the conjugated polymers. Additionally, introducing an electron donating group at the β position of a thiophene unit may decrease the band gap of the polymer. The vinylene spacers between the aromatic units reduce the steric hindrance between the substituents and therefore ensure the coplanarity of the conjugated polymer chain and thus the low band gap. It has been demonstrated that the incorporation of the vinylene linkages lowers the band gaps by about 0.4 eV[16].

3.2 Synthesis of poly(3,4-dichloro-2,5-thienylene vinylene) and poly(3,4-dibromo-2,5-thienylene vinylene) via the sulphinyl precursor route

In the synthesis of all the higher described substituted PTV derivatives, a precursor route was only applied once. However, the use of a precursor route is interesting with an eye on further applications. After all, if the conjugated polymer is insoluble, the synthesis of a soluble precursor polymer -that can be processed- can cancel this limitation.

In this paragraph, the use of the sulphinyl precursor route (scheme 3.9) in the synthesis of poly(3,4-disubstituted-2,5-thienylene vinylene)s will be examined. This route, designed to overcome the problems that are attached to the Gilch, Wessling and xanthate

precursor route, is the only route in which an unsymmetrical monomer **68** is used. This chemical differentiation between the polariser (a sulphinyl group) and the leaving group (a halogen atom) is what makes this route so attractive to use. The polariser makes the abstraction of the proton in the α position possible by stabilising the created anion in **69**. The *p*-quinodimethane system (*p*-QM) **70a-c** is formed by a 1,6-elimination of the leaving group. This QM molecule is the actual monomer in the polymerisation process. The sulphinyl group polarises the *p*-quinodimethane system in such a way that propagation occurs via consecutive head to tail additions. Thanks to the flexible side chain in the polariser, the non-conjugated precursor polymer **71** is soluble in different organic solvents. As the conversion of the precursor into the (non-processable) conjugated polymer **72** is performed via a thermal treatment, the polariser group should be stable at room temperature but convert smoothly at higher temperature.

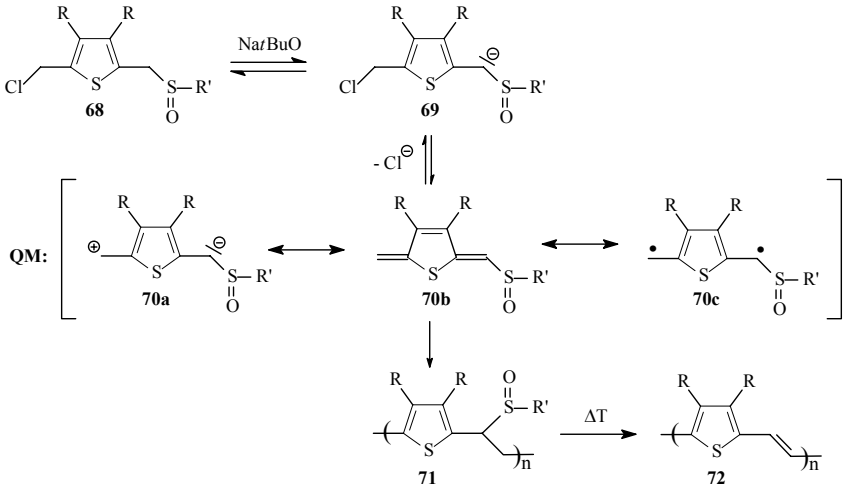

***Scheme 3.9**: The sulphinyl precursor route towards poly(3,4-disubstituted-2,5-thienylene vinylene)s*

As stated before, due to the electron rich character of the thiophene unit, it was difficult to synthesise premonomer **68** with R = H[33]. For that reason, our goal was to synthesise the dichloro and dibromo derivative. By choosing electron withdrawing R groups we hoped to obtain less reactive intermediates in the monomer synthesis.

3.2.1 Monomer synthesis

In the synthesis of the asymmetric, electron poor premonomer **68a** (R = Cl), different pathways were tested. They all started from the commercially available tetrachlorothiophene **73** which was also successfully synthesised in our lab by refluxing hexachloro-1,3-butadiene and sulphur[58]. The synthesis of 3,4-dichlorothiophene-2,5-dicarbaldehyde **75** however proved to be a problem. By using 2.2 equivalents of *n*-BuLi 3,4-dichlorothiophene-2-carbaldehyde **76** was obtained. (Scheme 3.10) This is rather surprisingly since other research groups succeeded in the synthesis of other 3,4-disubstituted 2,5-thiophenedialdehydes[48, 50, 51] by using the method of Feringa[59]. Also starting from 2,5-dibromothiophene the synthesis of 2,5-thiophenedialdehyde has been reported with a yield of 59%[60]. Our problem was not so much the synthesis of the dilithium salt **74** seeing that the salt precipitated as a white solid. The problems thus started with the addition of anhydrous *N,N*-dimethylformamide (DMF). Insufficient drying of the reagents and the glassware could therefore be the problem.

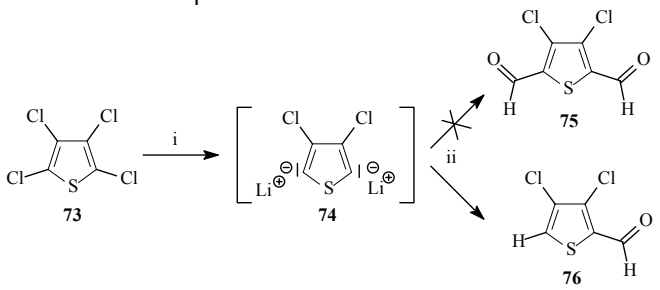

***Scheme 3.10**: Attempt to synthesise 3,4-dichlorothiophene-2,5-dicarbaldehyde: i) n-BuLi; ii) DMF*

Other attempts in which the Vilsmeier reagent ($POCl_3$/DMF) or ethyl formate (HC(O)OEt) were used as formylating reagents also failed. Nevertheless the reaction with *n*-BuLi and DMF could be tuned in such a way that only one equivalent of *n*-BuLi was used to obtain 3,4,5-trichlorothiophene-2-carbaldehyde **77**. (Scheme 3.11) Subsequent reduction of the aldehyde with $NaBH_4$ yielded alcohol **78** which was chlorinated with thionyl chloride. Further transfer into thioether **80** was accomplished using 1-octanethiol. At this level we tried to build in a second aldehyde. Unfortunately no aldehyde was detected in the NMR spectrum of the reaction mixture.

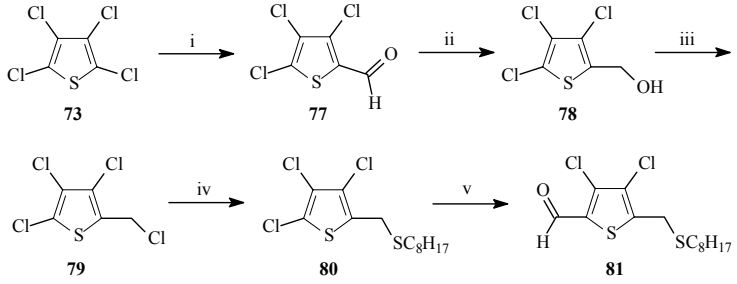

***Scheme 3.11**: Attempt to synthesise 2-thiooctylmethyl-3,4-dichlorothiophene-5-carbaldehyde **81**: i) n-BuLi, DMF; ii) $NaBH_4$, THF; iii) $SOCl_2$, THF; iv) $C_8H_{17}SH$; v) n-BuLi, DMF*

Another way to obtain compound **81** was via the route presented in scheme 3.12. In this approach first the mono-aldehyde was protected after which the second aldehyde could be built in. Again the aldehyde was reduced with $NaBH_4$ to yield the corresponding alcohol. But when **84** was treated with thionyl chloride, the protective group went off due to the high acidity of the reaction mixture. The chlorination therefore mainly yielded compound **86** and the protected variant **85** was only for less than 15% present in the reaction mixture. The next step, the conversion to the thioether, had a disappointing yield of 5% and purification of **81** was difficult because the R_f values of starting and end product were similar.

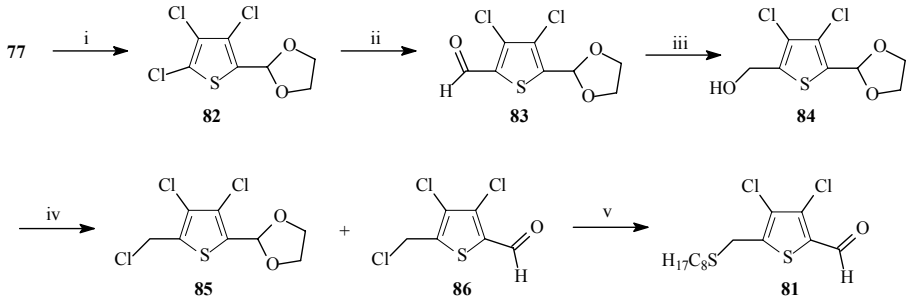

***Scheme 3.12**: Second pathway to obtain compound **81**: i) $HOCH_2CH_2OH$, p-TsOH; ii) n-BuLi, DMF; iii) $NaBH_4$, THF; iv) $SOCl_2$, THF; v) $C_8H_{17}SH$*

Due to the complexity and low overall yields of the reactions described above, we started with the synthesis of the 2,5-bischloromethylthiophenes **88a** and **88b**. (Scheme 3.13) This symmetric product could be synthesised from the corresponding dihalothiophene by means of a chloromethylation reaction[61]. We opted to use the method reported by Becker *et al.*[62]. This reaction is an electrophilic substitution of formaldehyde in acid

conditions to the substrate, followed by a nucleophilic substitution of the formed diol to the chlorine anions in the reaction mixture. 3,4-Dibromothiophene is commercially available but 3,4-dichlorothiophene had to be synthesised. By treatment of **73** with *n*-BuLi, the dilithium salt **74** was again formed as a white precipitate[63]. After addition of water and acidification with an aqueous HCl solution until neutral, **87a** could be obtained.

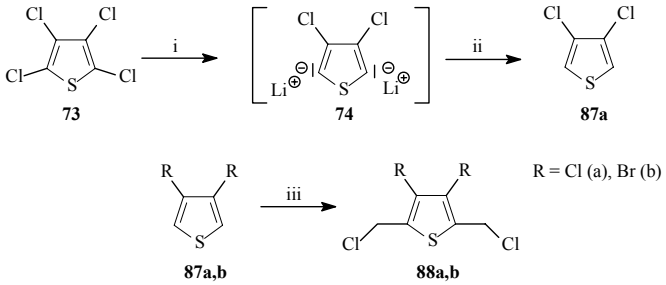

73 **74** **87a** **87a,b** **88a,b**

***Scheme 3.13**: Synthesis of the symmetric 3,4-dihalo-2,5-bischloromethylthiophene: i) n-BuLi; ii) H_2O; iii) CH_2O, HCl, Ac_2O*

The next step in the monomer synthesis involves the formation of the monosulphide. This sulphide could be formed directly via a classical nucleophilic substitution of the halide with an alkylthiolate or indirectly via the bissulphonium salt[64]. (Scheme 3.14) The reaction towards **89a** is a nucleophilic substitution of the chlorine atoms with tetrahydrothiophene (THT) groups. Subsequently, a thiolate anion extracts a proton and a 1,6-elimination can occur. The intermediary *p*-quinodimethane system immediately reacts to form monosulphide **90a** which is however not isolated. An azeotropic distillation with *n*-octane leads to monosulphide **91a**. Because it was difficult to isolate bissulphonium salt **89a**, we only performed the indirect synthesis for the chloro variant. An increase in reaction time and temperature could possibly lead to an improved synthesis of the salt. This was already proven earlier[65] but was however not tested here. The direct synthesis involves a two phase reaction in which a phase transfer catalyst, methyltrioctylammonium chloride (Aliquat 336®), is used to ensure the transfer of the hydroxyl anions (OH^-) from the water phase to the organic (toluene) phase. The overall yield for the reaction from **88a** to **68a** (direct synthesis) was 35% (R' = octyl) and 18% (R' = ethyl). However in these procedures respectively 55% and 71% of the starting product could be recovered.

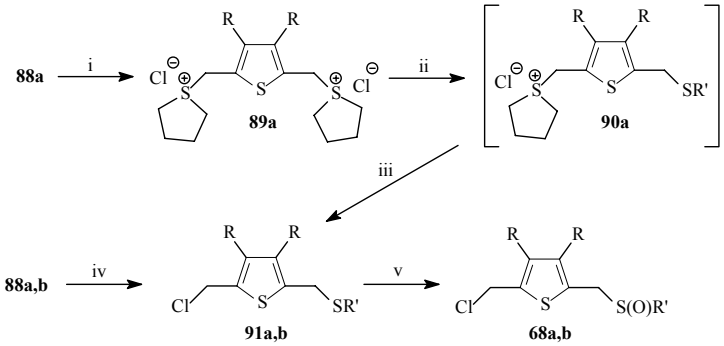

***Scheme 3.14**: Synthesis of the sulphinyl premonomers (R = Cl, Br; R' = ethyl, octyl): i) THT, MeOH; ii) R'SH, NatBuO; iii) n-octane; iv) R'SH, NaOH, Aliquat 336; v) H_2O_2, TeO_2, MeOH*

The last step in the preparation of the sulphinyl monomer is the oxidation of the corresponding sulphide. Since the tellurium dioxide (TeO_2) catalysed oxidation of thioethers with hydrogen peroxide (H_2O_2) in methanol had proven to work properly[64, 66], it was also applied here.

3.2.2 Stop flow UV-Vis measurements on the monomers: formation of *p*-QM

To learn something about the polymerisation capabilities of the monomer, the formation of the *p*-quinodimethane (*p*-QM) system was followed by means of UV-Vis measurements. This was possible because a *p*-QM system has a strong absorption in the UV area. For this purpose, a stop flow apparatus, depicted in figure 3.2, was used. With syringe 1 and 2, the monomer and base solutions were brought together at the same time into the measuring cell of the spectrometer.

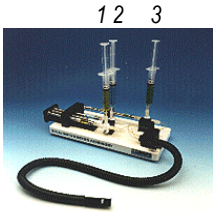

Syringe 1: monomer solution
Syringe 2: base solution
Syringe 3: waste

***Figure 3.2**: Stop flow apparatus*

The concentrations used for the monomer (10^{-4} M) and the base (10^{-3} M) solutions, were too low to initiate polymerisation of the *p*-quinodimethane system. For the

measurements on **68a**, 1,4-dioxane was used as the solvent and for **68b** this was *2*-BuOH. In both cases, sodium *tert*-butoxide (Na*t*BuO) was used as the base. Figure 3.3 shows the UV-Vis spectra of **68a** after monomer and base solutions were brought together. In figure 3.4 the absorption at 366, 378 and 357 nm are plotted as a function of time. The formation of the *p*-QM -with absorption at 357 nm- is clearly visible in this way.

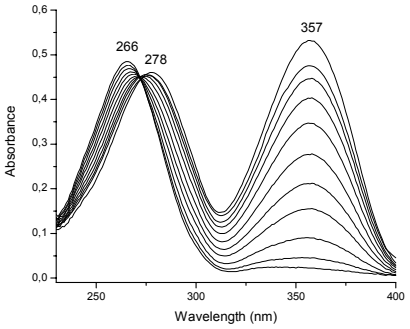

***Figure 3.3**: UV-Vis spectra of **68a** (R'=octyl) after addition of NatBuO*

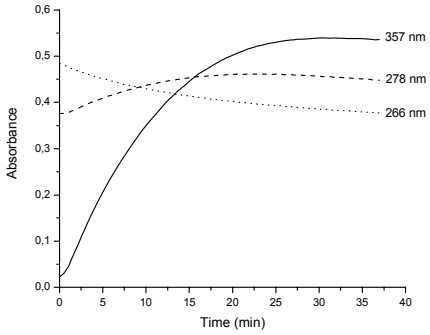

***Figure 3.4**: Absorption at 266, 278 and 357 nm versus time*

This measurement was performed in triplicate to check the reproducibility. Since the solubility of Na*t*BuO in 1,4-dioxane is poor, the base precipitated. As a result the *p*-quinodimethane system was formed slower when looking at the successive measurements. From the figures presented here, we can not draw conclusions regarding the kinetics of the *p*-quinodimethane formation but we can say that polymerisation of monomer **68a** looks possible since the corresponding quinoid formation is possible.

Exactly the same measurement could be done for **68b**. *2*-BuOH was used as the solvent thus no solubility problems occurred here. In figure 3.5 we can see that the quinoid absorption also here is at 357 nm. The quinoid formation was however so fast that, when the absorbance is plotted as a function of time, we can not see the formation anymore but only the decline in absorption at 357 nm. (Figure 3.6)

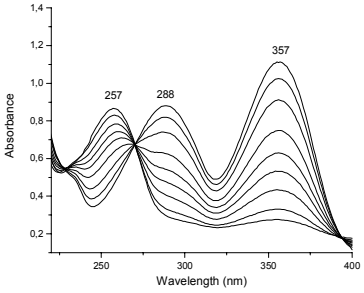

***Figure 3.5**: UV-Vis spectra of **68b** (R' = octyl) after addition of NatBuO*

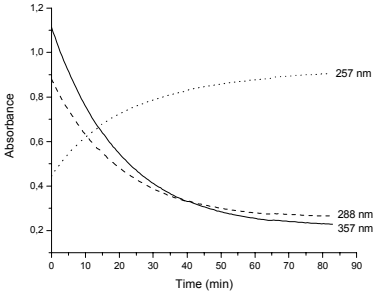

***Figure 3.6**: Absorption at 257, 288 and 357 nm versus time*

3.2.3 Polymerisation via the sulphinyl precursor route

The polymerisation of the premonomer **68** was performed in a thermostatic flask in which the monomer solution was inserted first. (Scheme 3.15) The base, dissolved in the same solvent, was added in one go via a thermostatic funnel after both solutions were made oxygen free by passing nitrogen gas through them. The monomer concentration was set at 0.1 M, calculated on the total volume of solvent that was used. After one hour the mixture was poured into ice water, acidified to neutral with an aqueous solution of HCl (1 M) and extracted with chloroform. After the solvent was removed, the polymer was precipitated in an ice-cold hexane/ether (3/1) mixture, collected and dried. The residual fraction was concentrated in vacuo.

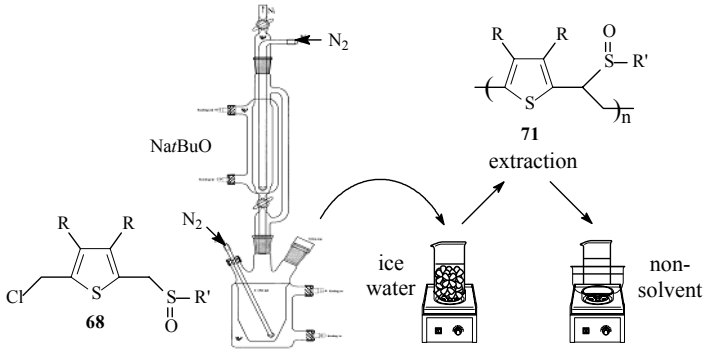

***Scheme 3.15**: Synthesis of precursor polymer **71** (R = Cl, Br and R' = ethyl, octyl)*

The yield, the weight-average molecular weight (M_w in g/mol) and the polydispersity (PD) depend on the polymerisation conditions. In contrast to other precursor routes, the

sulphinyl precursor route is not limited by one or two conditions. The parameters that can be varied in the polymerisation process are: the choice of solvent, base, temperature … It was not our intention to fully optimize the polymerisation conditions. The polymerisations presented in table 3.1, were performed to indicate that polymer could be obtained in the applied conditions. The temperature was kept constant at 30°C during the whole polymerisation process (1 hour) and Na*t*BuO was used as the base. The molecular weight of the precursor polymers was determined by Gel Permeation Chromatography (GPC) relative to polystyrene (PS) standards and THF was used as the eluent. All GPC analyses present a monomodal molecular weight distribution.

Entry	R	R'	Solvent	#Eq base	Yield (%)	M_w (x 10^{-3})	PD
1	Cl	Octyl	2-BuOH	1.2	89	89.2	2.3
2	Cl	Octyl	2-BuOH	1.05	75	63.5	2.3
3	Cl	Octyl	THF	1.05	30	48.9	2.4
4	Br	Octyl	2-BuOH	1.05	70	121	4.8
5	Br	Octyl	THF	1.05	48	86.5	3.0
6	Cl	Ethyl	2-BuOH	1.05	48	2.8	1.6

Table 3.1**: Polymerisation results for the monomers **68a,b

The best results were obtained with the synthesis of the octylsulphinyl precursor. The dichloro and dibromo premonomers behaved more or less in the same way and 2-BuOH was particularly suitable as the polymerisation solvent. The latter had already been proven in previous polymerisations of other sulphinyl monomers[67, 68]. In cases where the residual fraction was analysed with ^{1}H NMR only starting product was found.

3.2.4 Study of the thermal conversion of the precursor polymers to the conjugated structure

To obtain the conjugated polymer, the precursor polymer had to be submitted to a thermal treatment. The thermal elimination of the sulphinyl group towards 3,4-dihalo substituted PTV as well as the stability of the conjugated polymer could be studied with

different techniques. *In-situ* UV-Vis and *in-situ* FT-IR measurements as well as DIP-MS (Direct Insert Probe Mass Spectrometry) were used to study the thermal elimination reaction and the thermal stability behaviour of the polymer. For the first two, a thermo-cell was especially designed to fit in both a UV-Vis and a FT-IR spectrometer. A dynamic heating rate of 2°C/min up to 300°C under a continuous flow of nitrogen was used. DIP-MS measurements were performed at a heating rate of 10°C/min up to 600°C in order to get information on the elimination products. In this technique the material is brought directly on the heating element of the probe as a thin film and enables to study the products that are liberated in the high vacuum (4.10^{-4} Pa) inside the spectrometer upon elimination. Liberated products were ionised by electron impact.

UV-Vis measurements:

A precursor route has the advantage of producing a soluble and processable precursor polymer. An inherent drawback however is the elimination step needed to obtain fully conjugated polymers. The temperature program, applied after the precursor is spin-coated, is contributory for the functioning of the device. For example: when the heating rate is too high, cracks can arise in the polymer film resulting in a low device performance. When the applied temperature is too low, the precursor will not be fully converted which also results in poor or non-functioning of the device. In order to deduce the protocol one has to use to convert the precursor into the conjugated form, an *in-situ* UV-Vis measurement is indispensable. In figure 3.7, the gradual formation of the conjugated structure for poly{(3,4-dichlorothienylene)-[1-(*n*-octylsulphinyl)ethylene]} **71a** (M_w = 63 500) is shown. The higher the degree of conjugation, the more the absorption maximum shifts to higher wavelength. With an eye on further applications of the materials in TFTs, a high absorption maximum is favourable. After all, a large π-conjugation length results in wide valence and conduction bands, leading to a higher carrier mobility[69, 70]. The maximum wavelength (λ_{max}) of the conjugated polymer **72a** is 583 nm. Though, we should make the remark that this value has been measured at 150°C and that λ_{max} at room temperature is expected to have a higher value. This could be attributed to the 'thermochromic effect'. Indeed on cooling down, a bathochromic shift is visible because at lower temperature, the conjugation is better and thus a higher maximum wavelength is seen. In order to obtain the λ_{max} at room temperature, the precursor was heated at 2°C per minute up till 150°C. After this, the sample was hold at

this temperature for 5 minutes and cooled back to 25°C. A λ_{max} value of 595 nm could then be observed. By plotting the absorbance at the absorption maximum (at 150°C) as a function of temperature (figure 3.8), an increase in this absorbance could be seen between 65 and 95°C. In the region between 55 and 95°C, the formation and disappearance of oligomeric fragments (388 nm) is visible. Their formation goes up to a maximum and is then taken over by the absorption at 583 nm, in favour of the longer conjugated chains. The decrease in absorbance at 267 nm, which corresponds to the λ_{max} of the precursor polymer **71a**, takes place in the same temperature interval as the increase in the absorbance at 583 nm. We thus can conclude that elimination takes place in a temperature range from 65 up to 95°C.

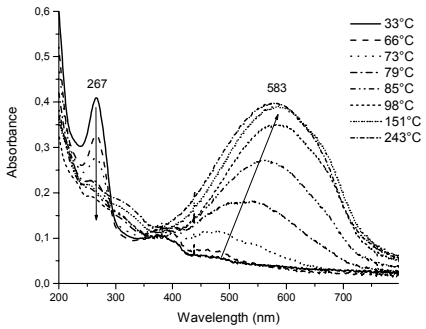

***Figure 3.7**: UV-Vis spectra of **71a** (R' = octyl) at different temperatures*

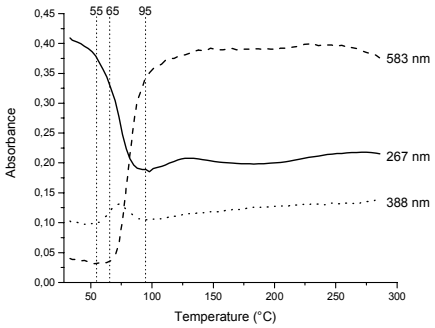

***Figure 3.8**: Absorption at 583, 388 and 267 nm as a function of temperature*

As explained in chapter one, we can derive the band gap of the conjugated polymer from its UV-Vis spectrum. At a temperature of 240°C, elimination of the sulphinyl group is completed. When drawing the tangent on the low energetic side of the spectrum taken at 243°C (figure 3.7), the intersection with the abscissa is at 776 nm which corresponds to a band gap of 1.6 eV. But due to the thermochromic effect the band gap should be determined from the UV-Vis spectrum recorded at room temperature. The value of the band gap thus derived was 1.55 eV.

Exactly the same UV-Vis profiles could be derived from the measurements of poly-{(3,4-dibromothienylene)-[1-(*n*-octylsulphinyl)ethylene]} **71b**. The corresponding conjugated polymer also has a band gap of 1.55 eV and the λ_{max} value measured at 150°C was 598

nm. A λ_{max} value of 609 nm was observed at 25°C after performing an analogue heating-cooling experiment as done for the conversion of **71a**.

Since the absorbance at 583 nm for **71a** and at 598 nm for **71b** stayed constant until at least 250°C, the degradation of the conjugated polymer occurred at a temperature higher than 250°C. To have a better idea of the stability, an additional experiment was performed. Here **71b**, spin-coated on a quartz disc, was exposed to four successive temperature ramps from ambient temperature to 250°C at 2°C per minute (dotted line in figure 3.9). The absorbance at 268 and at 590 nm is plotted as a function of time. When an overlay of the absorbance at 590 nm in the second and third temperature ramp is made, we can see that this overlay is quite good. (Figure 3.10) However, in an experiment where the successive temperature ramps only went to a temperature of 200°C, the same overlay was better, indicating possibly some signs of degradation at 250°C.

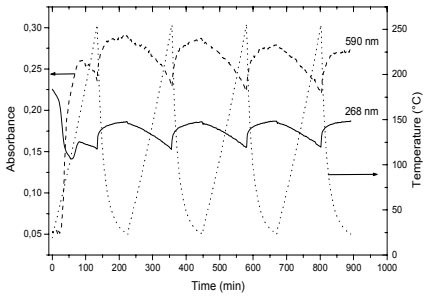

Figure 3.9**: Heating-cooling experiment on **71b

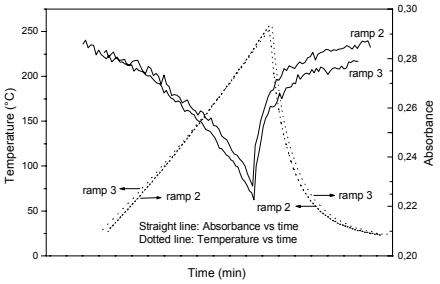

***Figure 3.10**: Overlay of ramp two and three*

The undulating motion in the absorbance as a function of time in figure 3.9 is caused by the thermochromic effect. With decreasing temperature, the absorbance at 268 and 590 nm will increase as there is a bathochromic shift on cooling down the polymer. To be sure that no changes occurred at these two wavelengths due to the quartz disc on which the polymer was spin-coated, also a pure quartz disc was heated from ambient temperature to 250°C at 2°C per minute. In figure 3.11 the absorbance at 258 and 587 nm is plotted as a function of time. The absorbance remains unchanged which means that the quartz disc itself has no influence on the absorbance at these wavelengths. Nevertheless the quartz disc does influences the absorbance at higher wavelengths (1304 nm) but this is of no

importance since these wavelengths are not studied during the elimination and degradation process of the polymers.

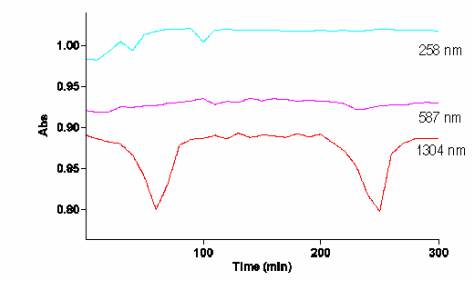

***Figure 3.11**: The absorbance at different wavelengths as a function of temperature for a quartz disc*

FT-IR measurements:

In-situ FT-IR spectroscopy is a second technique to get more insight in the elimination process of the polariser and thus the formation of the conjugated system. The same dichloro precursor polymer as used in the UV-Vis measurements was examined here. In the IR spectrum of the precursor polymer the signal at 1048 cm^{-1} originates from the octyl sulphinyl group. (Figure 3.12) The formation of the vinylene double bond is visible at 926 cm^{-1}. The intensity of these bands is plotted as a function of temperature in figure 3.13. The decrease in intensity of the signal at 926 cm^{-1} is probably not due to degradation of the conjugated system but can possibly be attributed to the thermochromic effect.

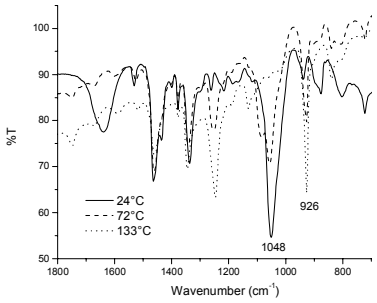

***Figure 3.12**: IR spectra of **71a** (R' = octyl) at different temperatures*

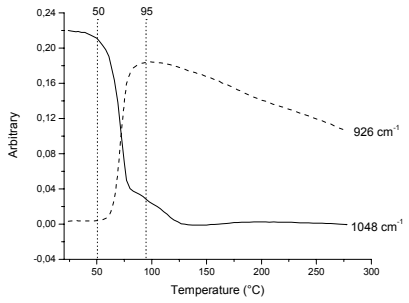

***Figure 3.13**: Absorption at 926 and 1048 cm^{-1} as a function of temperature*

From the absorption profiles we can conclude that UV-Vis and FT-IR are complementary techniques. The absorption at 583 nm increases in more or less the same

temperature interval than the absorption at 926 cm^{-1}. Also here exactly the same FT-IR profiles could be derived from the measurements of **71b**.

DIP-MS measurements:

With the thermal analysis of a precursor polymer by DIP-MS, information about the structure of the elimination products can be obtained as well as the kinetics of the evaporation process. In the thermogram of both the dichloro and the dibromo octylsulphinyl precursor polymer shown in figure 3.14, the total ion current (TIC) is plotted as a function of temperature. It shows two signals of which the first has a maximum at 101°C. By looking at the fragments observed in the mass spectrum of the first peak, this signal could be assigned to the elimination of the octylsulphinyl polariser. The second signal shows its maximum at 398°C for **71a** and at 379°C for **71b** and corresponds to the evaporation of degradation products of the conjugated polymer.

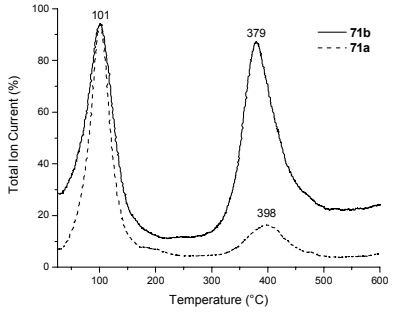

***Figure 3.14**: DIP-MS thermogram of **71a** and **71b** both with R' = octyl*

3.2.5 Photovoltaic studies

3.2.5.1. Introductory experiments needed for photovoltaic studies

The main difference between the material described in this chapter and the soluble PITNs described in chapter two is their solubility in the conjugated phase. Up till now, all polymer materials, tested for their applicability in solar cells, were soluble in the conjugated form thanks to side chains on the monomer unit. Here, the precursor polymer is soluble but

once transferred to the conjugated form, the material becomes insoluble. To test these materials in solar cell devices, we first have to spin-coat the precursor material and afterwards do a conversion at high temperature. Since we mix the precursor with [6,6]-PCBM and the elimination temperature sometimes can be quite high, we first investigated the thermal stability of this C_{60} derivative. Two techniques were used to evaluate the resistance of PCBM towards high temperatures and thus the applicability of PCBM as electron acceptor in a solar cell device even with high temperature processing. First, a simple *in-situ* UV-Vis measurement was done. The PCBM was dissolved in chlorobenzene 1% (w:v%) and brought on a quartz disc which is then placed in the temperature cell positioned in the beam of the UV-Vis spectrophotometer. The sample was heated at 2°C per minute from ambient temperature to 350°C and this under nitrogen atmosphere. The UV-Vis absorption spectra of [6,6]-PCBM at different temperatures are given in figure 3.15. Here we can see clearly the decrease in absorbance at 267 nm beyond 220°C. When plotting the absorbance at this wavelength as a function of temperature (figure 3.16) a decrease can be observed between 215 and 250°C. We thus expect no problems concerning the thermal stability on *in-situ* conversion of the precursor polymer to the conjugated structure in the presence of [6,6]-PCBM.

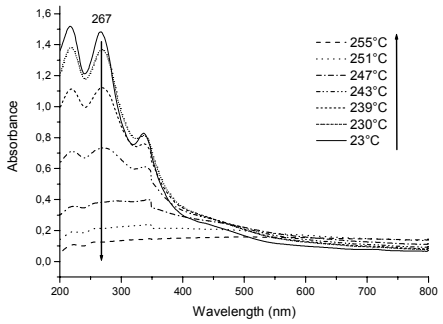

***Figure 3.15**: UV-Vis spectra of [6,6]-PCBM*

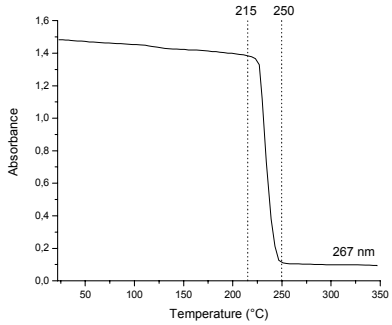

***Figure 3.16**: Absorption at 267 nm as a function of temperature*

These conclusions were confirmed by Thermo Gravimetric Analysis (TGA). A [6,6]-PCBM sample was inserted in the solid state in a thermogravimetric analyser. A continuous flow of nitrogen (50 mL/min) and a heating rate of 10°C per minute were used. In TGA, the weight of the sample is measured as a function of temperature. (Figure 3.17) As no weight

loss is observed before 350°C, there is no degradation of the PCBM before this temperature.

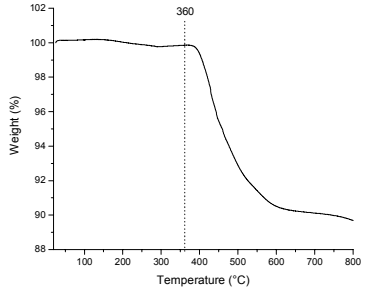

***Figure 3.17**: TGA spectrum of [6,6]-PCBM*

3.2.5.2. Solar cell behaviour of poly(3,4-dichloro-2,5-thienylene vinylene) and poly(3,4-dibromo-2,5-thienylene vinylene)

Photovoltaic studies on solar cell devices were performed by Martin Knipper at the physics division of the Institute for Materials Research (IMO). Solar cells were prepared according to the following procedure. Glass substrates coated with ITO (resistance ~ 90 ohm per square) were cleaned first with isopropanol in an ultrasonic bath for 20 minutes and dried in a nitrogen flow. The samples were brought into a glove box with a nitrogen atmosphere. Inside the glove box, an 80 nm layer of PEDOT/PSS (BAYTRON P from Bayer AG) was spin-coated on top of the ITO and heat treated for 10 minutes at 180°C on a hot plate. After this, the sample was cooled down to room temperature and the photoactive layer was spin-coated on top of the PEDOT. It was cast from a 0.5 wt% solution of poly{(3,4-dichlorothienylene)-[1-(*n*-octylsulphinyl)ethylene]} **71a** (M_w = 48 900) mixed with PCBM in chlorobenzene. The ratio by weight from **71a** and PCBM was 1:4 (1.5 mg of **71a**; 6 mg of PCBM). The solution was stirred with a magnetic stirrer overnight at room temperature. The spin-coating of the active layer was a two-step procedure: the first step, to determine the thickness, was with a closed cover at 600 rpm for 5 seconds. The second step, to dry the film, was with an open cover at 40 rpm for 2 minutes. The converted film was approximately 150 nm thick. The conversion of the precursor polymer was done on a hot plate from room temperature to 150°C with a temperature increase of 2°C per minute after which the

temperature was held constant at 150°C for 10 minutes. Then the top electrode was evaporated in a vacuum of 2.10^{-6} mbar. First a 0.7 nm thick layer of LiF and then a second layer of 70 nm aluminium were evaporated. The active area of each cell was 6 mm^2. Afterwards the samples were measured with a solar simulator (AM1.5 spectrum, 1000 W/m^2). A postproduction heat treatment took place at 70°C for several times, starting with 5 minutes. Then the samples were measured again at room temperature and after that annealed again (55 minutes, in total 1 hour). Five annealing steps were done with a total time of 9 hours.

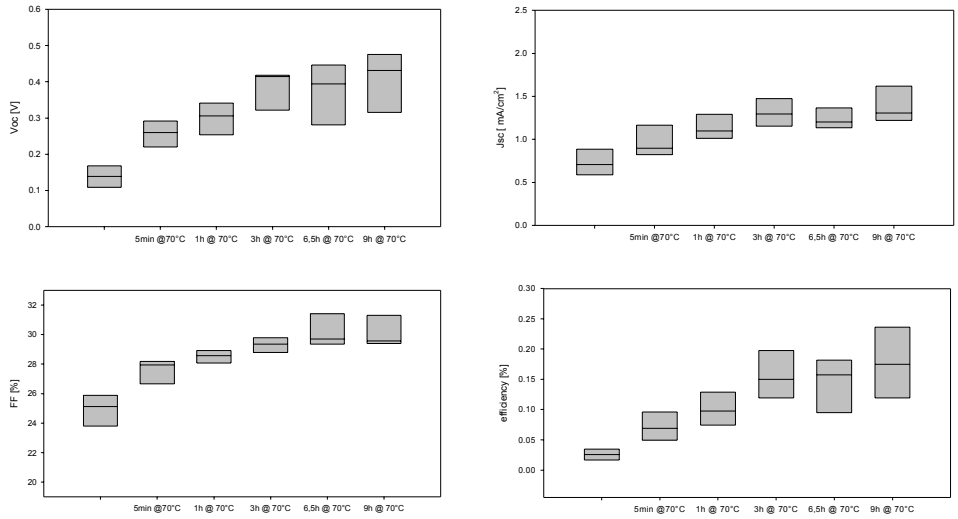

Figure 3.18 to 3.21**: V_{oc}, J_{sc}, FF and efficiency as a function of annealing time for **71a

Recently, Padinger *et al.* reported on an improvement of the performance of solar cells after a postproduction treatment[71]. Also here it is shown (figures 3.18 to 3.20) that the open circuit voltage (V_{oc}), the short circuit current density (J_{sc}) and the fill factor (FF) increase with postproduction temperature treatment. Therefore also the efficiency (product of these three values) increases as shown in figure 3.21. Since there were eight solar cells on each substrate, the boxes present the data off all eight measurements. The boundary of the box closest to zero indicates the 25th percentile, the line within the box marks the median, and the boundary of the box farthest from zero indicates the 75th percentile. The values listed in table 3.2 are the averages of the eight data points.

The same procedure as described above was used to construct devices with an active layer that was produced from precursor polymer **71b** (M_w = 121 000). As shown in figures 3.22 to 3.25 analogous curves were obtained.

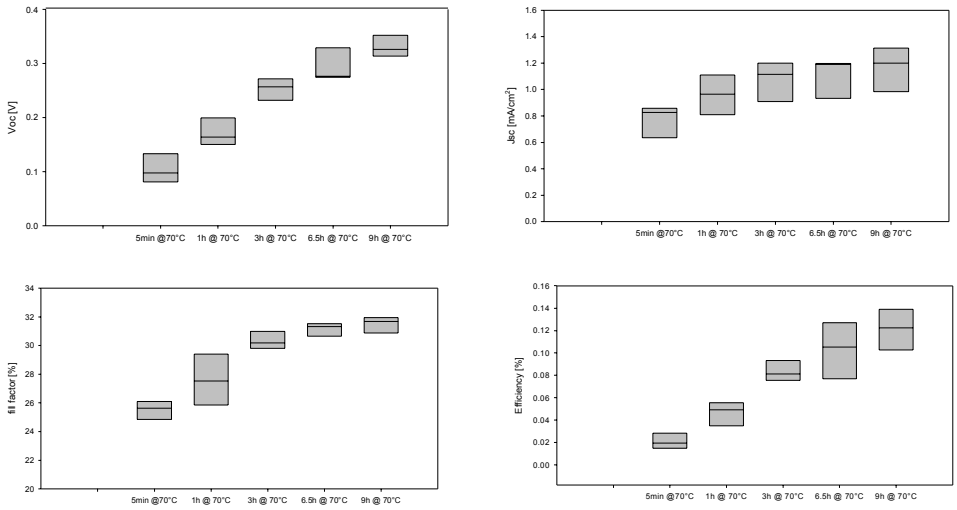

Figure 3.22 to 3.25**: V_{oc}, J_{sc}, FF and efficiency as a function of annealing time for **71b

Polymer	Annealing time	V_{oc} (mV)	J_{sc} (mA/cm^2)	FF (%)	η (%)
71a	5 minutes	252	0.966	27.3	0.070
71a	9 hours	408	1.437	29.9	0.18
71b	5 minutes	106	0.781	25.4	0.021
71b	9 hours	333	1.165	31.4	0.12

***Table 3.2**: Device characteristics*

The increase in V_{oc} and FF can be due to a burning of shunts in the bulk. The leakage current decreased with heat treatment as shown in figures 3.26a and 3.26b. We still have a high leakage current, but we see a little bit of rectification in the solid line of figure 3.26b. Due to the postproduction thermal treatment an improved diode behaviour is observed.

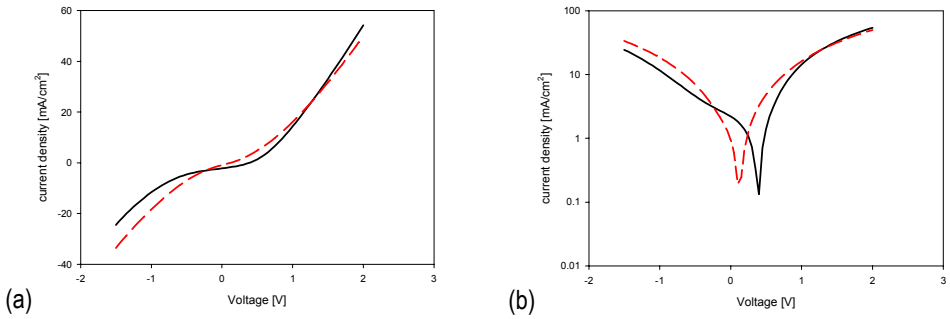

***Figure 3.26**: JIV curves before annealing (dashed line) and after 9 hours (solid line) for **71a**, (b): log-scale*

The increase in J_{sc} normally results from an increase of the charge carrier mobility[71]. In this case it can be due to an ongoing conversion from the precursor to the conducting polymer. To know if this is the case a comparative UV-Vis study was set up between the conversion of pristine **71a** and the conversion of a mixture of **71a** and PCBM. If the elimination temperature of the mixture was higher compared to the temperature of the precursor polymer alone, an explanation for the observed solar cell characteristics could be given.

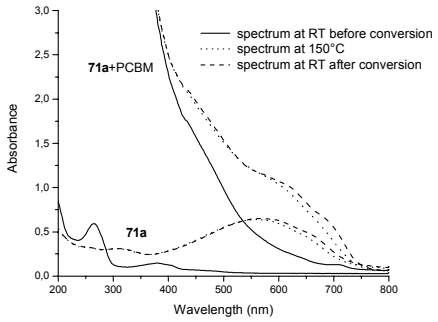

***Figure 3.27**: UV-Vis spectra of **71a** and the mixture of **71a** with PCBM*

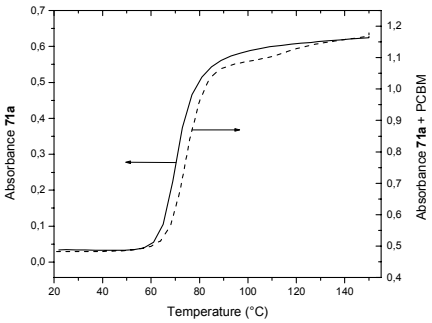

***Figure 3.28**: Absorption at 558 nm as a function of temperature*

In these two experiments, the precursor polymer and the polymer mixed with PCBM were heated at 2°C per minute from ambient temperature up till 150°C. After the sample was hold at this temperature for 10 minutes, it was cooled back to room temperature. For both samples the UV-Vis spectra at room temperature (solid line), at 150°C (dotted line) and after cooling down (dashed line) are given in figure 3.27. The strong absorption of the

mixture before 500 nm is due to the presence of the C_{60} derivative of which the UV-Vis spectrum is shown in figure 3.15. If we compare the profile of the absorption at 558 nm for the conjugated polymer alone with the profile for the polymer mixed with PCBM (figure 3.28), we observe a slight shift (5°C) towards higher temperature for the mixture. This small change however is in our view too small to be helpful to explain the improved characteristics with increasing annealing time.

3.2.6 Transistor behaviour of poly(3,4-dichloro-2,5-thienylene vinylene) and poly(3,4-dibromo-2,5-thienylene vinylene)

The two sulphinyl precursor polymers **71a** and **71b** were also tested in a TFT device. The measurements were performed on a bottom-contact ring transistor (L = 10 μm; W = 2500 μm) and carried out by Patrick Baesjou at Philips Research in Eindhoven, The Netherlands. Despite the good stability of the material, the transistor properties were very bad. For this reason, we looked for other possible substituents and the synthesis of 3,4-diphenyl substituted PTV was planned and started.

3.3 Synthesis of poly(3,4-diphenyl-2,5-thienylene vinylene)

Since the synthesis of non-substituted poly(2,5-thienylene vinylene) via the sulphinyl route has proven to be difficult, the synthesis of poly(3,4-diphenyl-2,5-thienylene vinylene) via this precursor route would probably be impossible. After all, substituting the β positions of the thiophene with electron donating phenyl groups, makes the aromatic core even more electron rich. Therefore, the xanthate precursor route was used to test the applicability of this route in the synthesis of electron rich PTV derivatives. At first, not much has been published about the use of the xanthate route[72, 73] in comparison to the other three precursor routes. It is only in the past few years that the number of reports on this route is increasing[74-82]. An important drawback inherent to the xanthate route is the strict conditions in which the polymerisation has to be performed. Whereas in the sulphinyl route a whole range of solvents and temperatures could be tested, here the use of dry THF as the solvent is necessary and the polymerisation has to be performed at a sufficiently low temperature.

3.3.1 Monomer synthesis

In the reports on the xanthate precursor route, the bisxanthate monomer was always synthesised in one step by addition of the potassium salt of ethylxanthic acid to the corresponding bishalomethyl compound. Thus, to obtain the bisxanthate monomer, 2,5-bisethoxy(thiocarbonyl)thiomethyl-3,4-diphenylthiophene, the first goal was finding a synthetic route towards 3,4-diphenyl-2,5-bischloromethylthiophene **97**. In this regard, two possible routes were successfully tested. The first route (scheme 3.16) started with the esterification of the two carboxylic groups of the commercially available thiodiglycolic acid **92** with ethanol[83]. Next, the Hinsberg reaction between diethyl thiodiacetate **93** and benzil produced the thiophene ring system[84]. Consecutive reduction of the two carboxylic groups of **95** with lithium aluminium hydride ($LiAlH_4$) followed by chlorination of the diol with thionyl chloride ($SOCl_2$) yielded the desired dichloride **97**. Compound **97** is quite unstable and degradation occurred in the attempt to purify it by means of column chromatography.

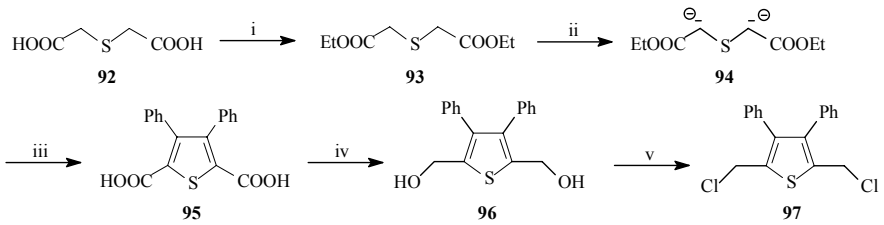

Scheme 3.16*: First possibility in the synthesis of 3,4-diphenyl-2,5-bischloromethylthiophene: i) 2 EtOH; ii) NaOH, EtOH; iii) PhC(O)C(O)Ph; iv) $LiAlH_4$, THF; v) $SOCl_2$, THF*

In the second possible route towards dichloride **97**, first 3,4-diphenylthiophene **101** was synthesised. (Scheme 3.17) Compound **101** could be obtained either via a Suzuki coupling reaction between the commercially available phenylboronic acid **102** and 3,4-dibromothiophene **103**, or via the method developed by Nakayama *et al*.[85, 86]. The latter involves the synthesis of thiophenes with two substituents on the 3- and 4-positions. Starting from commercially available 2-bromoacetophenon **98**, the reaction with sodium sulphide nonahydrate ($Na_2S.9H_2O$) yielded 1,5-diphenyl-3-thiapentane-15-dione **99**. Next 3,4-diphenylthiolane-3,4-diol **100** was formed by the intramolecular reductive coupling reaction with a low-valent titanium reagent prepared from titanium(IV)chloride ($TiCl_4$) and Zn powder. Treatment of the diol with *p*-toluenesulphonic acid ($TsOH.H_2O$) in refluxing benzene gave

3,4-diphenylthiophene **101**. The synthesis via the Suzuki coupling reaction is preferred since it requires only one step and the yield (77%) is better than the overall yield (29%) of the three step synthesis towards **101**.

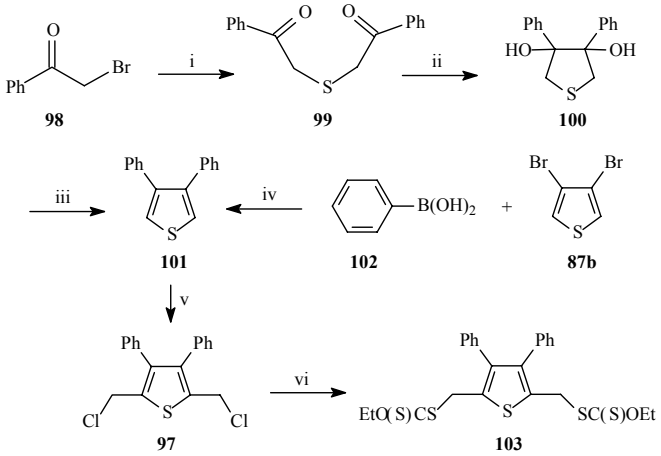

***Scheme 3.17**: Second possibility in the synthesis of 3,4-diphenyl-2,5-bischloromethylthiophene: i) $Na_2S.9H_2O$, Me_2CO/H_2O; ii) $TiCl_4$, Zn, THF; iii) $TsOH.H_2O$, PhH; iv) $Pd(PPh_3)_4$, KF, toluene/H_2O; v) CH_2O, HCl, Ac_2O; vi) KSC(S)OEt, MeOH*

The desired dichloride **97** was then obtained via the same chloromethylation reaction as used in the synthesis of **88a**. Another possible route to obtain compound **97** was reported in literature[87]. It involved the synthesis of 2,5-dibromo-3,4-diphenylthiophene by dibromination of 3,4-diphenylthiophene with *N*-bromosuccinimide (NBS) which was treated with *t*-BuLi. The resulting 2,5-dilithiated thiophene was treated with *N,N*-dimethylformamide (DMF) to give 3,4-diphenylthiophene-2,5-dicarbaldehyde, which was then reduced to **97** by $NaBH_4$. This route however was not applied in our lab because we already had experienced problems to obtain 3,4-dichlorothiophene-2,5-dicarbaldehyde (paragraph 3.2.1). Finally the bis-(*O*-ethyl xanthate) monomer **103** was synthesised as mentioned earlier from the bischloromethyl compound **97** by reaction with the potassium salt of ethylxanthic acid.

3.3.2 Polymerisation via the xanthate precursor route

When Son *et al.* reported for the first time on the xanthate route, they proposed that the polymerisation proceeded via a *p*-quinodimethane intermediate since the solution became red after addition of the base (K*t*BuO)[72]. However no real evidence could be found.

We neither could demonstrate the presence of a *p*-QM intermediate with stop flow UV-Vis measurements on monomer **103**. Nevertheless polymerisation in dry THF with 1.05 equivalents of Na*t*BuO as the base was possible. The polymerisations were performed using the same procedure as described in paragraph 3.2.3 and the results are given in table 3.3. The eluent used to determine the molecular weight of the precursor polymers by GPC was THF. After the precursor polymer is precipitated in the cold *n*-hexane/ether solution, the filtrate was evaporated which yielded the residual fraction. Analysis of this fraction with ^{1}H NMR spectroscopy indicated that it consisted only of monomer **103**.

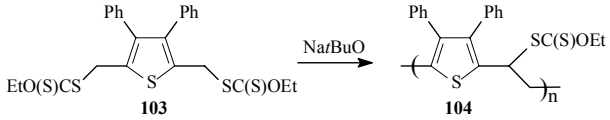

103 **104**

Entry	Temperature (°C)	Yield (%)	M_w (x 10^{-3})	PD
1	-15	32	7.2	1.4
2	0	38	35.7	8.4
3	15	34	16.1	3.9

Table 3.3**: Polymerisation results for monomer **103

Precursor polymers could be synthesised from the bisxanthate monomer **103** but their molecular weights were rather low. From *in-situ* UV-Vis and FT-IR measurements it could be seen that the elimination of the xanthate groups occurred between 105 and 175°C. The UV-Vis spectra of the precursor polymer **104** and of poly(3,4-diphenyl-2,5-thienylene vinylene) are given in figure 3.29. The band gap derived from the low energy side of the spectrum of the conjugated polymer (dashed line) is 1.6 eV.

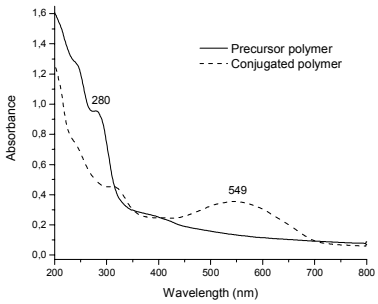

***Figure 3.29**: UV-Vis spectra of precursor polymer **104** and of poly(3,4-diphenyl-2,5-thienylene vinylene)*

3.4 Synthesis of poly(3,4-dichloro-2,5-thienylene vinylene) and poly(3,4-dibromo-2,5-thienylene vinylene) via the xanthate precursor route

Since the synthesis of electron rich PTV derivatives was possible via the xanthate precursor polymerisation route, this route was also tested for the electron poor dichloro PTV derivative discussed earlier. Starting from compound **88a**, the monomer was obtained using exactly the same procedure as described in the previous paragraph. (Scheme 3.18)

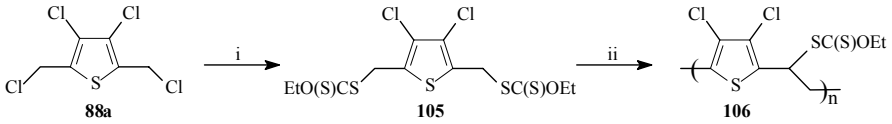

***Scheme 3.18**: Synthesis of xanthate monomer and precursor polymer: i) KSC(S)OEt, MeOH; ii) NatBuO, THF*

Also the polymerisation conditions were analogous as describes above. An overview of the polymerisation results is depicted in table 3.4. THF and chloroform are the two eluents used in the GPC analyses. Except for entry 2, a higher molecular weight was found with $CHCl_3$ as the eluent indicating that the latter is a better solvent for precursor polymer **106**. Very high polydispersities were detected and analysis of the residual fraction indicated that it consisted only of monomer **105**.

Entry	Temperature (°C)	Yield (%)	M_w (x 10^{-3}) (THF)	PD (THF)	M_w (x 10^{-3}) ($CHCl_3$)	PD ($CHCl_3$)
1	-15	20	475.7	69.9	491.3	50.5
2	0	40	439.4	35.1	172.9	28.0
3	15	14	397.4	67.6	440.1	67.7
4	40	9	38.5	7.5	43.7	6.6

Table 3.4**: Polymerisation results for monomer **105

It has now been proven that both electron rich and electron poor monomers can be polymerised via the xanthate precursor route.

The high elimination temperature of the xanthate groups in the precursor polymer is an important drawback of the xanthate route. *In-situ* UV-Vis and complementary *in-situ* FT-IR studies on polymer **106** with M_w = 439 400 in THF, showed that the elimination occurred in a temperature range from 125 to 175°C. In figure 3.30 the absorption at λ_{max} of the conjugated polymer (492 nm) and at λ_{max} of the precursor polymer (285 nm) is plotted as a function of increasing temperature.

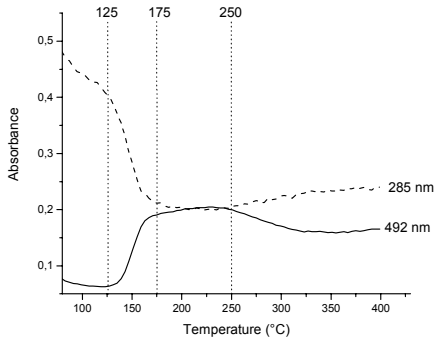

***Figure 3.30**: UV-Vis profiles for the absorption at 285 nm and 492 nm as a function of temperature*

3.5 Conclusion

Two different precursor routes towards poly(3,4-disubstituted-2,5-thienylene vinylene)s were successfully tested. Whereas the use of the sulphinyl precursor route is limited to electron poor derivatives like poly(3,4-dichloro-2,5-thienylene vinylene) and poly(3,4-dibromo-2,5-thienylene vinylene), the xanthate precursor route can be used in the synthesis of both electron poor and electron rich derivatives. The synthesis of the bischloromethyl monomer of an electron rich system still forms the most important obstacle in the synthesis of the bisxanthate monomer. This however does not alter the fact that the xanthate route could be an alternative in the cases where the synthesis of the sulphinyl monomer is problematic. For this reason an investigation of the xanthate route towards poly(2,5-thienylene vinylene) was performed. This will be dealt with in chapter four.

3.6 Experimental part

Materials: All solvents used in the synthesis were distilled before use. Tetrahydrofuran (THF) was refluxed under nitrogen with sodium metal and benzophenone until a blue colour persisted and was then distilled. All commercially available products were purchased from Acros or Aldrich.

Characterisation: ^{1}H NMR spectra were taken at 300 MHz on a Varian Inova spectrometer. For all synthesised compounds, ^{1}H NMR spectra were recorded in deuterated chloroform or deuterated water; chemical shifts (δ) in ppm were determined relative to the residual $CHCl_3$ or H_2O absorption at 7.24 ppm and 4.72 ppm respectively. ^{13}C NMR spectra were recorded at 75 MHz on the same spectrometer. Chemical shifts are determined relative to the ^{13}C resonance shift of $CHCl_3$ at 77.0 ppm. All spectra were obtained at ambient temperature.

The molecular weights and molecular weight distributions were determined in the same way as described in chapter two. Not only a DMF solution of oxalic acid ($1.1\ 10^{-3}$ M) was used as the eluent but also THF could be used. To characterise the materials further (TLC, GC/MS, CV), the same instruments were used as described in chapter two.

Fourier transform-infrared (FT-IR) spectroscopy was performed on a Perkin Elmer Spectrum One FT-IR spectrometer (nominal resolution 4 cm^{-1}, summation of 16 scans). Samples for the FT-IR characterisation were prepared by spin-coating the precursor polymer from a chloroform solution (6 mg/mL) onto NaCl discs (diameter 25 mm and thickness 1 mm) at 500 rpm. The NaCl discs were heated in a Harrick oven high temperature cell (purchased from Safir), which was positioned in the beam of the FT-IR to allow *in-situ* measurements. The temperature of the sample and the heating source were controlled by a Watlow temperature controller (serial number 999, dual channel). The heating source was in direct contact with the NaCl disc. Spectra were taken continuously and the heating rate was 2°C/min up to 400°C. All measurements were performed under a continuous flow of nitrogen. Timebase software was used to investigate regions of interest.

Ultraviolet visible (UV-Vis) spectroscopy was performed on a VARIAN CARY 500 UV-Vis-NIR spectrophotometer (interval: 1 nm, scan rate: 600 nm/min, continuous run from 200 to 700 nm). The precursor polymer was spin-coated from a chloroform solution (6 mg/mL) onto quartz glass (diameter 25 mm and thickness 3 mm) at 700 rpm. The quartz

glass was heated in the same Harrick oven high temperature cell as was used in the FT-IR measurements. The cell was placed in the beam of the UV-Vis spectrophotometer and spectra were taken continuously. The heating rate was 2°C/min. All measurements were performed under a continuous flow of nitrogen. Scanning kinetics software was used to investigate the regions of interest.

Direct insertion probe mass spectroscopy (DIP-MS) was performed on a FINNIGAN TSQ 70, in electron impact mode, mass range of 35-650 and scan rate of 2 s. The electron energy was 70 eV. A chloroform solution of the precursor polymer was placed directly on the heating element of the probe and measurements were performed under high vacuum (4.10^{-4} Pa). The polymer was heated from ambient temperatures till 650°C at a heating rate of 10°C/min.

Thermo Gravimetric analysis (TGA) was carried out on a TA INSTRUMENT 951 thermo gravimetric analyser with a continuous flow of nitrogen (50 mL/minute) and a heating rate of 10°C/min. The sample was inserted in the solid state.

Tetrachlorothiophene (73)

A flask with hexachloro-1,3-butadiene (15.06 g, 57.75 mmol) was placed in a heating mantle and refluxed. Sulphur (5.54 g, 0.173 mol) was added in portions. After this, the mixture was refluxed for 13 hours. A vacuum distillation resulted in 9.5 g (75% yield) of the pure product. MS (EI, m/e): 220 (M^+), 185 (M^+ - Cl), 150 (M^+ – 2 Cl), 115 (M^+ – 3 Cl), 79 (M^+ – 4 Cl)

3,4-Dichlorothiophene-2-carbaldehyde (76)

A solution of tetrachlorothiophene **73** (1 g, 4.545 mmol) in dry ether (10 mL) was cooled to 5°C on an ice-bath. A 1.6 M solution of *n*-BuLi in hexane (6.25 mL) was added to the solution over a period of 15 to 20 minutes. When the precipitation of the dilithium salt started, the ice bad was removed and the mixture was stirred for two hours at room temperature. Then the solvents were removed and dry THF (40 mL) was added. The mixture was cooled to -40°C and anhydrous DMF (0.94 mL, 12.27 mmol) was added drop wise. The mixture was first warmed to room temperature and then refluxed overnight. The reaction mixture was poured into 100 mL of an aqueous HCl solution (0.1 M) and a saturated aqueous sodium hydrogen carbonate ($NaHCO_3$) solution was added until the mixture was neutral. Further work-up consisted in extracting the mixture with $CHCl_3$ (3 x 10

mL) and drying the combined organic phases over $MgSO_4$. Evaporation of the solvent yielded only compound **76**. ^1H NMR ($CDCl_3$): 9.99 (s, 1H), 7.60 (s, 1H)

3,4,5-Trichlorothiophene-2-carbaldehyde (77)

The procedure is quite similar to the one described above but here only one equivalent of *n*-BuLi is used instead of 2.2 equivalents. After 3 g (13.64 mmol) of **73** was dissolved in dry THF (20 mL) and cooled to 0°C, 8.5 mL of a 1.6 M solution of *n*-BuLi in hexane was added. After two hours of stirring at room temperature, the mixture was cooled to -40°C and anhydrous DMF (1.41 mL, 18.41 mmol) was added. The work-up was analogous as described for **76** and the crude product was purified by column chromatography (silica gel, *n*-hexane/chloroform 7/3). 1.3 g (45% yield) of **77** was obtained as a white solid. ^1H NMR ($CDCl_3$): 9.96 (s, 1H); MS (EI, m/e): 214 (M^+), 185 (M^+ - C(O)H), 150 (M^+ - C(O)H - Cl), 115 (M^+ - C(O)H - 2 Cl)

2-Chloromethyl-3,4,5-trichlorothiophene (79)

A solution of aldehyde **77** (1 g, 4.672 mmol) in THF (20 mL) was cooled on an ice-bath. After $NaBH_4$ (0.27 g, 7.009 mmol) was added portion wise, the mixture was allowed to warm to ambient temperature. Then it was stirred at this temperature for one hour. An aqueous solution of HCl (1M) was added until the mixture was neutral. After extraction with $CHCl_3$ (3 x 20 mL) the combined organic layers were dried over $MgSO_4$ and the solvent was evaporated. The alcohol formed in this way was used without further purification. To an ice-cold solution of the alcohol in THF (5 mL), thionyl chloride (0.38 mL, 5.14 mmol) was added drop wise. The mixture was stirred at room temperature for one hour and $NaHCO_3$ was added until the mixture was neutral. After extraction with $CHCl_3$ (3 x 20 mL), the combined organic layers were dried over $MgSO_4$ and the solvent was evaporated. Overall yield: 60%; ^1H NMR ($CDCl_3$): 4.68 (s, 2H); MS (EI, m/e): 234 (M^+), 199 (M^+ - Cl), 164 (M^+ - 2 Cl), 129 (M^+ - 3 Cl)

2-Thiooctylmethyl-3,4,5-trichlorothiophene (80)

1-Octanethiol (0.45 g, 3.056 mmol) was added drop wise to a solution of sodium *tert*-butoxide (0.4 g, 4.167 mmol) in dry THF (10 mL). The mixture was stirred at room temperature for half an hour. Then compound **79** (0.65 g, 2.778 mmol) in dry THF (10 mL)

was added and the mixture was stirred for two hours. An aqueous solution of HCl (1M) was added until the mixture was neutral. After extraction with $CHCl_3$ (3 x 20 mL) the combined organic layers were dried over $MgSO_4$ and the solvent was evaporated. Yield: 85%; ^{1}H NMR ($CDCl_3$): 3.80 (s, 2H), 2.50 (t, 2H), 1.58 (m, 2H), 1.14-1.45 (m, 10H), 0.86 (t, 3H); MS (EI, m/e): 344 (M^+), 231 (M^+ - C_8H_{17}), 199 (M^+ - SC_8H_{17}), 164 (M^+ - SC_8H_{17} - Cl), 129 (M^+ - SC_8H_{17} - 2 Cl)

2,3,4-Trichloro-5-(dioxolan-2-yl)thiophene (82)

To a solution of 3,4,5-trichlorothiophene-2-carbaldehyde **77** (1 g, 4.673 mmol) in 20 mL of toluene, ethylene glycol (1,2-ethanediol) (0.29 mL, 5.14 mmol) and a catalytic amount of *p*-TsOH were added. The mixture was kept under reflux, and an azeotrope of toluene/H_2O was collected in a Dean – Stark apparatus. After three hours, the reaction was completed. The solvent was evaporated and the crude reaction product was purified by column chromatography (silica gel, *n*-hexane/$CHCl_3$ 1/1) which yielded 1.02 g of the pure product. Yield: 85%; ^{1}H NMR ($CDCl_3$): 6.10 (s, 1H), 4.07 (td, 2H), 4.01 (td, 2H); MS (EI, m/e): 258 (M^+), 223 (M^+ - Cl), 188 (M^+ - 2 Cl), 73 ($C_3H_5O_2^+$)

3,4-Dichloro-5-(dioxolan-2-yl)thiophene-2-carbaldehyde (83)

This compound was obtained in an analogous way as described for **77**, starting from **82** (1 g, 3.876 mmol), 2.5 mL of a 1.6 M solution of *n*-BuLi in hexane and DMF (0.4 mL, 5.232 mmol). The crude reaction product was purified by column chromatography (silica gel, *n*-hexane/$CHCl_3$ 1/1). Yield: 51%; ^{1}H NMR ($CDCl_3$): 10.03 (s, 1H), 6.18 (s, 1H), 4.11 (td, 2H), 4.06 (td, 2H); MS (EI, m/e): 252 (M^+), 217 (M^+ - Cl), 182 (M^+ - 2 Cl), 73 ($C_3H_5O_2^+$)

3,4-Dichloro-5-chloromethylthiophene-2-carbaldehyde (86)

This compound was obtained in an analogous way as described for **79**, starting from **83** (0.5 g, 1.984 mmol) in THF (10 mL), $NaBH_4$ (0.11 g, 2.976 mmol) and $SOCl_2$ (0.16 mL, 2.183 mmol). The crude reaction product was purified by column chromatography (silica gel, *n*-hexane/$CHCl_3$ 3/7) which yielded a white solid. Yield: 40%; ^{1}H NMR ($CDCl_3$): 10.03 (s, 1H), 4.73 (s, 2H); MS (EI, m/e): 228 (M^+), 193 (M^+ - Cl). For compound **85** which was obtained as a side product: ^{1}H NMR ($CDCl_3$): 6.14 (s, 1H), 4.70 (s, 2H), 4.10 (td, 2H), 4.02 (td, 2H); MS (EI, m/e): 272 (M^+), 237 (M^+ - Cl), 73 ($C_3H_5O_2^+$)

3,4-Dichloro-5-thiooctylmethylthiophene-2-carbaldehyde (81)

This compound was obtained in an analogous way as described for **80**. However, the yield after column chromatography (silica gel, *n*-hexane/$CHCl_3$ 7/3) was only 5%. ^1H NMR ($CDCl_3$): 10.00 (s, 1H), 3.85 (s, 2H), 2.52 (t, 2H), 1.57 (m, 2H), 1.14-1.44 (m, 10H), 0.86 (t, 3H)

3,4-Dichlorothiophene (87a)

Tetrachlorothiophene **73** (15 g, 0.0682 mol) was dissolved in dry ether (10 mL) and cooled down to 5°C. 93.75 mL of a 1.6 M *n*-BuLi solution in hexane (0.15 mol) was dropped to the solution over 15 to 20 minutes. When the precipitation of the dilithium salt started, the ice bad was removed and the mixture was stirred for two hours at room temperature. Then water (10 mL) and a 1 M HCl aqueous solution was added until the mixture was neutral. Further work-up consisted in extracting the mixture with $CHCl_3$ (3 x 10 mL) and drying of the combined organic phases over $MgSO_4$. The crude reaction product was purified by column chromatography (silica gel, *n*-hexane) which yielded 6.9 g of the pure product as a colourless oil. Yield: 67%; ^1H NMR ($CDCl_3$): 7.19 (s, 2H); MS (EI, m/e): 152 (M^+), 117 (M^+ - Cl)

3,4-Dichloro-2,5-bischloromethylthiophene (88a)

To paraformaldehyde (2.67 g, 0.0888 mol) and 3,4-dichlorothiophene (5 g, 0.0329 mol) in a three-necked flask, concentrated HCl (18.25 g, 0.1875 mol) and acetic anhydride (33.55 g, 0.329 mol) were added under nitrogen atmosphere. After 22 hours refluxing this mixture at 70°C, 10 mL of a cold saturated aqueous solution of sodium acetate and 10 mL of a 25% aqueous solution of sodium hydroxide were added. The mixture was extracted with $CHCl_3$ (3 x 50 mL) and dried over $MgSO_4$. Purification by column chromatography (silica, $CHCl_3$/*n*-hexane 1/1) gave the pure product as white crystals. Yield: 79%; ^1H NMR ($CDCl_3$): 4.71 (s, 4H); MS (EI, m/e): 248 (M^+), 213 (M^+ - Cl), 178 (M^+ – 2 Cl), 143 (M^+ – 3 Cl), 108 (M^+ – 4 Cl)

3,4-Dibromo-2,5-bischloromethylthiophene (88b)

This compound was obtained in an analogous way as described for **58a**, starting from 3,4-dibromothiophene (5 g, 20.661 mmol), paraformadehyde (1.67 g, 55.785 mmol), HCl (11.46

g, 117.768 mmol) and acetic anhydride (21.07 g, 0.2066 mol). Yield: 67%; ^{1}H NMR ($CDCl_3$): 4.73 (s, 4H); MS (EI, m/e): 338 (M^+), 303 (M^+ – Cl), 268 (M^+ – 2 Cl)

3,4-Dichloro-2,5-bis(tetrahydrothiopheniomethyl)thiophene dichloride (89a)

A solution of 3,4-dichloro-2,5-bischloromethylthiophene (820 mg, 3.306 mmol) and THT (1.28 g, 14.548 mmol) in methanol (10 mL) was stirred for five days at room temperature. The reaction mixture was precipitated in cold acetone. The salt was filtered off and dried in an exsiccator. Yield: 12%; ^{1}H NMR (D_2O): 4.80 (s, 4H), 3.53 (m, 8H), 2.34 (m, 8H)

3,4-Dichloro-2-chloromethyl-5-thiooctylmethylthiophene (91a)

A mixture of sodium *tert*-butoxide (153 mg, 1.595 mmol) and 1-octanethiol (233 mg, 1.595 mmol) in methanol (10 mL) and a mixture of 3,4-dichloro-2,5-bis(tetrahydrothiophenio-methyl)thiophene dichloride **89a** in methanol (50 mL) were stirred at room temperature for half an hour. Then the anion was added to the salt and the mixture was stirred at room temperature for one hour. Methanol was removed and the oil thus obtained was diluted with *n*-octane or petroleum ether (boiling range 100-130°C) and concentrated to remove tetrahydrothiophene. The sequence was repeated three times to afford a crude mixture that was purified by column chromatography (silica, $CHCl_3$/*n*-hexane 1/9). Yield: 35%; ^{1}H NMR ($CDCl_3$): 4.70 (s, 2H), 3.83 (s, 2H), 2.50 (t, 2H), 1.56 (m, 2H), 1.12-1.45 (m, 10H), 0.86 (t, 3H); MS (EI, m/e): 358 (M^+), 323 (M^+ – Cl), 213 (M^+ – SC_8H_{17})

3,4-Dichloro-2-chloromethyl-5-(*n*-octylsulphinyl)methylthiophene (68a, R' = octyl)

An aqueous (35 wt%) solution of H_2O_2 (1 mL) was added drop wise to a solution of **91a** (1.82 g, 5.096 mmol), TeO_2 (84 mg, 0.526 mmol) and three drops of concentrated HCl in methanol (30 mL). After three hours the reaction was quenched by adding a saturated aqueous NaCl solution (10 mL). The reaction mixture was extracted with $CHCl_3$ (3 x 20 mL), the combined organic layers were dried over $MgSO_4$, and concentrated in vacuo to afford a reaction mixture that was purified by column chromatography (silica, $CHCl_3$/diethyl ether 8/2). Yield: 95%

Direct synthesis of 68a, R' = octyl

A mixture of 3,4-dichloro-2,5-bischloromethylthiophene **88a** (2 g, 8.065 mmol) in 10 mL of toluene, NaOH (839 mg, 20.97 mmol) in 10 mL of H_2O and a catalytical amount of

methyltrioctylammonium chloride or Aliquat 336, was stirred at room temperature. A solution of 1-octanethiol (589 mg, 4.032 mmol) in toluene (5 mL) was dropped to this mixture. The reaction mixture was then stirred at room temperature for an additional five hours. After extraction with $CHCl_3$ (3 x 30 mL), drying over $MgSO_4$ and evaporation of the solvent, the product was oxidised as described above. Overall yield: 35%; ^{1}H NMR ($CDCl_3$): 4.71 (s, 2H), 4.18 (d, J = 14.1 Hz, 1H), 4.09 (d, J = 14.1 Hz, 1H), 2.62 (t, 2H), 1.73 (m, 2H), 1.42 (m, 2H), 1.16-1.37 (m, 8H), 0.86 (t, 3H); UV-Vis ($CHCl_3$): λ_{max} at 266 nm

3,4-Dichloro-2-chloromethyl-5-(*n*-ethylsulphinyl)methylthiophene (68a, R' = ethyl)
This compound was obtained in an analogous way as described for the direct synthesis of **68a** with R' = octyl, starting from **88a** (2 g, 8.065 mmol), NaOH (839 mg, 20.97 mmol) and ethanethiol (250 mg, 4.032 mmol). Overall yield: 18%; ^{1}H NMR ($CDCl_3$): 4.70 (s, 2H), 4.18 (d, J = 14.1 Hz, 1H), 4.08 (d, J = 14.1 Hz, 1H), 2.65 (m, 2H), 1.34 (t, 3H); UV-Vis ($CHCl_3$): λ_{max} at 265 nm

3,4-Dibromo-2-chloromethyl-5-(*n*-octylsulphinyl)methylthiophene (68b, R' = octyl)
This compound was obtained in an analogous way as described for the direct synthesis of **68a** with R' = octyl, starting from **88b** (2 g, 5.917 mmol), NaOH (615 mg, 15.38 mmol) and 1-octanethiol (432 mg, 2.959 mmol). Overall yield: 38%; ^{1}H NMR ($CDCl_3$): 4.73 (s, 2H), 4.23 (d, J = 14.1 Hz, 1H), 4.13 (d, J = 14.1 Hz, 1H), 2.63 (t, 2H), 1.75 (m, 2H), 1.42 (m, 2H), 1.16-1.37 (m, 8H), 0.85 (t, 3H); ^{13}C NMR ($CDCl_3$): 136.36, 127.56, 115.97, 115.06, 51.88, 51.27, 39.52, 31.66, 29.11, 28.92, 28.77, 22.56, 22.51, 14.05; UV-Vis ($CHCl_3$): λ_{max} at 266 nm

Poly{(3,4-dichlorothienylene)-[1-(*n*-octylsulphinyl)ethylene]} (71a, R' = octyl)
A solution of monomer **68a**, R' = octyl (250 mg, 0.668 mmol) and a solution of sodium *tert*-butoxide (77 mg, 0.802 mmol for entry 1 and 67 mg, 0.702 mmol for entry 2-3) were degassed for one hour at 30°C by passing through a continuous stream of nitrogen. The base solution was added in one portion to the stirred monomer solution. After one hour the reaction mixture was poured in a well-stirred amount (100 mL) of ice water. The mixture was neutralised with aqueous hydrogen chloride solution (1 M) and extracted with $CHCl_3$ (3 x 100 mL). The combined organic layers were concentrated in vacuo. The crude product was dissolved in $CHCl_3$ and precipitated in 100 mL of an ice-cold *n*-hexane/diethyl ether (3/1)

solution. The polymer was collected and dried. The residual fraction was concentrated in vacuo. The polymerisation results are summarised in table 3.1. UV-Vis ($CHCl_3$): λ_{max} at 267 nm

Poly{(3,4-dibromothienylene)-[1-(*n*-octylsulphinyl)ethylene]} (71b, R' = octyl)

This compound was obtained in an analogous way as described for **71a,** R' = octyl, starting from monomer **68b** (250 mg, 0.541 mmol) and sodium *tert*-butoxide (55 mg, 0.568 mmol). UV-Vis ($CHCl_3$): λ_{max} at 267 nm

Poly{(3,4-dichlorothiophene)-[1-(ethylsulphinyl)ethylene]} (71a, R' = ethyl)

This compound was obtained in an analogous way as described for **71a,** R' = octyl, starting from monomer **68a**, R' = ethyl (250 mg, 0.862 mmol) and sodium *tert*-butoxide (87 mg, 0.905 mmol)

Diethyl thiodiacetate (93)

Thiodiglycolic acid (10 g, 0.0667 mol) was refluxed with 30 mL of absolute ethanol in the presence of 3 drops of concentrated H_2SO_4 as a catalyst. After the reaction mixture was refluxed overnight, an extraction with $CHCl_3$ (3 x 50 mL) was performed, the combined organic layers were dried over $MgSO_4$ and the solvent was evaporated. Yield: 90%; ^{1}H NMR ($CDCl_3$): 4.17 (qu, 4H), 3.60 (s, 4H), 1.26 (t, 6H); MS (EI, m/e): 206 (M^+), 161 (M^+ – OEt), 133 (M^+ – COOEt), 104 (M^+ – COOEt – Et)

3,4-Diphenylthiophene-2,5-dicarboxylic acid (95)

To a mixture of thiodiglycolic ethylester **93** (2 g, 9.709 mmol) and benzil (2.04 g, 9.709 mmol) in methanol (15 mL), NaOMe (1.57 g, 29.13 mmol) was added as a solid. The mixture was stirred at ambient temperature for three days. Water was added and the alcohol was evaporated. The solid (benzil) was filtered off and the filtrate was acidified with HCl. The white solid that was formed in this way was filtered off. Yield: 64%; ^{1}H NMR (CD_3OD): 7.12-7.05 (m, 6H), 7.02-6.93 (m, 4H); DIP MS (CI, m/e): 325 (M^+ + 1), 281 (M^+ + 1 - COO)

3,4-Diphenyl-2,5-bischloromethylthiophene (97)

3,4-Diphenylthiophene-2,5-dicarboxylic acid **95** (1 g, 3.086 mmol) in dry THF was added to a solution of $LiAlH_4$ (0.35 g, 9.259 mmol) in dry THF, cooled on an ice-bath. The mixture was allowed to warm to ambient temperature, was stirred at this temperature for two hours and was afterwards refluxed for another two hours. The reaction was worked up by the addition of HCl (1M). After extraction with $CHCl_3$ (3 x 20 mL) the combined organic layers were dried over $MgSO_4$ and the solvent was evaporated. The alcohol formed in this way was used without further purification [DIP MS (EI, m/e): 296 (M^+), 279 (M^+ - OH), 249]. To an ice-cold solution of the alcohol in THF (5 mL), thionyl chloride (0.5 mL, 6.790 mmol) was added drop wise. The mixture was stirred at room temperature for two hours and $NaHCO_3$ was added until the mixture was neutral. After extraction with $CHCl_3$ (3 x 20 mL) the combined organic layers were dried over $MgSO_4$ and the solvent was evaporated. Yield: 42%; ^1H NMR ($CDCl_3$): 7.24-7.21 (m, 6H), 7.08-7.05 (m, 4H), 4.67 (s, 4H); MS (EI, m/e): 332 (M^+), 297 (M^+ - Cl), 261 (M^+ – 2 Cl)

1,5-Diphenyl-3-thiapentane-1,5-dione (99)

A solution of $Na_2S.9H_2O$ (10.47 g, 43.60 mmol) in water (50 mL) was added to an ice-cold solution of 2-bromoacetophenon (15 g, 87.21 mmol) in acetone (70 mL) in a period of one hour. The mixture was allowed to warm to ambient temperature and was stirred for one hour. After dilution with water, an extraction with $CHCl_3$ (3 x 50 mL) was performed, the combined organic layers were dried over $MgSO_4$ and the solvent was evaporated. Yield: 42%; ^1H NMR ($CDCl_3$): 7.97 (dd, 4H), 7.60-7.55 (tt, 2H), 7.48-7.43 (t, 4H), 3.97 (s, 4H); MS (EI, m/e): 270 (M^+), 237, 165, 105

3,4-Diphenythiolane-3,4-diol (100)

To a well-stirred solution of Zn powder (7.22 g, 111.11 mmol) and 1,5-diphenyl-3-thiapentane-1,5-dione **99** (5 g, 18.52 mmol) in dry THF (60 mL) under argon and at –18°C, $TiCl_4$ (6.1 mL, 55.56 mmol) was dropped over a period of three hours. The mixture was allowed to warm to 0°C and stirred for three hours at 0 – 15°C. The reaction was quenched by addition of crushed ice and the pH of the solution was brought to 9 by adding an aqueous solution of K_2CO_3. Dichloromethane was added and the mixture was stirred overnight. The mixture was filtered by a large glass filter on which a pad of Celite was placed. The organic

layer of the filtrate was washed with water 5 times, dried over $MgSO_4$ and evaporated. Yield: 89%; ^1H NMR ($CDCl_3$): 7.19-7.05 (m, 10H), 3.62 (d, 2H), 3.15 (d, 2H); MS (EI, m/e): 236 ($M^+ - H_2O$), 152, 120, 105

3,4-Diphenylthiophene (101)

(a) A mixture of 3,4-diphenythiolane-3,4-diol **100** (4.5 g, 16.544 mmol) and $TsOH.H_2O$ (1.57 g, 8.272 mmol) in benzene (30 mL) was refluxed for 4 hours and an azeotrope of toluene/H_2O was collected in a Dean – Stark apparatus. The obtained mixture was washed with an aqueous solution of $NaHCO_3$ (5%) and then with water, dried over $MgSO_4$ and evaporated. The crude mixture was purified by column chromatography (silica, $CHCl_3$/*n*-hexane 1/4). Yield: 77%

(b) Phenylboronic acid (5 g, 40.984 mmol), 3,4-dibromothiophene (2.14 g, 8.852 mmol) and KF (2.10 g, 36.204 mmol) were dissolved in water (40 mL) and toluene (40 mL). $Pd(PPh_3)_4$ (730 mg) was added as a catalyst. After refluxing the mixture for 18 hours, an extraction with $CHCl_3$ (3 x 50 mL) was performed and the combined organic phases were dried over $MgSO_4$. The crude reaction product was purified by column chromatography (silica, *n*-hexane). Yield: 77%; ^1H NMR ($CDCl_3$): 7.30 (s, 2H), 7.25-7.21 (m, 6H), 7.19-7.16 (m, 4H); MS (EI, m/e): 236 (M^+)

3,4-Diphenyl-2,5-bischloromethylthiophene (97)

To paraformaldehyde (343 mg, 11.440 mmol) and 3,4-diphenylthiophene (1 g, 4.237 mmol) in a three-necked flask, concentrated HCl (2.35 g, 24.151 mmol) and acetic anhydride (4.32 g, 42.372 mmol) were added under nitrogen atmosphere. After 4.5 hours refluxing this mixture at 70°C, 10 mL of a cold saturated aqueous solution of sodium acetate and 10 mL of a 25% aqueous solution of sodium hydroxide were added. The mixture was extracted with $CHCl_3$ (3 x 50 mL) and dried over $MgSO_4$. Yield: 98%; ^1H NMR ($CDCl_3$): 7.24-7.21 (m, 6H), 7.08-7.05 (m, 4H), 4.67 (s, 4H); MS (EI, m/e): 332 (M^+), 297 (M^+ - Cl), 261 ($M^+ – 2$ Cl)

2,5-Bisethoxy(thiocarbonyl)thiomethyl-3,4-diphenylthiophene (103)

A mixture of 3,4-diphenyl-2,5-bischloromethylthiophene **97** (1.5 g, 4.518 mmol) and ethylxanthic acid potassium salt (3.61 g, 22.59 mmol) in 10 mL of methanol was stirred for three hours at room temperature. The mixture was extracted with $CHCl_3$ (3 x 50 mL), dried

over $MgSO_4$ and after the solvent was evaporated, 1.9 g (82% yield) of bisxanthate monomer was obtained as an orange solid; ^1H NMR ($CDCl_3$): 7.22-7.18 (m, 6H), 7.01-6.97 (m, 4H), 4.65 (q, 4H), 4.43 (s, 4H), 1.42 (t, 6H)

Poly{(3,4-diphenylthienylene)-[1-(*O*-ethylxanthate ethylene]} (104)

This compound was obtained in an analogous way as described for **71a**, starting from a solution of monomer **103** (250 mg, 0.496 mmol) in dry THF (3 mL) and a solution of sodium *tert*-butoxide (50 mg, 0.521 mmol) in dry THF (2 mL); UV-Vis ($CHCl_3$): λ_{max} at 280 nm

2,5-Bisethoxy(thiocarbonyl)thiomethyl-3,4-dichlorothiophene (105)

This compound was obtained in an analogous way as described for **103**, starting from **88a** (1 g, 4.032 mmol) and ethylxanthic acid potassium salt (3.23 g, 20.16 mmol). Yield: 1.63 g of monomer (96%) as a white solid; ^1H NMR ($CDCl_3$): 4.65 (q, 4H), 4.47 (s, 4H), 1.42 (t, 6H); ^{13}C NMR ($CDCl_3$): 212.45, 131.06, 122.98, 70.64, 33.02, 13.77; UV-Vis ($CHCl_3$): λ_{max} at 280 nm

Poly{(3,4-dichlorothienylene)-[1-(*O*-ethylxanthate ethylene]} (106)

This compound was obtained in an analogous way as described for **71a**, starting from a solution of monomer **105** (250 mg, 0.595 mmol) in dry THF (4 mL) and a solution of sodium *tert*-butoxide (60 mg, 0.625 mmol) in dry THF (2 mL), the reaction temperature here is not 30°C but –15°C (entry 1), 0°C (entry 2), 15°C (entry 3) or 40°C (entry 4); UV-Vis ($CHCl_3$): λ_{max} at 285 nm

3.7 References

1. H. Fuchigami, A. Tsumura, H. Koezuka, *Appl. Phys. Lett.* **1993**, 63, 10, 1372.
2. K. Kaeriyama, in: H. S. Nalwa, *Handbook of Organic Conductive Molecules and Polymers*, John Wiley & Sons, Chichester, **1997**, 271.
3. J. Roncali, *Chem. Rev.* **1997**, 97, 1, 173.
4. G. Kossmehl, M. Härtel, G. Manecke, *Macromol. Chem.* **1970**, 131, 1, 15.
5. G. Kossmehl, A. Yaridjanian, *Macromol. Chem.* **1981**, 182, 12, 3419.
6. L. Kreja, M. Kurzawa, J. Kurzawa, W. Czerwinski, *Pol., No 177165*, **1994**.

7. L. Kreja, M. Kurzawa, J. Kurzawa, *Macromol. Chem. Phys.* **1997**, 198, 2, 643.
8. C. Méalares, Z. Hui, A. Gandini, *Polymer* **1996**, 37, 11, 2273.
9. K. Harper, W. J. W. West, *Eur. Pat. Appl., No 182548*, **1985**.
10. R. A. Wessling, R. G. Zimmerman, *U.S. Patent No 3401152*, **1968**.
11. M. Kanbe, M. Okawara, *J. Polym. Sci., Part A-1* **1968**, 6, 4, 1058.
12. K.-Y. Jen, R. Jow, H. Eckhardt, R. L. Elsenbaumer, *Polym. Mater. Sci. Eng.* **1987**, 56, 49.
13. K.-Y. Jen, M. Maxfield, L. W. Shacklette, R. L. Elsenbaumer, *J. Chem. Soc., Chem. Commun.* **1987**, 4, 309.
14. K.-Y. Jen, R. Jow, L. W. Shacklette, M. Maxfield, H. Eckhardt, R. L. Elsenbaumer, *Mol. Cryst. Liq. Cryst* **1988**, 160, 69.
15. M. Onada, S. Morita, T. Iwasa, H. Nakayama, K. Yoshino, *J. Chem. Phys.* **1991**, 95, 11, 8584.
16. H. Eckhardt, L. W. Shacklette, K.-Y. Jen, R. L. Elsenbaumer, *J. Chem. Phys.* **1989**, 91, 2, 1303.
17. S. Yamada, S. Tokito, T. Tsutsui, S. Saito, *J. Chem. Soc., Chem. Commun.* **1987**, 19, 1448.
18. S. Tokito, T. Momii, H. Murata, T. Tsutsui, S. Saito, *Polymer* **1990**, 31, 6, 1137.
19. H. Murata, S. Tokito, T. Tsutsui, S. Saito, *Synth. Met.* **1990**, 36, 95.
20. T. Tsutsui, H. Murata, T. Momii, K. Yoshiura, S. Tokito, S. Saito, *Synth. Met.* **1991**, 41, 1-2, 327.
21. I. Murase, T. Ohnishi, T. Noguchi, M. Hirooka, *Polym. Commun.* **1987**, 28, 229.
22. I. Murase, T. Ohnishi, T. Noguchi, *Ger. Offen., No 3704411*, **1987**.
23. O. M. Gelsen, D. D. C. Bradley, H. Murata, N. Takada, T. Tsutsui, S. Saito, *J. Appl. Phys.* **1992**, 71, 2, 1064.
24. W. Eevers, D. De Schrijver, T. Dierick, C. Peten, J. Van Der Looy, H. J. Geise, *Synth. Met.* **1992**, 51, 329.
25. W. Eevers, M. De Wit, J. Briers, H. J. Geise, R. Mertens, P. Nagels, R. Callaerts, W. Herrebout, B. Vanderveken, *Polymer* **1994**, 35, 4573.
26. H.-Q. Xie, C.-M. Liu, J.-S. Guo, *Eur. Polym. J.* **1996**, 32, 9, 1131.
27. S. Iwatsuki, M. Kubo, H. Yamashita, *Chem. Lett.* **1989**, 5, 729.
28. M. Kubo, H. Yamashita, S. Iwatsuki, *Kobunshi Ronbunshu* **1989**, 46, 4, 241.
29. W. S. Trahanovsky, D. L. Miller, Y. Wang, *J. Org. Chem.* **1997**, 62, 8980.
30. Y. H. Lu, C. S. Hsu, C. H. Chou, T. H. Chou, *Macromolecules* **1996**, 29, 17, 5546.
31. T. Itoh, *Prog. Polym. Sci.* **2001**, 26, 1019.
32. W. Ten Hoeve, M. M. de Kok, B.-H. Huisman, P. T. Herwig, A. J. J. M. Van Breemen, *PCT Int. Appl., No 1290059*, **2001**.

33. S. Gillissen, *Ph. D. Dissertation* **2002**, Limburgs Universitair Centrum, Diepenbeek, Belgium.
34. K.-Y. Jen, R. L. Elsenbaumer, L. W. Shacklette, *Int. Patent Appl. PCT/US87/01688*, **1987**.
35. P. C. Van Dort, J. E. Pickett, M. L. Blohm, *Synth. Met.* **1991**, 42, 3, 2305.
36. M. L. Blohm, P. C. Van Dort, J. E. Pickett, *Abstr. Pap. Am. Chem. Soc.* **1991**, 201, 123.
37. M. L. Blohm, P. C. Van Dort, J. E. Pickett, *Chemtech* **1992**, 22, 2, 105.
38. M. L. Blohm, J. E. Pickett, P. C. Van Dort, *Macromolecules* **1993**, 26, 11, 2704.
39. L. D. Peeters, *Ph. D. Dissertation* **1996**, University of Antwerp, Belgium.
40. J. K. Stille, *Angew. Chem., Int. Ed. Engl.* **1986**, 25, 508.
41. R. Galarini, A. Musco, R. Pontellini, A. Bolognesi, S. Destri, M. Catellani, M. Mascherpa, G. Zhuo, *J. Chem. Soc., Chem. Commun.* **1991**, 6, 364.
42. A. Bolognesi, M. Catellani, A. Musco, R. Pontellini, *Synth. Met.* **1993**, 55, 2-3, 1255.
43. A. Bolognesi, M. Catellani, W. Porzio, F. Speroni, R. Galarini, A. Musco, R. Pontellini, *Polymer* **1993**, 34, 19, 4150.
44. E. E. Havinga, C. M. J. Mutsaers, L. W. Jenneskens, *Chem. Mater.* **1996**, 8, 769.
45. R. S. Loewe, R. D. McCullough, *Chem. Mater.* **2000**, 12, 10, 3214.
46. J. E. McMurry, M. P. Fleming, K. L. Kees, L. R. Krepski, *J. Org. Chem.* **1978**, 43, 17, 3255.
47. R. Dams, M. Malinowski, I. Westdorp, Y. J. Geise, *J. Org. Chem.* **1982**, 47, 248.
48. S. Iwatsuki, M. Kubo, Y. Itoh, *Chem. Lett.* **1993**, 1085.
49. Y. Itoh, T. Itoh, S. Iwatsuki, M. Kubo, *Polymer Bulletin* **1996**, 37, 155.
50. J. J. L. M. Cornelissen, E. Peeters, R. A. J. Janssen, E. W. Meijer, *Acta Polym.* **1998**, 49, 471.
51. F. Goldini, R. A. J. Janssen, E. W. Meijer, *J. Polym. Sci., Part A: Polym. Chem.* **1999**, 37, 4629.
52. Z. Guijiang, L. Junchao, Y. Cheng, *Synth. Met.* **2003**, 135-136, 485.
53. L. K. Bicknell, M. J. Marsella, T. M. Swager, *Polym. Prepr.* **1994**, 35, 1, 269.
54. F. Wudl, S. Hoger, C. Zhang, K. Pakbaz, A. J. Heeger, *Polym. Prepr.* **1993**, 34, 1, 197.
55. H. Cheng, R. L. Elsenbaumer, *J. Chem. Soc., Chem. Commun.* **1995**, 1451.
56. K.-Y. Jen, H. Eckhardt, T. R. Jow, L. W. Shacklette, R. L. Elsenbaumer, *J. Chem. Soc., Chem. Commun.* **1988**, 3, 215.
57. B. M. Trost, T. N. Salzmann, K. Hiroi, *J. Am. Chem. Soc.* **1976**, 98, 4887.
58. E. J. Geering, *J. Org. Chem.* **1959**, 24, 1128.
59. B. L. Feringa, R. Hulst, R. Rikers, L. Brandsma, *Synthesis* **1988**, 316.
60. T.-H. Tong, L.-C. Chien, *J. Polym. Sci., Part A: Polym. Chem.* **2000**, 38, 1450.
61. M. Takeshita, M. Tashiro, *J. Org. Chem.* **1991**, 56, 8, 2837.

62. H. Becker, H. Spreitzer, K. Ibrom, W. Kreuder, *Macromolecules* **1999**, 32, 4925.

63. M. R. Smith, H. Gilman, *J. Organometal. Chem.* **1972**, 42, 1.

64. A. J. J. M. Van Breemen, D. J. M. Vanderzande, P. J. Adriaensens, J. M. J. V. Gelan, *J. Org. Chem.* **1999**, 64, 9, 3106.

65. M. Van Der Borght, *Ph. D. Dissertation* **1998**, Limburgs Universitair Centrum, Diepenbeek, Belgium.

66. K. S. Kim, H. J. Hwang, C. S. Cheong, C. S. Hahn, *Tetrahedron Lett.* **1990**, 31, 20, 2893.

67. A. J. J. M. Van Breemen, A. C. J. Issaris, M. M. de Kok, M. J. A. N. Van Der Borght, P. J. Adriaensens, J. M. J. V. Gelan, D. J. M. Vanderzande, *Macromolecules* **1999**, 32, 18, 5728.

68. A. J. Van Breemen, *Ph. D. Dissertation* **1999**, Limburgs Universitair Centrum, Diepenbeek, Belgium.

69. R. H. Baughman, J. L. Brédas, R. R. Chance, R. L. Elsenbaumer, L. W. Shacklette, *Chem. Rev.* **1982**, 82, 209.

70. R. H. Baughman, L. W. Shacklette, *Phys. Rev. B* **1989**, 39, 9, 5872.

71. F. Padinger, R. S. Rittberger, N. S. Sariciftci, *Adv. Funct. Mater.* **2003**, 13, 1, 85.

72. S. Son, A. Dodabalapur, A. J. Lovinger, M. E. Galvin, *Science* **1995**, 269, 376.

73. S. Son, A. J. Lovinger, M. E. Galvin, *Polym. Mater. Sci. Eng.* **1995**, 72, 567.

74. J. Yang, H. Hong, M. E. Thompson, *Polym. Prepr.* **1999**, 40, 2, 1244.

75. S.-C. Lo, A. K. Sheridan, D. W. Samuel, P. L. Burn, *J. Mater. Chem.* **1999**, 9, 9, 2165.

76. S.-C. Lo, A. K. Sheridan, D. W. Samuel, *J. Mater. Chem.* **2000**, 10, 2, 275.

77. S.-C. Lo, L.-O. Palsson, M. Kilitziraki, P. L. Burn, I. D. W. Samuel, *J. Mater. Chem.* **2001**, 11, 9, 2228.

78. G. Arbuckle-Keil, Y. Liszewski, J. Peng, B. Hsieh, *Polym. Prepr.* **2000**, 41, 1, 826.

79. G. Arbuckle-Keil, Y. Liszewski, J. Wilking, B. Hsieh, *Polym. Prepr.* **2001**, 42, 1, 306.

80. W. J. Mitchell, C. Pena, P. L. Burn, *J. Mater. Chem.* **2002**, 12, 2, 200.

81. E. Kesters, S. Gillissen, F. Motmans, L. Lutsen, D. Vanderzande, *Macromolecules* **2002**, 35, 21, 7902.

82. S. Gillissen, A. Henckens, L. Lutsen, D. Vanderzande, J. Gelan, *Synth. Met.* **2003**, 135-136, 225.

83. B. Sankaran, J. R. Reynolds, *Macromolecules* **1997**, 30, 9, 2582.

84. O. Hinsberg, *Chem. Ber.* **1910**, 43, 901.

85. J. Nakayama, R. Hasemi, *J. Am. Chem. Soc.* **1990**, 112, 5654.

86. J. Nakayama, R. Hasemi, K. Yoshimura, Y. Sugihara, S. Yamaoka, *J. Org. Chem.* **1998**, 63, 4912.

87. J. Nakayama, Y. Hasegawa, Y. Sugihara, A. Ishii, *Sulfur Letters* **1999**, 22, 4, 131.

Chapter 4
Poly(2,5-thienylene vinylene)

4.1 Introduction

Poly(2,5-thienylene vinylene) (PTV) is a conjugated polymer that has attracted a lot of attention because of its high electrical conductivity upon doping[1] and its possible application as a semi-conductor in all-polymer field effect transistors[2] or as a chemiresistor[3, 4]. However, as mentioned in the introduction of chapter three, still no good polymerisation process toward PTV is developed. Given that substituted PTV derivatives could be synthesised via the xanthate precursor route[chapter three], the xanthate route is a possible alternative to obtain PTV. It was recently reported that xanthate leaving groups do not react with ITO (indium tin oxide), a commonly used electrode material, and hence xanthate groups should be suitable for device applications[5]. Moreover, the elimination products that are liberated during the elimination of xanthate groups are unstable and further react to form ethanol and carbon disulphide (CS_2) on one hand and ethanethiol (EtSH) and carbonoxy sulphide (OCS) on the other[6, 7]. These are all products with low boiling points and therefore evaporate fast. As a result they do not stay in the polymer film and the resulting conjugated polymer shows a high stability, which is of course of utmost importance for applications. So we decided to evaluate the applicability of the xanthate route in the synthesis of PTV.

4.2 Synthesis of PTV via the xanthate precursor route

4.2.1 Monomer synthesis

As already mentioned in chapter three, the bisxanthate monomer was always synthesised from the corresponding bishalomethyl compound. Synthesis of 2,5-

bischloromethylthiophene via a chloromethylation reaction of thiophene was already reported by different groups[8-10]. However, in the synthesis of the sulphinyl monomer, another procedure, which was more suitable towards upscaling and avoided the health risks of a chloromethylation reaction, was developed[11]. Here first the commercially available 2,5-thiophenedicarboxylic acid **107** was converted to diester **108** which subsequently was transferred into diol **109** using $LiAlH_4$. (Scheme 4.1) Then 2,5-bischloromethylthiophene **110** was obtained by reaction with thionylchloride ($SOCl_2$). Since also here the dichloride proved to be highly unstable, an *in-situ* reaction towards 2,5-bis(tetrahydrothiopheniomethyl)-thiophene dichloride **111** was performed. This hygroscopic bissulphonium salt was less reactive and as already reported was best stored under N_2 atmosphere at low temperature[10]. The synthesis of the xanthate monomer was a very easy, single step reaction from the bissulphonium salt **111**: the salt was dissolved in acetonitrile with a minimal amount of water and ethylxanthic acid potassium salt was added as a solid.

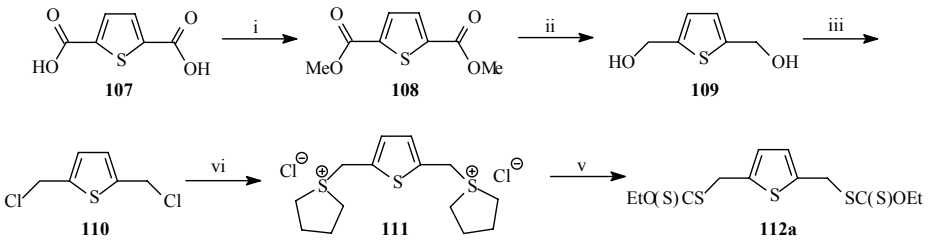

***Scheme 4.1**: Synthesis of xanthate monomer **112a**:*
i) MeOH, H_2SO_4, ΔT; ii) $LiAlH_4$, THF; iii) $SOCl_2$, THF; vi) THT; v) $KSC(S)OEt$, CH_3CN/H_2O

It was of course also possible to synthesise the xanthate monomer **112a** directly from dichloride **110**. But owing to the possibility of storage of salt **111**, the synthesis via scheme 4.1 was preferred. When new monomer was needed, only one step had to be performed and it was not necessary to go through the synthesis of the unstable dichloride.

4.2.2 Polymerisation

The polymerisation of monomer **112a** was not performed in a thermostatic flask as described in chapter three but in a three-necked flask. In this flask, the monomer was dissolved in dried THF or dried 1,4-dioxane and degassed for 1 hour by passing through a continuous stream of nitrogen. Depending on the applied polymerisation temperature, this

was done at -78°C, 0°C or ambient temperature. Then, an equimolar amount of base solution was added. When the polymerisation was performed at 0°C and K*t*BuO (or Na*t*BuO) was used as the base, precursor polymer was obtained in relatively low yield (18%) and low molecular weight (M_w of 21 900)[11]. By using lithium diisopropyl amide (LDA) as the base, the yield could be increased thanks to the improved solubility of LDA at low temperature. In all the performed polymerisations a 2 M LDA solution in THF/*n*-hexane was used and it was added through a septum that was placed on one neck of the flask. After the addition of the base solution, the reaction was stirred at a given temperature for 90 minutes under nitrogen atmosphere. Then, the mixture was poured out in ice water. When the polymerisation temperature was -78°C, first the mixture was quenched with ethanol because water would freeze at this temperature. After extraction with chloroform, the combined organic layers were concentrated in vacuo. The crude product was dissolved in chloroform, precipitated in a 1/1 mixture of diethyl ether and *n*-hexane at 0°C, collected and dried in vacuo. An overview of the performed polymerisations is given in table 4.1. The molecular weights listed in this table were determined by GPC relative to PS standards and THF was used as the eluent. The residual fractions consisted of monomer **112a**.

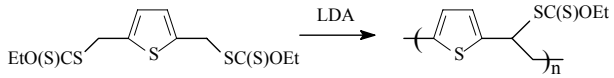

112a **113a**

Entry	Solvent	Monomer conc. (M)	Polymerisation temperature	M_w (x 10^{-3}) (g/mol)	PD	Yield (%)
1	THF	0.05	-78°C → 0°C*	108.7	21.7	31
2	THF	0.1	-78°C → 0°C	238.6	30.0	36
				258.3	22.1	34
3	THF	0.2	-78°C → 0°C	360.6	19.7	36
4	THF	0.3	-78°C → 0°C	107.6	28.3	38
5	THF	0.1	Room temp.	48.7	11.1	16
6	THF	0.1	0°C	37.0	6.7	18
7	THF	0.1	-78°C	350.8	26.0	37
8	1,4-dioxane	0.1	Room temp.	6.0	2.2	8
9	1,4-dioxane	0.2	Room temp.	3.85	1.8	11

* Polymerisation at -78°C for 90 minutes, warming up to 0°C for 15 minutes and afterwards quenching with ice water

Table 4.1**: Polymerisation results for monomer **112a

These data demonstrate that the concentration and especially the temperature are important parameters in the polymerisation process. By changing the concentration (entry 1-4), the yield stayed more or less constant but it seems that the molecular weight reached an optimum for a monomer concentration of 0.2 M. To check the influence of temperature, four polymerisations were executed at different polymerisation temperatures (entry 2, 5-7). Increasing the temperature decreased the yield and the molecular weight so that apparently a low temperature is favourable for the xanthate polymerisation route. The need to use a sufficiently low polymerisation temperature in this route was already reported earlier[12-14]. THF proved to be a better solvent compared to 1,4-dioxane (entry 8-9). Due to the high melting point of 1,4-dioxane (12°C), only the polymerisation at higher temperatures could be executed which is certainly unfavourable. All the precursor polymers had very broad molecular weight distributions. The polydispersity values range from 7 to 30. This could be an indication for the occurrence of different polymerisation mechanisms in competition with each other.

After these results were obtained in our lab, also Burn *et al.* published an article on the preparation of PTV via the xanthate precursor route[15]. They polymerised monomer **112a** as a 1 M (dried) THF solution at room temperature with 0.9 equivalents of K*t*BuO. Under these conditions the precursor polymer was isolated in a 16% yield. A weight-average molecular weight of 78.10^3 and a polydispersity of 4.5 were found. These results are in good agreement with the ones obtained in our lab. The rather low yield and low molecular weight result from the choice of the base and the relatively high temperature that was used.

4.3 Variation of the xanthate group

Because the elimination temperature of the commonly used *O*-ethyl xanthate group was quite elevated (see next paragraph), the idea to alter this group arose. After all, a different eliminable group could possibly lower the temperature necessary for the conversion of the precursor polymer to the conjugated polymer. Another disadvantage inherent to the *O*-ethyl xanthate group in the xanthate monomer is the lower leaving group capacity compared to the chlorine atom in the sulphinyl monomer. As a result the yield of a polymerisation via this route is lower than of a polymerisation via the sulphinyl precursor

route. By placing electron withdrawing groups on the xanthate salt, the group could possibly be a better leaving group and as a result increase the yield. For this purpose, first new xanthic acid salts had to be synthesised since they were not commercially available. Alkali metal salts of the *O*-alkyl dithiocarbonates (xanthates) are prepared by the reaction of carbon disulphide (CS_2) with an alcohol (ROH) and an alkali metal hydroxide[16].

$$ROH + KOH + CS_2 \rightarrow KSC(S)OR + H_2O$$

Two new salts with electron withdrawing groups could be prepared. After refluxing the corresponding alcohol (2-methoxyethanol or 2,2,2-trifluoroethanol) in the presence of potassium hydroxide, carbon disulphide was added under constant stirring. The salt precipitated and could be filtered off. Reaction of the 2-methoxyethyl xanthate salt **114b** with bissulphonium salt **111** yielded monomer **112b**. (Scheme 4.2) This reaction was performed in the same way as for monomer **112a**.

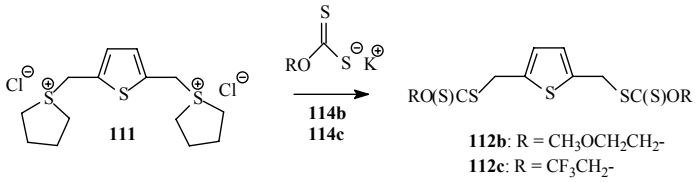

***Scheme 4.2**: Synthesis of new xanthate monomers*

By adding the trifluoroethyl xanthate salt **114c** to bissulphonium salt **111**, no trifluoroethyl xanthate monomer **112c** could be obtained. Instead an insoluble orange solid was formed which was characterised by solid state NMR (Cross Polarisation/Magic Angle Spinning ^{13}C NMR) as PTV. This could be explained by assuming that a Wessling polymerisation had occurred. The pH of an aqueous solution of **114c** was 14 and thus basic enough to start the polymerisation of the bissulphonium salt. Diluting the reaction mixture 350 times reduced the formation of PTV but despite the correct mass spectrum, the NMR spectrum was not in agreement with monomer **112c**. Direct synthesis from the reaction of dichloride **110** with **114c** did also not yield the new monomer. Therefore, only the methoxyethyl xanthate monomer **112b** was polymerised. The procedure, as described above, to polymerise the ethyl xanthate monomer was also applied here. The polymerisation results are listed in table 4.2. The molecular weights were determined by GPC in THF relative to PS standards.

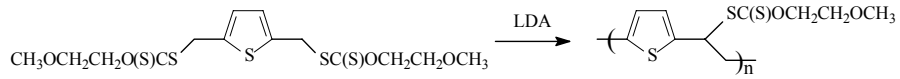

112b **113b**

Entry	Solvent	Monomer conc. (M)	Polymerisation temperature	M_w (x 10^{-3}) (g/mol)	PD	Yield (%)
1	THF	0.05	-78°C → 0°C*	31.7	6.9	11
2	THF	0.2	-78°C → 0°C	28.6	6.2	15
3	THF	0.3	-78°C → 0°C	20.2	6.5	16

* Polymerisation at -78°C for 90 minutes, warming up to 0°C for 15 minutes and afterwards quenching with ice water

Table 4.2**: Polymerisation results for monomer **112b

Compared to the *O*-ethyl xanthate precursor polymers, the yield and molecular weight decreased dramatically. From synthetic point of view we can thus conclude that the use of the methoxyethyl xanthate functional group does not lead to a good alternative for the synthesis of PTV.

4.4 Comparative study of the elimination of the two different xanthate groups

Also here the last step in the synthesis of the polymer (PTV) is the thermal elimination of the xanthate groups in the precursor polymer to obtain the double bonds and thus the conjugated structure. The techniques to investigate this conversion are the same as described for the poly(3,4-dihalo-2,5-thienylene vinylene)s in chapter three: *in-situ* UV-Vis spectroscopy, *in-situ* FT-IR spectroscopy and DIP-MS. For the *in-situ* techniques, a non-isothermal heating program of 2°C per minute up to 350°C under a continuous flow of nitrogen was used. Since one of the reasons to perform the synthesis of the new xanthate was to reduce the elimination temperature, the results derived from these techniques for both xanthate precursor polymers **113a** and **113b** are compared below.

The gradual formation of the conjugated structure, starting from the ethyl (Et) and the methoxyethyl ($CH_3OCH_2CH_2$) xanthate precursor polymers, as obtained from UV-Vis measurements are shown in figures 4.1 and 4.2 respectively. The ethyl xanthate precursor polymer shows a maximum absorption at 289 nm, the methoxyethyl xanthate precursor

polymer at 252 nm. On heating the precursor, a new absorption band is formed which red shifts by increasing the temperature. The absorption peaks at 520 nm for the ethyl and at 480 nm for the methoxyethyl xanthate. We should however again make the remark that this maximum wavelength has been measured at high temperature (200°C). If we want to compare our λ_{max} values with the reported values from *ex-situ* UV-Vis measurements, the thermochromic effect has to be taken into account as explained in chapter three. To acquire λ_{max} at room temperature, an additional experiment was performed. Here the ethyl xanthate precursor **113a** was heated from ambient temperature to 185°C at 2°C per minute under a continuous flow of nitrogen. After the sample was heated for 5 minutes at 185°C, it was cooled back to room temperature. The λ_{max} value then measured at 25°C was 536 nm which is, as expected, higher than λ_{max} at 200°C. In a previous report from Kossmehl, where PTV oligomers ($Th[CH=CHTh]_n$) were prepared via the Wittig reaction, it has already been shown that the maximum increased with increasing conjugation length from λ_{max} = 340 nm for n = 1 via λ_{max} = 460 nm for n = 3 and λ_{max} = 490 nm for n = 4 to the limiting value of λ_{max} = 520 nm[17]. By looking at a series of oligomers and extrapolating to high polymer, Kossmehl[18] predicted that the absorption maximum for PTV should be 550 nm. Jen *et al.*[19] observed an absorption maximum at about 600 nm and therefore concluded that PTV prepared by the modified Kanbe[20] and Wessling[21, 22] procedure is extensively conjugated and of high quality. The by us observed value of 536 nm is therefore quite low compared to the higher values reported in literature. This blue shift was also reported by Burn *et al.*[15] and may relate to defects in the structure of the PTV obtained.

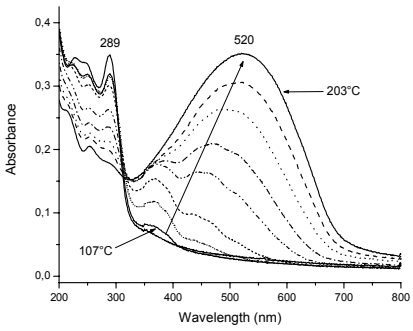

***Figure 4.1**: UV-Vis spectra of **113a** at different temperatures*

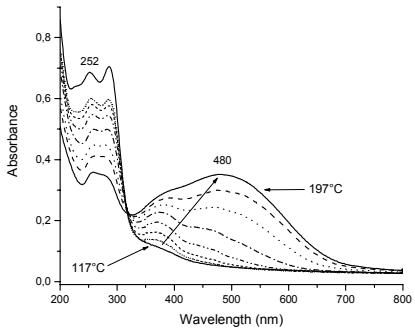

***Figure 4.2**: UV-Vis spectra of **113b** at different temperatures*

When these two characteristic wavelengths of both polymers are plotted as a function of temperature, the trends in elimination behaviour are clearly observed. For the ethyl xanthate, the formation of the first conjugated segments begins at about 115°C and the elimination is completed at 175°C. For the methoxyethyl xanthate, similar results are obtained. However, PTV obtained via the new xanthate seems to be less stable since the temperature area of stability of the conjugated polymer is smaller. In the region between 175°C and 250°C, no decrease in the absorbance of the double bond is visible for PTV from **113a** but for PTV from **113b** there is a slight decrease.

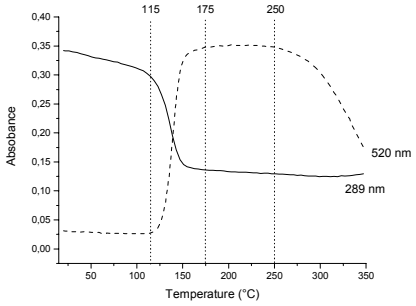

Figure 4.3**: Absorbance profiles at 289 and 520 nm as a function of temperature for **113a

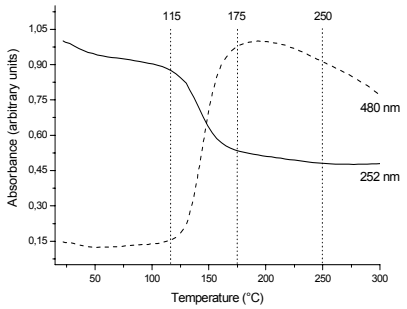

Figure 4.4**: Absorbance profiles at 252 and 480 nm as a function of temperature for **113b

In-situ FT-IR measurements are strictly speaking expected to yield a confirmation of the conclusions derived from the *in-situ* UV-Vis measurements. In the precursor polymer, most of the IR absorptions arise from stretchings within the xanthate group. From the ethyl xanthate group, strong absorption bands at 1216 cm^{-1}, 1109 cm^{-1} and 1044 cm^{-1} are visible which is in perfect agreement with previous reported values[6]. From the methoxy ethyl xanthate group an absorption band at 1060 cm^{-1} appears. When heating the precursor, a new absorption band at 930 cm^{-1} is formed for both precursors. This band is assigned to the *trans*-vinylene C-H out-of-plane bending band[15, 23]. At the same time as this band is formed, the bands from the xanthate group decline in intensity which is an indication that the xanthate group is being eliminated. The changes in intensity for the different peaks are shown in figure 4.5 and 4.6 where an overlay of IR spectra at different temperatures is plotted. By plotting these absorptions as a function of temperature, we can again see the trends in elimination behaviour. (Figure 4.7 and 4.8) The slight decrease in intensity of the

signal at 930 cm^{-1} at increasing temperature in the region between 115 and 250°C, is difficult to interpret because a very small signal is followed here.

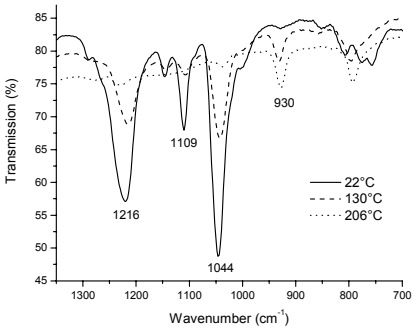

***Figure 4.5**: IR spectra of **113a** at 22, 130 and 206°C*

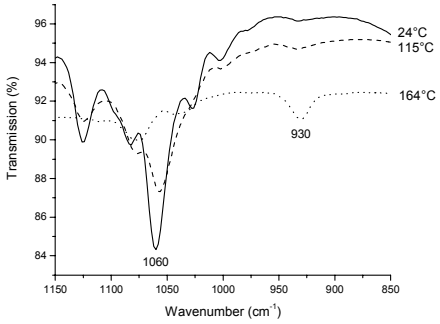

***Figure 4.6**: IR spectra of **113b** at 24, 115 and 164°C*

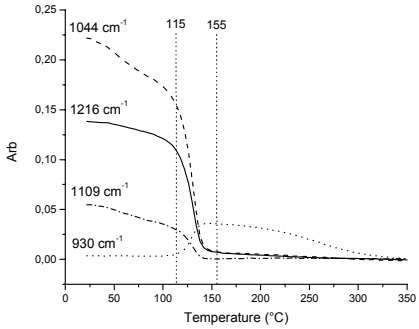

Figure 4.7**: IR absorption profiles at 1216, 1109, 1044 and 930 cm^{-1} as a function of temperature for **113a

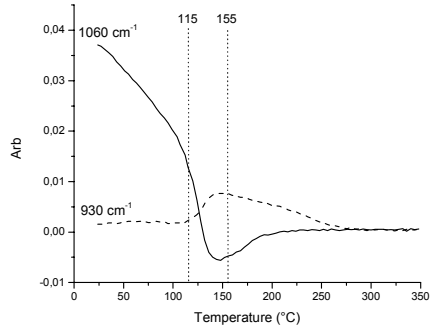

Figure 4.8**: IR absorption profiles at 1060 and 930 cm^{-1} as a function of temperature for **113b

The comparison of the profiles for the two different xanthate groups, obtained from these *in-situ* techniques, reveals no major difference in elimination temperature. We can thus conclude that placing a methoxy group on the ethyl xanthate functionality does not cause a decrease in elimination temperature.

From the last technique (DIP-MS), information on the elimination and degradation products is obtained. In this technique the precursor polymer is heated from ambient temperatures till 600°C under reduced pressure (4.10^{-4} Pa). The elimination products of the ethyl xanthate precursor polymer correspond well with the elimination products reported before[5, 12, 14]. When the total ion current is plotted as a function of temperature (figure 4.9

and 4.10), two signals are observed of which the first one (ethyl: 170-240°C, methoxyethyl: 150-250°C), based on the fragments detected (EtO(S)CS, EtO(S)C and CS_2 for the ethyl xanthate and $CH_3OCH_2CH_2O(S)CS$, $CH_3OCH_2CH_2O(S)C$, $CH_3OCH_2CH_2$ and CS_2 for the methoxyethyl xanthate), can be assigned to the elimination of the xanthate groups and the second one (ethyl: 350-450°C, methoxyethyl: 350-470°C) to the evaporation of the degradation products of the conjugated polymer. The higher elimination temperature observed with this technique compared to *in-situ* UV-Vis and FT-IR is assigned to the difference in heating rate (DIP-MS: 10°C/min, *in-situ* UV-Vis and IR measurements: 2°C/min).

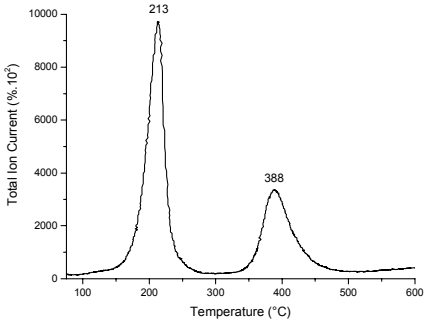

Figure 4.9**: DIP-MS thermogram of **113a

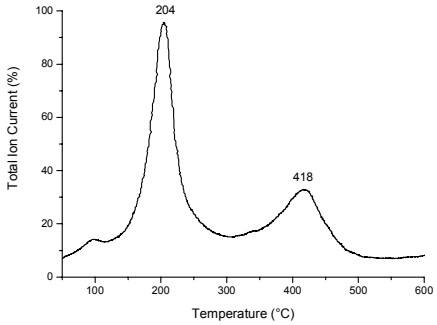

Figure 4.10**: DIP-MS thermogram of **113b

4.5 Transistor behaviour of poly(2,5-thienylene vinylene)

The xanthate precursor polymer **113a** was also tested in a TFT device. The measurements were performed on a top-contact parallel transistor (L[‡] = 75 μm; W[§] = 2000 μm) and carried out by Tom Aernouts at IMEC in Leuven. After dissolving the precursor polymer in chlorobenzene in a concentration of 1% (w:v%), it was spin-coated. Subsequently the gold contacts (source and drain) were evaporated on top of the device. Before starting the measurement, the precursor was converted to PTV by heating the sample from room temperature to 185°C at 2°C per minute. After the sample was hold at 185°C for 10 minutes, it was cooled back to ambient temperature. The results of the transistor measurements are listed in table 4.3.

[‡] L is the length of the channel between the source and the drain electrode
[§] W is the width of the channel between the source and the drain electrode

M_w x 10^{-3} (g/mol)	Mobility (cm^2/Vs)	I_{on}/I_{off}	Threshold voltage (V)
37	1.2 x 10^{-6}	2	-13
100.7	2.7 x 10^{-4}	4 400	-10
186	9.5 x 10^{-4}	9 400	-0.3
282.3	1.6 x 10^{-4}	4 500	-6
360.6	5.6 x 10^{-4}	72 000	-7

Table 4.3**: Transistor properties of **113a

For the low molecular weights, an increase of mobility, I_{on}/I_{off} ratio and threshold voltage is observed with increasing molecular weight. This confirms the trend which was already observed before[11]. Unfortunately, when the molecular weight increases further, the mobility seems to become lower. We have no explanation for the deviation of the mobility for the last two measurements and as a result no relevant conclusion can be drawn.

However the mobility is much lower than the value of 0.22 cm^2 $V^{-1}s^{-1}$ reported by Fuchigami *et al.*[24]. In this report PTV was obtained from a methoxy leaving group precursor polymer. Nevertheless this result has not yet been reproduced and the values listed in table 4.3 are in good agreement with the values reported by Vandamme *et al.*[25], by Brown *et al.*[26], and with the value of 1.4 10^{-4} cm^2 $V^{-1}s^{-1}$ reported by M. De Wit[27] for the same type of PTV as Fuchigami used.

4.6 Conclusion

It was found that the xanthate precursor route can be used to obtain PTV. Due to the low boiling points of the elimination products, an improved stability of the corresponding conjugated polymer was found. Drawbacks however in the use of this route were the rather low yield and the high polydispersities of the obtained polymers. The latter is a strong indication that more than one polymerisation mechanism is active during the polymerisation process. The deviation of λ_{max} of PTV obtained via the xanthate route compared with literature values for PTV seems to point to a defective structure of PTV so obtained.

Synthesis of a new xanthate monomer bearing other groups than the commonly used *O*-ethyl xanthate group was possible. In spite of this, the yield and molecular weights of the obtained precursor polymer were quite low. Use of these groups could not lead to a lowering of the elimination temperature. The transistor properties observed for PTV prepared from the *O*-ethyl xanthate precursor polymer were in good agreement with the values reported by other groups.

4.7 Experimental part

For the characterisation methods and materials used here we would like to refer to the experimental part of chapter two and three. The synthesis of compounds **108** to **111** is described elsewhere[11].

2,5-Bis[ethoxy(thiocarbonyl)thiomethyl]thiophene (112a)

To 80 mL of an acetonitrile/water solution (5 vol% water) of bissulphonium salt **111** (8 g, 0.0224 mol), ethylxanthic acid potassium salt (8.25 g, 0.0515 mol) was added as a solid after which the mixture was stirred at ambient temperature for two hours. Then, water was added and the desired xanthate monomer was extracted with ether (3 x 100 mL) and dried over $MgSO_4$. Evaporation of the solvent yielded 7 g (89%) of the pure product as a white solid; Mp: 36.0-37.4°C; ^{1}H NMR ($CDCl_3$): 6.80 (s, 2H), 4.65 (q, 4H), 4.48 (s, 4H), 1.41 (t, 6H). ^{13}C NMR ($CDCl_3$): 213.13, 138.61, 126.74, 70.27, 35.02, 13.77; MS (EI, m/e): 231 (M^+ – SC(S)OEt), 110 (M^+ – 2 x SC(S)OEt); UV-Vis ($CHCl_3$): λ_{max} at 294 nm

Polymerisation of monomer 112a (113a)

All polymerisations were carried out in dry THF or dry 1,4-dioxane at different temperatures and concentrations of monomer. A solution of monomer **112a** (250 mg, 0.71 mmol) in dry solvent (14.2, 7.1, 3.55 or 2.37 mL = 0.05, 0.1, 0.2 or 0.3 M respectively) at –78°C (or rt or 0°C) was degassed for 1 hour by passing through a continuous nitrogen flow. An equimolar LDA solution (355 μL[**] of a 2 M solution in THF/*n*-hexane) was added in one go to the stirred monomer solution. The mixture was kept at –78°C (or rt or 0°C) for 90 minutes and the passing of nitrogen was continued. After this, the solution was allowed to come to 0°C or

[**] This 0.35 ml of solvent from the base solution was neglected in the calculation of the monomer concentration

ethanol (5 mL) was added at -78°C to stop the reaction (this was not necessary if the polymerisation was performed at rt or 0°C). The polymer was precipitated in ice water (100 mL) and extracted with chloroform (3 x 60 mL). The solvent of the combined organic layers was evaporated under reduced pressure and a second precipitation was performed in a 1/1 mixture (100 mL) of diethyl ether and hexane at 0°C. The polymer was collected and dried in vacuo. ^{1}H NMR ($CDCl_3$): 6.62-6.69 (br s, 1H), 6.44-6.53 (br s, 1H), 5.01-5.12 (br s, 1H), 4.53-4.66 (br q, 2H), 3.46-3.58 (br m, 1H), 3.25-3.37 (br m, 1H), 1.35-1.41 (br t, 3H); ^{13}C NMR ($CDCl_3$): 212.16, 140.51, 140.12, 126.24 (2C), 70.13, 51.03, 37.67, 13.83; UV-Vis ($CHCl_3$): λ_{max} at 289 nm. The residual fractions only contained monomer residues.

2-Methoxyethylxanthic acid potassium salt (114b)

In a flask, potassium hydroxide (KOH) pellets (20 g, 0.357 mol) and 2-methoxyethanol (110 mL, 1.389 mol) were refluxed for 1 hour. Then, CS_2 (27.14 g, 0.357 mol) was slowly added under constant stirring. After cooling the reaction mixture in an ice-bath, the resulting solid was filtered off and washed with ether (3 x 10 mL). After drying the salt in an exsiccator, 34.4 g (55%) of the pure salt was yielded as a white solid. ^{1}H NMR (D_2O): 4.45 (t, 2H), 3.68 (t, 2H), 3.31 (s, 3H).

2,2,2-Trifluoroethylxanthic acid potassium salt (114c)

The preparation of **114c** is analogous to that described for **114b** but here 2,2,2-trifluoroethanol (89 mL, 1.237 mol) was used. Yield: 20% (15.03 g, 0.0702 mol); ^{1}H NMR (D_2O): 3.82 (q, 2H)

2,5-Bis[2-methoxyethoxy(thiocarbonyl)thiomethyl]thiophene (112b)

The preparation of **112b** is analogous to that described for **112a** but here 2-methoxyethylxanthic acid potassium salt was used. Yield: 70%; ^{1}H NMR ($CDCl_3$): 6.82 (s, 2H), 4.72 (t, 4H), 4.50 (s, 4H), 3.72 (t, 4H), 3.39 (s, 6H); ^{13}C-NMR ($CDCl_3$): 213.06, 138.24, 126.74, 72.59, 69.49, 58.87, 35.00; MS (EI, m/e): 261 (M^+ – $SC(S)OCH_2CH_2OCH_3$), 142 (M^+ - $C_8H_{14}O_4S_3$), 110 (M^+ – 2 x $SC(S)OCH_2CH_2OCH_3$); UV-Vis ($CHCl_3$): λ_{max} at 220 and 261 nm

2,5-Bis[2,2,2-trifluoroethoxy(thiocarbonyl)thiomethyl]thiophene (112c)

Via bissulphonium salt (111)

The preparation in analogous to that described for **112a** but here 2,2,2-trifluoroethylxanthic acid potassium salt was used. ^{1}H NMR ($CDCl_3$): not correct; MS (EI, m/e): 285 (M^+ – $SC(S)OCH_2CF_3$), 110 (M^+ – 2 x $SC(S)OCH_2CF_3$)

Via dichloride (110)

To a solution of 2,5-bischloromethylthiophene (freshly prepared from diol **109** (3.5 g, 0.0243 mol)) in methanol, 2,2,2-trifluoroethylxanthic acid potassium salt (11.9 g, 0.0556 mol) was added as a solid after which the mixture was stirred at ambient temperature for two hours. Then, water was added and the desired xanthate monomer was extracted with ether (3 x 100 mL). The organic layer was dried over $MgSO_4$ and filtered, the solvent was evaporated, and column chromatography was performed (eluent: hexane/EtOAc, 1/1). This resulted in 3 g of a product as yellow oil. ^{1}H NMR ($CDCl_3$): not correct; MS (EI, m/e): 285 (M^+ – $SC(S)OCH_2CF_3$), 110 (M^+ – 2 x $SC(S)OCH_2CF_3$)

Polymerisation of monomer 112b (113b)

The polymerisation method is the same as described for the polymerisation of monomer **112a**. ^{1}H NMR ($CDCl_3$): 6.60-6.69 (br s, 1H), 6.44-6.51 (br s, 1H), 4.99-5.13 (br s, 1H), 4.57-4.72 (br m, 2H), 3.62-3.74 (br m, 2H), 3.60-3.50 (br s, 2H), 3.27-3.40 (br s, 3H); UV-Vis ($CHCl_3$): λ_{max} at 252 nm

4.8 References

1. G. A. Kossmehl, in: T. A. Skotheim, *Handbook of Conducting Polymers*, Dekker, Basel, New York, **1986**, 351.

2. C. J. Drury, C. M. J. Mutsaers, C. M. Hart, M. Matters, D. M. de Leeuw, *Appl. Phys. Lett.* **1998**, 73, 1, 108.

3. M. De Wit, E. Vanneste, F. Blockhuys, H. J. Geise, *Synth. Met.* **1997**, 85, 1303.

4. M. De Wit, E. Vanneste, H. J. Geise, L. J. Nagels, *Sensors and Actuators B* **1998**, 50, 2, 164.

5. S.-C. Lo, L.-O. Palsson, M. Kilitziraki, P. L. Burn, I. D. W. Samuel, *J. Mater. Chem.* **2001**, 11, 9, 2228.

6. G. Arbuckle-Keil, Y. Liszewski, J. Peng, B. Hsieh, *Polym. Prepr.* **2000**, 41, 1, 826.

7. G. Arbuckle-Keil, Y. Liszewski, J. Wilking, B. Hsieh, *Polym. Prepr.* **2001**, 42, 1, 306.
8. J. M. Griffing, L. F. Salisbury, *J. Am. Chem. Soc.* **1948**, 70, 3416.
9. M. Takeshita, M. Tashiro, *J. Org. Chem.* **1991**, 56, 8, 2837.
10. W. Eevers, D. De Schrijver, T. Dierick, C. Peten, J. Van Der Looy, H. J. Geise, *Synth. Met.* **1992**, 51, 329.
11. S. Gillissen, *Ph. D. Dissertation* **2002**, Limburgs Universitair Centrum, Diepenbeek, Belgium.
12. S. Son, A. Dodabalapur, A. J. Lovinger, M. E. Galvin, *Science* **1995**, 269, 376.
13. S.-C. Lo, A. K. Sheridan, D. W. Samuel, P. L. Burn, *J. Mater. Chem.* **1999**, 9, 9, 2165.
14. E. Kesters, S. Gillissen, F. Motmans, L. Lutsen, D. Vanderzande, *Macromolecules* **2002**, 35, 21, 7902.
15. W. J. Mitchell, C. Pena, P. L. Burn, *J. Mater. Chem.* **2002**, 12, 2, 200.
16. B. S. Furniss, A. J. Hannaford, P. W. G. Smith, A. R. Tatchell, *Vogel's Textbook of Practical Organic Chemistry*, 5th ed., Longman: New York, **1989**, p. 793.
17. G. Kossmehl, M. Härtel, G. Manecke, *Macromol. Chem.* **1970**, 131, 1, 15.
18. G. Kossmehl, *Ber. Bunsenges. Phys. Chem.* **1979**, 83, 417.
19. K.-Y. Jen, R. Jow, H. Eckhardt, R. L. Elsenbaumer, *Polym. Mater. Sci. Eng.* **1987**, 56, 49.
20. M. Kanbe, M. Okawara, *J. Polym. Sci., Part A-1* **1968**, 6, 4, 1058.
21. R. A. Wessling, R. G. Zimmerman, *U.S. Patent No 3401152*, **1968**.
22. R. A. Wessling, R. G. Zimmerman, *U.S. Patent No 3706677*, **1968**.
23. M. Onada, S. Morita, T. Iwasa, H. Nakayama, K. Yoshino, *J. Chem. Phys.* **1991**, 95, 11, 8584.
24. H. Fuchigami, A. Tsumura, H. Koezuka, *Appl. Phys. Lett.* **1993**, 63, 10, 1372.
25. L. K. J. Vandamme, R. Feyaerts, G. Trefan, C. Detcheverry, *J. Appl. Phys.* **2002**, 91, 2, 719.
26. A. R. Brown, C. P. Jarrett, D. de Leeuw, M. Matters, *Synth. Met.* **1997**, 88, 37.
27. M. De Wit, *Ph. D. Dissertation* **1997**, UIAntwerpen, Belgium.

Chapter 5
The dithiocarbamate precursor route

5.1 Introduction

An *N,N*-dialkyl dithiocarbamate group (-SC(S)NR_2) can be seen as a modified xanthate group (-SC(S)OR). When looking in literature, mono- and bis-dithiocarbamate molecules have been used as photoiniferters. An example of such a bifunctional iniferter is *p*-xylylene bis(*N,N*-diethyl dithiocarbamate) (XDC or XDT). (Figure 5.1) It was first synthesised in 1984 by Otsu *et al.*[1] and used for the living radical polymerisation of styrene and methyl methacrylate. Today, 16 papers[1-16] and 12 patents[17-28] exist on the use of this compound as an iniferter. The number of reports on the iniferter polymerisation in general is of course much higher. Recently, Otsu wrote an extensive review on the iniferter concept and the living radical polymerisation[29].

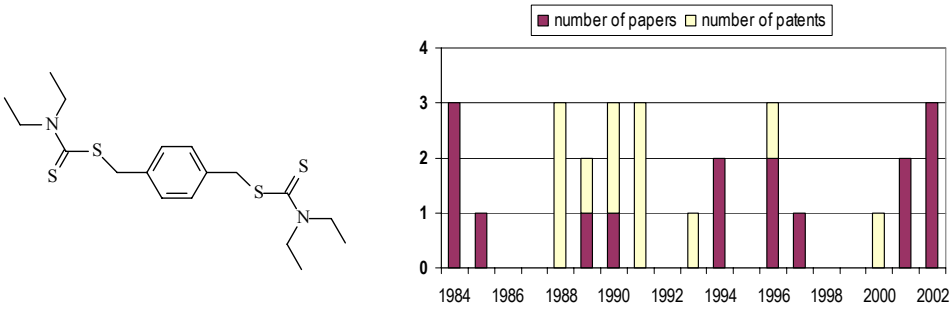

Figure 5.1: *Reports on p-xylylene bis(N,N-diethyl dithiocarbamate)*

The iniferter (*ini*tiator-trans*fer* agent-*ter*minator)[30] controlled free-radical polymerisation technique developed by Otsu and Kuriyama[1, 4, 29] is used in the synthesis of block copolymers. The graph in figure 5.1 shows that nowadays block copolymers still are being synthesised by using this technique. Bowman *et al.*[9] investigated the kinetics and the

mechanism of iniferter photopolymerisations of methacrylates. Here XDC acts as a photoinitiator which on irradiation produces a chain-initiating carbon-centred radical (b) and a sulphur-centred dithiocarbamyl radical (a) which can reversibly terminate the propagating chains. (Scheme 5.1) Because the dithiocarbamyl (DTC) radical (a) is stable and relatively unreactive to propagation, the carbon radicals (b) constitute the active centres and the initiation by DTC radicals is negligible as compared to the initiation by carbon radicals[5, 6, 31]. Dika Manga *et al.* however claimed that initiation by DTC radicals must not be neglected[32]. In the polymerisation there are two possible termination pathways: the carbon-carbon radical termination and the carbon-dithiocarbamyl radical termination. The first one results in a dead polymer while the second forms a polymer of which the end group can be reinitiated. It was reported that definitive termination reactions took place simultaneously with (but more slowly than) the reversible terminations reactions[32]. The iniferter consequently serves to reduce the concentration of the propagating species and thus the incidence of radical-radical termination during irradiation.

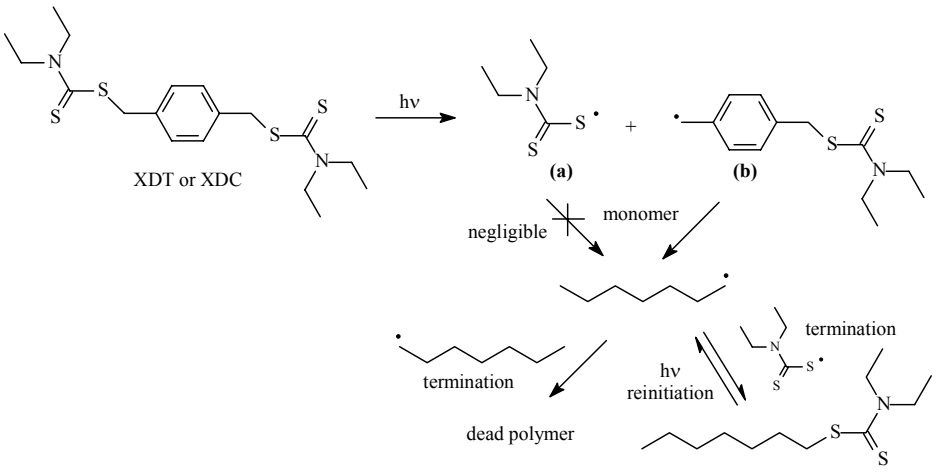

***Scheme 5.1**: Living radical iniferter polymerisation mechanism for XDC*

Despite the fact that the dithiocarbamate group's structure is similar to the one of the xanthate group, no reports on the use of *p*-xylylene bis(*N,N*-diethyl dithiocarbamate) as a monomer were found. Our goal was to test if it was possible to polymerise this potential monomer and if so to check the characteristics of the precursor polymer. A next step then could be the use of this new precursor route in the synthesis of PTV. Nishiyama *et al.*[33]

patented the synthesis of thiophene-2,5-diylbismethylene dialkylthiocarbamates for their herbicidal activities but no report exists on the diethyl**di**thiocarbamate analogue. Since the mechanism of the iniferter photopolymerisation has already been elucidated, the polymerisation of bis-dithiocarbamate monomers maybe could give suggestions for the processes occurring during polymerisation and thus eventually for the high polydispersities obtained via the xanthate route.

5.2 Synthesis of the poly(*p*-phenylene vinylene) precursor

The 'monomer' synthesis was similar to the synthesis of the bisxanthate monomer described in the previous chapter. Addition of sodium diethyldithiocarbamate trihydrate to α-α'-dichloro-p-xylene **115**[1, 4] or to bissulphonium salt **116** yielded the bis-dithiocarbamate 'monomer' **117**. (Scheme 5.2)

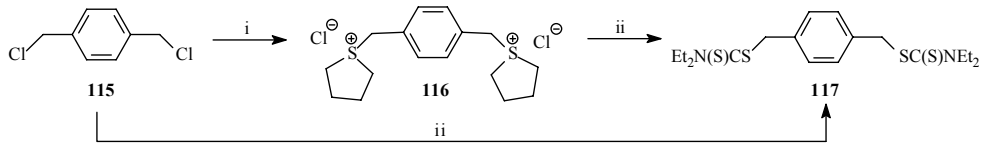

***Scheme 5.2**: Synthesis of dithiocarbamate monomer **117**: i) THT; ii) $NaSC(S)NEt_2.3H_2O$*

Polymerisation of this 'monomer' was performed in an analogous way as described in the previous chapter (paragraph 4.2.2). For the four test polymerisations of which the results are listed in table 5.1, LDA was used as the base, dried THF as the solvent and the monomer concentration was set at 0.2 M. All polymerisation reactions were terminated after 90 minutes. In an attempt to check the influence of the polymerisation temperature, four different temperatures were applied (entry 1-4). From the data in table 5.1 it could be concluded that by using the new dithiocarbamate precursor route, it was possible to obtain polymer in an excellent yield for all the applied temperatures (ranging from -78°C to room temperature). Molecular weights were determined by GPC relative to PS standards with DMF and THF as the eluents. It is clear that DMF is a much better solvent for precursor polymer **118** than THF: weight-average molecular weights going from 7 300 g/mol to 36 500 g/mol could be reached when DMF was used as the eluent compared to values going from 1 300 g/mol to 3 400 g/mol when THF was used. The molecular weights of the precursor

polymers **118** were in general lower than of the xanthate precursor polymers obtained in similar polymerisation conditions[34, 35].

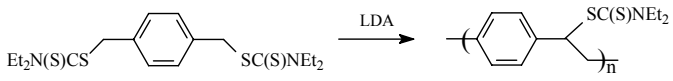

117 **118**

Entry	Polymerisation temperature	Yield (%)	M_w (x 10^{-3}) (DMF)	PD (DMF)	M_w (x 10^{-3}) (THF)	PD (THF)
1	-78°C	89	7.3	1.6	3.4	1.4
2	-78°C → 0°C*	88	15.0	2.1	3.0	1.6
3	0°C	87	31.2	4.1	1.7	2.1
4	Room temp.	88	36.5	5.5	1.3	2.2

* Polymerisation at -78°C for 90 minutes, warming up to 0°C for 15 minutes and afterwards quenching with ice water

Table 5.1**: Polymerisation results for monomer **117

To demonstrate the effect of temperature on the molecular weights, an overlay of the chromatograms (DMF as eluent) of the four different entries is presented in figure 5.2. This overlay is zoomed in the region between 12 and 20 minutes of elution time. The chromatogram of precursor polymer **118** prepared at -78°C (solid line) shows a monomodal molecular weight distribution. As the polymerisation temperature is increased an extra peak at the high molecular weight side of the chromatogram occurs and a bimodal molecular weight distribution is observed. This explains the increase of M_w and PD with increasing polymerisation temperature.

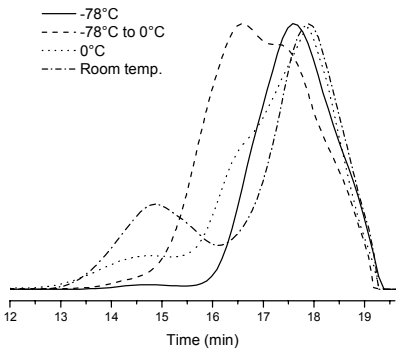

Figure 5.2**: Overlay of GPC-chromatograms of precursor polymer **118

5.3 Synthesis of the poly(2,5-thienylene vinylene) precursor

After having polymerised the phenyl dithiocarbamate monomer successfully, the possibility of polymerising the thiophene dithiocarbamate monomer (thiophene-2,5-diylbismethylene *N,N*-diethyl dithiocarbamate) was investigated. Monomer and precursor polymer synthesis were analogous to the synthesis applied above and the polymerisation results are presented in table 5.2. The residual fractions contained only unreacted monomer **119**.

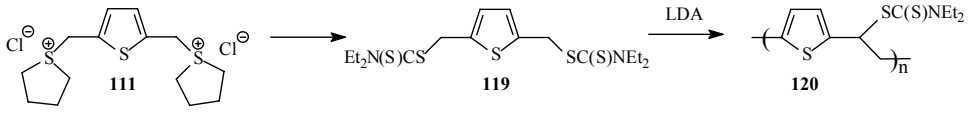

Entry	Conc. (M)	Polymerisation temperature	Yield (%)	M_w (x 10^{-3}) (DMF)	PD (DMF)	M_w (x 10^{-3}) (THF)	PD (THF)
5	0.1	-78°C	47	62.8	2.9	21.5	2.2
6	0.2	-78°C	57	94.4	3.1	14.0	1.8
7	0.1	-78°C → 0°C	55	90.0	5.4	17.8	2.9
8	0.2	-78°C → 0°C	56	66.1	4.9	29.2	4.7
9	0.3	-78°C → 0°C	53	12.8	1.4	5.8	1.6
10	0.1	0°C	42	23.8	3.8	1.4	1.2

Table 5.2**: Polymerisation results for monomer **119

The data in table 5.2 confirm the fact that DMF is a better solvent for the dithiocarbamate precursors than THF is. The yields are lower than those obtained with the phenyl analogue but are still higher than when the xanthate route was applied (chapter four). The M_w's range from 12 800 to 94 400 g/mol whereas this was from 6 000 to 360 000 g/mol for the PTV precursor polymers obtained via the xanthate precursor route. Thus in general lower molecular weights are observed. But by using the dithiocarbamate route also the polydispersity of the precursors is lowered dramatically. Their values range from 1.4 to 5.3 while in chapter four values from 7 to 30 were observed after the polymerisation of the xanthate monomer in THF.

5.4 Conversion of the precursors to PPV and PTV

When studying the thermal conversion to the conjugated structure by means of *in-situ* UV-Vis spectroscopy, it could be seen that the absorption maxima of the polymers prepared by the dithiocarbamate precursor route are shifted to longer wavelength (lower energy) compared to the precursors prepared by the xanthate route. For the PPV xanthate precursor a λ_{max} value of 396 nm[35] was found while for the dithiocarbamate precursor λ_{max} was 408 nm. (Figure 5.3) The same is true for the comparison of the PTV xanthate precursor with a λ_{max} value of 520 nm (chapter four) with the dithiocarbamate precursor of which λ_{max} was 546 nm. (Figure 5.4) This is an indication of an improved conjugation of the π-electron system.

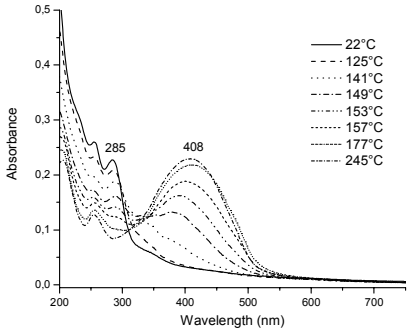

***Figure 5.3**: UV-Vis spectra of **118** (entry 4) at different temperatures*

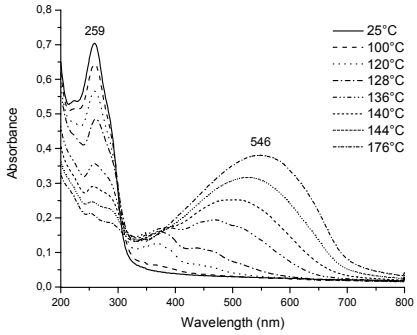

***Figure 5.4**: UV-Vis spectra of **120** (entry 5) at different temperatures*

The λ_{max} values mentioned above are all measured at high temperature and thus the thermochromic effect has not yet been taken into account. If the precursor was cooled down to ambient temperature after conversion, a higher λ_{max} could be observed. For the PPV dithiocarbamate precursor λ_{max} was 420 nm and the PTV dithiocarbamate precursor showed a λ_{max} value of 571 nm at room temperature. This is a red shift of 12 nm and 25 nm respectively. The band gaps, as determined from the low energy edges of the π-π^* absorption bands, are 2.37 and 1.67 eV for PPV and PTV respectively. This is in good agreement with the values reported by Elsenbaumer *et al.*[36] (2.40 and 1.64 eV).

In figure 5.5 and 5.6, the absorbance at the absorption maximum of both dithiocarbamate precursors and conjugated polymers are plotted as a function of increasing

temperature. From these profiles, it can be seen that the elimination of the dithiocarbamate groups of the phenyl precursor **118** starts at about 115°C and is completed around 175°C. For the thienyl precursor **120** elimination also starts around 115°C and is completed around 160°C. In the region between 95 and 160°C the formation and disappearance of oligomeric fragments (368 nm) is visible.

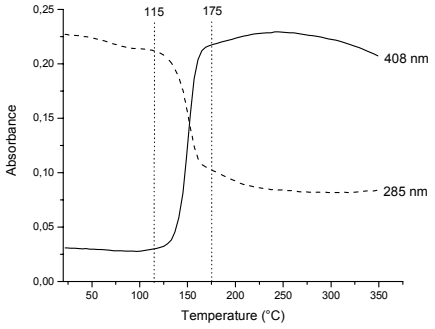

Figure 5.5**: Absorbance profiles at 285 and 408 nm as a function of temperature for **118

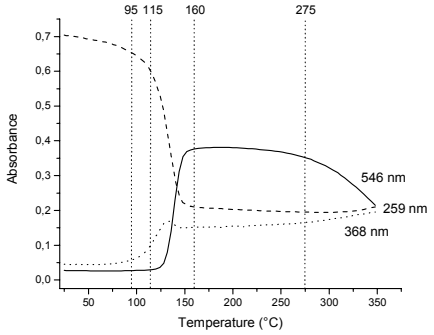

Figure 5.6**: Absorbance profiles at 259, 368 and 546 nm as a function of temperature for **120

Also *in-situ* FT-IR spectroscopy measurements were carried out as described in the previous chapters. Figures 5.7 and 5.8 show a part of the IR spectra at different temperatures starting from precursor polymer **118** and **120** respectively. Dithiocarbamate precursor polymer **118** shows strong absorption bands at 1486, 1414, 1266 and 1205 cm^{-1} which all arise from the dithiocarbamate leaving group. For precursor **120** similar bands are observed.

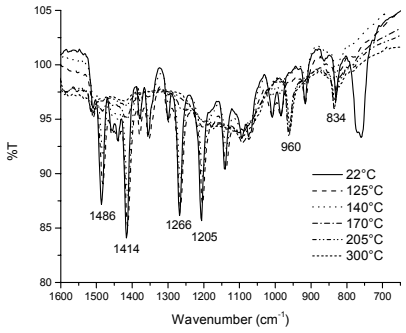

***Figure 5.7**: IR spectra of **118** at different temperatures*

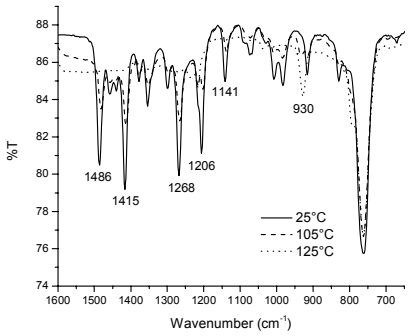

***Figure 5.8**: IR spectra of **120** at different temperatures*

By heating polymer **118**, the elimination of the dithiocarbamate groups is observed and a new absorption signal appears at 960 cm^{-1} which originates from the *trans*-vinylene double bond. The signal at 834 cm^{-1} of the *p*-phenylene C-H out-of-plane deformation[35, 37] also increases during the elimination process. Both the decline in dithiocarbamate absorption and the increase in double bond absorption start around 105°C as visualised in figure 5.9. There is no indication for the formation of *cis* double bonds, which differs from the observations for the corresponding xanthate precursor polymer[35]. For precursor polymer **120**, the signal of the *trans*-vinylene double bond appears at 930 cm^{-1} and the elimination takes place in the temperature interval between 85 and 140°C as shown in figure 5.10.

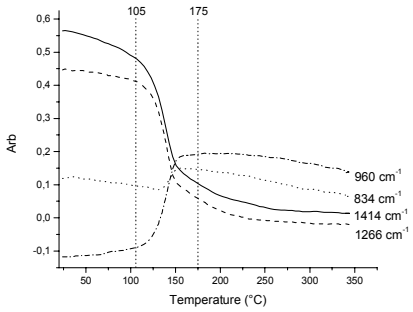

Figure 5.9**: IR absorption profiles at 1414, 1266, 960 and 834 cm^{-1} as a function of temperature for **118

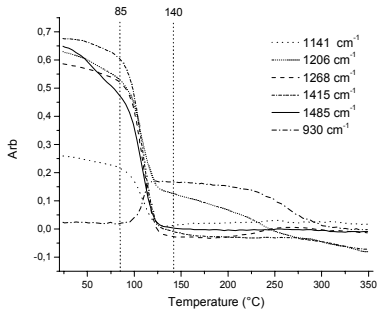

Figure 5.10**: IR absorption profiles at 1415, 1268 and 930 cm^{-1} as a function of temperature for **120

Two TGA experiments of both precursor polymers **118** and **120** were performed at a heating rate of 10°C per minute up to 670°C and 600°C respectively and with a continuous flow of nitrogen (50 mL/min). Here the weight loss of the samples is plotted as a function of increasing temperature (solid lines in figure 5.11 and 5.12). Also the derivative of weight loss to the temperature is calculated and plotted in the same figures (dashed lines). In this way the temperature of maximum weight loss is determined. For each precursor polymer two major steps of weight loss are visible above 100°C: at 211 and 538°C for **118** and at 194 and 424°C for **120**. The first step is related to the elimination of the dithiocarbamate group and to the evaporation of the elimination products that are liberated. The second step of weight loss is assigned to the evaporation of the degradation products of the conjugated system of PPV or PTV. For PPV this is in agreement with the literature data[38, 39]. The loss of weight below 100°C, which is clearly visible for **120** at 62°C, is assigned to the

evaporation of solvent residues. After all, insufficient drying of the precursor polymer results in remainders of $CHCl_3$ (bp: 61°C) and *n*-hexane (bp: 69°C) on the polymer.

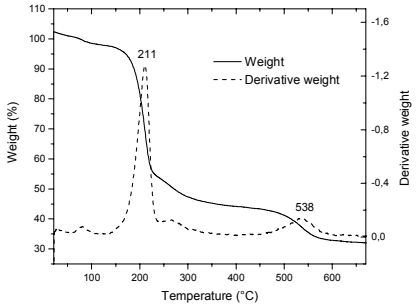

Figure 5.11**: TGA thermogram of phenyl precursor polymer **118

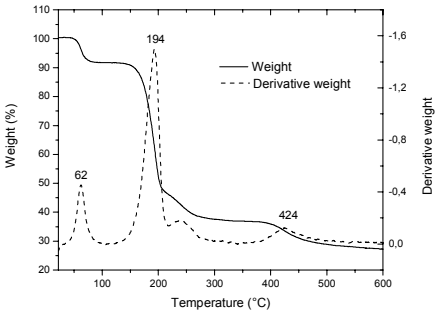

Figure 5.12**: TGA thermogram of thienyl precursor polymer **120

A study on the thermal stability of the PPV and PTV dithiocarbamate precursors **118** and **120** by DIP-MS (heating rate of 10°C per minute) resulted in the thermograms presented in figure 5.13 and 5.14 respectively. The thermogram of **118** shows two distinct signals at a maximum temperature of 227 and 471°C and for polymer **120** at 200 and 400°C. The first signal, based on the fragments detected ($Et_2N(S)CS$, $Et_2N(S)C$ and NEt_2), can be assigned to the elimination of the dithiocarbamate groups and the second one to the evaporation of the degradation products of the conjugated polymer. These observations are comparable with those obtained with TGA. The signal observed at lower temperature, which is clearly visible for **118** at 139°C, originates from remainders of monomer in the precursor polymer fraction.

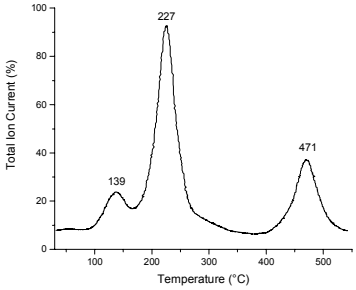

Figure 5.13**: DIP-MS thermogram of **118

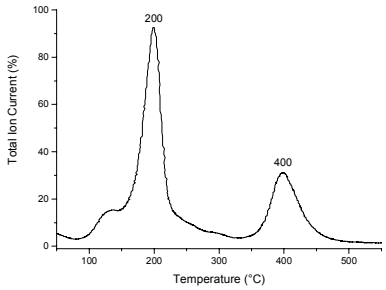

Figure 5.14**: DIP-MS thermogram of **120

The fact that a similar elimination temperature is observed in TGA (nitrogen atmosphere) and DIP-MS (vacuum) implies that at this temperature the elimination products that are liberated will evaporate immediately. The elimination reaction itself and the evaporation of the elimination products thus are not kinetically separated. The elimination temperature observed with these techniques is higher than that obtained from *in-situ* UV-Vis and *in-situ* FT-IR results. This difference is attributed to the difference in heating rate (10°C/min versus 2°C/min).

5.5 Cyclic voltammetry

The HOMO and LUMO energy levels of the thienyl dithiocarbamate precursor polymer **120** (entry 5) and of the -after thermal treatment- resulting PTV could be estimated from the cyclic voltammograms depicted in figure 5.15.

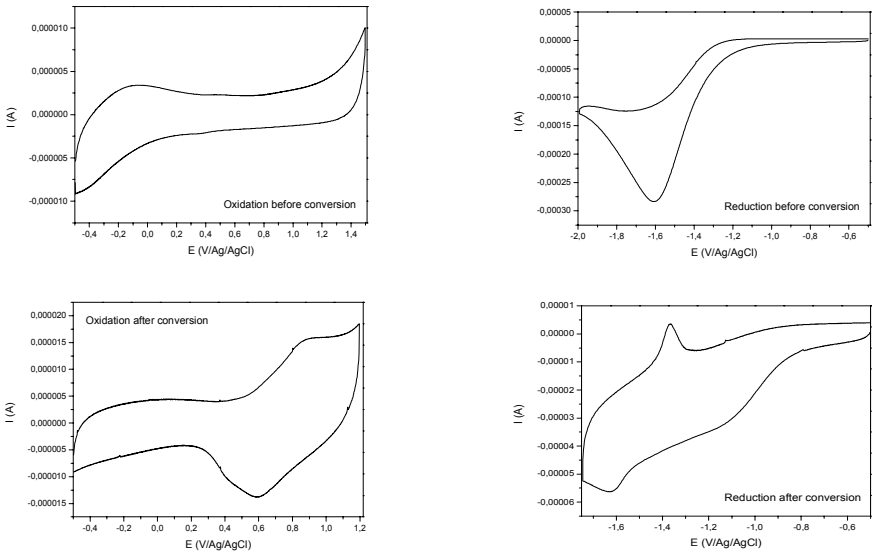

***Figure 5.15**: Cyclic voltammograms of the polymer films drop-casted on Pt in an electrolytic solution of Bu_4NClO_4 (0.1 M) in CH_3CN at a scan rate of 50 mV s^{-1}*

The energy values of LUMO and HOMO were determined in the same way as described in paragraph 2.1.5. After determination of the onset potentials of both p- and n-doping, the values could be transferred to the following equations: $E_{HOMO} = - (4.8 + E_{onset}^{ox})$

eV and E_{LUMO} = - (4.8 + E_{onset}^{red}) eV. The onset potentials in oxidation and in reduction were determined, respectively, at 1.15 and - 1.23 V for **120** and at 0.51 and - 0.91 V for **PTV** versus Ag/AgCl, corresponding to 0.65 and - 1.73 V for **120** and 0.002 and - 1.41 V for **PTV** versus F_c/F_c^+ ($E°'$ F_c/F_c^+ = 0.43 V vs. Ag/AgCl). The redox data and the energy levels are listed in table 5.3.

Polymer	E_{onset}^{ox} (V)	E_{onset}^{red} (V)	E_{HOMO} (eV)	E_{LUMO} (eV)	E_g^{el} (eV)
120	1.15	-1.23	-5.45	-3.07	2.38
PTV	0.51	-0.91	-4.80	-3.39	1.41

Table 5.3**: Electrochemical characteristics of polymer **120** and **PTV

The band gap of PTV determined in this way (1.4 eV) is quite low compared to the value determined from the optical absorption data and the value of about 1.8 eV reported in literature[40].

5.6 Exploratory measurements for applications in organic solar cells and transistors

Photovoltaic studies on solar cell devices with PTV (obtained from precursor polymer **120**, entry 5) as electron donor and [6,6]-PCBM as electron acceptor as well as transistor measurements with this polymer material as an active layer, were performed by Tom Aernouts at IMEC in Leuven. For both measurements the precursor was converted by first heating the sample from room temperature to 185°C at 2°C per minute, then holding it at this temperature for 10 minutes and finally cooling it down again to ambient temperature.

Solar cell tests

Two ITO (indium tin oxide)/PEDOT (poly(3,4-ethylene dioxythiophene))/PTV/Al devices on a glass substrate were tested. The glass substrates, coated with ITO (100 nm, resistance < 20 ohm per square), were first cleaned with acetone in an ultrasonic bath. On top of the ITO, a dispersion of PEDOT/PSS (BAYTRON P) was spin-coated for 60 seconds at 3000 rpm resulting in a 30 nm thick layer. The first test was with the pristine material as active layer. The second device was made by first converting the spin-coated precursor **120**

and afterwards spin-coating [6,6]-PCBM on top of it. In this way a bilayer device was obtained. In both cases, the precursor polymer was dissolved in chlorobenzene in a concentration of 1% (w:v%), stirred overnight and afterwards spin-coated at 600 rpm. Eventually, an aluminium electrode was evaporated in a high vacuum. On each substrate, eight solar cells, with an active area of 2 mm^2, were present.

Figure 5.16 shows the plot of the J/V curves of the devices in the dark and under illumination of 100 mW/cm^2 light from a halogen lamp. The observed short current density (J_{sc}) and the open circuit voltage (V_{oc}) as well as the fill factor (FF) and the efficiency (η) for both devices are listed in table 5.4.

	J_{sc} ($\mu A/cm^2$)	V_{oc} (mV)	FF (%)	η (%)
Pristine	430	435	34	0.06
Bilayer	1 430	515	48.5	0.36

***Table 5.4**: Device characteristics*

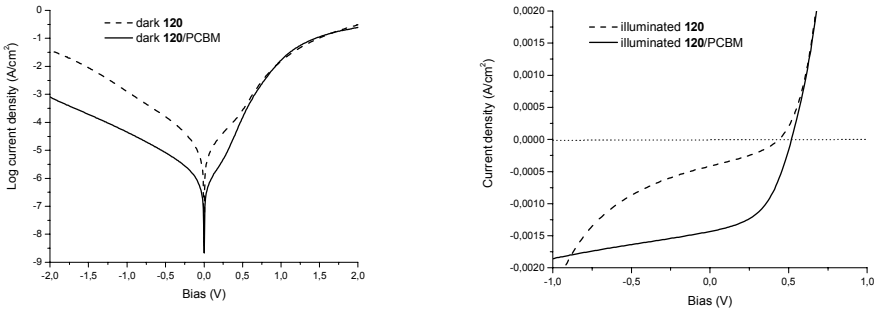

***Figure 5.16**: J/V curves of a photovoltaic device with PTV as the active material; in the dark (left, log-scale) and under white light illumination (right)*

The results for the bilayer device already look very promising for a first trial. Certainly if we compare these results with the ones obtained with other bilayer devices where PPV or soluble derivatives of PPV were used as active layer[41, 42]. However reports state that the appliance of a LiF/Al electrode in stead of a pristine Al electrode guarantees a good ohmic contact between the metal and the organic layer and thus can improve the device performance[43-45]. For this reason the LiF layer beneath the Al electrode is widely used at this moment[46-48]. Also a composite device instead of a bilayer device could improve the FF and the efficiency. The fill factor here (48.5%) is only slightly lower than the values reported

for OC_1C_{10}-PPV/PCBM composite solar cell devices (50%[49] without the use of LiF and 60%[46, 48, 49] when LiF was used) which have almost the highest power conversion efficiencies reported in literature so far[48]. It is obvious that it is interesting to perform additional tests which imply the use of LiF and a device with a composite layer of PCBM and PTV. Further experiments are being executed at the moment of writing this dissertation.

Transistor tests

Dithiocarbamate precursor polymer **120** was tested in the same transistor device as described in chapter four (top-contact, W = 2000 μm, L = 75 μm). In figure 5.17, the square root of the drain-source current as a function of the gate voltage of the transistor is plotted.

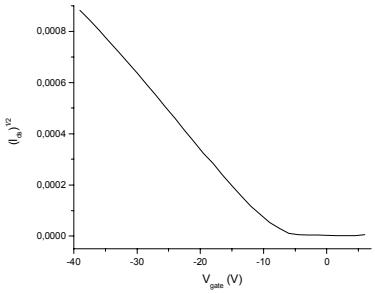

***Figure 5.17**: Plot of the square root of $I_{ds,sat}$ as a function of V_{gs}*

As stated in chapter one, the mobility μ can be derived from the slope of the straight line (equation (1-6)) and V_t from the extrapolation to the V_{gs} axis. The mobility was 1.7 x 10^{-3} cm^2 $V^{-1}s^{-1}$, a value that is higher than any other PTV xanthate precursor that was measured in this device. A threshold voltage of -7 V and an I_{on}/I_{off} ratio of 92 300 was determined.

5.7 Copolymerisation

The synthesis of copolymers can be an attractive approach to combine the interesting physical and/or chemical properties of different polymers. It has been proven in the past that copolymerisations lead to new materials with intermediate (or even improved) properties[50, 51].

Since the yields of the polymerisation of the phenyl dithiocarbamate monomer were higher compared to the thiophene analogue, a combination of the monomers could improve

the yield. Also copolymers of other PPV derivatives as OC_1C_{10}-PPV with PTV could be of interest. After all, in this way the good performance of OC_1C_{10}-PPV is combined with the 'band gap lowering' thiophene unit which can lead to a supplementary improvement of the device performance. Additionally, the obtained conjugated polymers are soluble as a result of the long alkoxy side chains on the phenyl core. The copolymer of PTV with other conducting polymers (PPV and its derivatives) was already studied by Shim *et al.*[52, 53] and Gregorius *et al.*[54, 55]. These copolymers were all synthesised via the Wessling-Zimmerman precursor polymer route but the difference in reactivity between the two monomers made it difficult to control the composition of the desired copolymers. Gregorius and co-workers investigated the copolymeric nature by using an IR analysis method that distinguishes the vinylene units linking the phenylene and thienylene units. In this way they tried to overcome the uncertainty whether the materials synthesised were indeed copolymers or homopolymer blends. The relative reactivity ratios of the PPV/PTV system were found to be heavily skewed toward TV incorporation.

The molecular weights of the precursor polymers obtained via the polymerisation of the thiophene xanthate monomer (chapter four) were higher than those of the thienyl dithiocarbamate precursors. By copolymerising these different monomers, polymers with an intermediate M_w could possibly arise. We therefore chose not only to test the copolymerisation behaviour between the phenyl and thiophene dithiocarbamate monomers but also between the thiophene xanthate and the thiophene dithiocarbamate monomers. The chemical structures of the monomers and the precursor polymers which are normally derived from the performed copolymerisations are given in scheme 5.3.

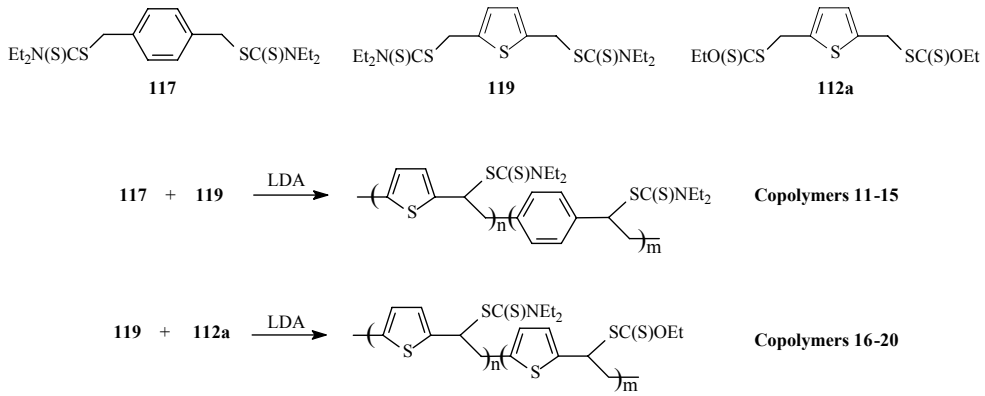

Scheme 5.3**: Copolymerisations of monomers **117**, **119** and **112a

The two monomers were dissolved together in dry THF (monomer concentration of 0.2 M) and the polymers were obtained in the same way as described for the homopolymers. All the polymerisation reactions were performed at -78°C and were terminated after 90 minutes by quenching with ethanol. For each set of copolymerisations, the comonomer ratios were 75/25, 50/50 and 25/75. The ratios of 100/0 and 0/100 are those of the homopolymerisations described in the previous paragraphs or chapter. The chemical composition of the polymer was determined on the precursor stage with quantitative ^{13}C NMR spectroscopy. The residual fraction was analysed with ^{1}H NMR spectroscopy to determine the ratio of the different monomers.

5.7.1 Thienyl and phenyl dithiocarbamate copolymers

The results of the (co)polymerisations of monomer **117** (phenyl) and **119** (thiophene) are listed in table 5.5. GPC measurements were performed versus PS standards and DMF was used as the eluent since it was already proven that this is a better eluent for the dithiocarbamate precursors than THF.

	Monomers		**Copolymer**					**Residual fraction**	
Entry	**117**	**119**	**Yield (%)**	**M_w (x 10^{-3}) (g/mol)**	**PD**	**Phenyl**	**Thioph**	**Phenyl (117)**	**Thioph (119)**
11	100	0	89	7.3	1.6	100	0	100	0
12	75	25	90	17.2	3.4	73	27	100	0*
13	50	50	89	24.7	3.2	45	55	100	0*
14	25	75	89	109.8	9.9	24	76	100	0*
15	0	100	57	94.4	3.1	0	100	0	100

* No traces of thiophene monomer visible in ^{1}H NMR spectrum (< 5%)

Table 5.5**: Copolymerisation results for monomer **117** and **119

From ^{13}C NMR spectroscopy it seemed that no statistical copolymers were formed as no additional signals occurred in the carbon spectrum. The two starting monomers would then have polymerised without any real contact and the copolymer actually is either a homopolymer blend or a material that is extremely blocky. It should however be noted that

there was a lot of noise in the signals and that it is thus difficult to draw conclusions. Since the phenyl homopolymer (entry 11) has a lower M_w than the thienyl homopolymer (entry 15), it is not surprisingly that the more phenyl monomer **117** is used in the starting mixture in proportion to thiophene monomer **119**, the lower the average molecular weight of the mixture of polymers is. This is visually shown in figure 5.18 where an overlay of the different GPC-chromatograms is plotted.

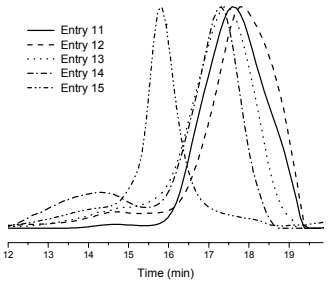

***Figure 5.18**: Overlay of the GPC-chromatograms of the five precursor (co)polymers*

To follow the conversion of the precursor polymer into the conjugated form, *in-situ* UV-Vis measurements were carried out for (co)polymers 11-15. A dynamic heating program of 2°C per minute up to a temperature of 350°C was used and the measurements were performed under a continuous flow of nitrogen. The normalised UV-Vis spectra at maximal conversion of the different (co)polymers are plotted in figure 5.19. The PPV homopolymer has a λ_{max} value of 396 nm. The more thiophene monomer was present in the initial comonomer feed, the more the value of λ_{max} shifts to the absorption maximum of the PTV homopolymer at 546 nm.

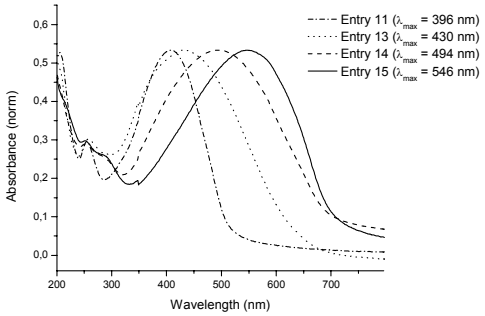

***Figure 5.19**: Normalised absorption spectra for (co)polymers 11, 13, 14 and 15*

From the UV-Vis spectra it looks like copolymers are formed since only one band is visible. However it may be possible that this band is an intermediate of two bands, although the difference in λ_{max} between PPV and PTV is quite large (150 nm).

The copolymeric nature of the systems can also be investigated by the method used by Gregorius *et al.*[54], who based their method on the oligomeric model studies of Kossmehl[56, 57]. They studied the IR spectra obtained for the putative PPV-co-PTV copolymers in the vinylene out-of plane region and found that they looked different compared to spectra for the homopolymer blends. For the copolymers, the absorption maxima shifted as the TV fraction in the copolymer composition increased. But there were no absorption maxima at 970 and 930 cm^{-1} (*trans* vinylene wagging band) which suggests that "blocks" (> six units) were not produced. In the blends the central absorption between 940 and 960 cm^{-1} was absent and both homopolymeric absorption maxima were apparent throughout the entire range of blend compositions. Therefore also *in-situ* FT-IR measurements were carried out for (co)polymers 11-15 and the same dynamic heating program of 2°C per minute up to a temperature of 350°C was used. The overlay of the IR spectra of the conjugated polymers is depicted in figure 5.20.

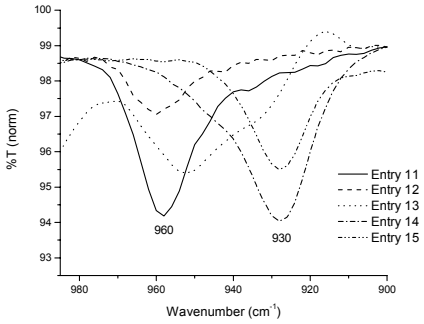

***Figure 5.20**: Vinylene out-of-plane infrared spectral region for entry 11-15*

In the FT-IR spectrum of entry 13 no homopolymeric absorption maxima appear. This suggests that "blocks" are not present in this polymer. However, the FT-IR spectra of entry 12 and 14 look the same as for the blends reported by Gregorius and co-workers with the exception of the lack of an absorption maximum at 930 and 960 cm^{-1} respectively.

We can conclude that the different data from ^{13}C NMR, UV-Vis and FT-IR spectroscopy at the moment available, lead to contradictory conclusions making a more detailed investigation of these polymers necessary.

5.7.2 Thiophene xanthate and thiophene dithiocarbamate copolymers

A second set of copolymerisations were performed by starting from two different types of thiophene monomers: the xanthate and the dithiocarbamate monomer. The polymerisation results are listed in table 5.6. Molecular weights were determined by GPC relative to PS standards with DMF (underlined) and THF as the eluents. It is clear that the more xanthate monomer is present, the higher the molecular weight of the copolymer is. This is consistent with our expectations since the molecular weights of the homopolymers obtained via the xanthate route were also much higher than the ones of the homopolymers obtained via the dithiocarbamate route.

	Monomers		**Copolymer**					**Residual fraction**	
Entry	**119**	**112a**	**Yield (%)**	**M_w (x 10^{-3}) (g/mol)***	**PD***	**Carb**	**Xanth**	**Carb (119)**	**Xanth (112a)**
16	100	0	57	<u>94.4</u> 14.0	<u>3.1</u> 1.8	100	0	100	0
17	75	25	56	<u>372.6</u> 18.6	<u>13.4</u> 3.5	73	27	92	8
18	50	50	69#	<u>309.9</u> 165.8	<u>12.8</u> 11.3	45	55	94	6
19	25	75	70#	<u>202.7</u> 118.5	<u>10.3</u> 9.0	21	79	90	10
20	0	100	50	<u>137.2</u> 282.3	<u>7.8</u> 9.5	0	100	0	100

* For the underlined values GPC was performed in DMF, for the others GPC was performed in THF
# The GPC chromatograms shows that there is still some monomer left in the precursor polymer

Table 5.6**: Copolymerisation results for monomer **119** and **112a

Also here ^{13}C NMR spectroscopy was performed to determine the composition of the copolymer and it could be seen that the incorporation of the xanthate monomer was slightly preferred. In contrast with the absence of additional peaks in the ^{13}C NMR spectra of the PPV/PTV precursor polymers (entry 12-14), extra peaks were observed in the spectra of the dithiocarbamate/xanthate PTV precursor polymers (entry 17-19). Whereas the carbon resonance for the carbon directly attached to the dithiocarbamate group in the homopolymer is at 52.5 ppm and for the carbon on which the xanthate group is attached is at 70.1 ppm, a new, intermediary resonance at 65.8 ppm is observed for the copolymer. In this set of copolymerisations, the difference in reactivity between the two monomers is not as big as it was for the thiophene and phenyl dithiocarbamate monomers. Consequently it is less problematic to obtain copolymers.

^{1}H NMR spectroscopy was used to analyse the residual fractions. The benzylic protons adjacent to the xanthate group or the dithiocarbamate group at 4.48 ppm and 4.69 ppm respectively, were compared. For all the copolymerisations, it was found that the dithiocarbamate monomer remained almost exclusively in the residual fraction.

5.8 The dithiocarbamate route: solution for electron rich systems?

In our search for new low band gap materials, the use of precursor routes always stayed a problem for electron rich systems. The synthesis of PTV via the sulphinyl route turned out to be very problematic. The xanthate route was another option to obtain this polymer but high polydispersities of the precursor polymer and a quite low λ_{max} value for the corresponding conjugated polymer were found. This was improved with the use of the dithiocarbamate route. If we want to go to soluble systems in the conjugated phase, the introduction of long side chains is a solution. In this way an even more electron rich system is created. In the past, attempts to use precursor routes as the Gilch and the Wessling-Zimmerman route in the preparation of electron rich polymers failed. The high reactivity and instability of the monomers always seemed to be the problem. Since also the sulphinyl route developed in our lab was not up to these systems, the new dithiocarbamate precursor route could be a possible answer to this limitation.

In the synthesis of electron rich monomers the instability of the 2,5-bis(chloromethyl) compound often was a big problem. If the dithiocarbamate monomer could be synthesised from the corresponding diol this step would not be necessary anymore. Therefore some preliminary tests were done. Elsenbaumer *et al.*[58] already applied the direct synthesis of benzylic thioethers from benzylic alcohols -in the presence of zinc iodide as a Lewis acid-[59, 60] in the monomer synthesis towards poly(3,4-dialkoxy-2,5-thienylene vinylene)s. Because of the good results obtained via this procedure, we tried to synthesise the dithiocarbamate monomer **119** directly from the alcohol **109** using this method. (Scheme 5.4) The alcohol and the Lewis acid (2 equivalents) were dissolved in dichloromethane and sodium diethyldithiocarbamate trihydrate was added in small portions. After two hours of stirring at room temperature, water was added and the mixture was extracted with CH_2Cl_2. The organic layers were separated, dried over $MgSO_4$ and filtered. However, evaporating the solvent only resulted in zinc complex **121** and alcohol **109**.

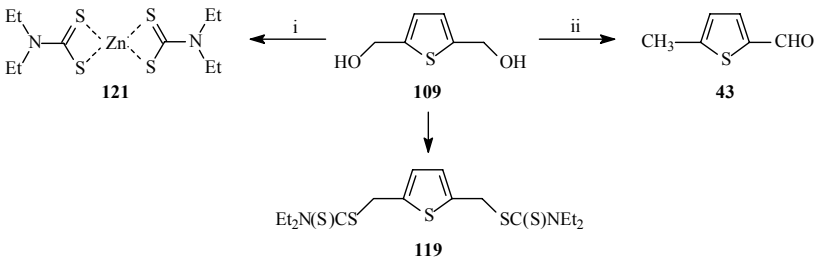

***Scheme 5.4**: Synthesis of dithiocarbamate monomer **119** via diol **109**: i) ZnI_2, $NaSC(S)NEt_2.3H_2O$; ii) CF_3COOH, $NaSC(S)NEt_2.3H_2O$*

Another reaction involving the use of trifluoroacetic acid[61] was tested. Dissolving the alcohol and CF_3COOH (2 eq.) in acetone led to a brown solution in which an insoluble solid (polymer) precipitated. By first adding the sodium diethyldithiocarbamate trihydrate (3 eq.) to the alcohol and afterwards the acid (5 eq.), no precipitation was formed. Thus the order of addition of the reagent seems to be important. After work-up the obtained product was again not the dithiocarbamate monomer **119** but 5-methyl-2-thiophenecarbaldehyde **43** was isolated. In this reaction, one of the two hydroxymethyl groups was reduced to the methyl group, whilst the other was oxidised to the formyl group. These findings were in agreement with recently reported data. Komatsu *et al.*[62] reported on the reaction of **109** with trifluoromethanesulphonic acid (CF_3SO_3H) to form cyclic oligomers **122**. (Figure 5.21)

Nakayama *et al.*[63] performed a reaction with 3,4-diphenyl-2,5-bishydroxymethylthiophene and *p*-toluenesulphonic acid monohydrate and found that 5-methyl-3,4-diphenylthiophene-2-carbaldehyde was formed due to the acid-catalysed intramolecular disproportionation of the bishydroxymethylthiophene compound. According to them, the structures of the polymeric materials, obtained as side products, seem to be acyclic such as **123** rather than cyclic. A higher concentration of diol also increased the amount of these polymeric products.

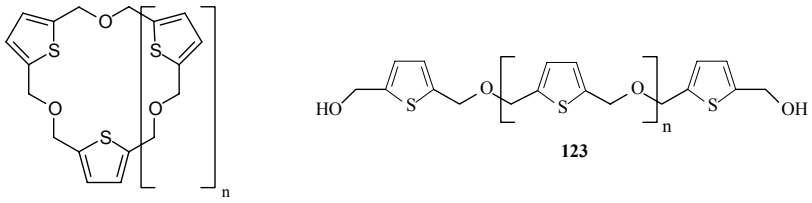

122 **123**

***Figure 5.21**: Chemical structure of the polymeric material*

In the cited reference the mechanism of this novel disproportionation is clarified. The initial step involves the acid-catalysed formation of a carbocation intermediate **124** by dehydration (-H_2O) of the alcohol. (Scheme 5.5) This stabilised carbocation is then converted to the intermediate enol form by deprotonation. Finally this is followed by acid-catalysed isomerisation to the aldehyde **43**.

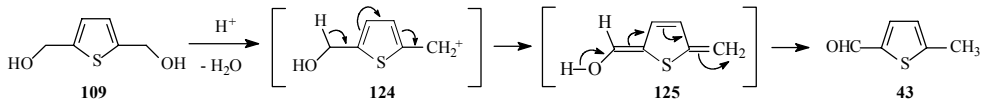

109 **124** **125** **43**

***Scheme 5.5**: Mechanism of the disproportionation*

Although these first trials to simplify the synthesis of the dithiocarbamate monomer systems failed, the use of the dithiocarbamate route towards electron rich polymers is still an option. Further experiments are planned to study the applicability of this route (see chapter seven).

5.9 Conclusion

A new precursor route for the synthesis of poly(aromatic vinylene)s: the dithiocarbamate route was developed. Synthesis of the non-substituted phenyl and thiophene bismethylene *N,N*-diethyl dithiocarbamate monomers was easily achieved. Their polymerisation involved a reaction with an equimolar amount of base (LDA) in dry THF. This new route had superior properties compared to the xanthate route: (i) the polydispersities of the resulting polymers were much lower than those of the xanthate precursor polymers; (ii) the λ_{max} values of the conjugated polymers acquired after thermal treatment of the dithiocarbamate precursors lay higher than the corresponding polymers acquired from the xanthate polymers and (iii) devices with PTV obtained from a dithiocarbamate precursor showed an improved performance compared to those with PTV obtained from a xanthate precursor. All these observation indicate that this new precursor route is an improved version of the xanthate route and that it is interesting to look more into detail in the scope and limitations of this route (chapter seven). Copolymerisations between the phenyl and thiophene dithiocarbamate monomers and between the thiophene dithiocarbamate and xanthate monomers were both performed and the resulting (co)polymers were examined.

5.10 Experimental part

For the characterisation methods and materials used here we would like to refer to the experimental part of chapter two and three. Before CV was performed on PTV obtained from polymer **120**, this precursor was heated from room temperature to 175°C at 2°C per minute, hold at this temperature for five minutes and then cooled back to room temperature. The synthesis of compound **116** is described elsewhere[64].

***p*-Xylylene bis(*N,N*-diethyl dithiocarbamate) (117)**

To 50 mL of an acetonitrile/water solution (5 vol% water) of 1,4-bis(tetrahydrothiophenio-methyl)xylene dichloride **116** (6 g, 17.143 mmol), sodium diethyldithiocarbamate trihydrate (or diethyldithiocarbamic acid sodium salt trihydrate) (8.87 g, 39.429 mmol) was added as a solid after which the mixture was stirred at ambient temperature for two hours. Then, water was added and the desired monomer was extracted with ether (3 x 100 mL) and dried over

$MgSO_4$. Evaporation of the solvent yielded 6.2 g (90%) of the pure product as a white solid; ^{1}H NMR ($CDCl_3$): 7.31 (s, 4H), 4.49 (s, 4H), 4.01 (q, J = 7.2 Hz, 4H), 3.69 (q, J = 7.2 Hz, 4H), 1.26 (2t, J = 7.2 Hz, 12H). ^{13}C NMR ($CDCl_3$): 195.10, 135.27, 129.57, 49.46, 46.70, 41.79, 12.44, 11.56; MS (EI, m/e): 253 (M^+ – $SC(S)NEt_2$), 148 ($SC(S)NEt_2$), 105 (M^+ – 2 x $SC(S)NEt_2$), 72 (NEt_2)

Polymerisation of 117 (118)

A solution of monomer **117** (500 mg, 1.25 mmol) in dry THF (6.25 mL, 0.2 M) at –78°C (or rt or 0°C) was degassed for 1 hour by passing through a continuous nitrogen flow. An equimolar LDA solution (625 μL[††] of a 2 M solution in THF/*n*-hexane) was added in one go to the stirred monomer solution. The mixture was kept at –78°C (or rt or 0°C) for 90 minutes and the passing of nitrogen was continued. After this, the solution was allowed to come to 0°C or ethanol (6 mL) was added at -78°C to stop the reaction (this was not necessary if the polymerisation was performed at rt or 0°C). The polymer was precipitated in ice water (100 mL) and extracted with chloroform (3 x 60 mL). The solvent of the combined organic layers was evaporated under reduced pressure and a second precipitation was performed in a 1/1 mixture (100 mL) of diethyl ether and hexane at 0°C. The polymer was collected and dried in vacuo. ^{1}H NMR ($CDCl_3$): 6.78-7.14 (br s, 4H), 5.00-5.30 (br s, 1H), 3.82-4.10 (br s, 2H), 3.51-3.78 (br s, 2H), 2.92-3.12 (br s, 2H), 1.04-1.34 (br t, 6H). ^{13}C NMR ($CDCl_3$): 194.38, 138.07, 137.17, 129.35, 128.30, 56.92, 49.15, 46.68, 42.63, 12.58, 11.65. The residual fractions only contained monomer residues.

Thiophene-2,5-diylbismethylene *N,N*-diethyl dithiocarbamate (119)

The preparation of **119** is analogous to that described for **117** but here bissulphonium salt **111** was used. Yield: 81%; ^{1}H NMR ($CDCl_3$): 6.84 (s, 2H), 4.69 (s, 4H), 4.01 (q, J = 7.2 Hz, 4H), 3.69 (q, J = 7.2 Hz, 4H), 1.26 (t, J = 7.2 Hz, 12H); ^{13}C NMR ($CDCl_3$): 194.29, 138.76, 126.77, 49.46, 46.70, 36.72, 12.46, 11.53; MS (EI, m/e): 258 (M^+ – $SC(S)NEt_2$), 148 ($SC(S)NEt_2$)

[††] The solvent from the base solution was neglected in the calculation of the monomer concentration

Polymerisation of 119 (120)

The preparation of **120** is analogous to that described for **118**. ^{1}H NMR ($CDCl_3$): 6.56-6.72 (br s, 1H), 6.72-6.36 (br s, 1H), 5.22-5.55 (br s, 1H), 3.81-4.12 (br q, 2H), 3.48-3.81 (br q, 2H), 3.11-3.40 (br s, 2H), 1.01-1.37 (br t, 6H). ^{13}C NMR ($CDCl_3$): 193.61, 140.77, 140.36, 126.15, 125.89, 52.50, 49.20, 46.73, 38.37, 12.45, 11.60

Copolymerisation of 117 and 119 (copolymers 12-14)

A solution of monomer **117** (369, 246, 123 mg respectively) and monomer **119** (125, 250, 375 mg respectively) in dry THF (6.16 mL, 0.2 M) at –78°C was degassed for 1 hour by passing through a continuous nitrogen flow. An equimolar LDA solution (616 μL‡‡ of a 2 M solution in THF/*n*-hexane) was added in one go to the stirred monomer solution. The mixture was kept at –78°C for 90 minutes and the passing of nitrogen was continued. After this, ethanol (6 mL) was added at -78°C to stop the reaction. The polymer was precipitated in ice water (100 mL) and extracted with chloroform (3 x 60 mL). The solvent of the combined organic layers was evaporated under reduced pressure and a second precipitation was performed in a 1/1 mixture (100 mL) of diethyl ether and hexane at 0°C. The polymer was collected and dried in vacuo.

Copolymerisation of 119 and 112a (copolymers 17-19)

The preparation of copolymers 17-19 is analogous to that described for copolymers 12-14 but here monomers **119** (375, 250, 125 mg respectively) and **112a** (108, 217, 325 mg respectively) were used.

Zinc bis(*N,N*-diethyldithiocarbamate) (121)

The alcohol **109** (2 g, 13.89 mmol) and ZnI_2 (8.86 g, 27.78 mmol) were dissolved in CH_2Cl_2 (30 mL) and sodium diethyldithiocarbamate trihydrate (12.5 g, 55.56 mmol) was added in small portions. After two hours of stirring at room temperature, water was added and the mixture was extracted with CH_2Cl_2. The organic layers were separated, dried over $MgSO_4$ and filtered. Evaporating the solvent and a flash chromatographic separation (silica gel, CH_2Cl_2) gave the pure zinc complex of the diethyldithiocarbamate salt as a white solid in quantitative yield. ^{1}H NMR ($CDCl_3$): 3.82 (q, J = 7.2 Hz, 8H), 1.28 (t, J = 7.2 Hz, 12H); MS

‡‡ The solvent from the base solution was neglected in the calculation of the monomer concentration

(EI, m/e): 360 (M^+), 244 (M^+ – $C(S)NEt_2$), 212 (M^+ – $SC(S)NEt_2$), 148 ($SC(S)NEt_2$), 116 ($C(S)NEt_2$), 72 (NEt_2)

5-Methyl-2-thiophenecarbaldehyde (43)

To a solution of alcohol **109** (2 g, 13.89 mmol) in acetone (20 mL), sodium diethyldithiocarbamate trihydrate (9.38 g, 41.67 mmol) was added in small portions. CF_3COOH (5.4 mL) was added over four hours and after three days of stirring at room temperature, water and CH_2Cl_2 were added. A saturated aqueous solution of $NaHCO_3$ was added until the water layer was neutral and the mixture was further extracted with CH_2Cl_2. The organic layers were separated, dried over $MgSO_4$ and filtered. The crude reaction product was purified by column chromatography (silica gel, CH_2Cl_2) which resulted in pure **43**. ^1H NMR ($CDCl_3$): 9.92 (s, 1H), 7.68 (dd, 1H), 6.96 (dd, 1H), 2.61 (s, 3H); MS (EI, m/e): 126 (M^+), 97 (M^+ – CHO)

5.11 References

1. T. Otsu, A. Kuriyama, *Polym. Bull.* **1984**, 11, 2, 135.
2. A. Kuriyama, T. Otsu, *Polym. J.* **1984**, 16, 6, 511.
3. T. Otsu, A. Kuriyama, *J. Macromol. Sci., Chem.* **1984**, A21, 8-9, 961.
4. T. Otsu, A. Kuriyama, *Polym. J.* **1985**, 17, 1, 97.
5. T. Otsu, T. Matsunaga, A. Kuriyama, M. Yoshioka, *Eur. Polym. J.* **1989**, 25, 7-8, 643.
6. P. Lambrinos, M. Tardi, A. Polton, P. Sigwalt, *Eur. Polym. J.* **1990**, 26, 10, 1125.
7. T. Doi, A. Matsumoto, T. Otsu, *J. Polym. Sci., Part A: Polym. Chem.* **1994**, 32, 12, 2241.
8. Z. Guan, J. B. McClain, E. T. Samulski, J. M. DeSimone, *Polym. Prepr.* **1994**, 35, 1, 725.
9. A. R. Kannurpatti, S. Lu, G. M. Bunker, C. N. Bowman, *Macromolecules* **1996**, 29, 23, 7310.
10. A. R. Kannurpatti, S. Lu, C. N. Bowman, *Polym. Mater. Sci. Eng.* **1996**, 74, 358.
11. A. R. Kannurpatti, K. J. Anderson, J. W. Anseth, C. N. Bowman, *J. Polym. Sci., Part B: Polym. Phys.* **1997**, 35, 14, 2297.
12. L. G. Lovell, J. E. Elliott, J. R. Brown, C. N. Bowman, *Polymer* **2001**, 42, 2, 421.
13. L. G. Lovell, K. A. Berchtold, J. E. Elliott, H. Lu, C. N. Bowman, *Polym. Adv. Technol.* **2001**, 12, 6, 335.

14. M. E. Arnold, K. Nagai, R. J. Spontak, B. D. Freeman, D. Leroux, D. E. Betts, J. M. DeSimone, F. A. DiGiano, C. K. Stebbins, R. W. Linton, *Macromolecules* **2002**, 35, 9, 3697.
15. K. Dean, W. D. Cook, *Macromolecules* **2002**, 35, 21, 7942.
16. J. H. Ward, A. Shahar, N. A. Peppas, *Polymer* **2002**, 43, 6, 1745.
17. S. Himori, *Japan Kokai Tokkyo Koho, No 88278910*, **1988**.
18. S. Himori, *Japan Kokai Tokkyo Koho, No 88314223*, **1988**.
19. T. Otsu, S. Himori, T. Kiriyama, *European Pat. Appl., No 286376*, **1988**.
20. S. Himori, *Japan Kokai Tokkyo Koho, No 8924879*, **1989**.
21. H. A. Milton, A. B. Mahfuza, R. A. Olsen, *European Pat. Appl., No 349232*, **1990**.
22. S. Ozoe, H. Yamakawa, *Japan Kokai Tokkyo Koho, No 90300217*, **1990**.
23. S. Ozoe, H. Yamakawa, *European Pat. Appl., No 421149*, **1991**.
24. A. B. Mahfuza, *European Pat. Appl., No 434335*, **1991**.
25. S. B. Mitra, A. B. Mahfuza, *European Pat. Appl., No 434334*, **1991**.
26. A. B. Mahfuza, G. N. Babu, P. G. Zimmerman, *PCT international, No 9320164*, **1993**.
27. P. Le Barny, L. Bouteiller, *France Demande, No 2729670*, **1996**.
28. H. Oki, Y. Okamoto, M. Sawamoto, Y. Kano, K. Kitahata, K. Yamada, Y. Okano, M. Nishimura, K. Terada, H. Ita, *Japan Kokai Tokkyo Koho, No 2000273131*, **2000**.
29. T. Otsu, *J. Polym. Sci., Part A: Polym. Chem.* **2000**, 38, 12, 2121.
30. T. Otsu, M. Yoshida, *Macromol. Chem. Rapid Commun.* **1982**, 3, 127.
31. P. M. Kazmaier, K. A. Moffat, M. K. Georges, R. P. N. Veregin, G. K. Hamer, *Macromolecules* **1995**, 28, 1841.
32. J. Dika Manga, A. Polton, M. Tardi, P. Sigwalt, *Polym. Int.* **1998**, 45, 1, 14.
33. R. Nishiyama, R. Takahashi, T. Haga, S. Sometani, *Jpn. Tokkyo Koho, No 50004732*, **1975**.
34. S. Son, A. Dodabalapur, A. J. Lovinger, M. E. Galvin, *Science* **1995**, 269, 376.
35. E. Kesters, S. Gillissen, F. Motmans, L. Lutsen, D. Vanderzande, *Macromolecules* **2002**, 35, 21, 7902.
36. H. Eckhardt, L. W. Shacklette, K.-Y. Jen, R. L. Elsenbaumer, *J. Chem. Phys.* **1989**, 91, 2, 1303.
37. D. H. Williams, I. Fleming, *Spectroscopic Methods in Organic Chemistry*, 5th ed., The McGraw-Hill Companies, London, **1995**, p. 53.
38. G. Montaudo, D. Vitalini, R. W. Lenz, *Polymer* **1987**, 28, 5, 837.
39. M. M. De Kok, A. J. J. M. Van Breemen, R. A. A. Carleer, P. J. Adriaensens, J. M. Gelan, D. J. Vanderzande, *Acta Polym.* **1999**, 50, 1, 28.

40. M. Onada, S. Morita, T. Iwasa, H. Nakayama, K. Yoshino, *J. Chem. Phys.* **1991**, 95, 11, 8584.

41. N. S. Sariciftci, D. Braun, C. Zhang, V. I. Srdanov, A. J. Heeger, G. Stucky, F. Wudl, *Appl. Phys. Lett.* **1993**, 62, 6, 585.

42. J. J. M. Halls, K. Pichler, R. H. Friend, S. C. Moratti, A. B. Holmes, *Appl. Phys. Lett.* **1996**, 68, 22, 3120.

43. L. S. Hung, C. W. Tang, M. G. Mason, *Appl. Phys. Lett.* **1997**, 70, 2, 152.

44. G. E. Jabbour, Y. Kawabe, S. E. Shaheen, J. F. Wang, M. M. Morrell, B. Kippelen, N. Peyghambarian, *Appl. Phys. Lett.* **1997**, 71, 13, 1762.

45. G. E. Jabbour, B. Kippelen, N. R. Armstrong, N. Peyghambarian, *Appl. Phys. Lett.* **1998**, 73, 9, 1185.

46. S. E. Shaheen, C. J. Brabec, F. Padinger, T. Fromherz, J. C. Hummelen, N. S. Sariciftci, *Appl. Phys. Lett.* **2001**, 78, 6, 841.

47. C. Winder, D. Mühlbacher, H. Neugebauer, N. S. Sariciftci, C. J. Brabec, R. A. J. Janssen, J. C. Hummelen, *Mol. Cryst. Liq. Cryst* **2002**, 385, 93.

48. T. Munters, T. Martens, L. Goris, V. Vrindts, J. V. Manca, L. Lutsen, P. De Ceuninck, D. Vanderzande, L. De Schepper, J. Gelan, N. S. Sariciftci, C. J. Brabec, *Thin Solid Films* **2002**, 403, 247.

49. C. J. Brabec, N. S. Sariciftci, J. C. Hummelen, *Adv. Funct. Mater.* **2001**, 11, 1, 15.

50. H. Spreitzer, H. Becker, E. Kluge, W. Kreuder, H. Schenk, R. Demandt, H. Schoo, *Adv. Mater.* **1998**, 10, 16, 1340.

51. R. E. Martin, F. Geneste, B. S. Chuah, C. Fischmeister, Y. Ma, A. B. Holmes, R. Riehn, F. Cacialli, R. H. Friend, *Synth. Met.* **2001**, 122, 1, 1.

52. H. K. Shim, R. W. Lenz, J. I. Jin, *Macromol. Chem.* **1989**, 190, 2, 389.

53. J.-I. Jin, H. K. Shim, R. W. Lenz, *Synth. Met.* **1989**, 29, 1, E53.

54. R. M. Gregorius, P. M. Lahti, F. E. Karasz, *Macromolecules* **1992**, 25, 24, 6664.

55. R. M. Gregorius, F. E. Karasz, *Synth. Met.* **1992**, 53, 1, 11.

56. G. Kossmehl, M. Härtel, G. Manecke, *Macromol. Chem.* **1970**, 131, 1, 15.

57. G. Kossmehl, M. Härtel, G. Manecke, *Macromol. Chem.* **1970**, 131, 1, 37.

58. H. Cheng, R. L. Elsenbaumer, *J. Chem. Soc., Chem. Commun.* **1995**, 1451.

59. Y. Guindon, R. Frenette, R. Fortin, J. Rokach, *J. Org. Chem.* **1983**, 48, 1357.

60. M. C. Wang, T.-Y. Luh, *J. Org. Chem.* **1992**, 57, 2178.

61. T. W. Greene, P. G. M. Wuts, *Protective Groups in Organic Synthesis*, John Wiley & Sons, New York, **1991**, p. 285.

62. N. Komatsu, A. Taniguchi, A. Suzuki, *Tetrahedron Lett.* **1999**, 40, 19, 3749.

63. J. Nakayama, Y. Hasegawa, Y. Sugihara, A. Ishii, *Sulfur Letters* **1999**, 22, 4, 131.

64. A. J. J. M. Van Breemen, D. J. M. Vanderzande, P. J. Adriaensens, J. M. J. V. Gelan, *J. Org. Chem.* **1999**, 64, 9, 3106.

Chapter 6
Thienyl substituted poly(*p*-phenylene vinylene)s

6.1 Introduction

Among the conjugated polymers, poly(*p*-phenylene vinylene)s (PPV) and its derivatives are one of the most widely studied. Especially after the report of Burroughes *et al.*[1] on the electroluminescent properties of PPV, a lot of papers appeared on this subject and many different synthetic pathways to obtain this polymer were described. In our group, a lot of effort has been put into the development of the sulphinyl precursor route[2-4]. This has led to several soluble poly(*p*-phenylene vinylene) precursors. As mentioned in chapter three, a chemical differentiation between the leaving group (halide) and the polariser (sulphinyl group) is introduced in this route in order to have control over the polymerisation process. The synthesis of soluble phenyl substituted PPVs via the Gilch route was reported by different research groups[5-9] and also poly(2,3-diphenyl-1,4-phenylene vinylene) (DP-PPV) was made by using the chlorine precursor route[10-12]. Yet the use of a thiophene ring as a substituent was never described. Therefore the synthesis of thienyl substituted sulphinyl monomers was tested. By selecting the thiophene unit, the possibility for further electrochemical polymerisation is built in. In this regard, Advincula *et al.*[13] reported on the formation of very uniform ultra-thin films of a conjugated polymer network in which a siloxane polymer was cross-linked through the 2,5 linkages of the substituted thiophene ring by electrochemical or oxidative methods.

A transport regime often operational around room temperature in π-conjugated systems is hopping[14]. The hole-hopping process can be depicted as an electron-transfer (ET) reaction in which an electron is exchanged between two neighbouring molecules, one being in the neutral state and the other being in the radical cation state [T(a) + $T(b)^{+\cdot} \rightarrow$

$T(a)^{+\cdot}$ + T(b)][15]. Two major parameters determine the electron-transfer rate and ultimately the charge mobility: i) the electronic coupling between adjacent molecules, which needs to be maximised and ii) the reorganisation energy, which needs to be small for efficient transport[16]. In this respect, the origin of the improved mobility of OC_1C_{10}-PPV compared to PPV can possibly be explained. After all, the geometric reorganisation, which costs energy, can be localised in the ring via the stabilisation effect of the alkoxy chains on the hole as a charge carrier. A thiophene ring on the PPV backbone may therefore be even more interesting and responsible for an improved stabilisation which consequently simplifies hopping.

6.2 Monomer synthesis

Initially the monomer synthesis towards 2,5-di(2'-thienyl) substituted PPV was tested. For this reason 1,4-dichloromethyl-2,5-di(2'-thienyl)benzene **132** was synthesised starting from the commercially available 2,5-dibromo-*p*-xylene **126**. (Scheme 6.1)

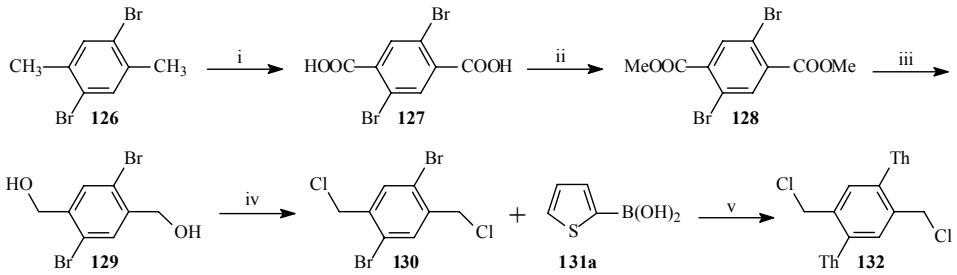

***Scheme 6.1**: Synthesis of 1,4-dichloromethyl-2,5-di(2'-thienyl)benzene **132**: i) $KMnO_4$; ii) MeOH, H_2SO_4; iii) $LiAlH_4$; iv) $SOCl_2$; v) $Pd(PPh_3)_4$, KF*

First the two methyl groups were oxidised by using potassium permanganate. Esterification of the resulting carbonic acids was followed by the transformation of the esters into the corresponding diol. And after this reduction, compound **129** was easily converted into dichloride **130** by means of thionyl chloride. The substitution of the thiophene rings on the phenyl core was performed by means of a Suzuki coupling reaction which is a cross coupling reaction between an organoboron reagent and an -in this case- unsaturated halide. Noteworthy is the use of KF as the base. In Suzuki coupling reactions aqueous carbonate is the most frequently used base[17]. However Wright *et al.*[18] described fluoride-mediated

boronic acid coupling reactions and found that fluoride salts allow these reactions to occur rapidly and in good yields.

The route described above involves a lot of steps, which makes the synthesis of **132** via this path time-consuming. Another path, via the dichlorobenzene analogue, to obtain the same dithienyl substituted intermediary product **132** is shown in scheme 6.2. Here several synthetic pathways towards 1,4-dichloromethyl-2,5-dichlorobenzene **135** were explored. A first approach was to start with the radical bromination of the commercially available 2,5-dichloro-*p*-xylene **133** with NBS and benzoyl peroxide (BPO) towards 1,4-dibromomethyl-2,5-dichlorobenzene **134**. This reaction was followed by converting the bromine atoms into chlorine atoms by means of LiCl. The conversion of **133** into **135** could also be accomplished in a single step by treating **133** with sulphuryl chloride in the presence of a catalytical amount of BPO[19]. The latter is preferred since the yield (36%) is comparable with the overall yield (34%) of the two step synthesis. The substitution of the thiophene units then was performed in the same way as described for the bromo analogue.

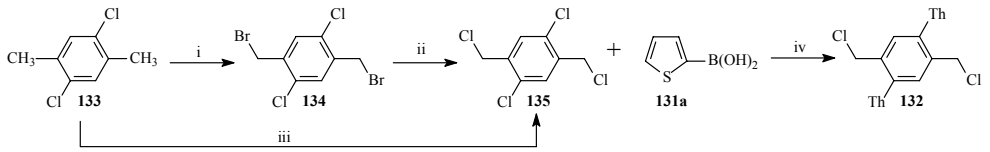

***Scheme 6.2**: Synthesis of **132** via 1,4-dichloromethyl-2,5-dichlorobenzene **135**: i) NBS, BPO; ii) LiCl; iii) SO_2Cl_2, BPO; iv) $Pd(PPh_3)_4$, KF*

Further functionalisation of the dichloride **132**, necessary to obtain the sulphinyl premonomer, seemed to be a problem. Different trials to synthesise the monosulphide always resulted in starting product and dioctyl disulphide (RSSR). Also an attempt to obtain the corresponding bissulphonium salt failed and yielded only starting product. Given that the sulphinyl monomer could not be synthesised, we tried to synthesise the xanthate monomer. Under the normal reaction conditions (addition of the potassium salt of ethylxanthic acid, reaction in methanol) again no reaction occurred. Even when methanol as the solvent was replaced by acetonitrile, which normally reduces the solvation of the anions and as a result improves the reactivity of the thiolate anions, only the starting product **132** was recovered. When also a Gilch polymerisation of dichloride **132** -with the use of K*t*BuO as the base- was unsuccessful, we decided to continue with the mono substituted derivative. Starting from

dichloride **135** the next step involved the introduction of the non-symmetrical differentiation into the monomer via the synthesis of the sulphide. (Scheme 6.3) For that reason dichloride **135** was dissolved in toluene and NaOH in water was added. Aliquat 336® or methyltrioctylammonium chloride was used as a phase transfer reagent. After this, the monosulphide **136** was oxidised using the H_2O_2/TeO_2 system. The substitution of the thiophene ring on the phenyl core was again performed by means of a Suzuki coupling. Since we are dealing with a non-symmetrical monomer, two regioisomers **138** and **139** can be formed when coupling monomer **137** with 2-thiophene (a) or 3-thiophene (b) boronic acid. NMR spectroscopy demonstrated the formation of exclusively the steric most favoured monomers **138a** and **138b** in a yield of 74% and 71%, respectively. The structure was certified by an extensive NMR study (see below).

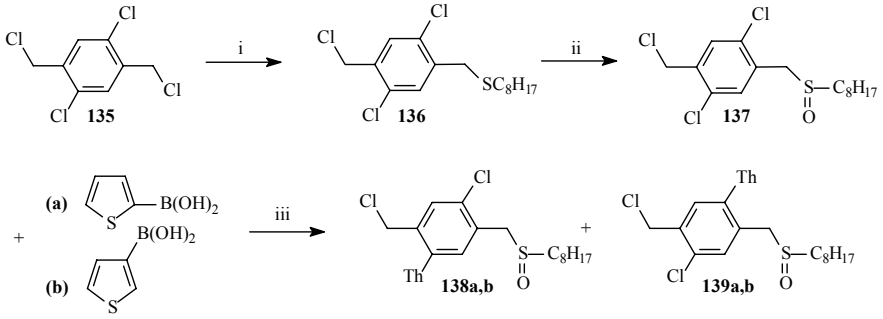

***Scheme 6.3**: Synthesis of the monomers: i) $C_8H_{17}SH$, NaOH, Aliquat 336; ii) H_2O_2, TeO_2; iii) $Pd(PPh_3)_4$, KF*

6.3 Structural characterisation of monomer 138a and 138b by NMR spectroscopy

For a consistent study of the polymers, a proper characterisation of the initial monomers is indispensable. The thienyl substituted monomers described above allow extensive NMR characterisation. In this paragraph the complete assignment of the ^1H and ^{13}C chemical shifts by different NMR techniques is discussed. The atomic numbering scheme used for this purpose is presented in figure 6.1.

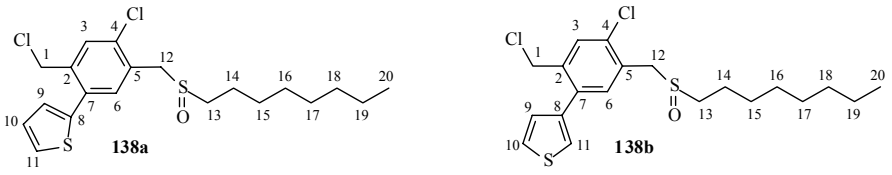

***Figure 6.1**: Atomic numbering scheme of the two monomers*

6.3.1 NMR signal assignment of the chemical shifts of the aliphatic part

Signal assignment of the side chain resonances

Assignment of the octyl side chain for non-substituted sulphinyl monomers was already accomplished in our group[20] and identical chemical shift values were observed for the side chain of these two new monomers. Nevertheless, the assignment was once confirmed by the INADEQUATE carbon-carbon connectivity technique in order to evaluate a much faster assignment criterion found in the determination of the T_{1C}-decay times of the carbon nuclei. Remark that heteronuclear C-H correlation experiments only allow the assignment of the carbon resonances C_{13}, C_{14}, C_{15} and C_{20} because the signals of H_{16}-H_{19} overlap in the proton spectrum. The INADEQUATE experiment reveals carbon-carbon *J*-coupling interactions via double quantum coherence. In figure 6.2 the spectrum of **138a** optimised for $^1J_{C\text{-}C}$ = 34 Hz is depicted. Remark that the signal at 32.9 ppm arises from C_1 and will be handled later.

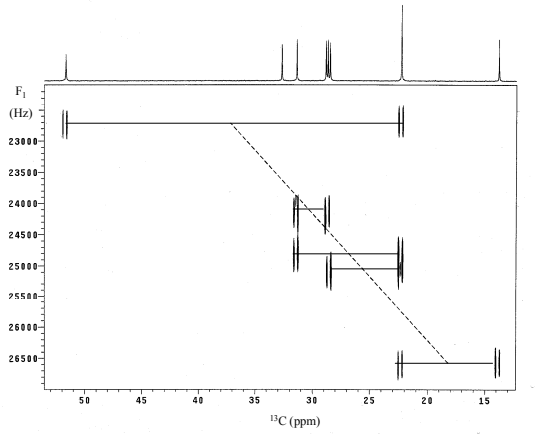

Figure 6.2**: INADEQUATE spectrum of monomer **138a

Beginning from the C_{20} methyl group at 14.0 ppm, a correlation is observed at a F_1 frequency of 26600 Hz, correlating the methyl carbon with the C_{19} methylene signal at 22.5 ppm. The C_{19} methylene correlates further with the C_{18} methylene signal at 31.6 ppm via a double-quantum correlation at 24800 Hz. C_{18} correlates with C_{17} at 28.9 ppm via a double-quantum correlation around 24100 Hz. For the assignment of C_{15} and C_{16}, a new start was made from C_{13} (51.8 ppm). Starting from C_{13}, a correlation is observed at a F_1 frequency of about 22700 Hz, correlating C_{13} with C_{14} at 22.5 ppm. C_{14} is correlated with C_{15} at 28.7 ppm via a double-quantum correlation around 25050 Hz. The remaining signal was assigned to C_{16} at 29.1 ppm.

When looking at the T_{1C} relaxation decay times (table 6.1), we can see a systematic increase in the decay time of the carbon nuclei in going from C_{13} to C_{20} due to an increase in molecular mobility towards the end of the flexible side chain. It is demonstrated that the T_{1C} decay times offer a rigid and fast (less than ½ h) criterion to assign the carbon resonances in long and flexible side chains.

An overview of the side chain resonances of the monomers **138a** and **138b** is given in table 6.1.

	Monomer 138a			**Monomer 138b**		
#	**Proton**	**Carbon**	**T_{1C} value (sec)***	**Proton**	**Carbon**	**T_{1C} value (sec)***
13	2.71	51.84	0.48	2.70	51.87	0.49
14	1.77	22.51	0.65	1.77	22.58	0.65
15	1.43	28.70	0.83	1.43	28.77	0.83
16	1.16-1.36	29.05	1.10	1.16-1.36	29.12	1.03
17	1.16-1.36	28.90	1.40	1.16-1.36	28.95	1.39
18	1.16-1.36	31.61	1.91	1.16-1.36	31.67	1.92
19	1.16-1.36	22.51	2.48	1.16-1.36	22.58	2.48
20	0.86	14.00	3.20	0.86	14.05	3.24
1	4.21	32.94	0.75	4.03	33.58	0.71
12	4.01 and 4.13	55.08	0.39	3.97 and 4.12	55.11	0.37

*** Average error is about 2%**

Table 6.1**: ^{1}H and ^{13}C-NMR chemical shifts and T_{1C} values of the aliphatic part of the carbon and proton spectra of monomer **138a** and **138b

Signal assignment of the remaining aliphatic resonances

The two remaining aliphatic signals in the ^{1}H and ^{13}C spectra are those of the benzylic methylenes. Since the H_{12} methylene protons are diastereotopic owing to the neighbouring asymmetric sulphinyl group and give rise to a typical AB pattern as demonstrated in figure 6.3a, the H_1 methylene group can be assigned to the singlet at 4.21 ppm. Their carbon chemical shifts are derived from a single bond optimised heteronuclear ($^{1}J_{C\text{-}H}$) correlation (direct HETCOR) NMR experiment. Both proton and carbon chemical shifts as well as the T_{1C} relaxation decay times are shown in table 6.1.

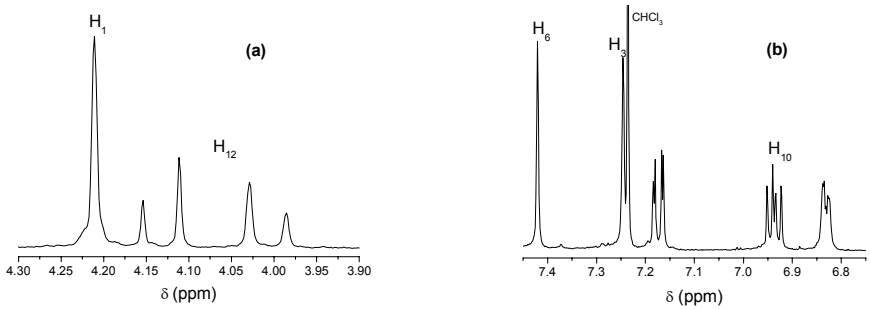

Figure 6.3**: (a) C<u>H2</u>Cl and C<u>H2</u>S(O)R region and (b) aromatic region of the proton spectrum of **138a

6.3.2 NMR signal assignment of the aromatic part (-$C_6H_2Cl(C_4H_3S)$-)

The proton spectra of both monomers consist of five aromatic spin systems. The two singlets represent the phenyl protons H_3 and H_6 which can be differentiated by means of a NOE difference experiment. Frequency selective irradiation of the aliphatic H_1 methylene protons of **138a** at 4.21 ppm yields a clear NOE enhancement of the resonance at 7.25 ppm which therefore can be assigned to the H_3 protons. (Figure 6.3b) The remaining singlet at 7.42 ppm can thus be assigned to the H_6 protons. A similar strategy was used to assign the corresponding resonances of **138b**. From the remaining three proton spin systems of the thiophene ring, one can already be assigned based on the coupling pattern: H_{10} of **138a** (two ortho couplings) and H_{11} of **138b** (only meta couplings). The two remaining proton signals will be assigned later. After assigning these proton chemical shifts, the assignment of the corresponding carbon signals is straightforward by means of direct HETCOR. (Figure

6.4) An overview of the proton and carbon resonance assignments for the monomers **138a** and **138b** is presented in table 6.2 and table 6.3, respectively.

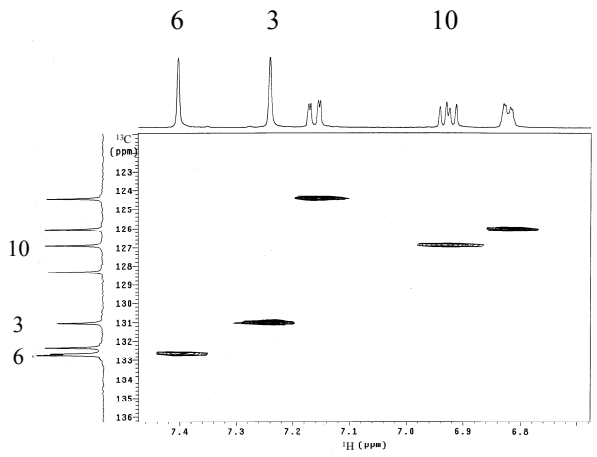

Figure 6.4**: Direct HETCOR spectrum of the aromatic part of monomer **138a

As in a long range HETCOR spectrum of phenylic systems mainly (vicinal) heteronuclear $^{3}J_{C\text{-}H}$ couplings are visualised, we expect for the monomers mainly $^{3}J_{C\text{-}H}$ couplings between H_3 and the quaternary carbons C_5 and C_7 and between H_6 and the quaternary carbons C_4, C_2 and C_8. According to the correlations observed in figure 6.5a for H_3 and H_6, the resonances at 128.4/132.4 ppm and those at 132.8/140.0/140.2 thus originate from C_5/C_7 and $C_4/C_2/C_8$, respectively. Since H_{12} can only couple with C_4, C_5 and C_6, the correlation between H_{12} and the carbon resonance at 128.4 ppm (figure 6.5b) has to arise from the $^{2}J_{C\text{-}H}$ coupling between H_{12} and C_5, leaving the C_7 resonance at 132.4 ppm and the C_4 resonance at 132.8 ppm (almost coinciding with the protonated C_6 resonance). In the same way H_1 can only couple with C_2, C_3 (protonated; already assigned at 131.1 ppm) and C_7 and the correlation between H_1 and the carbon resonance at 132.4 ppm (figure 6.5b) confirms the assignment of C_7. The remaining correlation allows assigning the C_2 resonance at 140.0 ppm leaving the C_8 resonance at 140.2 ppm. Interesting to notice is the appearance of $^{2}J_{C\text{-}H}$ couplings only for the benzylic protons; all other correlations in the long range HETCOR spectrum of the phenylic part are due to $^{3}J_{C\text{-}H}$ couplings.

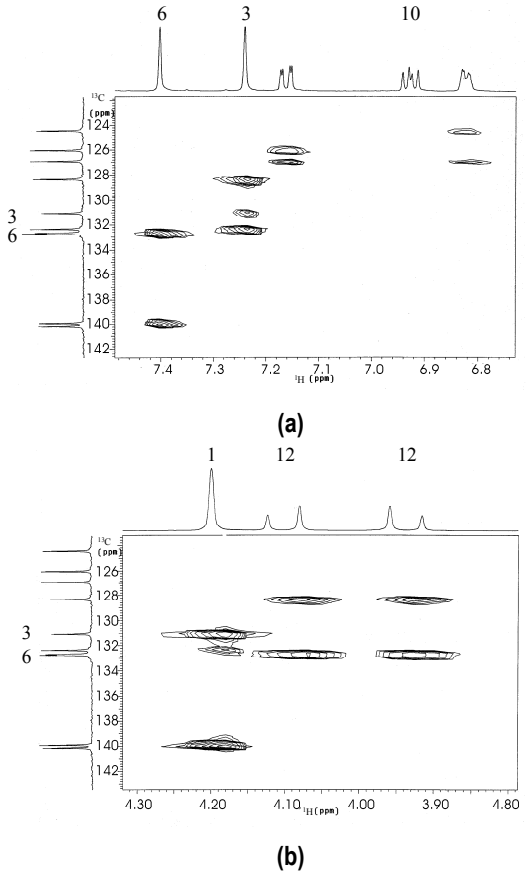

Figure 6.5**: Long range HETCOR spectrum of the central part of monomer **138a

Unfortunately, no correlation is observed between C_7 (132.4 ppm) and H_9 of the thiophene ring in the long range HETCOR spectra. The assignment of the missing thiophene resonances therefore had to be based on INADEQUATE experiments. Figure 6.6 shows the spectrum, optimised for $^1J_{C\text{-}C}$ = 52 Hz for the monomer **138b**. Starting from C_{11} at 122.0 ppm, a correlation is observed at a F_1 frequency of about 26750 Hz, correlating C_{11} with C_8 at 138.0 ppm. C_8 correlates with C_9 at 128.0 ppm via a double-quantum correlation around 26150 Hz. C_9 correlates further with C_{10} at 125.9 ppm via a double-quantum correlation around 27400 Hz. An overview is presented in table 6.2 and table 6.3.

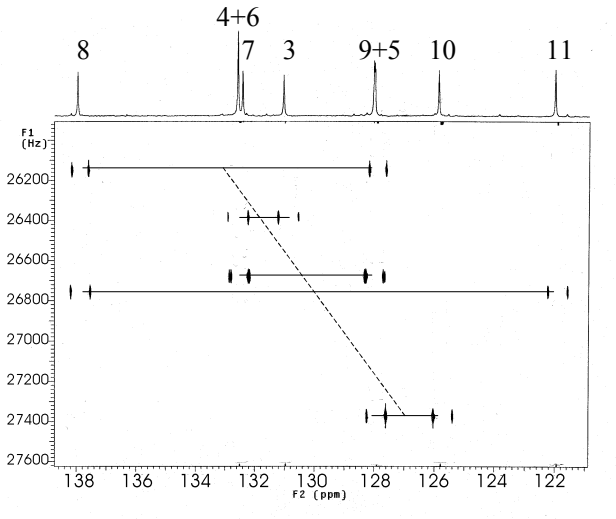

Figure 6.6**: INADEQUATE spectrum of monomer **138b

For this type of monomers, some degree of classification of the aromatic carbon resonances can also be found in the T_{1C} decay times. The protonated carbons C_3 and C_6 have T_{1C} values below 1 sec while those of the thiophene ring are situated between about 1 and 3 sec. The quaternary carbons next to the methylene carbon (C_2 and C_5) relax with a decay time between 2.8 and 3.6 sec while those next to a methine carbon have much longer decay times > 4.5 sec. Since the relaxation of carbon nuclei mainly occurs via neighbouring protons, the higher the surrounding proton density, the shorter the T_{1C} decay time. An overview of the T_{1C} values for both monomers is presented in table 6.2 and table 6.3, respectively.

#	Proton	Carbon	Long range HETCOR	T_{1C} value (sec)*
2		139.99 (C_q)	$^2J_{H1-C2}$	3.44
			$^3J_{H6-C2}$	
3	7.25	131.10 (CH)	$^3J_{H1-C3}$	0.67
4		132.78 (C_q)	$^3J_{H6-C4}$	4.54
5		128.41 (C_q)	$^3J_{H3-C5}$	2.80
			$^2J_{H12-C5}$	
6	7.42	132.72 (CH)	$^3J_{H12-C6}$	0.88
7		132.41 (C_q)	$^3J_{H3-C7}$	6.81
8		140.21 (C_q)		7.54
9	6.83	126.10 (CH)		2.17
10	6.94	126.97 (CH)		2.06
11	7.18	124.51 (CH)		1.32

*** Average error is about 2%**

Table 6.2**: ^1H and ^{13}C-NMR chemical shifts and T_{1C} values of the aromatic part of the carbon and proton spectra of monomer **138a

#	Proton	T_{1C} value (sec)*	Carbon	Long range HETCOR
2		3.57	140.14 (C_q)	$^2J_{H1-C2}$
				$^3J_{H6-C2}$
3	7.19	0.68	131.04 (CH)	$^3J_{H1-C3}$
4		5.03	132.57 (C_q)	$^3J_{H6-C4}$
5		2.80	127.99 (C_q)	$^3J_{H3-C5}$
				$^2J_{H12-C5}$
6	7.41	0.58	132.57 (CH)	$^3J_{H12-C6}$
7		6.37	132.42 (C_q)	$^3J_{H3-C7}$
8		8.55	137.95 (C_q)	
9	6.92	3.11	128.02 (CH)	
10	7.28	1.89	125.88 (CH)	
11	6.98	2.49	122.02 (CH)	

*** Average error is about 2%**

Table 6.3**: ^1H and ^{13}C-NMR chemical shifts and T_{1C} values of the aromatic part of the carbon and proton spectra of monomer **138b

6.4 Synthesis of the precursor polymer and conversion to the conjugated structure

The polymerisations of monomer **138a**, **138b** and **137** were performed in the same way as described in paragraph 3.2.3. Also here the temperature was kept constant at 30°C during the whole polymerisation process (1 hour) and Na*t*BuO (1.2 equivalents) was used as the base. Surprisingly no polymer could be obtained from the polymerisation of the monomers **138a** or **138b**. Even when the solvent was changed into 1,4-dioxane or when the polymerisation temperature was increased to 60°C, no polymer could be observed. Polymerisation in 2-BuOH at 30°C of the dichloro substituted monomer **137** did yield polymer **140**. (Scheme 6.4) The molecular weight (M_w = 142 000, PD = 1.7) of this precursor polymer was determined by Gel Permeation Chromatography (GPC) in THF relative to polystyrene (PS) standards. A monomodal molecular weight distribution was observed.

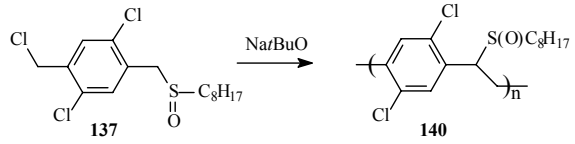

Scheme 6.4**: Polymerisation of monomer **137

The residual fraction was analysed with ^{1}H NMR spectroscopy and it was found that the solvent substituted product **142** was formed. In scheme 6.5 the formation of this compound, from the reaction of the *p*-quinodimethane system from monomer **137** with the solvent (2-BuOH), is presented.

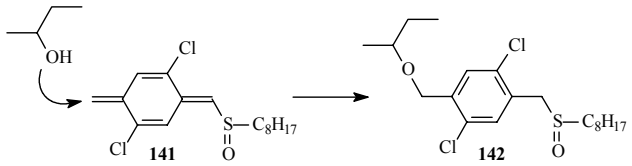

Scheme 6.5**: Formation of the solvent substituted monomer **142

The impossibility to polymerise monomers **138a,b** and the fact that the residual fraction there consist only of monomer is an indication that there is no *p*-QM formation for these monomers. In order to follow the formation of the *p*-QM system, a UV-Vis experiment

was carried out. Here a 10^{-4} M solution of monomer (**138a**) and a 10^{-3} M solution of base (Na*t*BuO), both in *2*-BuOH, were brought together in the measuring cell of the spectrometer by using a stop-flow apparatus. However after the assemblage of the two solutions, no difference in the absorption spectrum of the monomer was observed. After 100 minutes still no new absorption band was formed and so we could conclude that no formation of the QM system was visible. By way of comparison, for the 2,5-dichloro substituted monomer **137** the maximum of *p*-QM formation was already reached within two to three seconds. The QM system of this monomer with a bromine atom as the leaving group was also formed quickly[21] and it was previously demonstrated that this monomer also did polymerise in *2*-BuOH at 20°C in a yield of 65%[22].

The presence of the thiophene ring can be the reason for the fact that the *p*-QM system of **138a** is not formed. Due to the steric hindrance of this ring, the C-Cl bond can possibly not be in a perpendicular position relative to the plane of the phenyl ring, which is necessary for the elimination of the chlorine atom. In this way no 1,6-elimination can occur after the proton next to the polariser is abstracted. This is consistent with the fact that no nucleophilic substitution occurs on the compound **132** where two thiophene rings are attached on the phenyl core. In the synthesis of the phenyl substituted PPVs by means of the Gilch route, mentioned in the introduction, this is not a problem since a symmetrical monomer is started with. When one steric hindering group (R) is attached on the phenyl ring of the monomer (scheme 6.6), the *p*-QM system in which the polariser is next to the R group preferentially will be formed and thus polymerisation can occur.

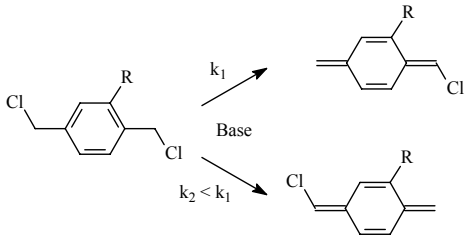

***Scheme 6.6**: Formation of the two possible p-QM systems*

To confirm this idea, a theoretical calculation is planned by the research group of J.L. Brédas and R. Lazzaroni in Mons to clarify the conformational aspects in the most stable conformation of the ground state of these monomers. Although an attractive hypothesis

could be formulated to explain our results, contradictive data can be found in the synthesis of the DP-PPV reported by Hsieh *et al.*[10-12]. They were able to synthesise a 2,3-diphenyl substituted monomer and to polymerise it successfully. This may indicate that our observations are specifically related to the presence of a thiophene ring.

The conversion of the precursor polymer **140** to its conjugated form was again followed by means of *in-situ* UV-Vis and FT-IR spectroscopy. The UV-Vis spectra recorded at different temperatures (figure 6.7) show the decline in absorbance at the absorption maximum of the precursor polymer (210 nm) as well as the red shift of the newly formed absorption maximum at increasing temperature. At 150°C, a conjugated polymer with a λ_{max} of 421 nm was obtained. A band gap of 535 nm or 2.3 eV was determined from the low energy edge of the π-π^* absorption band.

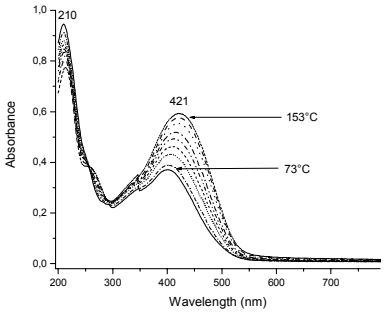

***Figure 6.7**: UV-Vis spectra at different temperatures*

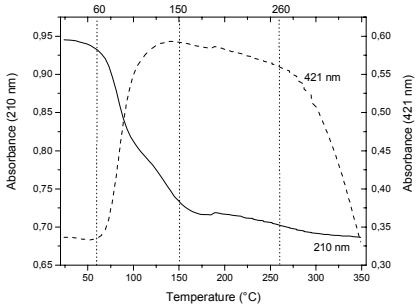

***Figure 6.8**: Absorbance profiles at 210 and 421 nm as a function of temperature*

From the profiles of the absorbance at λ_{max} of precursor and conjugated polymer, (figure 6.8) we could conclude that the elimination takes place between 50 and 150°C and that degradation starts around 260°C.

The FT-IR absorption profiles (figure 6.10) were in accordance with the results obtained from the UV-Vis measurements. The formation of the conjugated structure occurs in the temperature domain between 50 and 150°C as can be seen from the decrease of the sulphoxide stretching at 1052 cm^{-1} and the increase of the *trans* vinylene double bond at 960 cm^{-1}. The decline in absorption at 960 cm^{-1} above 150°C is probably caused by a thermochromic effect and not by the degradation of the structure.

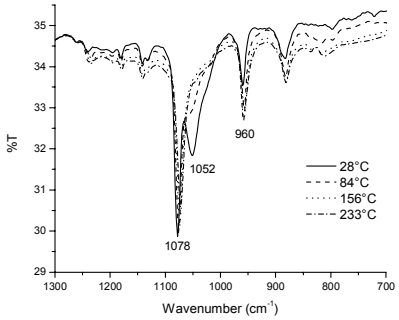

***Figure 6.9**: FT-IR spectra at different temperatures*

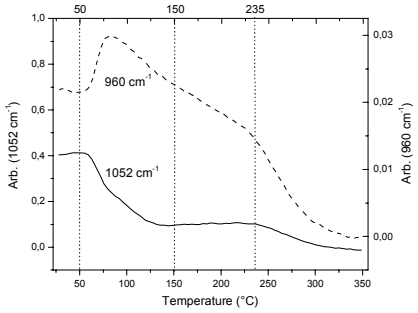

***Figure 6.10**: Absorption at 960 and 1052 cm^{-1} as a function of temperature*

6.5 Conclusion

Since thienyl substituted PPVs never were synthesised, we tried to obtain them via the sulphinyl precursor route. Problems occurred in the synthesis of the dithienyl substituted monomer but a straightforward synthesis of two sulphinyl monomers substituted with one thiophene ring is presented. Also the complete assignment of the ^{1}H and ^{13}C resonances of these monomers is discussed in this chapter. The latter can be of high value towards the optimalisation of chemical shift prediction software since reports that describe the experimental assignment of sulphoxide substituted benzylic positions are rather seldom. A very fast and robust criterion for the assignment of the carbon nuclei of the flexible side chain that is based on the T_{1C}-decay times is presented. Despite the easy synthesis of these two thienyl substituted monomers, they could not be polymerised. It is probably due to the steric hindrance caused by the thiophene ring that the elimination of the chlorine atom was impossible which blocked the formation of the *p*-QM system, the actual monomer in the polymerisation process. It is very likely that thienyl substituted PPVs can be obtained via the Gilch precursor route because then a symmetrical monomer is used which consequently can lead to the corresponding *p*-QM. This was however not tested yet.

6.6 Experimental part

Characterisation: ^{1}H NMR spectra were obtained in $CDCl_3$ at 300 MHz on a Varian Inova spectrometer using a 5 mm probe. The chemical shifts (δ) in ppm were determined

relative to the residual $CHCl_3$ absorption at 7.24 ppm. The ^{13}C NMR experiments were recorded at 100 MHz on a 9.4 Tesla Varian Inova spectrometer using a 10 mm probe. Chemical shifts were defined relative to the ^{13}C resonance of $CDCl_3$ (77.0 ppm). A ^{13}C APT (attached proton test) was used to detect methyls and methines in opposite intensity with respect to methylenes and quaternary carbons and this to confirm the results described in the previous paragraphs. The HETCOR (heteronuclear chemical shift correlation) pulse sequence was optimised to observe the direct couplings ($^1J_{CH}$) or the long range two-bond couplings ($^2J_{CH}$) and three-bond couplings ($^3J_{CH}$). The 2D-INADEQUATE spectrum was obtained using the pulse sequence described by Bax and co-workers[23, 24] using quadrature detection in both frequency domains at 21.0 ± 0.1°C. The delay time ¼ *J*(C,C) was set to be 8.5 or 13 ms, corresponding to the ^{13}C-^{13}C coupling constant of aliphatic or aromatic carbons of 34 or 52 Hz, respectively. The sweep width used in the t_1 time domain was set to be twice the sweep width in t_2 (16000 and 2100 Hz for aliphatic and aromatic region respectively), yielding a spectrum with cross peaks symmetric about a pseudo-diagonal. A total of 200 scans were collected in 4096 complex points for each of the 128 t_1 values and eight dummy scans were used to establish a pseudo-steady state. A preparation delay of 6 s was used between scans. NOE difference spectroscopy was accomplished by subtracting a selective irradiated (during the preparation delay) spectrum from a normal spectrum. The T_{1C} relaxation times were derived from an inversion recovery experiment and by fitting the carbon signal intensity versus the evolution time *t* according to equation (6-1).

$$M(t) = M_0 (1 - 2 \exp(-t/T_{1C})) \qquad (6\text{-}1)$$

In this equation, M(t) and M_0 is the magnetisation as a function of the variable evolution time t and at equilibrium, respectively. All relaxation decay curves were analysed on a Macintosh computer using the program Kaleidagraph 3.0.

For the other characterisation methods and the materials used, we would like to refer to the experimental part of chapter two and three.

2,5-Dibromoterephthalic acid (127)

This compound was prepared according to a procedure reported in the literature[25].

Dimethyl-2,5-dibromoterephthalate (128)

To a solution of 2,5-dibromoterphthalic acid (5 g, 15.43 mmol) in MeOH (38.6 mL), 15 mL of concentrated H_2SO_4 was added and the mixture was refluxed for 24 hours. Then the mixture was poured in water (77 mL) and made basic with NaOH (25% aqueous solution). After extraction with $CHCl_3$ (3 x 100 mL), the organic layer was dried over $MgSO_4$ and the solvent was removed in vacuo. Yield: 87% (4.7 g, 13.35 mmol); ^{1}H NMR ($CDCl_3$): 8.03 (s, 2H), 3.93 (s, 6H); MS (EI, m/e): 352 (M^+), 321 (M^+ – OMe), 293 (M^+ – COOMe), 261 (M^+ – COOMe - OMe), 233 (M^+ – 2 COOMe)

1,4-Dibromo-2,5-dichloromethylbenzene (130)

To a solution of $LiAlH_4$ (0.65 g, 17.143 mmol) in dry THF cooled in an ice-bath, dimethyl-2,5-dichloroterephthalate (2.0 g, 5.714 mmol) dissolved in dry THF was added. The mixture was removed from the ice-bath and stirred for two hours at room temperature. After another two hours refluxing, the mixture was again placed in an ice-bath and a 1 M aqueous HCl solution was added until neutral. The mixture was extracted with $CHCl_3$ (3 x 20 mL), dried over $MgSO_4$ and the solvent was removed in vacuo. The alcohol formed in this way was used without further purification. [MS (EI, m/e): 296 (M^+), 265 (M^+ – CH_2OH), 249 (M^+ – CH_2OH - OH), 216 (M^+ – Br), 197 (M^+ – Br - OH), 185 (M^+ – Br - CH_2OH)] To an ice-cold solution of the alcohol in THF (10 mL), thionyl chloride (0.5 mL, 6.790 mmol) was added drop wise. The mixture was stirred at room temperature for two hours and $NaHCO_3$ was added until the mixture was neutral. After extraction with $CHCl_3$ (3 x 20 mL) the combined organic layers were dried over $MgSO_4$ and the solvent was evaporated. Yield: 79%; ^{1}H NMR ($CDCl_3$): 7.69 (s, 2H), 4.61 (s, 4H); MS (EI, m/e): 332 (M^+), 297 (M^+ - Cl), 262 (M^+ – 2 Cl), 182 (M^+ – 2 Cl – Br), 102 (M^+ – 2 Cl – 2 Br)

1,4-Dibromomethyl-2,5-dichlorobenzene (134)[22, 26]

In a three-neck flask, 2,5-dichloro-p-xylene **133** (17.5 g, 0.1 mol) was dissolved in benzene (100 mL). After NBS (*N*-bromosuccinimide) (35.6 g, 0.2 mol) and BPO (benzoyl peroxide) (0.01 g, 0.041 mol) as initiator were added, the mixture was refluxed under nitrogen and lighted with a lamp of 200 Watt. After 24 hours, the succinimide was filtered off and the solvent was evaporated. The product was dissolved in $CHCl_3$, an extraction with $CHCl_3$ (3 x 50 mL) was performed, the combined organic layers were washed with a $NaHCO_3$ solution

and with water, dried over $MgSO_4$ and the solvent was evaporated partially. The flask was placed in the fridge and the crystals that were formed were filtered off. Yield: 36% (12.1 g, 0.0364 mol); Mp: 123.0-125.4°C; ^{1}H NMR ($CDCl_3$): 7.46 (s, 2H), 4.48 (s, 4H); MS (EI, m/e): 332 (M^+), 252 (M^+ – Br), 172 (M^+ – 2 Br)

1,4-Dichloromethyl-2,5-dichlorobenzene (135)

(a) A mixture of 1,4-dibromomethyl-2,5-dichlorobenzene **134** (12 g, 0.0361 mol) and LiCl (15.18 g, 0.361 mol) in acetone (150 mL) was refluxed for 24 hours. Water was added and an extraction with $CHCl_3$ (3 x 50 mL) was performed, the combined organic layers were dried over $MgSO_4$ and the solvent evaporated which yielded **135** as white crystals. Yield: 94% (8.2 g, 0.0339 mol).

(b) To a solution of 2,5-dichloro-*p*-xylene **133** (10 g, 57.14 mmol) in CCl_4 (20 mL), sulphuryl chloride (4.58 mL, 57.14 mmol) and a catalytic amount of benzoyl peroxide (BPO) were added. The solution was refluxed for 12 hours after which the solvent was removed in vacuo. The crude reaction product was purified by column chromatography (silica, n-hexane) which yielded **135** as white crystals. Yield: 36% (5 g, 20.661 mmol); Mp: 98.9-99.9°C; ^{1}H NMR ($CDCl_3$): 7.51 (s, 2H), 4.62 (s, 4H); MS (EI, m/e): 242 (M^+), 207 (M^+ – Cl), 172 (M^+ – 2 Cl), 137 (M^+ – 3 Cl), 102 (M^+ – 4 Cl)

1,4-Dichloromethyl-2,5-di(2'-thienyl)benzene (132)

2-Thiopheneboronic acid (1.22 g, 9.566 mmol), **135b** (0.5 g, 2.066 mmol) and KF (490 mg, 8.450 mmol) were dissolved in a mixture of water (20 mL) and toluene (20 mL). $Pd(PPh_3)_4$ (150 mg) was added as a catalyst. After refluxing the mixture for 24 hours, an extraction with $CHCl_3$ (3 x 30 mL) was performed and the combined organic phases were dried over $MgSO_4$. The crude reaction product was purified by column chromatography (silica, *n*-hexane). Yield: 52% (0.36 g, 1.065 mmol); ^{1}H NMR ($CDCl_3$): 7.21 (s, 2H), 7.16 (dd, 2H), 6.93 (dd, 2H), 6.81 (dd, 2H), 4.19 (s, 4H); MS (EI, m/e): 338 (M^+), 303 (M^+ – Cl), 219 (M^+ – Cl - Th), 184 (M^+ – 2 Cl - Th)

1-Chloromethyl-4-(*n*-octylsulphinyl)methyl-2,5-dichlorobenzene (137)

A mixture of 1,4-dichloromethyl-2,5-dichlorobenzene **135** (850 mg, 3.512 mmol) in toluene (10 mL), NaOH (365 mg, 9.132 mmol) in H_2O (10 mL) and a catalytical amount of the phase

transfer catalyst, trioctylmethylammoniumchloride (Aliquat 336®), was stirred at room temperature. A solution of 1-octanethiol (513 mg, 3.512 mmol) in toluene (5 mL) was added dropwise and stirred for five hours. After extraction with $CHCl_3$ (3 x 20 mL), drying over $MgSO_4$ and evaporation of the solvent, the product was oxidised by adding dioxane (15 mL), H_2O_2 (0.42 mL), TeO_2 (35 mg) and three drops of concentrated HCl. The reaction was followed on TLC and proceeded until traces of overoxidation were visible, then it was quenched by adding brine (20 mL) and afterwards extracted with $CHCl_3$ (3 x 20 mL). The combined organic layers were dried over $MgSO_4$ and concentrated. After column chromatographic purification (silica, $CHCl_3/Et_2O$ 8/2), compound **137** was obtained as a white solid. Yield: 46% (600 mg, 1.630 mmol); Mp: 53.0-54.8°C; ^{1}H NMR ($CDCl_3$): 7.56 (s, 1H), 7.46 (s, 1H), 4.62 (s, 2H), 4.14 (d, ^2J = 12.9 Hz, 1H), 3.96 (d, ^2J = 12.9 Hz, 1H), 2.73 (m, 2H), 1.79 (m, 2H), 1.43 (m, 2H), 1.25 (m, 8H), 0.86 (t, 3H); MS (CI, m/e): 369 (M^+), 333 (M^+ – Cl)

1-Chloromethyl-2-(2'-thienyl)-4-(*n*-octylsulphinyl)methyl-5-chlorobenzene (138a)

2-Thiopheneboronic acid (2.0 g, 15.625 mmol), 1-chloromethyl-4-(n-octylsulphinyl)methyl-2,5-dichlorobenzene **137** (2.5 g, 6.794 mmol) and KF (788 mg, 13.587 mmol) were dissolved in a mixture of water (20 mL) and toluene (20 mL). $Pd(PPh_3)_4$ (115 mg) was added as a catalyst. After refluxing the mixture for 23 hours, an extraction with $CHCl_3$ (3 x 30 mL) was performed and the combined organic phases were dried over $MgSO_4$. The crude reaction product was purified by column chromatography (silica, $CHCl_3$). Yield: 74% (2.1 g, 5.048 mmol); Mp: 54.1-55.4°C; MS (EI, m/e): 416 (M^+), 255 (M^+ – $S(O)C_8H_{17}$); UV-Vis ($CHCl_3$): λ_{max} at 208 nm; FT-IR (ν, cm^{-1}): 2954 (s), 2926 (s), 2855 (s), 1478 (m), 1418 (w), 1371 (m), 1080 (s), 1047 (s), 888 (w), 851 (w), 695 (s)

1-Chloromethyl-2-(3'-thienyl)-4-(*n*-octylsulphinyl)methyl-5-chlorobenzene (138b)

The preparation of **138b** is analogous to that described for **138a** but here 3-thiopheneboronic acid was used. Yield: 71% (2.0 g, 4.808 mmol); Mp: 57.0-57.8°C; MS (EI, m/e): 416 (M^+), 255 (M^+ – $S(O)C_8H_{17}$); UV-Vis ($CHCl_3$): λ_{max} at 208 nm; FT-IR (ν, cm^{-1}): 2954 (s), 2926 (s), 2855 (s), 1478 (m), 1411 (w), 1368 (m), 1079 (s), 1047 (s), 888 (w), 832 (w), 813 (w), 770 (m), 636 (w)

Polymerisation of monomer 137

A solution of the monomer (300 mg, 0.815 mmol) in *sec*-butanol (4.6 mL) and a solution of sodium *tert*-butoxide (96 mg, 0.978 mmol) in *sec*-butanol (2.5 mL) were degassed for 1 hour at 30°C by a continuous stream of nitrogen. The base solution was added in one portion to the stirred monomer solution. After one hour the reaction mixture was poured in a well-stirred amount (150 mL) of ice water. The mixture was neutralised with aqueous hydrogen chloride (1 M) and extracted with $CHCl_3$ (3 x 100 mL). The combined organic layers were concentrated in vacuo. The crude product was dissolved in $CHCl_3$ and precipitated in 100 mL of an ice-cold *n*-hexane/diethyl ether (3/1) solution. The polymer was collected and dried. The residual fraction was concentrated in vacuo. UV-Vis ($CHCl_3$): λ_{max} at 210 nm

6.7 References

1. J. H. Bourroughes, D. D. C. Bradley, A. R. Brown, R. N. Marks, K. MacKay, R. H. Friend, P. L. Burn, A. B. Holmes, *Nature* **1990**, 347, 539.

2. F. Louwet, D. Vanderzande, J. Gelan, *Synth. Met.* **1995**, 69, 509.

3. F. Louwet, D. Vanderzande, J. Gelan, J. Mullens, *Macromolecules* **1995**, 28, 1330.

4. M. Van Der Borght, D. Vanderzande, P. Adriaensens, J. Gelan, *J. Org. Chem.* **2000**, 65, 284.

5. H. Spreitzer, H. Becker, E. Kluge, W. Kreuder, H. Schenk, R. Demandt, H. Schoo, *Adv. Mater.* **1998**, 10, 16, 1340.

6. H. Becker, H. Spreitzer, W. Kreuder, E. Kluge, H. Schenk, I. Parker, Y. Cao, *Adv. Mater.* **2000**, 12, 1, 42.

7. H. Becker, H. Spreitzer, W. Kreuder, E. Kluge, H. Vestweber, H. Schenk, K. Treacher, *Synth. Met.* **2001**, 122, 1, 105.

8. D. M. Johansson, G. Srdanov, G. Yu, M. Theander, O. Inganäs, M. R. Anderson, *Macromolecules* **2000**, 33, 2525.

9. D. M. Johansson, X. Wang, T. Johansson, O. Inganäs, G. Yu, G. Srdanov, M. R. Anderson, *Macromolecules* **2002**, 35, 4997.

10. B. R. Hsieh, H. Antoniadis, D. C. Bland, W. A. Feld, *Adv. Mater.* **1995**, 7, 1, 36.

11. H. Antoniadis, D. Roitman, B. Hsieh, W. A. Feld, *Polym. Adv. Technol.* **1997**, 8, 7, 392.

12. W. C. Wan, H. Antoniadis, V. E. Choong, H. Razafitrimo, Y. Gao, W. A. Feld, B. R. Hsieh, *Macromolecules* **1997**, 30, 21, 6567.

13. R. Advincula, C. Xia, K. Onishi, P. Tarenekar, S. Deng, A. Baba, W. Knoll, *Polym. Prepr.* **2002**, 514.

14. J. H. Schön, C. Kloc, B. Batlogg, *Phys. Rev. Lett.* **2001**, 86, 3843.

15. M. Malagoli, J.-L. Brédas, *Chem. Phys. Lett.* **2000**, 327, 1-2, 13.

16. N. E. Gruhn, D. A. da Silva Filho, T. G. Bill, M. Malagoli, V. Coropceanu, A. Kahn, J.-L. Brédas, *J. Am. Chem. Soc. Comm.* **2002**, 124, 27, 7918.

17. A. Suzuki, *Pure & Appl. Chem.* **1985**, 57, 1749.

18. S. W. Wright, D. L. Hageman, L. D. McClure, *J. Org. Chem.* **1994**, 59, 6095.

19. B. S. Furniss, A. J. Hannaford, P. W. G. Smith, A. R. Tatchell, *Vogel's Textbook of Practical Organic Chemistry*, 5th ed., Longman: New York, **1989**, p. 864.

20. A. J. J. M. Van Breemen, P. J. Adriaensens, A. C. Issaris, M. M. de Kok, D. J. M. Vanderzande, J. M. J. V. Gelan, *Magn. Reson. Chem.* **2000**, 38, 129.

21. Results obtained by F. Motmans, Limburgs Universitair Centrum, Diepenbeek, Belgium.

22. M. Van Der Borght, *Ph. D. Dissertation* **1998**, Limburgs Universitair Centrum, Diepenbeek, Belgium.

23. A. Bax, R. Freeman, T. A. Frenkiel, *J. Am. Chem. Soc.* **1981**, 103, 2102.

24. A. Bax, R. Freeman, T. A. Frenkiel, M. H. Levitt, *J. Magn. Reson.* **1981**, 43, 478.

25. Y. X. Yao, J. M. Tour, *Macromolecules* **1999**, 32, 8, 2455.

26. R. K. McCoy, F. E. Karasz, A. Sarker, P. M. Lahti, *Chem. Mater.* **1991**, 3, 5, 941.

Chapter 7
Perspectives

7.1 Introduction

The work described in this dissertation is of course far from finished. In 1998 McCullough[1] wrote in an article: "A large portion of both the pioneering and future work in conjugated polymers strongly depends on synthetic chemists creating new polymers that can be fabricated into new devices and whose physics and chemistry can be understood in detail". This statement is still true today, especially the last part. The knowledge and understanding of the chemistry in the applied synthesis of new materials is indispensable. Therefore well defined and reliable synthetic pathways are necessary. With these routes, new low band gap materials can be synthesised. The work that has to be done regarding this subject is still enormous. The challenge for synthetic chemists is to come to new and better materials than there are known today. The dithiocarbamate route described in chapter five can be an interesting and new tool in this search for new materials. This route offers a whole range of possibilities: new materials can be made and additionally materials that are already known can be made in an improved way. This was already demonstrated for PTV which had better characteristics compared to the PTV obtained via the xanthate route. Since it is a new precursor route a lot of work can be devoted to the synthesis of other polymers than PTV and PPV described in chapter five and to gain a better insight into the mechanisms of this polymerisation process.

7.2 Further study on the dithiocarbamate route

Further investigations towards the polymerisation conditions which can be used to obtain precursor polymers via the dithiocarbamate route are planned. As we applied for a patent regarding this route, additional information is needed.

First an extensive study on the influence of different reaction conditions on the course of the polymerisation has to be planned. Up till now, only LDA was used as the base, the polymerisation time was always 90 minutes and the reaction was performed in dried THF. As mentioned in paragraph 5.3, the residual fractions contained monomer after the polymerisation. By elevating the reaction time it is perhaps possible to reduce this amount of monomer and hereby increase the polymerisation yield. Other bases such as K*t*BuO instead of LDA have to be tested as well. If similar results can be obtained when K*t*BuO is used as the base, this will be preferable to the use of LDA seeing that LDA is less suitable on large scale and therefore is less used in industry. Another aspect of the polymerisation that has to be checked is the choice of solvent. In summary, our goal is to find the optimal conditions for the polymerisation of dithiocarbamate monomers.

After these conditions are determined, we have to evaluate the scope of the dithiocarbamate route by trying to synthesise and polymerise different monomers of interest via this new route. The characteristics of the 3,4-disubstituted PTVs described in chapter three can be compared with the same polymers obtained via the new precursor route. An example of such a substituted PTV is the 3,4-diphenyl substituted polymer. An example of an even more electron rich system is EDOT. Attempts to synthesise monomer **143** will be made in the future in order to obtain poly(3,4-ethylene dioxythiophene vinylene) (PEDOTV). (Scheme 7.1)

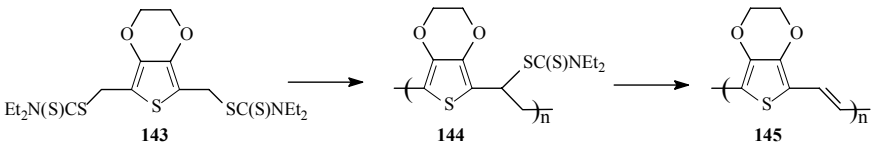

***Scheme 7.1**: Synthesis of PEDOTV via the dithiocarbamate precursor route*

It would also be interesting to synthesise polymers with another aromatic system. An example is the synthesis of the naphthalene monomer **146**. (Scheme 7.2) This compound was already reported in literature for its fungicidal activity[(2)] and the reason for the use of this compound as a monomer is related to the fact that this monomer could lead to a polymer with an extended aromatic system.

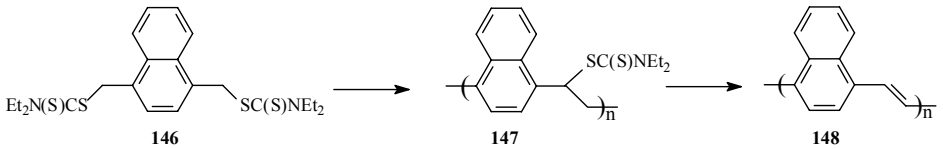

146 **147** **148**

***Scheme 7.2**: Synthesis of poly(p-naphthalene vinylene) via the dithiocarbamate precursor route*

The electron poor polymers are the last group of materials which have to be tested to determine the scope of the dithiocarbamate route. Examples of such polymers are poly(2,5-pyridylene vinylene) and poly(2,2'-bipyridylene vinylene). These polymers were already synthesised via the sulphinyl precursor route[3] and thus no additional problems are being expected for the synthesis of monomer **150** and **152** via the corresponding dichlorides. (Scheme 7.3) Dichloride **149** was synthesised by chlorinating the commercially available 2,5-lutidine (2,5-dimethylpyridine) with NCS. The pathway towards dichloride **151** comprised more steps. The synthesis started with the dimerisation of 3-picoline (3-methylpyridine) with a Raney Nickel catalyst. The 5,5'-dimethyl-2,2'-bipyridine in this way formed, was oxidised towards the diacid which was consecutively esterified. Reduction of the ester and chlorination of the corresponding diol with $SOCl_2$ yielded compound **151**.

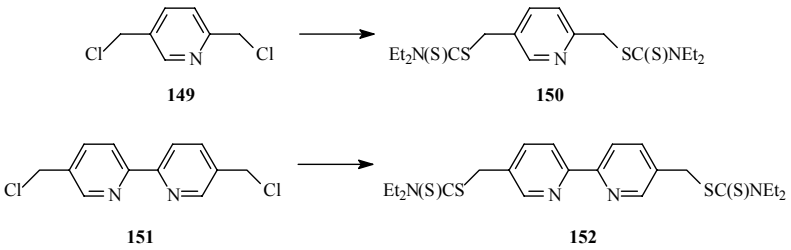

149 **150**

151 **152**

***Scheme 7.3**: Synthesis of the pyridine and bipyridine dithiocarbamate monomers*

The very last reactions to investigate are the copolymerisations between different dithiocarbamate monomers.

7.3 Synthesis of low band gap polymers which are soluble in the conjugated state

As mentioned in chapter five, the use of the dithiocarbamate route can be a solution to the synthesis of electron rich conjugated polymers. By making PTV derivatives with long

chains (R) on the thiophene core, the system becomes even more electron rich. (Scheme 7.4)

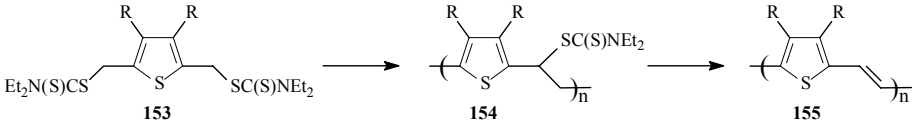

***Scheme 7.4**: Synthesis of soluble PTV via the dithiocarbamate route (R = alkyl, alkoxy, PEO)*

Furthermore, the obtained polymer is soluble not only in its precursor but also in its conjugated form. This will have the advantage that no heat treatment is necessary in the device preparation. The elimination of the dithiocarbamate groups can be done in solution and after that the in this way obtained conjugated polymer is precipitated in a non-solvent, it can be spin-coated on the device. It has already been proven that the elimination in solution has several advantages over the elimination in film. An example is the improved photoluminescence of OC_1C_{10}-PPV, prepared via the sulphinyl precursor route, when the (spin-coated) conjugated polymer was obtained from the in solution eliminated precursor polymer compared to when the polymer was obtained by converting the soluble precursor polymer in film[4]. After all, the subsequent reactions of the elimination products, such as the disproportionation reaction of thiosulphinate, do not affect the conjugated polymer anymore since the elimination products are removed (they remain dissolved in the non-solvent).

The different R-groups we attempt to implant are not only alkyl or alkoxy chains but also oligo ethylene oxide (PEO) chains. By introducing these hydrophilic side chains, a polar polymer, which is soluble in polar solvents, is obtained. This can be of interest for several applications since environment-friendly solvents (alcohols, water) can be used in this way.

7.4 Elucidation of the polymerisation mechanism(s)

To obtain more insight in the processes that occur during the polymerisation of the xanthate or dithiocarbamate monomers, two mutilated monomers **157** and **158** were synthesised starting from benzyl bromide. (Scheme 7.5)

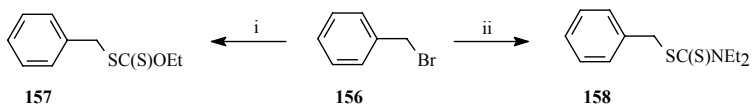

***Scheme 7.5**: Synthesis of the mutilated monomers: i) KSC(S)OEt; ii) $NaSC(S)NEt_2.3H_2O$*

To these monomers, an equimolar amount of base (LDA) was added and the obtained reaction mixture was investigated. From TLC it was clear that something happened with these mutilated monomers (different spots). This indicates that the xanthate or dithiocarbamate eliminable group in the intermediary formed precursor polymer induces side reactions during the polymerisation process. It was difficult to investigate the nature of the different products that were formed. Further investigations are necessary to clarify the polymerisation mechanism. In the future especially the mechanism of the dithiocarbamate precursor route will be studied. The influence of additives such as a radical inhibitor (2,2,6,6-tetramethylpiperinoxyl (TEMPO)) or of a chain transfer reagent (CBr_4) on the reaction and its products will be tested. This way of investigating a polymerisation mechanism was also applied in the mechanistic study on the sulphinyl and the Gilch route[5-7]. Additionally, the polymerisation reaction of the bis-dithiocarbamate monomer **117** in the presence of the corresponding mutilated monomer **158** will be performed and the effect on the molecular weight will be checked.

7.5 The use of the dithiocarbamate group in the precursor polymer as an iniferter

Another part of the plans for future work is the further use of the dithiocarbamate polariser in the precursor polymers obtained via the dithiocarbamate route. Such a dithiocarbamate group can function as an iniferter and the task of such a group is already explained in the introduction of chapter five. Attempts to polymerise styrene (S) and methyl methacrylate (MMA) in this way will then lead to block copolymers with the PPV or PTV precursor polymer as is visualised for the latter in scheme 7.6.

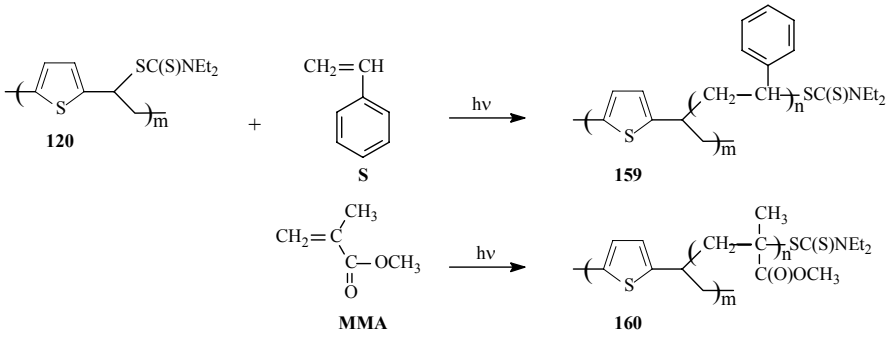

***Scheme 7.6**: Further use of the dithiocarbamate group as an iniferter*

The dithiocarbamate groups can principally induce further radical polymerisation but not all dithiocarbamate groups on the precursor have to function as an iniferter. This can be accomplished by performing first a partial elimination of these groups. Of course it is then preferable to start from a precursor polymer with side chains on the backbone (e.g. OC_1C_{10}-PPV) which make that the polymer stays soluble in the conjugated phase. The non-eliminated dithiocarbamate groups then can function as an iniferter and induce the polymerisation of the vinyl monomers. The in this way obtained block copolymer of a conjugated polymer with another polymer can be of interest in the use of new materials for solar cell devices. The vinyl monomer could then be chosen in such a way that a p- or n-type polymer is formed on the conjugated polymer by the radical polymerisation of the corresponding vinyl monomer.

Polymers with a dithiocarbamate photoiniferter group in a side-chain end were already synthesised by a chemical reaction. An example is the reaction of poly(vinyl chloride) (PVC) with sodium dithiocarbamate in DMF to form a polymer which was partially substituted with dithiocarbamate groups. (Scheme 7.7) These groups were then used as a photoiniferter for the preparation of, for one, new antithrombogenic heparinised polymers[8].

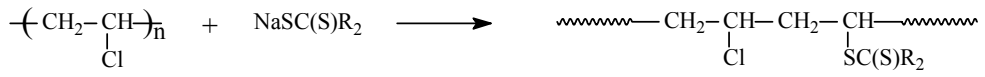

***Scheme 7.7**: Reaction of PVC with sodium dithiocarbamate*

Another application in which the iniferter technique was used is the surface grafting of hydrophilic monomers onto hydrophobic polymer surfaces. Inoue *et al.* reported on the preparation of a hydrophilic polydimethylsiloxane (PDMS) surface from a chlorine-containing PDMS which was first photocured on a glass plate and afterwards subjected to a reaction with sodium diethyldithiocarbamate[9]. This polymer was then photoirradiated in the presence of hydrophilic vinyl monomers to afford surface-grafted PDMS. Surface grafting techniques using this dithiocarbamate photoiniferter were also applied by Hadziioannou *et al.*[10] and in the group of Matsuda in a precision processing technology of polymer surfaces[11]. Since the polymerisation proceeds only during photoirradiation and at photoirradiated regions, different types of surfaces were realised: (i) regionally precise, microprocessed surfaces onto which different polymers were regionally grafted, (ii) surface

graft block copolymers in which different polymer blocks were sequentially formed in graft copolymers, and (iii) a gradient surface in which the thickness of the graft layer gradually varied in one direction. However, in all the cases mentioned above, the dithiocarbamate groups were introduced by a chemical reaction and these iniferter groups never were intrinsically present as a cause of the used polymerisation route.

7.6 Performance of materials in electronic devices

It is of course evident that new materials should be tested for their applications. Since low band gap materials already proved to be quite successful for the use in FETs and solar cells (chapter three), especially these devices will be interesting to do tests with. But not only tests towards the applicability of newly synthesised materials are needed; also further experiments on the materials that were already made are planned.

Tests with composite solar cell devices in which the active layer results from PTV or PTV derivatives made via the dithiocarbamate precursor route (chapter five) should normally give improved results. Additionally the use of a LiF layer in such device structures can be tested. Analysing the performance of a certain material in a device, not only will valorise the material itself but also the synthetical route by which the compound was made. All this requires an interdisciplinary approach. As already mentioned in chapter one an intense cooperation between chemists, physicists and engineers is indispensable to obtain the best results. Also in a physical viewpoint a lot of research can be done to improve the device configuration. From our collaboration with the physics department some CPM (Constant Photocurrent Method) measurements are planned to determine the band gap in another way and to obtain more information about the energy levels present between the conduction and valence band.

7.7 References

1. R. D. McCullough, *Adv. Mater.* **1998**, 10, 2, 93.
2. B. Tarasiuk, W. Podkoscielny, W. Fortuna, J. Ptaszkowska, *Przem. Chem.* **1991**, 70, 4, 162.
3. S. Gillissen, *Ph. D. Dissertation* **2002**, Limburgs Universitair Centrum, Diepenbeek, Belgium.

4. L. Lutsen, P. Adriaensens, H. Becker, A. J. Van Breemen, D. Vanderzande, J. Gelan, *Macromolecules* **1999**, 32, 6517.
5. A. Issaris, D. Vanderzande, J. Gelan, *Polymer* **1997**, 38, 10, 2571.
6. L. Hontis, M. Van Der Borght, D. Vanderzande, J. Gelan, *Polymer* **1999**, 40, 6615.
7. L. Hontis, *Ph. D. Dissertation* **2002**, Limburgs Universitair Centrum, Diepenbeek, Belgium.
8. M. Miyama, N. Haramiya, Y. Mori, H. Tanzawa, *J. Biomed. Mater. Res.* **1977**, 11, 251.
9. H. Inoue, S. Kohama, *J. Appl. Polym. Sci.* **1984**, 29, 3, 877.
10. B. de Boer, H. K. Simon, M. P. L. Werts, E. W. van der Vegte, G. Hadziioannou, *Macromolecules* **2000**, 33, 2, 349.
11. Y. Nakayama, T. Matsuda, *Macromolecules* **1996**, 29, 27, 8622.

Summary

Recent years have seen the increased use of organic materials for electronic applications as photovoltaic cells and field-effect transistors (FETs). Such applications require the use of conjugated polymers with a sufficiently high quality, purity and molecular weight (M_w > 30 000). This dissertation deals with the search for possible synthetic routes leading to low band gap (LBG) materials, conjugated polymers with a small energy gap between the valence and conduction band. Those materials show interesting properties which make them extremely attractive for applications in plastic electronics. The processability of these materials here is very important. This can be obtained either by introducing long chains or by the use of a precursor route. In this dissertation especially the latter is dealt with. Here first a soluble precursor polymer is synthesised which, after thermal treatment, gives rise to the conjugated polymer. We aim at efficient synthetical pathways in order to obtain well defined polymer materials. In cooperation with other research groups, different materials were characterised en tested with an eye to further applications.

Chapter one explains what conducting polymers and in particular low band gap materials are. The parameters that influence the band gap as well as some methods to determine the band gap are discussed. Also the applications of the materials are mentioned of which polymer solar cells and organic transistors are described in detail.

Chapter two copes with the synthesis of soluble low band gap materials by introducing long tails on the monomer unit. Especially the synthesis and characterisation of soluble poly(isothianaphthene) (PITN) derivatives, obtained via the thermal and non-oxidative polymerisation of 5,6-disubstituted dithiophthalides, is discussed. Besides a characterisation of such monomers and polymers with ^{1}H NMR spectroscopy, the band gap of the polymers is determined with UV-Vis spectroscopy and cyclic voltammetry. As predicted by theoretical calculations, the band gap of the obtained polymers is comparable to the band gap of PITN itself. After this, some exploratory measurements for applications in organic solar cells are discussed briefly. Despite the low power conversion efficiencies that

could be reached, a clear contribution of the measured photocurrent could be attributed to the polymer.

In the past poly(dithienylisothianaphthene) (PDTI) derivatives were already synthesised via oxidative polymerisation of the corresponding monomers. However this method has some important drawbacks and therefore we tried to functionalise some monomer derivatives for their use in reductive coupling reactions. We however experienced difficulties in the synthesis of these functionalised monomers so that the reductive polymerisation could not be valorised.

The polymers discussed in the subsequent chapters were all synthesised by applying a precursor route. In chapter three, 3,4-dihalo substituted poly(thienylene vinylene) (PTV) derivatives were synthesised via the sulphinyl and xanthate precursor route. The use of the sulphinyl route seemed possible due to the presence of the electron withdrawing halogen atoms on the 3- and 4-position of the thiophene ring. The electron richness is hereby lowered which is favourable for the monomer synthesis. The implementation of such a material in a solar cell device is discussed in detail. An improvement of the performance of the solar cell was seen after a postproduction heat treatment. Also 3,4-diphenyl substituted PTV was made. Since we are dealing with an electron rich system, the synthesis via the xanthate precursor route was preferred. It was found that this route can be used in the synthesis of both electron poor and electron rich PTV derivatives.

Previous research indicated that the use of the sulphinyl precursor route was problematic for the synthesis of PTV. For this reason, the use of the xanthate route was valorised. Chapter four not only highlights the synthesis and characterisation of precursors with the commonly used *O*-ethyl xanthate group, also new xanthate monomers were synthesised and polymerised. This in order to lower the elimination temperature and to increase the yield. Also here it was proven that the xanthate route can be used in the synthesis of PTV but important drawbacks in the use of this route are the rather low yield and the high polydispersities of the obtained precursor polymers. Furthermore, the deviation of the λ_{max} value with literature values for PTV seems to point to a defective structure of PTV so obtained. The yield and the molecular weight of the precursor polymers bearing other xanthate groups (-SC(S)$OCH_2CH_2OCH_3$) are quite low and the use of this group can also not lead to a lowering of the elimination temperature. Therefore this does not lead to a good alternative for the synthesis of PTV.

In chapter five a total new precursor route, the dithiocarbamate route, is presented. The idea for the synthesis came from the fact that the dithiocarbamate group has a chemical analogue structure as the xanthate group. Trials to polymerise the monomers to obtain precursors of poly(*p*-phenylene vinylene) (PPV) and PTV were successful. Not only the yields were good but the obtained polymer also had improved properties. Besides these homopolymers also trials were started to synthesise copolymers of dithiocarbamate PPV with dithiocarbamate PTV on the one hand and of dithiocarbamate PTV with xanthate PTV on the other hand.

In chapter six the sulphinyl route is again applied in the synthesis of thienyl substituted PPV derivatives. The assignment of the ^{1}H and ^{13}C chemical shifts of two sulphinyl monomers by different NMR techniques is discussed. In addition to the ^{1}H and ^{13}C NMR spectra, INADEQUATE, direct HETCOR and long range HETCOR experiments were performed. Also after the determination of the T_{1C} relaxation times it was demonstrated that this data offers a criterion to assign the carbon resonances. However, in the attempts to polymerise these two monomers, it was found that no *p*-QM system was formed after the addition of a base.

Finally some perspectives and suggestions for further work are presented in chapter seven. It is evident that the further use of the dithiocarbamate route is important.

Samenvatting

De laatste jaren kent men een toenemend gebruik van organische materialen voor elektronische toepassingen zoals fotovoltaïsche cellen en veld-effecttransistoren (FETs). Dergelijke toepassingen vereisen het gebruik van geconjugeerde polymeren met een voldoende hoge kwaliteit, zuiverheid en moleculair gewicht (M_w > 30 000). Deze thesis behandelt de zoektocht naar mogelijke syntheseroutes die leiden tot 'low band gap' (LBG) materialen, geconjugeerde polymeren met een kleine energieafstand tussen de valentie- en conductieband. Deze materialen vertonen interessante eigenschappen wat hun uitermate aantrekkelijk maakt voor toepassingen binnen de 'plastic electronica'. De verwerkbaarheid van de bekomen materialen is hierbij zeer belangrijk. Deze kan verkregen worden ofwel door het invoeren van lange staarten ofwel door het werken via precursorroutes. Vooral de laatste methode komt in deze thesis aan bod. Hierbij wordt altijd eerst een oplosbaar precursorpolymeer gemaakt dat, na een thermische behandeling, aanleiding geeft tot het geconjugeerde polymeer. Bij de bereidingen hebben we vooral gezocht naar efficiënte synthesemethoden om te komen tot goed gedefinieerde polymere materialen. In samenwerking met andere onderzoeksgroepen werden verschillende materialen gekarakteriseerd en getest met het oog op verdere toepassingen.

In hoofdstuk één wordt duidelijk gemaakt wat geleidende polymeren en meer bepaald low band gap of kleine bandafstand materialen zijn. De factoren die een invloed hebben op de bandafstand van een polymeer alsook de methodes om deze bandafstand te bepalen worden hierbij besproken. Ook de toepassingen van de materialen komen aan bod waarbij polymere zonnecellen en organische transistoren in detail beschreven worden.

Hoofdstuk twee beschrijft de synthese van oplosbare low band gap materialen door het inbouwen van lange staarten op de monomeer-eenheid. Vooral de synthese en karakterisatie van oplosbare poly(isothianafteen) (PITN) derivaten, bekomen via de thermische niet-oxidatieve polymerisatie van 5,6-digesubstitueerde dithioftalides, wordt besproken. Naast een karakterisatie van dergelijke mono- en polymeren met ^{1}H NMR

spectroscopie, wordt ook de bandafstand van de polymeren bepaald aan de hand van UV-Vis spectroscopie en cyclische voltammetrie. Zoals voorspeld door theoretische berekeningen is de bandafstand van de bekomen polymeren vergelijkbaar met de bandafstand van PITN zelf. Daarna worden enkele zonneceltesten in het kort besproken. Ondanks de lage efficiëntie, kon een duidelijke bijdrage van de gemeten fotostroom toegekend worden aan het polymeer.

Poly(dithienylisothianafteen) (PDTI) derivaten werden in het verleden reeds gesynthetiseerd via een oxidatieve polymerisatie van het overeenkomstige monomeer. Daar deze methode enkele nadelen kent, werden ook pogingen ondernomen om enkele monomeerderivaten te functionaliseren en vervolgens te gebruiken in reductieve koppelingen. We ondervonden echter problemen bij de synthese van deze gefunctionaliseerde monomeren zodat de reductieve polymerisatie niet gevaloriseerd kon worden.

De polymeren die beschreven worden in de hierop volgende hoofdstukken, werden allen bereid door het aanwenden van een precursorroute. De in hoofdstuk drie beschreven 3,4-dihalogesubstitueerde poly(thienyleen vinyleen) (PTV) derivaten werden via de sulfinyl- en xanthaat precursorroute aangemaakt. Het gebruik van de sulfinylroute bleek mogelijk door de aanwezigheid van de elektronzuigende halogenen op de 3- en 4- positie van de thiofeenring. Hierdoor wordt het systeem minder elektronenrijk hetgeen de monomeersynthese ten goede komt. De implementatie van een dergelijk materiaal in een zonnecel wordt hierbij uitvoerig behandeld. Een verbetering van de prestatie van de zonnecel werd waargenomen door het verhitten van deze cel. Hiernaast werd ook 3,4-difenylgesubstitueerd PTV gemaakt. Daar we hier met een elektronenrijk systeem te maken hebben, werd geopteerd voor een synthese via de xanthaat precursorroute. We toonden dus aan dat deze route gebruikt kan worden in de synthese van zowel elektronenarme als elektronenrijke PTV derivaten.

Uit eerder onderzoek bleek dat het gebruik van de sulfinyl precursorroute problematische was voor de synthese van PTV. Daarom werd het gebruik van de xanthaat-route gevaloriseerd. Hoofdstuk vier belicht niet enkel de synthese en de karakterisatie van de meest gebruikte *O*-ethylxanthaat groep, ook nieuwe xanthaat monomeren werden gesynthetiseerd en gepolymeriseerd. Dit om de eliminatietemperatuur te verlagen en het rendement te verhogen. Ook hier werd aangetoond dat de xanthaatroute gebruikt kan

worden in de synthese van PTV maar het lage rendement en de hoge polydispersiteit van de bekomen precursorpolymeren zijn belangrijke nadelen in het gebruik van deze route. Hierenboven wijst de afwijking van de λ_{max} waarde met de literatuurwaardes voor PTV op defecten in de structuur van het via deze route bekomen geconjugeerde polymeer. Het rendement en het moleculair gewicht van de precursorpolymeren met de andere xanthaatgroepen (-SC(S)$OCH_2CH_2OCH_3$) zijn laag en het gebruik van deze groep kan ook de eliminatietemperatuur niet verlagen. Daarom leidt dit niet tot een goed alternatief voor de synthese van PTV.

In hoofdstuk vijf wordt een totaal nieuwe precursorroute, de dithiocarbamaatroute, voorgesteld. De idee voor de synthese kwam naar aanleiding van de analogie in chemische structuur van een dithiocarbamaatgroep en een xanthaatgroep. Pogingen tot polymerisatie ter vorming van poly(*p*-fenyleen vinyleen) (PPV) en PTV precursoren verliepen positief. Niet alleen waren de rendementen zeer goed maar de bekomen polymeren bleken ook verbeterde eigenschappen te bezitten. Naast deze homopolymeren werden ook pogingen ondernomen voor de synthese van copolymeren tussen dithiocarbamaat PPV en PTV enerzijds en tussen dithiocarbamaat PTV en xanthaat PTV anderzijds.

In hoofdstuk zes wordt opnieuw gebruik gemaakt van de sulfinylroute. Ditmaal voor de synthese van een thiofeengesubstitueerd PPV derivaat. Hierbij worden de ^{1}H en ^{13}C chemische shiften van twee sulfinylmonomeren toegekend aan de hand van verschillende NMR technieken. Als aanvulling op de ^{1}H en ^{13}C NMR spectra, werden INADEQUATE, directe HETCOR en long range HETCOR experimenten uitgevoerd. Ook na de bepaling van de T_{1C} relaxatietijden bleek dat deze data een goede stafmaat waren voor de toekenning van de chemische shiften. Wanneer echter getracht werd de twee monomeren te polymeriseren door het toevoegen van een base, werd er geen vorming van een *p*-QM systeem waargenomen.

Tenslotte worden in hoofdstuk zeven enkele toekomstperspectieven en suggesties voor verder werk gegeven. Dat het verdere gebruik van de dithiocarbamaatroute hierbij een belangrijke rol zal spelen is vanzelfsprekend.

List of abbreviations

Ac_2O	acetic anhydride
Bp	boiling point
BPO	benzoyl peroxide or dibenzoyl peroxide
CB	conduction band
$CHCl_3$	chloroform
CH_2Cl_2	dichloromethane
CI	chemical ionisation
CV	cyclic voltammetry
DIP-MS	direct insert probe mass spectrometry
DMF	*N,N*-dimethylformamide
DP	degree of polymerisation
EI	electron impact
EL	electroluminescence
EtOAc	ethyl acetate
Et_2O	diethyl ether
E_g	band gap
eV	electronvolt
FT-IR	Fourier transform infrared
GC/MS	gas chromatography/mass spectrometry
GPC	gel permeation chromatography
HCl	hydrogen chloride
HETCOR	heteronuclear chemical shift correlation
HOMO	highest occupied molecular orbital
Iniferter	initiator-chain transfer-terminator agent
ITO	indium tin oxide
LBG	low band gap

LDA	lithium diisopropyl amide
LUMO	lowest unoccupied molecular orbital
KOH	potassium hydroxide
K*t*BuO	potassium *tertiar*-butoxide
MCPBA	3-chloroperbenzoic acid or m-chloroperbenzoic acid
MeOH	methanol
M_n	number-average molecular weight
M_w	weight-average molecular weight
Na*t*BuO	sodium *tertiar*-butoxide
NBS	*N*-bromosuccinimide
NCS	*N*-chlorosuccinimide
NMP	*N*-methylpyrrolidone
NMR	nuclear magnetic resonance
NOE	nuclear Overhauser effect
OFET	organic field-effect transistor
PA	poly(acetylene)
PD	polydispersity (M_w/M_n)
PDTI	poly(1,3-dithienylisothianaphthene)
PEDOT	poly(3,4-ethylene dioxythiophene)
PEDOT/PSS	
or BAYTRON P	poly(3,4-ethylene dioxythiophene) poly(styrene) sulphonate
PEDOTV	poly(3,4-ethylene dioxythiophene vinylene)
PF	poly(furan)
PITN	poly(isothianaphthene)
PLED	polymer light-emitting diode
PPP	poly(*p*-phenylene)
PPV	poly(*p*-phenylene vinylene)
PPy	poly(pyrrole)
PS	poly(styrene)
PT	poly(thiophene)
p-TsOH	*para*-toluenesulphonic acid
PTV	poly(2,5-thienylene vinylene)

P_4S_{10}	phosphorus pentasulphide
p-QM	*para*-quinodimethane
rpm	rotations per minute
rt	room temperature
SEC	size exclusion chromatography
$SOCl_2$	thionyl chloride
SO_2Cl_2	sulphuryl chloride
TFT	thin film transistor
TGA	thermogravimetric analysis
THF	tetrahydrofuran
THT	tetrahydrothiophene
TLC	thin-layer chromatography
T_1	spin-lattice relaxation time
T_2	spin-spin relaxation time
UV-Vis	ultraviolet visible
VB	valence band
λ_{max}	maximum absorption wavelength